IFM-GEOMAR REPORT

IFM-GEOMAR

Leibniz-Institut für Meereswissenschaften
an der Universität Kiel

FS Sonne
Fahrtbericht / Cruise Report
SO186 Leg 3
SeaCause II

Penang-Singapore

26.02.-16.03.2006

Berichte aus dem Leibniz-Institut
für Meereswissenschaften an der
Christian-Albrechts-Universität zu Kiel

Nr. 6
März 2006

IFM-GEOMAR
Leibniz-Institut für Meereswissenschaften
an der Universität Kiel

FS Sonne
Fahrtbericht / Cruise Report
SO186 Leg 3
SeaCause II

Penang-Singapore

26.02.-16.03.2006

Edited by
Heidrun Kopp & Ernst R. Flueh

Berichte aus dem Leibniz-Institut
für Meereswissenschaften an der
Christian-Albrechts-Universität zu Kiel

Nr. 6, März 2006

ISSN Nr.: 1614-6298

IFM-GEOMAR
Leibniz-Institut für Meereswissenschaften
an der Universität Kiel

Das Leibniz-Institut für Meereswissenschaften ist ein Institut der Wissenschaftsgemeinschaft Gottfried Wilhelm Leibniz (WGL)

The Leibniz-Institute of Marine Sciences is a member of the Leibniz Association (Wissenschaftsgemeinschaft Gottfried Wilhelm Leibniz).

Herausgeber / Editor:
Heidrun Kopp & Ernst R. Flueh

IFM-GEOMAR Report
ISSN Nr.: 1614-6298

Leibniz-Institut für Meereswissenschaften / Leibniz-Institute of Marine Sciences
IFM-GEOMAR
Dienstgebäude Westufer / West Shore Building
Düsternbrooker Weg 20
D-24105 Kiel
Germany

Leibniz-Institut für Meereswissenschaften / Leibniz-Institute of Marine Sciences
IFM-GEOMAR
Dienstgebäude Ostufer / East Shore Building
Wischhofstr. 1-3
D-24148 Kiel
Germany

Tel.: ++49 431 600-0
Fax: ++49 431 600-2805
www.ifm-geomar.de

Rücken (nur bei umfangreicheren Dokumenten)

IFM - GEOMAR REPORT Nr. 6 - FS Sonne Fahrtbericht / Cruise Report SO 186 SEACAUSE

IFM-GEOMAR
Leibniz-Institut für Meereswissenschaften
an der Universität Kiel

Das Leibniz-Institut für Meereswissenschaften ist ein Institut der Wissenschaftsgemeinschaft Gottfried Wilhelm Leibniz (WGL)

The Leibniz-Institute of Marine Sciences is a member of the Leibniz Association (Wissenschaftsgemeinschaft Gottfried Wilhelm Leibniz).

Leibniz-Institut für Meereswissenschaften / Leibniz-Institute of Marine Sciences
IFM-GEOMAR
Dienstgebäude Westufer / West Shore Building
Düsternbrooker Weg 20
D-24105 Kiel
Germany

Leibniz-Institut für Meereswissenschaften / Leibniz-Institute of Marine Sciences
IFM-GEOMAR
Dienstgebäude Ostufer / East Shore Building
Wischhofstr. 1-3
D-24148 Kiel
Germany

Tel.: ++49 431 600-0
Fax: ++49 431 600-2805
www.ifm-geomar.de

TABLE OF CONTENTS

1.1 Summary

The cruise SO 186 Leg 3 with research vessel SONNE started on February 26, 2006, in Penang, Malaysia, and ended in Singapore on March, 15, 2006. An international group of 23 scientists from Germany, Indonesia and the United Kingdom participated in this cruise. The cruise SO186-3 is a continuation of previous surveys, which were conducted in the same area since October 2005.

The cruise SO186-3 is a part of the SECAUSE project, which investigates the georisk potential along the active convergence zone between the Eurasian and Indo-Australian plates offshore Indonesia. The magnitude 9.3 and 8.7 earthquakes, which occurred at the Sumatra subduction zone on December 26, 2004 and on March 28, 2005 were the two largest earthquakes of the last 40 years. In contrary to the second event, the earthquake of December 26 generated a devastating tsunami, which took the live of more than 200000 people. As a consequence of this catastrophe Germany and Indonesia have been developing a Tsunami Early Warning System (GITEWS) for the Indian Ocean with the focus on the Indonesian coast. As a part of the system two buoys and ocean bottom units equipped with pressure sensors and seismometers were deployed during the previous legs of the RV SONNE cruise. During the previous cruises an array of Ocean Bottom Seismometers and Hydrophones was deployed and reflection-seismic and bathymetric surveys were performed.

It is the goal of this leg SO 186-3 in the framework of the SEACAUSE project to study the mechanisms of tsunami generation by using refraction seismic methods. During SO186-3 three active seismic wide-angle experiments were performed with Ocean Bottom Stations of IFM-GEOMAR and a BGR airgun source. The first experiment was a 150 nm long profile east of Simeulue Island. The profile was directed from the trench in the south-west to the coast of Sumatra in the north-east. 25 Ocean Bottom stations were deployed, while 7 stations were still in operation as part of the seismological network. The second seismic experiment was performed south of Simeulue Island. 21 Ocean Bottom stations were deployed and a 20 nm long profile was shot. The third experiment was performed north-west of Simeulue Island with 33 stations on two cross profiles. Additionally five methane sensors were deployed during all experiments, which sensors measured the methane concentration in the water; the quality of data was good. During profiles 1 and 2 several Ocean Bottom stations were equipped with paroscientific pressure sensors, which recorded the long period tides and signals from large earthquakes with high data quality. The data recorded during the seismic experiments are of high quality, and the same applies to seismological data recorded by the network during the last four months. All ocean bottom stations from the seismological network were recovered.
In the time between the seismic experiments the test buoy of the GITEWS system was inspected. The ocean bottom unit was recovered, the seismic data was collected, and the unit was redeployed.
During the cruise bathymetric measurements were performed with the SIMRAD system.

1.2 Zusammenfassung

Die Fahrt SO 186-3 mit dem Forschungsschiff SONNE begann am 26 Februar 2006 in Penang, Malaysia, und endete in Singapur am 15 März 2006. Eine internationale Gruppe mit 23 Wissenschaftlern aus Deutschland, Indonesien und Großbritannien nahm an der Fahrt teil. Diese Fahrt schloss an die vorhergehenden Vermessungen an, die seit Oktober 2005 in demselben Gebiet durchgeführt worden sind. Die Fahrt SO 186-3 fand im Rahmen des Projektes SEACAUSE statt, in dem das Geo-Risikopotential längs der aktiven Konvergenzzone zwischen der eurasischen und der indo-australischen Platte vor der Küste Indonesiens untersucht wird. Die Erdbeben mit Magnituden 9.3 und 8.7, die sich am 26. Dezember 2004 und am 28. März 2005 an der Sumatra Subduktionszone ereigneten, waren die zwei größten Erdbeben der letzten 40 Jahre. Im Gegensatz zum zweiten Beben erzeugte das Erdbeben am 26. Dezember einen verheerenden Tsunami, der mehr als 200000 Menschen das Leben kostete.

Als Konsequenz dieser Katastrophe entwickeln Deutschland und Indonesien ein Tsunami-Frühwarnsystem (GITEWS) für den indischen Ozean mit Schwerpunkt an der indonesischen Küste. Als Teil dieses Systems sind während der vorherigen Fahrtabschnitte des Forschungsschiffes SONNE zwei Bojen stationiert worden, zusammen mit Ozean Boden Einheiten, die mit Drucksensoren und Seismometern ausgestattet sind. Des Weiteren ist ein seismologisches Netz von Ozean-Boden-Seismometern und Hydrophonen implementiert und reflexionsseismische und bathymetrische Vermessungen sind durchgeführt worden.
Das Ziel dieses Fahrtabschnittes SO 186-3 innerhalb des SEACAUSE Projektes ist es, die Mechanismen der Entstehung des Tsunamis mit refraktionsseismischen Methoden zu untersuchen. Während der Fahrt SO 186-3 wurden, unter Verwendung von Ozean-Boden-Stationen des IFM-GEOMAR und einer Airgun-Quelle der BGR, drei aktive seismische Weitwinkel-Experimente durchgeführt. Das erste Experiment war ein 150 nm langes Profil östlich der Insel Simeulue. Das Profil war vom Graben im Südwesten ausgerichtet zur Küste Sumatras im Nordosten. 25 Ozean-Boden-Stationen wurden ausgesetzt, während 7 Stationen als Teil des seismologischen Netzes noch in Betrieb waren. Die nächsten beiden Experimente wurden innerhalb der Bruchzonen der Erdbeben durchgeführt. Das zweite seismische Experiment wurde südlich der Insel Simeulue durchgeführt, in der Nähe des Epizentrums des Bebens vom 28. März 2005, bei dem kein Tsunami erzeugt wurde. Es wurden 21 Ozean-Boden-Stationen eingesetzt, mit einem 20 nm langen Schussprofil. Das dritte Experiment wurde nordwestlich der Insel Simeulue, in der Nähe des Epizentrums des Bebens vom 26. Dezember 2004, durchgeführt, mit 33 Stationen auf zwei sich kreuzenden Profilen. Bei allen Experimenten wurden zusätzlich fünf Methansensoren eingesetzt, die die Methankonzentration im Wasser mit guter Datenqualität aufgezeichnet haben. Bei den Profilen 1 und 2 wurden bei mehreren Ozean-Boden-Stationen Paroscientific-Drucksensoren angebracht, die sehr gute Datenqualität lieferten. Neben dem langwelligen Tidenhub zeichnen sie Signale von größeren Erdbeben auf. Die während der seismischen Experimente gesammelten Daten sind von hoher Qualität. Dasselbe gilt für die Daten, die vom seismologischen Netz während der vergangenen vier Monate registriert wurden. Alle Ozean-Boden-Stationen des seismologischen Netzwerkes wurden eingeholt.

In der Zeit zwischen den seismischen Experimenten wurde die Testboje des GITEWS Systems inspiziert. Die Ozean Boden Einheit wurde eingeholt, die seismischen Daten überspielt, und die Einheit wurde wieder abgesetzt.

Während der Fahrt wurden bathymetrische Messungen mit dem SIMRAD System durchgeführt.

2. Introduction

The earthquake with a magnitude (Mw) 9.3 of Dec. 26, 2004 (Stein and Okal, 2005) on the Sumatra subduction zone was the largest earthquake within the past 40 years and the second-largest ever recorded (Figure 2.1). Rupture started at the southern end of the fault segment and propagated northwards. Duration and extent of the rupture were the longest ever recorded (Ishii et al., 2005). The observation that the slip did not propagate significantly southwards, even though the magnitude of slip was high at the southern end of the rupture, strongly suggests a segmentation of the subduction zone. The 2004 event was followed on March 28, 2005 by an earthquake with a magnitude (Mw) of 8.7, which was the second-largest event in the past 40 years. The 2004 and 2005 Sumatra earthquake couplet allows for the first time the use of modern recordings and modern scientific tools of investigation to unravel the linkage between fault segmentation and earthquake dynamics.

The segmentation of major fault systems controls earthquake magnitude and location, but the physical causes of segment boundaries and their impact on earthquake rupture dynamics are still poorly understood. One of the key issues in scientific research involves the influence of the properties of the earthquake generating fault zone on the generation and rupture propagation of such large earthquakes as observed along the Sumatra subduction zone.

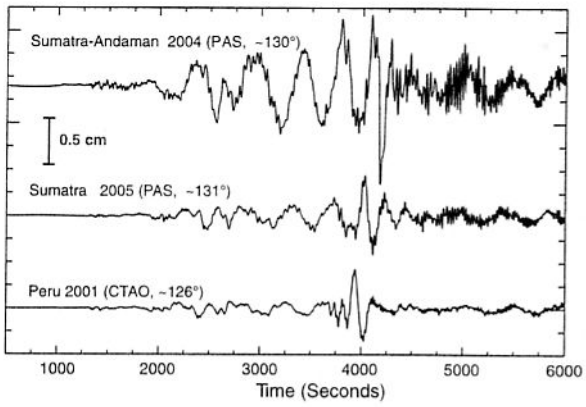

Figure 2.1: *Comparison of the three largest earthquakes in the past 40 years. Vertical-component ground displacements for periods <1000 s are displayed. The 2001 Peru earthquake had a magnitude of Mw=8.4 (from Lay et al., 2005).*

2.1 Aims of the project and objectives of cruise SO186 Leg 3

In the wake of the devastating tsunami generated by the 2004 Sumatra earthquake, the joint project SEACAUSE started in 2005 to investigate the segmentation of the Sunda megathrust as well as differences between the 2004 and 2005 events, as the latter did not cause a comparable tsunami.

Tsunamis may be generated by one of the following occurrences:

- Vertical motion along plate boundaries or fracture zones covered by a large water column
- Submarine, sedimentary slides
- Volcanic eruptions or extraterrestrial impacts
- the Earth's spheroidal modes (Lomnitz & Nilsen-Hofseth, 2005)

The SEACAUSE project contributes to the understanding of the Sumatra earthquakes and tsunami generation, which is an essential prerequisite for the implementation of an Early Warning System in the Indian Ocean.

The segmentation of the forearc is essential for an understanding of the differences between the two seismic events. Tectonic and structural variations in the forearc, especially in the region of the forearc wedge in the vicinity of the deformation front, play an important role in the different earthquake characteristics of the two events, including the generation of the tsunami.

The SEACAUSE project includes an integrated programme of seismic and seismological investigations, complemented by bathymetric measurements. In October 2005, a local seismological array consisting of 20 ocean bottom instruments was deployed around Simeulue Island in the area of the postulated segment boundary between the 2004 and 2005 earthquakes offshore northern Sumatra (Figure 2.1.1). This array was extended to and modified during the next cruises of RV SONNE from November 2005 through January 2006 (see Figure 2.1.1). In addition, 8 Güralp CMG-6TD sensors of the SeisUK equipment pool were deployed on Simeulue Island by the University of Cambridge (Figure 2.1.2).

The local seismological network was recovered during the course of cruise SO186 Leg 3 lasting from Feb. 26, to March 16, 2006. We expected that these instruments, together with the land stations deployed on Simeulue, would yield a state-of-the-art slip distribution related to the physical properties of the fault plane. To achieve this goal, several seismic wide-angle profiles were acquired during the cruise. The longest profile, running through the seismological network, will be used to calibrate seismological data. This profile coincides with a multichannel seismic (MCS) line acquired by the BGR during the previous leg. Additional profiles trend across-strike of the margin toe and cover the deformation front where the décollement is shallowest. These densely spaced lines serve to unravel changes in the physical properties of the décollement in the rupture areas of the 2004 and 2005 events, respectively.

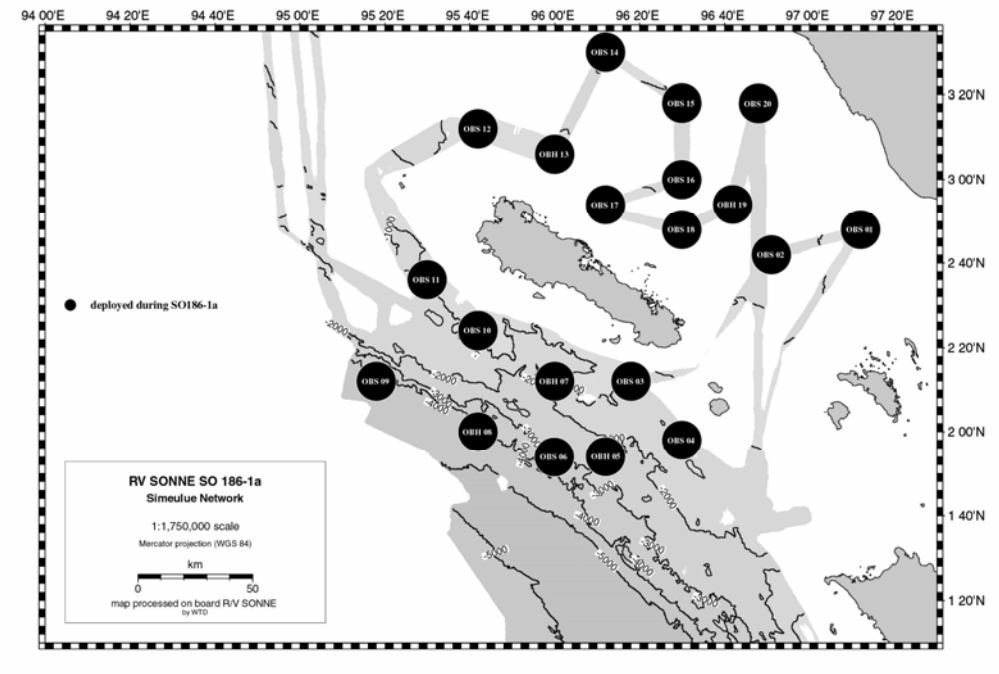

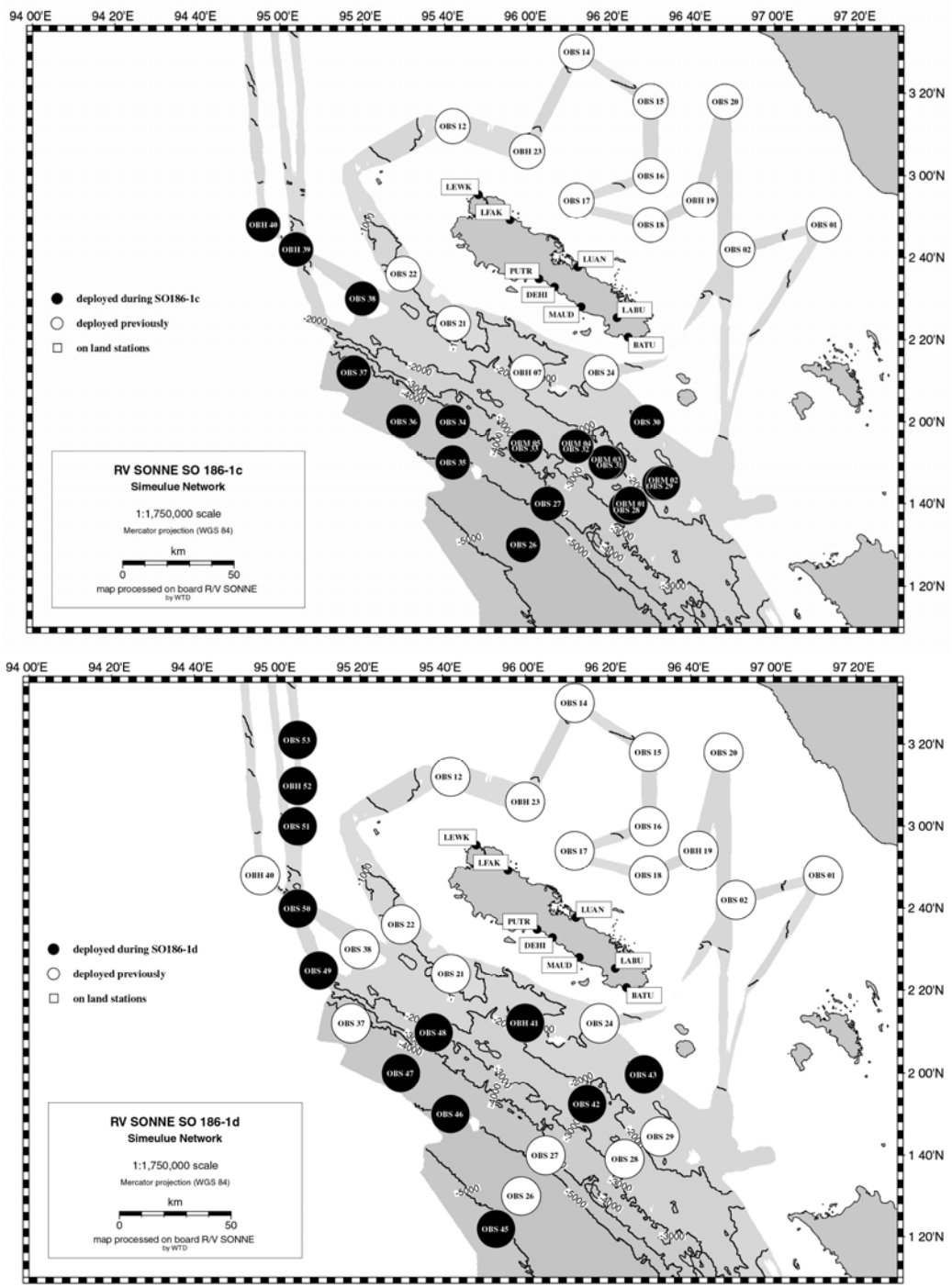

Figure 2.1.1: *Local seismological network deployed in Oct. 2005 around Simeulue Island offshore northern Sumatra. The segment boundary between the Dec. 26, 2004 earthquake and the March 28, 2005 event is believed to trend in a SW-NE direction through the network area. The upper panel displays locations of stations deployed during cruise SO186 Leg 1 (SO186-1a). Black dots mark stations deployed during the cruises of RV SONNE from Nov. 2005 through Jan. 2006.*

The lack of understanding of the role of segmentation for the extent and distribution of rupture during large earthquakes leaves a significant gap in our ability to assess seismic hazards of fault systems. A detailed knowledge of the physics and tectonics of the fault systems which were involved in the generation of these large earthquakes is the key to the understanding of the destructive 2004 tsunami and of the tsunamogenic behaviour of

earthquakes in general. These analyses are essential to societal benefits and to the implementation of an early warning system.

Regions of possible future large earthquakes are the Sumatra Fault and the area southeast of the 2005 event rupture (Sieh, 2005, Lay et al., 2005). The adjacent segment experienced rupture in 1833 and is likely to have accumulated substantial strain. The inevitability of future megathrust events along the Sumatra subduction zone necessitates efforts to establish early-warning capabilities in the Indian Ocean.

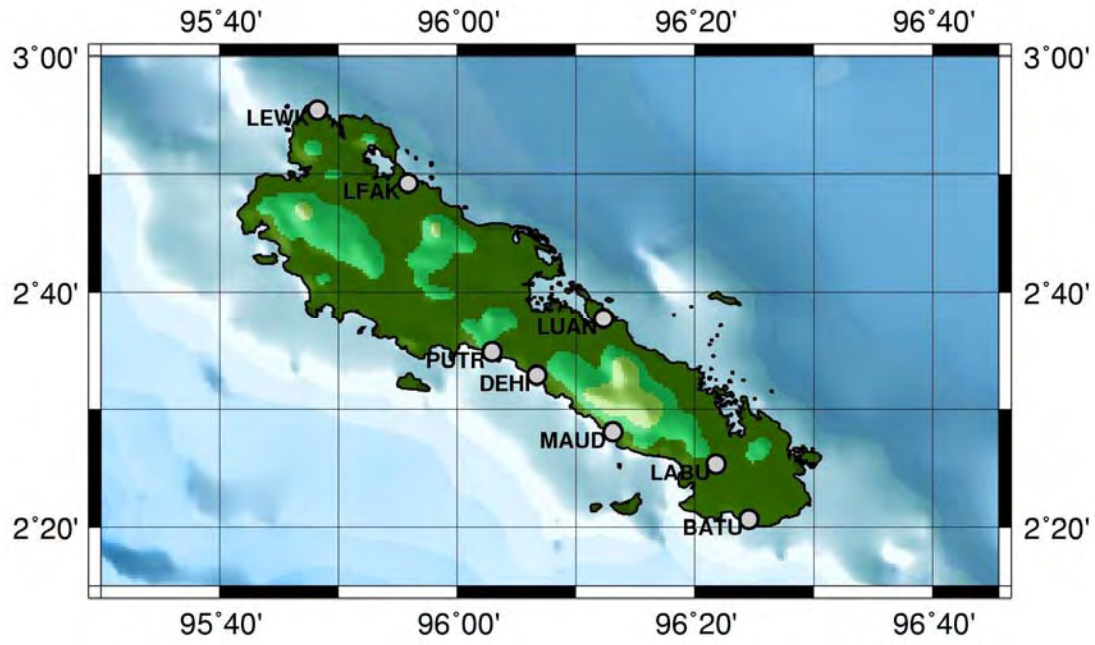

Figure 2.1.2: *Location map of seismological stations deployed on Simeulue Island offshore Sumatra in 2005. Eight seismometers were deployed by the University of Cambridge to record seismicity simultaneously to the offshore network.*

2.2 The Sumatra-Andaman earthquake of Dec. 26, 2004 and Nias earthquake of March 28, 2005

The Sunda subduction zone, which curves along the Indonesian archipelago, was the site of the seismic megathrust event with a moment magnitude (Mw) of 9.3 that occurred on Dec. 26, 2004. A moment magnitude (Mw) of 9.0 was obtained shortly after the earthquake, but was later revised by a factor of 2.5 based on analyses of normal-modes with longer periods (Stein and Okal, 2005). Rupture started approximately 100 km off the west coast of northern Sumatra at 3.3°N and 96.0°E at a depth of approximately 30 km at 00:58:53 GMT (Khan and Gudmundsson, 2005; Lay et al., 2005). The earthquake ruptured the tectonic boundary along which the Australian and Indian plates begin their descent beneath Southeast Asia (Sieh, 2005). Here, the Eurasian plate is segmented into the Burma and Sunda subplates (Figure 2.2.1). Convergence is highly oblique along the northern segment of the plate boundary from northern Sumatra into the Andaman Sea, becoming strike-slip. This feature presumably stopped further rupture to the north (Stein and Okal, 2005). As a result of slip partitioning, a plate sliver, referred to as the Andaman or Burma microplate, has sheared off in parallel to the subduction zone from Myanmar to Sumatra (Lay et al., 2005). This microplate is dotted by the Andaman and Nicobar archipelagos. Thrust motion predominates in the Andaman trench at a convergence rate of approximately 14 mm/year. The Andaman ridge transform system joins the lithospheric-scale right-lateral Sumatra strike-slip fault in the south. The pronounced

back-arc basin in the Andaman Sea results from oblique back-arc spreading, which accommodates the remaining plate motion.

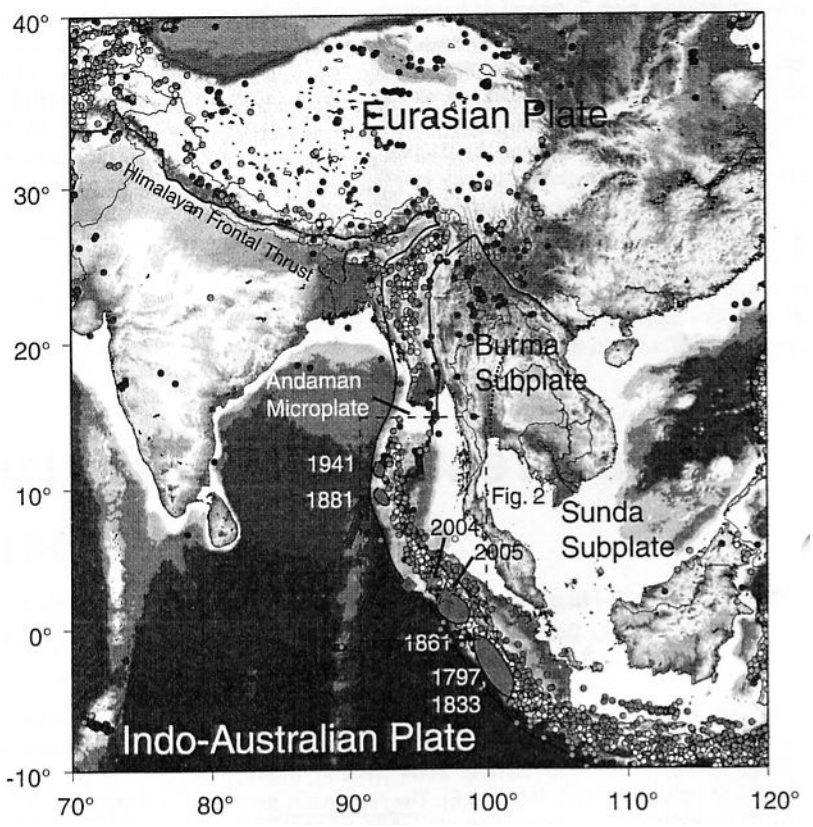

Figure 2.2.1: *Tectonic map of Southeast Asia showing earthquakes with a moment magnitude (Mw) of >5 from 1965 to 2004 from the earthquake catalogue of the National Earthquake Information Center (NEIC). Dashed areas mark rupture zones of historic and recent earthquakes (from Lay et al., 2005).*

The Global Seismographic Network (GSN), which includes 137 high dynamic range, broadband seismic stations distributed worldwide (Figure 2.2.2) is run by IRIS in collaboration with USGS. GSN data captured the broadband character and complexity of the seismic vibrations of Dec. 26 in exquisite detail (Figure 2.2.3) (Park et al., 2005a).

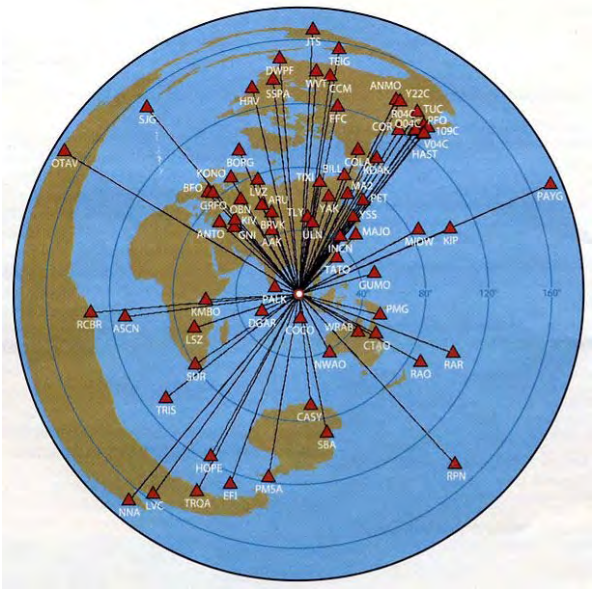

Figure 2.2.2: *Global station distribution of the GSN (Global Seismographic Network) array providing real-time data or data near real-time for the Sumatra-Andaman earthquake (from Park et al., 2005a).*

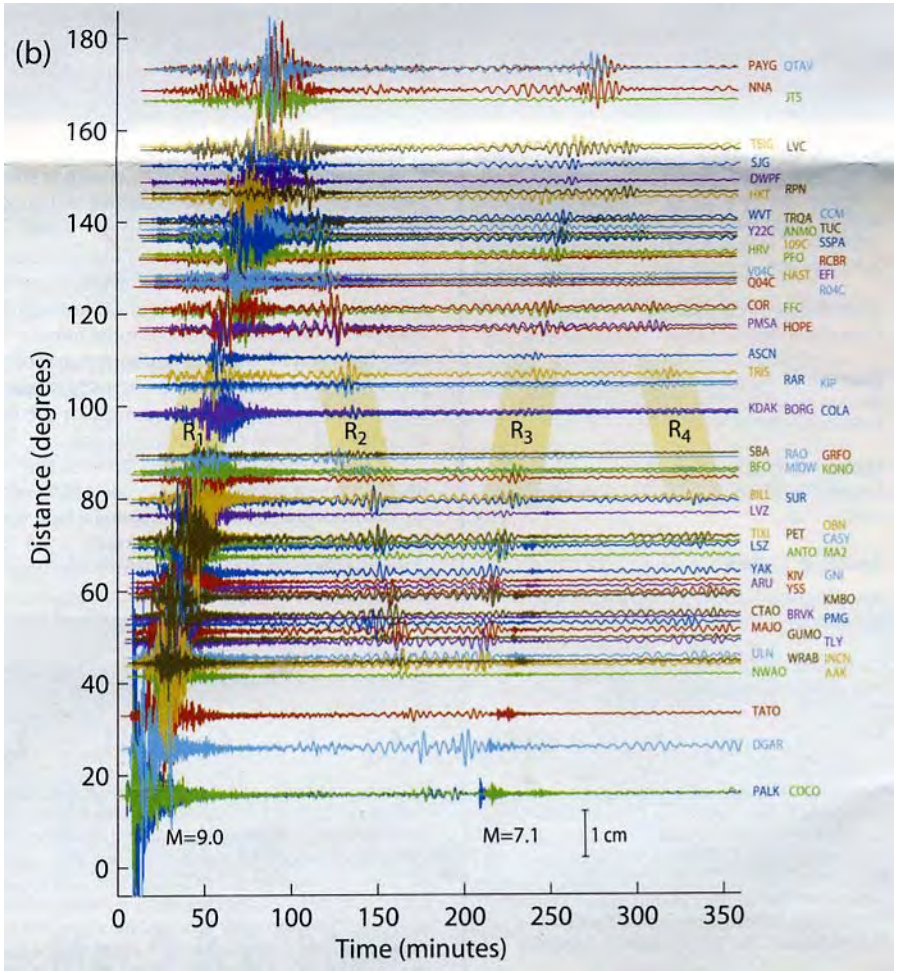

Figure 2.2.3: *Vertical component records for the first 6 hours after the 2004 Sumatra earthquake. R1-R4 denote arrivals of different Rayleigh wave phases. The closest stations (bottom) record a Mw=7.1 aftershock at a time delay of about 200 minutes (from Park et al., 2005a).*

Every position on the Earth's surface began to vibrate within 21 minutes after the 2004 mainshock with peak ground motions exceeding 1 cm at all locations on Earth's solid surface (Park et al., 2005a). The earthquake lasted 8-9 minutes and ruptured between 210 000 km^2 (Ishii et al., 2005) and 250 000 km^2 of the plate with 10-15 m of slip across the fault surface (Wilson, 2005). Fault slip reached approximately 15 m near Banda Aceh, Sumatra (Lay et al., 2005). This shift in the seafloor displaced more than 30 km^3 of seawater, causing a tsunami that could be detected globally (Bilham, 2005). It released as much strain energy as all earthquakes combined over the last fifteen years (Figure 2.2.4) (Wilson, 2005).

Energy release during an earthquake is partitioned into radiation of seismic waves, tectonic-mechanical processes such as creation of fractures, and frictional heat. The frequency and amplitude of the generated seismic waves depend on both the rupture propagation and the local slip history. Thus, variations in the rate and amount of slip will be documented in the seismic waves and may be reconstructed from the seismic wave field. Rupture speed plays an important role in the quantification of an earthquake, as fast ruptures radiate a relatively large portion of seismic energy. Rupture speed is about 70-95% of the shear wave velocity. Variations in rupture speed across segment boundaries are thus essential for an understanding of the complexity of a rupture (Ammon et al., 2005). The aftershock pattern of the 2004 event (Figure 2.2.5) suggests a rupture length of up to 1300 km extending from northern Sumatra to the Andaman Islands, with seismic activity being concentrated along the shallow part of the

subduction zone. A rupture length of 1200-1300 km is a common result of several papers published on this earthquake (e.g. Park et al., 2005a; Stein and Okal, 2005; Ni et al., 2005; Bilham, 2005; Lay et al., 2005; Ammon et al., 2005; Ishii et al., 2005; Guilbert et al., 2005). Krüger and Ohrnberger (2005) estimate a somewhat shorter rupture length of 1150 km based on teleseismic arrivals. Short-period radiation was generated for approximately 500 s (Lay et al., 2005). Along the northernmost segment (north of 10°N) the fault strike rotates N-NW. The Harvard centroid-moment tensor (CMT) solution of the mainshock indicates predominantly thrust faulting on a shallow (8°) dipping plane. Focal mechanisms for the aftershocks unveil a variety of geometries - mostly thrust faulting along the subduction zone and strike-slip and normal faulting in the Andaman Sea. These findings are consistent with nearly arc-normal thrusting in the shallow part of the subduction zone and right-lateral shearing due to slip partitioning in the back arc (Lay et al., 2005).

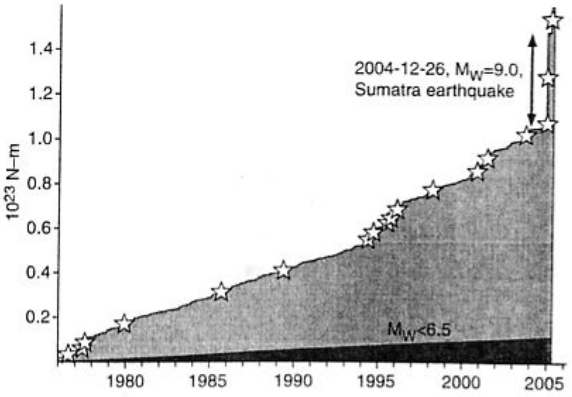

Figure 2.2.4: *Cumulative seismic moment for earthquakes of magnitude Mw >5.0 since 1976. (Stars indicate earthquakes of magnitude Mw >8). The released seismic moment of the 2004 event is comparable to the cumulative global moment released during the preceding decade (Lay et al., 2005).*

Figure 2.2.5: *Aftershock distribution of events in 2004 and 2005 with moment tensor solutions enlarged. Star indicates the epicenter location of the earthquake in 2004; dashed line marks the segment boundary between the two events (Lay et al., 2005).*

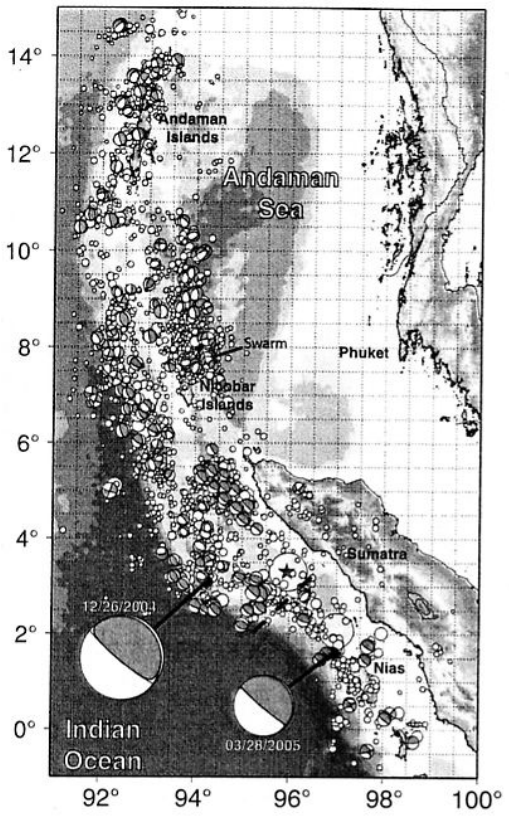

Rupture of the event in 2005 started at 2.1°N, 97.0°E near Nias Island offshore northern Sumatra at a depth of approximately 30 km (Lay et al., 2005). Rupture was directed primarily to the southeast (Ammon et al., 2005). Dip-slip thrusting was the predominant motion on a plate dipping shallowly by 7°. The aftershock distribution suggests that a 300-400 km long section of the plate broke with relatively uniform rupture geometry (Lay et al., 2005). The earthquake caused widespread destruction on the islands and is estimated to have caused about 2000 casualties (Nalbant et al., 2005). Peak slip near the hypocenter reached ~5-6 m (Ammon et al., 2005) and is concentrated at a depth between 20 km and 40 km. This, in conjunction with the substantial outer arc high, possibly helps explain the smaller tsunami generated by this event.

Changes in the trend of interplate motion and age variations of the subducting oceanic lithosphere apparently affect the nature of the faulting (Lay et al., 2005). The age of the oceanic plate increases from about 60 million to 90 million years between Sumatra and the Andaman Islands, presumably affecting the mechanical coupling between the downgoing plate and the upper plate. Large earthquakes are rare in subduction zones, which display back-arc spreading and an old oceanic plate, but are more common where young, strongly coupled lithosphere is subducted with shallow dip and a broad contact area. As different sectors along the Sumatra-Andaman trench show a high variation in geologic parameters (plate age, convergence direction), this segmentation is essential to the understanding of the rupture sequence and slip distribution of the 2004 and 2005 earthquakes.

2.2.1 Subduction zone segmentation along the Sumatra-Andaman trench

Segmentation of a subduction zone may either be linked to discontinuities in the geometry of the forearc (e.g. slab tears, topographic anomalies such as ridges, fracture zones or seamount chains, large scale structures on the upper plate) or to variations in the physical properties (e.g. changes in buoyancy of the subducted lithosphere due to thermal age differences). Physical property heterogeneity is associated with variations in temperature, rock strength, composition, stress state, or fluid content.

For the assessment of natural hazards, subduction zone segmentation is crucial as it controls the extent of slip, and thus the magnitude of an earthquake. Strong lateral variability in the amount of slip has been documented for the event in Dec. 26, 2004 (e.g. Ammon et al., 2005). It may be linked to differences in coupling strength due to topographic effects on the plate interface or changes in plate age or due to compositional heterogeneity or varying effective pressure associated with pore pressure variations. The maximum size of an earthquake on a fault system is controlled by the degree to which the propagating rupture can cross the boundaries between the single segments. While the 2004 earthquake extended far to the north, it did not propagate significantly southwards, even though slip focussed at the southern end of the rupture. This observation strongly suggests a barrier at that place (Krüger and Ohrnberger, 2005). The physical properties of a barrier that so abruptly terminated the rupture of the enormous magnitude of the event in 2004 still remain obscure. The question of whether the surface manifestation of segmentation is also reflected in the structure of the subduction zone at depth is the key to the assessment of the potential for natural hazards in global fault systems and represents one of the aspects to be tackled by the SEACAUSE project.

Segmentation of the Sumatra-Andaman subduction zone is established from a considerable variation of age, dip angle and obliquity along strike of the margin (Lay et al., 2005; Kennett and Cummins, 2005). The rupture zone of the Sumatra-Andaman earthquake extends along a segment where tomographic imaging and historic seismicity indicate a significant change in the morphology of the subduction zone and also the physical properties of the subducted slab (Kennett and Cummins, 2005). The region around the epicenter is characterized by a subduction zone sector of shallow dip (7°-8° according to Lay et al., 2005), which becomes much steeper at depth (Kennett and Cummins, 2005). The hypocenter is located within the shallow dipping portion. Subduction becomes much steeper to the north, where it becomes almost vertical underneath the Andaman Islands (Kennett and Cummins, 2005). Details of subduction zone geometry remain obscure, though, due to lack of modern data.
Multiple studies using different geophysical data sets and methods have been conducted on the Sumatra-Andaman earthquake. One common feature is the division of the subduction zone into several segments (Figure 2.2.1.1). Ammon et al. (2005) and Lay et al. (2005) propose

changes in rupture and slip speed at points A and B depicted in Figure 2.2.1.1. Ishii et al. (2005) suggest drops in radiated energy near these points. The model of Stein and Okal (2005) as well as the geodetic solution by Khan and Gudmundsson (2005) require slip to extend over region 4 (right panel in Figure 2.2.1.1). Results of a multi-wavespeed seismic tomography (Kennett and Cummins, 2005) image changes in the physical properties at the top of the subducting plate below 50 km depth near point A (at 7°N) and point B (at 10°N). The reasons for segmentation and the nature of the barriers between the segments remain obscure. Abrupt changes of plate age corresponding to subduction zone segmentation are not known. Kennett and Cummins (2005) speculate on the influence of the passage of the Ninetyeast Ridge as it enters the trench in the northern segment. Due to lack of geophysical data, any detailed analysis is not possible. It is striking that the segment transitions lie at changes in the strike of the subduction zone where the subducted slab is required to accommodate the change in the geometry of subduction. Again, lack of modern data prohibits any interpretation of the effects of variations in subduction zone geometry, which may include features such as slab tears or slab deformation due to roll-back.

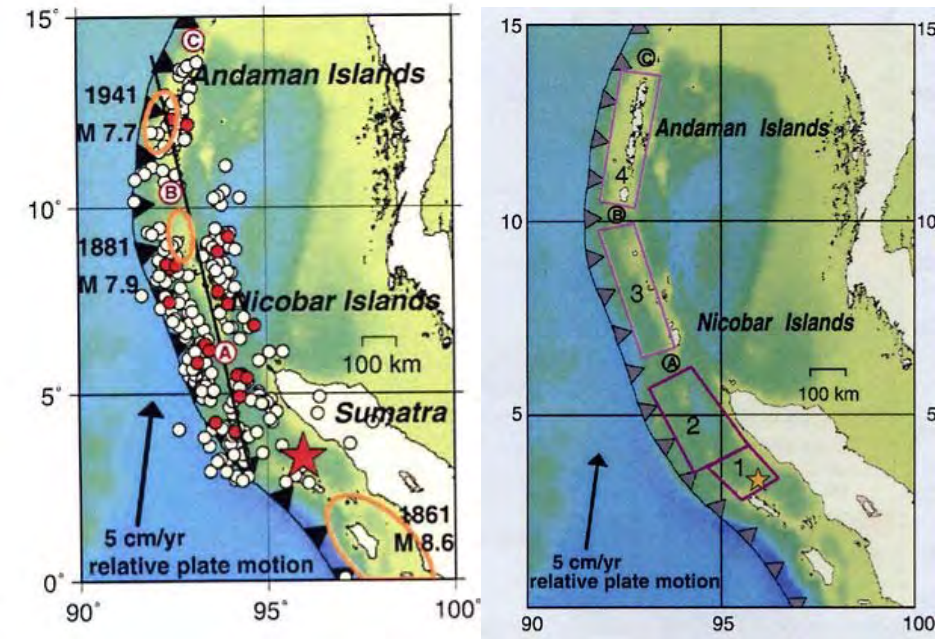

Figure 2.2.1.1: *Segmentation of the Sumatra-Andaman margin (from Kennett and Cummins, 2005). Left side shows the aftershock distribution in the 60 days after the Dec. 26, 2004 earthquake (aftershocks in the first 100 minutes shown as dark circles). Several studies imply segmentation into 4 different domains (right side). Point A corresponds to a temporary reduction in slip as suggested by Ishii et al. (2005). Point B marks the end of the main tsunamigenic segment as identified by Lay et al. (2005) and is the likely terminal point of the highest frequency radiation (Ammon et al., 2005; Ni et al., 2005). Point C indicates the northern segment required by geodetic observations (e.g. Khan and Gudmundsson, 2005) and normal-mode analysis (Stein and Okal, 2005).*

2.2.2 Rupture sequence of the 2004 Sumatra-Andaman earthquake

The Sumatra-Andaman earthquake ruptured with strong directionality, accumulating energy toward the northwest from the event epicenter (Park et al., 2005a). Analysis of surface waves and longer period body waves has shown that most of the slip concentrated in the southern half of the rupture zone, with diminishing, increasingly oblique slip toward the north of the fault (Figure 2.2.2.1) (Lay et al., 2005). Geodetic observations require approximately 10 m of

slip along the northern segment to account for tilting observed here. Vertical displacement exceeding 1 m is observed in the North Andaman Islands (Guilbert et al., 2005). The western margins of the Andaman and Nicobar Islands were uplifted while the eastern margins were submerged. This large-scale slip did not generate detectable seismic waves late in the rupture and must thus have a long source-process time of 1000 s and more (Lay et al., 2005). Analysis of amplitudes of hydroacoustic waves reported along the fault suggests that the northern area of the rupture did not radiate massive energy (Guilbert et al., 2005). Using spheroidal mode amplitudes, Park et al. (2005) postulate that the northern end of the rupture released one-third of the total energy of the earthquake, equivalent to a moment magnitude of 8.9.

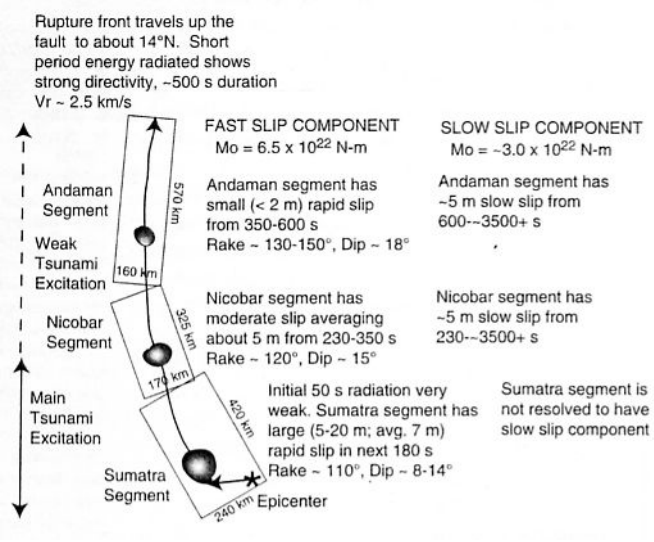

Figure 2.2.2.1: *Model of the rupture sequence for the 2004 Sumatra-Andaman earthquake (from Lay et al., 2005). The rupture zone is segmented into three sections according to the rupture process. Initial rupture started in the south with low energy release and slow rupture velocity. Rupture progressed to the north/northwest, extending about 1300 km. Rupture lasted for approximately 500 s. Large, rapid slip is observed in the Sumatra segment, diminishing northwards. The Sumatra segment roughly corresponds to segments 1 and 2 as shown in Figure 2.2.1.1.*

2.2.3 Slip distribution

The 2004 Sumatra-Andaman earthquake has been the focus of numerous analyses using different classes of geophysical data. While these studies provide many common features (e.g. rupture length and duration, unilateral rupture propagation), they differ in their interpretation of slip rate variation along the fault. Rupture progressed slowly (Ammon et al., 2005) or even stationary (Krüger and Ohrnberger, 2005) in the vicinity of the hypocenter with approximately 10 m of slip corresponding to reported uplift on Simeulue Island (Ammon et al., 2005). During the first minute after earthquake initiation approximately 100 km of the plate boundary ruptured northward (Bilham, 2005). Rapid slip at 3 km/s (Bilham, 2005) occurred for approximately 240 s in a northwestern direction along an area of 420 to 600 km length (Lay et al., 2005; Krüger and Ohrnberger, 2005). Large amounts of slip occurred off the west coast of northern Sumatra, reaching amplitudes of approximately 15 m (Ammon et al., 2005). Results by Ishii et al. (2005) based on observations of the Japanese Hi-Net seismic array imply a delayed energy maximum after 90 s and 300 s with an increased slip rate. Large slip, approaching 20 m, occurred in proximity to the Nicobar Islands (Ammon et al., 2005). Rupture then shifted direction to the north (Krüger and Ohrnberger, 2005). This northward rotation of rupture following the trench coincides with decreasing slip (Ammon et al., 2005). While Bilham (2005), Lay et al. (2005), and Ammon et al. (2005) support the slow-slip model for the northern segment of Stein and Okal (2005), results found by of Ishii et al. (2005), Ni et al. (2005), and Krüger and Ohrnberger (2005) contradict this model. The analysis of Stein and Okal (2005) is based on Earth's normal modes ${}_0S_2$, ${}_0S_3$ and ${}_0S_4$. These free oscillations, which are excited by great earthquakes, show discrete periods or eigenfrequencies, due to the rotation and ellipticity of the earth (Figure 2.2.3.1) (Park et al., 2005b). From the normal

modes Stein and Okal estimate a seismic moment magnitude of 9.3, which is about 2.5 times larger than initial reports suggested. This larger size is consistent with an average slip of 11 m (Stein and Okal, 2005) to 13 m (Sieh, 2005) along a 1200 km long rupture. They suggest that the larger moment reflects slow slip along the northern segment of the rupture that was not detected by using surface waves with periods below 300 s, which are commonly used for moment magnitude determination. While slip occurred at typical rupture speeds in the south (Bilham, 2005), the additional slow slip in the north arose over a time scale of 50 minutes or longer along the Nicobar and Andaman Islands sector of the rupture zone. Here, plate convergence is increasingly oblique, and slip is highly partitioned (Lay et al., 2005), which possibly contributed to the termination of rupture (Ammon et al., 2005). The slide of 7 to 20 m of this segment took more than half an hour (Bilham, 2005).

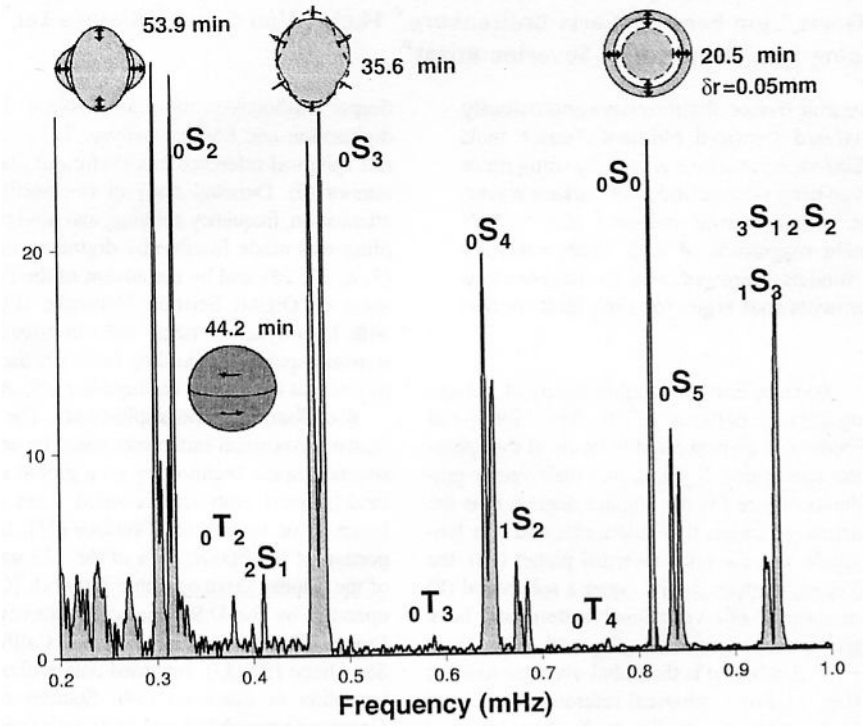

Figure 2.2.3.1: *Schematic of motion of free oscillations superimposed on a spectrum computed from 240 hours of vertical seismic motions recorded at an Australian Geoscope Network station (from Park et al., 2005b).*

Results obtained by most authors imply that the fault was well-coupled in the south in the vicinity of the epicenter, with interplate coupling steadily decreasing northwards. This decrease may be associated to an increase in dip angle, plate age and motion obliquity towards the Andaman Sea, although details in plate geometry are still not resolved.

2.3 Earthquake risk from co-seismic stress variation

As the entire ~1300 km rupture zone beneath the Burma microplate has slipped during the 2004 event, the strain accumulated along this subduction zone segment has been released, and there is no immediate danger of a similar earthquake or tsunami in this area as such earthquakes normally occur at least 400 years apart. Earthquake risk assessment thus focuses on the segments of the Sumatra megathrust located south of the 2004 earthquake. The boundary of the aftershock distribution of the event on Dec. 26, 2004, is very sharp to the south. As McCloskey et al. (2005) recognized correctly from the calculation of co-seismic stress distribution, the event in 2004 increased seismic hazard to the south, where it eventually

triggered the earthquake with a magnitude (Mw) of 8.7 on March 28, 2005. Megathrust earthquakes often occur in clusters on adjacent segments (e.g. Nankai trough subduction zone: five of the seven large earthquakes on the Nankaido segment were accompanied by similar events on the contiguous Tonankai/Tokai segment; the Izmit earthquake (Mw=7.4) followed earlier local events and subsequently triggered the Düzce earthquake (Mw=7.1)). Sieh (2005), McCloskey et al. (2005) and Nalbant et al. (2005) infer an increased risk of failure for the northern Sumatra strike-slip fault, which has been dormant in this area for ~100 years. An earthquake of magnitude (Mw) 7.0-7.5 is proposed to represent the most immediate threat.

The Nias earthquake has appreciably altered the state of stress in the vicinity of the hypocenter, and has increased stress on the Sumatra fault and the megathrust to the south (Figure 2.3.1). The earthquake of March 28, 2005 has brought closer to failure the megathrust immediately to the south, under the Batu and Mentawai islands from 0.7°S to 5.5°S. Palaeoseismic studies show that the seismic cycle of the Mentawai segment of the Sunda megathrust is well advanced, increasing the risk of triggered failure (Nalbant et al., 2005). This stress may be expected to migrate further south over time as a result of viscoelastic relaxation in the lower crust (McCloskey et al., 2005).

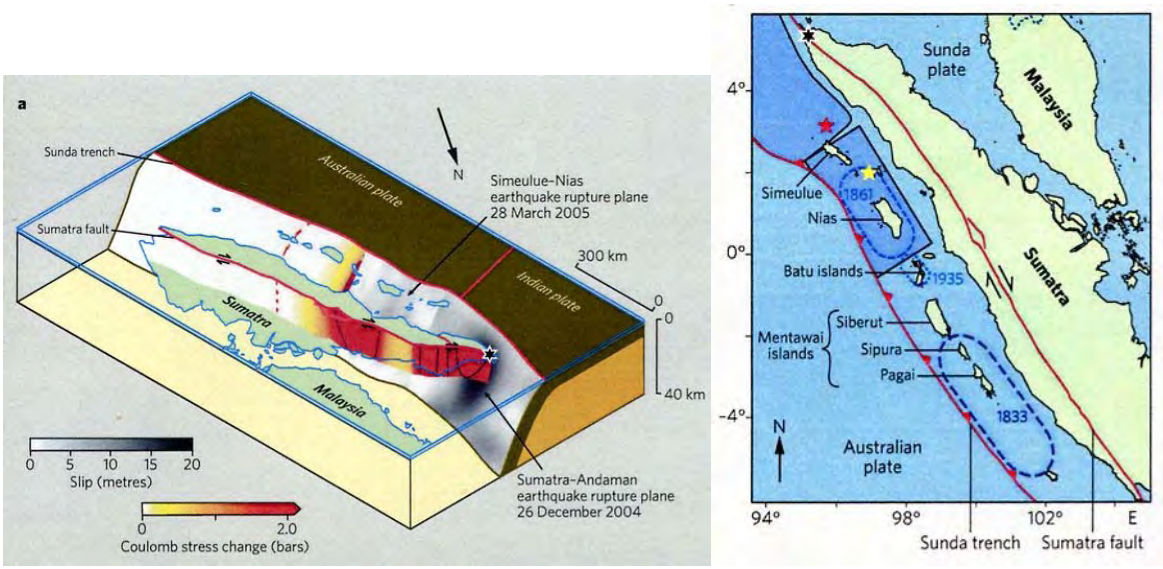

Figure 2.3.1: *Co-seismic stress changes generated by the events in 2004 and 2005 are projected onto the Sumatra Fault and the Sumatra-Andaman megathrust (figure to the left). The figure to the right displays rupture locations of recent and historic events (from Nalbant et al., 2005).*

The megathrust under the island of Siberut has not ruptured since 1797, when it slipped a few meters (Mw>8). An earthquake of magnitude (Mw) 8.5 in 1833 (with a presumed recurrence of 230 years as inferred from palaeoseismic studies) resulted in a megathrust rupture of 10 m. Both of these events caused large tsunamis running towards the islands and the mainland coast (Nalbant et al., 2005).

2.4 The 2004 Indian Ocean tsunami

The earthquake on Dec. 26, 2004, generated a destructive tsunami. It hit the shore of northern Sumatra with 10 m amplitude and expanded across the Indian Ocean, striking the coastlines of bordering nations within a few hours after the rupture. Its maximum strengths expanded perpendicular to the Sumatra trench (Yuan et al., 2005). The death toll reached 283 000 confirmed casualties, making this earthquake one of the most devastating natural disasters in human history (Park et al, 2005a). Tsunami waves propagate as solitons or nonlinear solitary waves, over distances of thousands of kilometers with a wavelength largely exceeding water depth (Lomnitz and Nielsen-Hofseth, 2005). A period of 200-2000 s and a speed of 150-250 m/s are common in open water (Yuan et al., 2005). Tide gauge stations located at shorelines and ocean bottom pressure gauges allow a direct monitoring of tsunamis (Yuan et al., 2005), whereas satellite altimetry observations are only relevant if the satellite directly passes the propagating tsunami (Gower, 2005). Altimetry measurements of the 2004 tsunami were acquired by the Jason-1 and Topex/Poseidon satellites as they transited the Indian Ocean about 150 km apart ~2 hours after the earthquake (Figure 2.4.1) (Fine et al., 2005). The tsunami was also detected seismically by Yuan et al. (2005), who infer an average speed of approximately 200 m/s for water depth of 4-5 km from the observed arrival times. The seismic signals closely match signals from tide gauge stations on nearby islands (Figure 2.4.1).

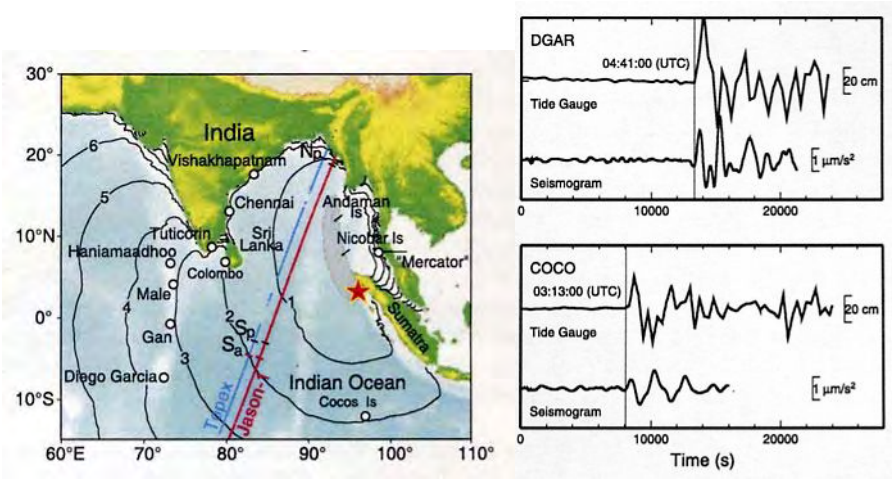

Figure 2.4.1: *Map of tide gauge stations in the Indian Ocean. Straight lines mark the tracks of the Topex/Poseidon and Jason-1 satellites that passed over the area approximately 2 hours after the Dec. 26, 2004 earthquake. Hourly isochrones of tsunami travel time are displayed (from Fine et al., 2005). The right side shows a comparison of acceleration seismograms of the 2004 earthquake with tide gauge data (DGAR=Diego Garcia; COCO=Cocos Islands; see left for location). Time axis origin corresponds to earthquake initiation (from Yuan et al., 2005).*

About 86% of all tsunamis are caused by earthquake processes, which lead to a massive displacement of seawater. The remaining events are generated by volcanic eruptions, submarine landslides, or extraterrestrial impact. An alternative process for the generation of the tsunami was proposed by Lomnitz and Nielsen-Hofseth (2005), who link the tsunami to Earth's normal modes. They propose that the vertical components of low-order spheroidal modes such as ${}_0S_2$, ${}_0S_3$ and ${}_0S_4$ (Figure 2.4.2) may have excited a waveguide in the ocean, which at least partially may have caused the tsunami. This physical mechanisms associated with waveguide propagation would explain the low dissipation and the directionality of tsunamis (Lomnitz and Nielsen-Hofseth, 2005).

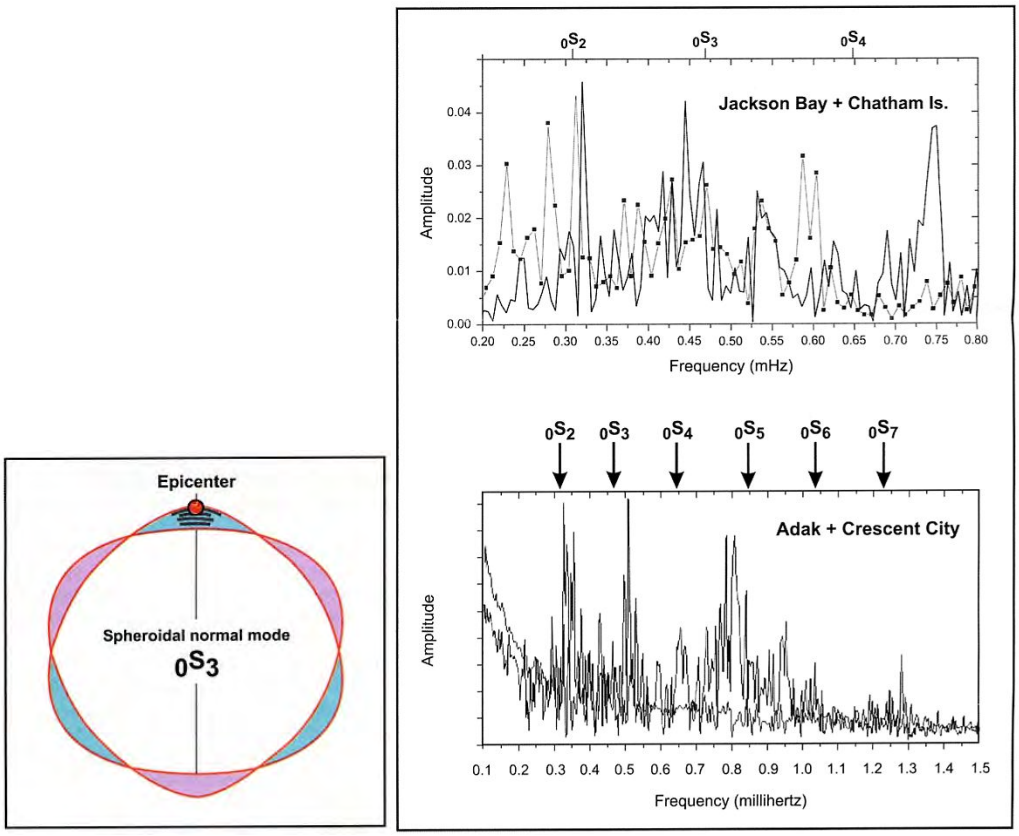

Figure 2.4.2: *Spheroidal normal mode $_0S_3$ shown to the left with greatly exaggerated amplitudes (from Lomnitz and Nilsen-Hofseth, 2005). To the right: Fourier amplitude spectra of tide gauge records of the 2004 tsunami recorded in New Zealand (top) and Alaska/California (bottom) (from Lomnitz and Nilsen-Hofseth, 2005).*

There are three prerequisites for an earthquake-generated tsunami:

- The earthquake's moment magnitude must exceed 7.0.
- The hypocenter must be located shallowly underneath the seafloor.
- Extensive vertical motion must lead to an offset in the seafloor causing substantial displacement of the water column.

The necessary vertical motion of the seafloor may be caused by two processes:

- Thrusting: The vertical motion trends along a rupture zone. The seafloor is offset along a zone of weakness (commonly a normal or thrust fault).
- 'Tensional buckling': accumulation of elastic stress in the upper plate causes flexure due to coupling of the forearc with the downgoing oceanic plate. During an earthquake the forearc will be decoupled along a thrust fault and stresses will be released. This causes large-scale uplift and subsidence, which may trigger a tsunami.

One of the most imminent questions regarding the generation of the tsunami involves the actual amplitude of the surface motions that triggered it (Khan and Gudmundsson, 2005). The Indian Ocean tsunami is attributed to an impulsive upheaval of the ocean floor by up to 10 m (Lomnitz and Nielsen-Hofseth, 2005). Another aspect concerns the displacement pattern in the affected area. These questions may be addressed e.g. by direct measurements of deformation (Khan and Gudmundsson, 2005) using continuous Global Positioning System (GPS) observations in the vicinity of the earthquake. For the event in 2004 the location of coupling between the fault plane and the water column, where the tsunami was generated, could not be definitely determined. Vertical motion is documented to have occurred in

northern Sumatra (subsidence in Aceh) and on the forearc islands. There is evidence of an uplift of ~1 m on Simeulue (Sieh, 2005). These observations correlate to the amplitude values of the tsunami gained from back-propagation of the initial tsunami wavefront: first recorded waves on tide gauge sites in India, Sri Lanka and the Maledives were positive (crests) due to uplift on the western side of the source area, whereas the eastern sites in Thailand and Indonesia recorded troughs caused by subsidence east of the source area (Fine et al., 2005). Sabadini et al. (2005) propose these differential vertical motions with an almost instantaneous occurrence of uplift and subsidence with an offset of ~6 m as the cause for the tsunami ('tensional buckling'). In contrast to the documented vertical displacements on the forearc islands and on northern Sumatra, GPS analyses by Khan and Gudmundsson (2005) do not reveal any vertical displacement. Khan and Gudmundsson (2005) employed four GPS stations: data for these sites are available at http://sopac.ucsd.edu/dataArchive. Site SAMP, which is located about 330 km west of the Dec. 26, 2004 earthquake on northern Sumatra, recorded north, east, and vertical displacements of –12.1±1.8, -145.2±3.2, and 6.1±7.7 mm, respectively. No vertical component was resolved as SAMP moved westward during the earthquake (W5°S) (Khan and Gudmundsson, 2005). Figure 2.4.3 shows averages for the north, east, and vertical displacements for station SAMP. The surface displacements caused by the earthquake are manifested in the offset, which separates the pre-event and post-event solutions (Khan and Gudmundsson, 2005). As the observed vertical motion was not detected by the GPS measurements of site SAMP, despite its resolution in the millimeter range, the overlying plate must have been decoupled along a north-south trending lineament. The most plausible location for the decoupling may be the Mentawai or Sumatra fault systems, which would also mark the landward extent of the rupture zone.

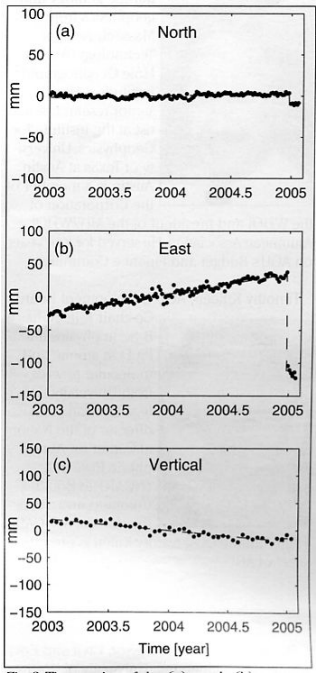

Figure 2.4.3: *Time series of the north, east, and vertical displacements (from Khan and Gudmundsson, 2005) of a GPS site located in northern Sumatra. The north and east displacements are averages over 5 days, the vertical displacement is averaged over 15 days. The dashed line is the best fitting linear term plus an offset introduced on Dec. 26, 2004.*

2.4.1 Source region of the 2004 tsunami

Fine et al. (2005) propose a dual source region for the tsunami associated with the southern fast-slip and northern slow-slip domains. Based on wave arrival times from coastal tide gauges and satellite altimetry records, they define an overall 250 km wide, 1000 km long tsunami source region, which coincides with the aftershock distribution. Inverse-wave tracing reveals a dual-source region: the southern source coincides with the fast-slip area of Stein and Okal (2005). According to Fine et al. (2005), this zone generated the destructive tsunami waves that hit the coasts of Sir Lanka, the Maledives and East and South Africa before propagating globally. The southern source region extends from about 600-650 km to the north of the mainshock epicenter (Fine et al., 2005). The northern source region, which coincides with the slow slip region of Stein and Okal (2005) immediately south of the Andaman Islands, produced the weaker waves that struck the coasts of Bangladesh, Myanmar, and eastern India. Using back-projection of tsunami waves, Lay et al. (2005) postulate a source region extending 600-800 km north of the 2004 epicenter, terminating near the Nicobar Islands. Bilham (2005) places the source region along the

southern 650 km of the 2004 earthquake, arguing that slip was too slow in the northern region to generate tsunami waves.

2.5 Seismic history of the Sumatra-Andaman margin

Historic records show a sequence of great earthquakes clustered in the interval from 1797 to 1861 (e.g. Newcomb and McCann, 1987). The event in 1861 with Mw~8.5 (Lay et al., 2005) overlaps the rupture area of the year 2005. Another event in 1907 with a magnitude (Mw) of ~7.8 (Lay et al., 2005) occurred just south of the rupture zone of 2004, thus overlapping the rupture area of 2005, and produced seismic and tsunami damage in northern Sumatra. Two large earthquakes occurred in the same sector of the megathrust south of the epicenter of 2005 in 1797 (Mw >8, (Nalbant et al., 2005), Mw=8.4 (Lay et al., 2005)) and in 1833 (Mw=8.5 (Nalbant et al., 2005), Mw~9 (Lay et al., 2005)). Stress transfer onto this region has brought it closer to failure (Nalbant et al., 2005). Repeat times of earthquakes on segments of the Sumatra megathrust are presumed to average ~150-500 years, however, deviations from this average are evident from recent events (2004/2005 couplet; 1797 and 1833 sequence). Seismicity in the Andaman trench includes a Mw~7.9 event beneath the Nicobar Islands in 1881 and a Mw~7.9 event near the Andaman Islands in 1941. The sector between the Nicobar Islands and northern Sumatra between the epicenters in 1881 and 2004 experienced little seismic activity in the past 40 years. A number of earthquakes occurred near the 2004 epicenter in the past decade, e.g. Mw=7.2 in 2002 (Lay et al., 2005). Seismicity was also low in the Nias segment before the 2005 rupture and still does not show much activity in the Mentawai segment to the south. This behavior is associated with long-term strain accumulation in the eventual rupture area and a stress focus in the area of the mainshock hypocenter (Lay et al., 2005).

2.6 Comparison to the earthquakes with magnitude (Mw) 9.5 / Chile (1960) and (Mw) 9.2 /Alaska (1964)

The moment magnitude of an earthquake is commonly gained from measurements of long-period surface waves (100-300 s for very large earthquakes; around 300 s for the Chile, Alaska and Sumatra-Andaman events). This allows direct comparison of different earthquakes and places the Sumatra-Andaman earthquakes as the second-largest recorded with seismic instrumentation. Though the aftershock areas of the two other largest earthquakes are comparable in size, the rupture length of the Sumatra-Andaman event (an estimated maximum of 1300 km) is the longest (Figure 2.6.1). This is consistent with rupture duration (estimated 500 s for Sumatra). Average durations for the Chile and Alaska earthquakes were ~345 s and ~340 s, respectively (Ishii et al., 2005). A common feature of all three earthquakes is the unilateral rupture propagation. Chile broke at ~3.5 km/s, Alaska at 3.0 km/s and Sumatra-Andaman at an average speed of 2.8 km/s. While the Chile event shows the largest slip area (followed by the Sumatra-Andaman earthquake), the 2004 earthquake exceeds all other recorded earthquakes in rupture length and duration (Ishii et al., 2005).

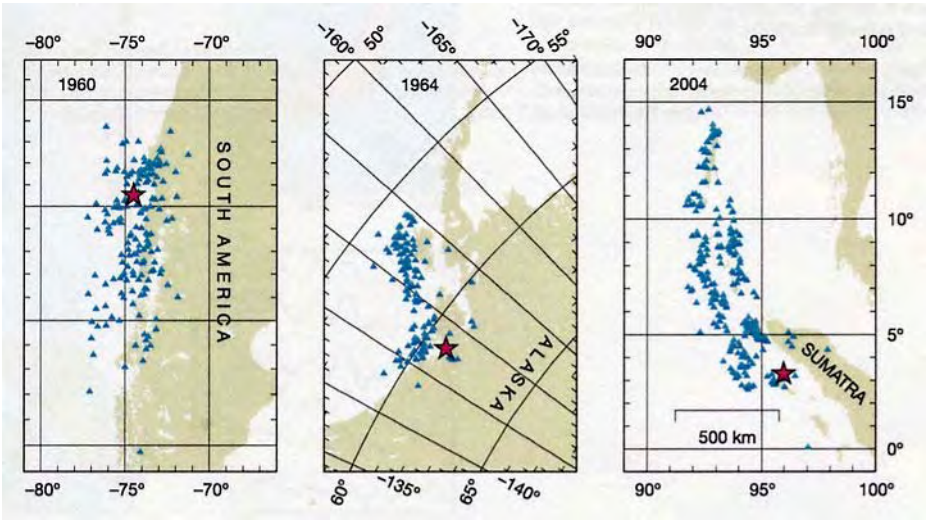

Figure 2.6.1: *Comparison of aftershock areas of the 1960 Chile earthquake, 1964 Alaska earthquake and the 2004 Sumatra-Andaman earthquake (modified from Ishii et al., 2005). Triangles denote aftershock distribution for the first month following the event, stars mark epicenter locations. The Sumatra-Andaman earthquake caused the largest aftershock zone. Slip region is greatest for the Chile event.*

3. Participants

3.1 Scientists - SO 186 Leg 3

Prof. Dr. Ernst R. Flueh	**IFM-GEOMAR, Chief Scientist**
John Armitage	NOC
Thomas Behrens	BGR
Wiebke Brunn	IFM-GEOMAR
Anke Dannowski	IFM-GEOMAR
Dr. Dieter Franke	BGR
PD Dr. Ingo Grevemeyer	IFM-GEOMAR
Claudia Hagen	CAU
Katja Iwanowski	CAU
Claudia Jung	CAU
Stefanie Kessling	FSU
Dr. Anne Krabbenhoeft	IFM-GEOMAR
Dr. Cord Papenberg	IFM-GEOMAR
Anne-Doerte Rohde	CAU
Achim Sievers	BGR
Klaus-Peter Steffen	IFM-GEOMAR
Wiebke Suhr	CAU
Eike Surburg	BGR
Dr. Matthias Zillmer	IFM-GEOMAR
Yudi Anantasena	BPPT
Dayuf Yusuf	BPPT
Rahardian	BPPT
Purwito	Indonesian Navy

3.2 Crew - SO 186 Leg 3

Oliver Meyer	Master
Detlef Korte	Chief Mate
Nils Aden	1st Mate
Matthias Linnenbecker	2nd Mate
Dr. Mathias Graessle	Surgeon
Werner Guzmann-Navarrete	Chief Engineer
Andreas Rex	2nd Engineer
Klaus-Dieter Klinder	2nd Engineer
Uwe Rieper	Electrician
Joeg Leppin	Chief Electrician
Matthias Grossmann	System Operator
Andreas Ehmer	System Operator
Holger Zeitz	Motorman
Volker Blohm	Motorman
Przem Marcinkowski	Motorman
Frank Tiemann	Chief Cook
Ryszard Kornaga	Cook
Gerlinde Gruebe	Chief Steward
Ryszard Kuzon	2nd Steward
Peter Mucke	Bosum
Winfried Jahns	A. B.
Torsten Bierstedt	A. B.
Juergen Kraft	A. B.
Nicki Meyer	A. B.
Hans-Juergen Vor	A. B.
Tino Foerster	Apprentice
Robert Noack	Apprentice
Tim Stegemann	Apprentice

3.3 Addresses of Participating Institutions

IFM-GEOMAR: Leibniz-Institut für Meeresforschung
der Christian-Albrechts-Universität zu Kiel
Wischhofstr. 1-3
24148 Kiel
Germany
Tel.: +49 - 431 - 600 - 2972
Fax: +49 - 431 - 600 - 2922
e-Mail: Iname@ifm-geomar.de
Internet: www.ifm-geomar.de

BGR: Bundesanstalt für Geowissenschaften und Rohstoffe
Dienstgebäude Alfred-Bentz-Haus
Stilleweg 2
30655 Hannover
Germany
Tel.: +49 – 0511 – 643 – 0
Fax: +49 – 0511 – 643 – 2304
e-mail: info@bgr.de
Internet: www.bgr.de

CAU: Christian-Albrechts-Universität zu Kiel
Olshausenstr. 98
24118 Kiel
Germany
Tel.: +49 - 431 - 880 – 3900
Fax: +49 - 431 - 880 – 4432
e-Mail: Iname@geophysik.uni-kiel.de
Internet: http://www.geophysik.uni-kiel.de/phpwebsite/index.php

FSU: Friedrich-Schiller-Universität Jena
Institut für Geowissenschaften
Burgweg 11
07749 Jena
Germany
Tel.: +49 - 3641 - 948601
Fax: +49 - 3641 – 948602
e-Mail: Iname@uni-jena.de
Internet: http://www.igw.uni-jena.de/start.html

NOC: National Oceanography Centre
University of Southampton
European Way
Southampton
SO14 3Z
England
e-Mail: j.armitage@noc.soton.ac.uk
Internet: http://www.noc.soton.ac.uk/

BPPT: **BPP Teknologi, Agency for the Assessment & Application of Technology**

Building 2, 19th Floor.
Jalan M.H. Thamrin 8
Jakarta 10340
Indonesia
Tel.: +62 - 21 - 3169706
Fax.: +62 - 21 - 3169720
e-mail: iyung@ceo.bppt.go.id, iyung24@yahoo.com
Internet: www.bppt.go.id

TNI-AL: Dinas Hidro Oseanografi – TNI AL (Indonesian Navy)
Jl. Pantai Kuta V/1, Ancol Timur,
Jakarta 14430
Tel.: +62 – 21 – 64714810 ext 3924, 3925
Fax: +62 – 21 – 64714819
e-mail: Infohid @ indo.net.id
Internet: www.dishidros.or.id

Fig. 3.1.1.1: *Participants of cruise SO186 Leg 3, Penang-Singapore.*

4. Agenda of cruise SO186-3

Cruise SO 186 Leg 3 "SEACAUSE II" started on February 26, 2006, in Penang, Malaysia, where we left the pier at 15:00 local time. Altogether 23 scientists embarked on RV SONNE in Penang, comprising the international group of scientists from Indonesia, Great Britain and Germany. As this cruise is a continuation of previous surveys conducted along the Sumatra margin, most of the scientific equipment was already set up and nearly no preparatory work was necessary in port. When we reached Indonesian waters the Simrad system was activated and was in continuous operation throughout the cruise.
After nearly two days of transit we reached our working area, where at first a seismological network – deployed during October to January - had to be recovered. Six instruments were left and 27 were additionally deployed along a 150 nm Profile from the trench to the coast of Sumatra. This work was completed by 05:30 on 03 March and we started to shoot along the profile (SO186-3-1) at a ship speed of 4 kn and with a trigger interval of 60 s. During the previous leg MCS data had already been collected along this line (BGR06-Line 135). Shooting terminated at 16:30 on 04 March, and subsequently the remaining 34 instruments were recovered by 21:30 on 05 March.
SONNE then headed towards the test buoy of the GITEWS-system and recovered the Bottom Station and an additional OBS. A close inspection of the buoy showed no sign of piracy, little physical damage and little fouling. The bottom station was redeployed after data had been downloaded.

At 05:00 on 07 March SONNE reached the area off Simeulue Island again, and 23 bottom instruments were deployed for a detailed investigation of the decollement. The location had been identified from previous bathymetric and multichannel seismic data. Instruments were spaced at only 0.1 nautical miles, making the deployment process a challenge as to instrument preparation and ship speed. Indeed, on average one instrument was deployed every three minutes. Four parallel profiles of about 20 nm each were shot along this array, using different trigger intervals (40 and 60 s) and different airgun configurations (one or two arrays). All instruments were recovered by midday 08 March.
After a 150 nm transit all 23 instruments were deployed again in a similar fashion in an area that broke during the 26 December 2004 event. Here at first six profiles, 20 nm long, were shot parallel to the trench with a spacing of 0.2 nm between the profiles. Both airgun arrays were used and the trigger interval was set to 30 sec. Thus, at the ship speed given, this resulted in a shot spacing of 30 m. Eleven of these instruments were recovered at 10.03 in the morning and subsequently redeployed perpendicular to the previous line, coincident with the MCS line BGR06-109. Subsequently another six profiles were shot, using the same parameters as before. All instruments were recovered during the evening of 11.03, and our transit to Singapore started. Simrad was turned off on 13.03 at 04:00 and this terminated the scientific mission. SONNE reached the pilot station in Singapore at 08:00 on 15 March and berthed at 10:30.

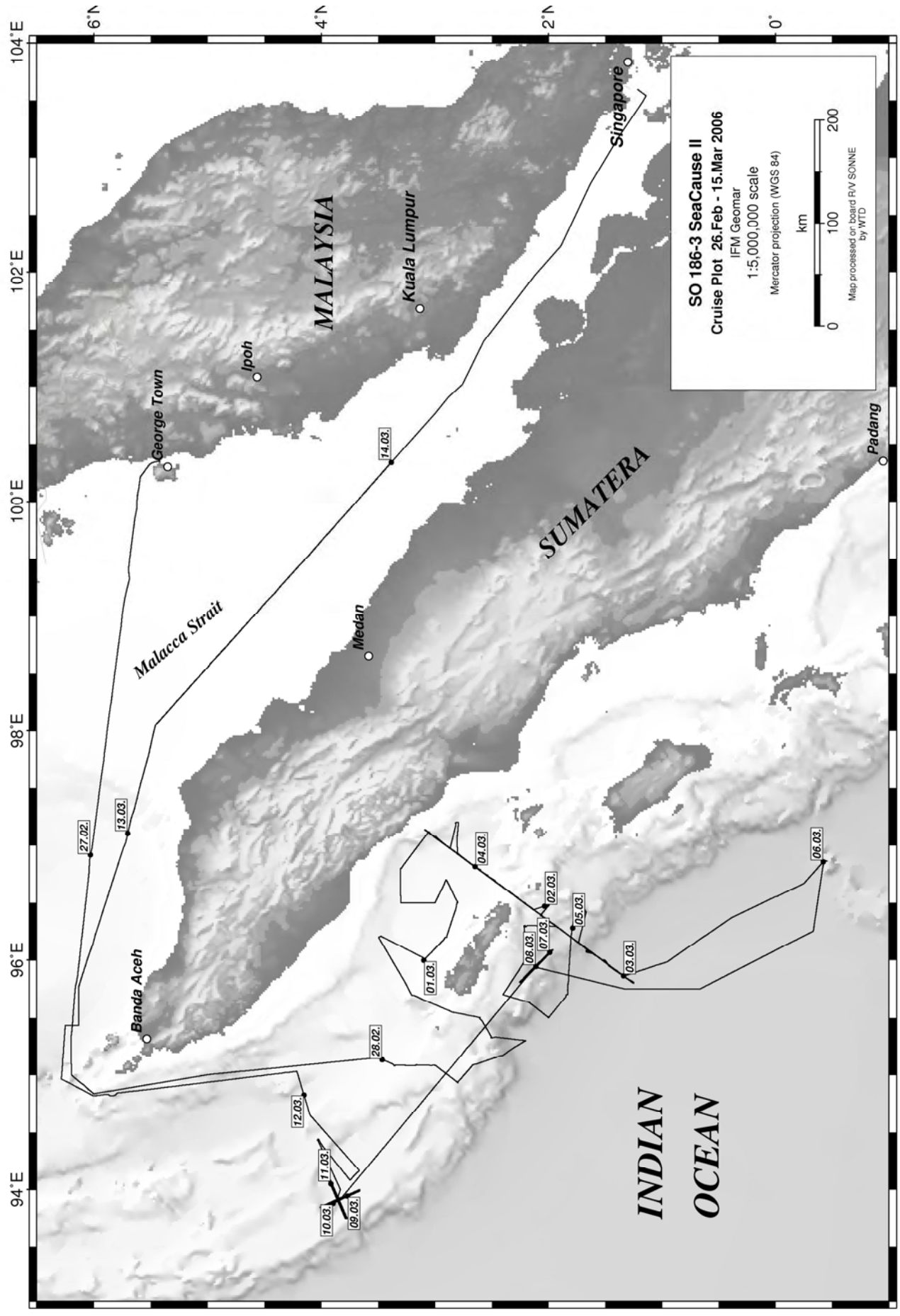

Figure 4.1: Track chart of cruise SO186 Leg 3

5. Scientific equipment
5.1 Shipboard equipment
5.1.1 Navigation

A precise knowledge of position information (latitude, longitude, altitude above/below a reference level) is a crucial prerequisite for all kinds of marine surveys. Since 1993 the global positioning system (GPS) has been commercially available and widely used for marine surveys. It operates 24 satellites in synchronous orbits, thus at least 3 satellites are visible anywhere at any moment (Seeber, 1996). The full precision of this originally military service yields positioning accuracies of a few meters. In the past the usage of the system was restricted to military forces and inaccessible to commercial users (Blondel and Murton, 1997). Since about the year 2000 the full resolution has been generally available (with an accuracy in the order of 15 m). During this cruise the operation of the differential (DGPS) option was not requested as standard precision coordinates are precise enough for seismological monitoring stations.

GPS-values as well as most other cruise parameters are continuously stored in the navigation database, and are distributed via the DVS ("data distribution system") on the ship's network.

5.1.2 Simrad EM120 swathmapping bathymetry system

The EM120 system is a multibeam echosounder (with 191 beams) providing accurate bathymetric mapping of areas at depths down to 11000 m. This system is composed of two transducer arrays fixed to the ship's hull, and it sends successive frequency-coded acoustic signals (11.25 to 12.6 kHz). Data acquisition is based on successive emission-reception cycles of this signal. The emission beam is 150° wide across track and 2° wide along track direction (Figure 5.1.2.1). The reception is obtained from 191 overlapping beams, with widths of 2° across track and 20° along it (Figure 5.1.2.1). The beam spacing can be defined as equidistant or equiangular, with the maximum seafloor coverage fixed or not fixed. The echoes from the intersection area between transmission and reception patterns (Figure 5.1.2.1) produce a signal from which depth and reflectivity are extracted.

For depth measurements, 191 isolated depth values are obtained perpendicular to the track for each signal. Depth is estimated for each beam by using the 2-way travel-time and the beam angle known for each beam, and by taking into account ray bending due to refraction in the water column by sound speed variations. A combination of phase (for the central beams) and amplitude (lateral beams) is used to provide a measurement accuracy practically independent of the beam pointing angle. The raw depth data need then to be processed to obtain depth-contour maps. In the first step, the data are merged with navigation files to compute their geographic position, and the depth values are plotted on a regular grid to obtain a digital terrain model (*DTM)*. In the last stage, the grid is interpolated, and finally smoothed to obtain a better graphic representation.

Together with depth measurement data, the acoustic signal is sampled each 3.2 ms and processed to obtain a cartographic representation, commonly named mosaic, where grey levels are representative of backscatter amplitudes. These data provide information on the sea-floor's nature and texture: a smooth and soft seabed will backscatter little energy, whereas a rough and hard relief will return a strong echo.

The EM120 was used continuously during cruise 186 Leg 3. Bathymetric data were processed routinely onboard during the survey by using the NEPTUNE software from Simrad and the

academic software MB-System from Lamont-Doherty Earth Observatory. Subsequently, data collected during SO186 were merged with data collected during the previous legs, and maps were generated which are shown in Figures 5.1.2.2 and 5.1.2.3.

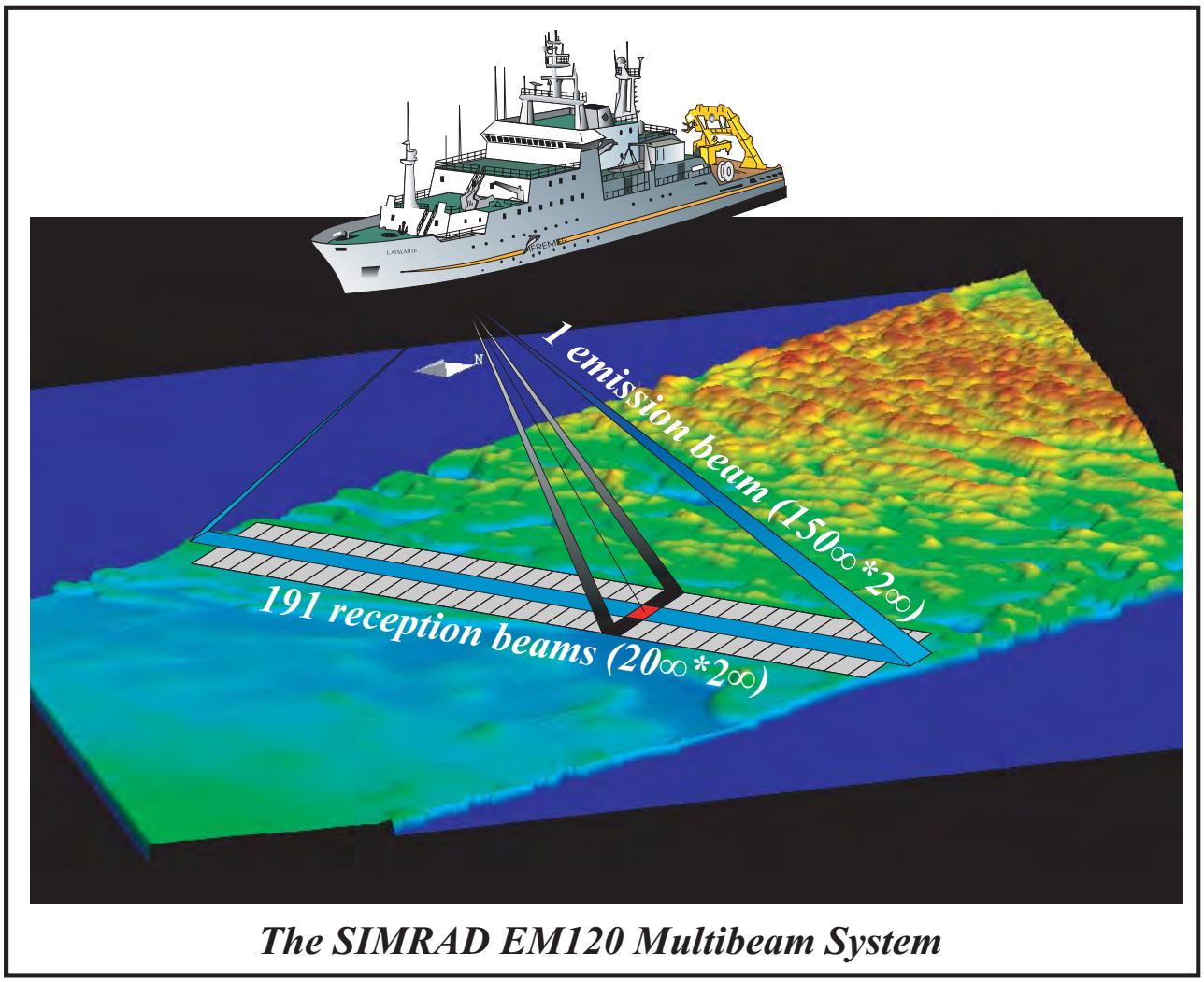

Figure 5.1.2.1: *Acquisition method for bathymetric and backscatter data from the Simrad EM120 system (crossed beams technique).*

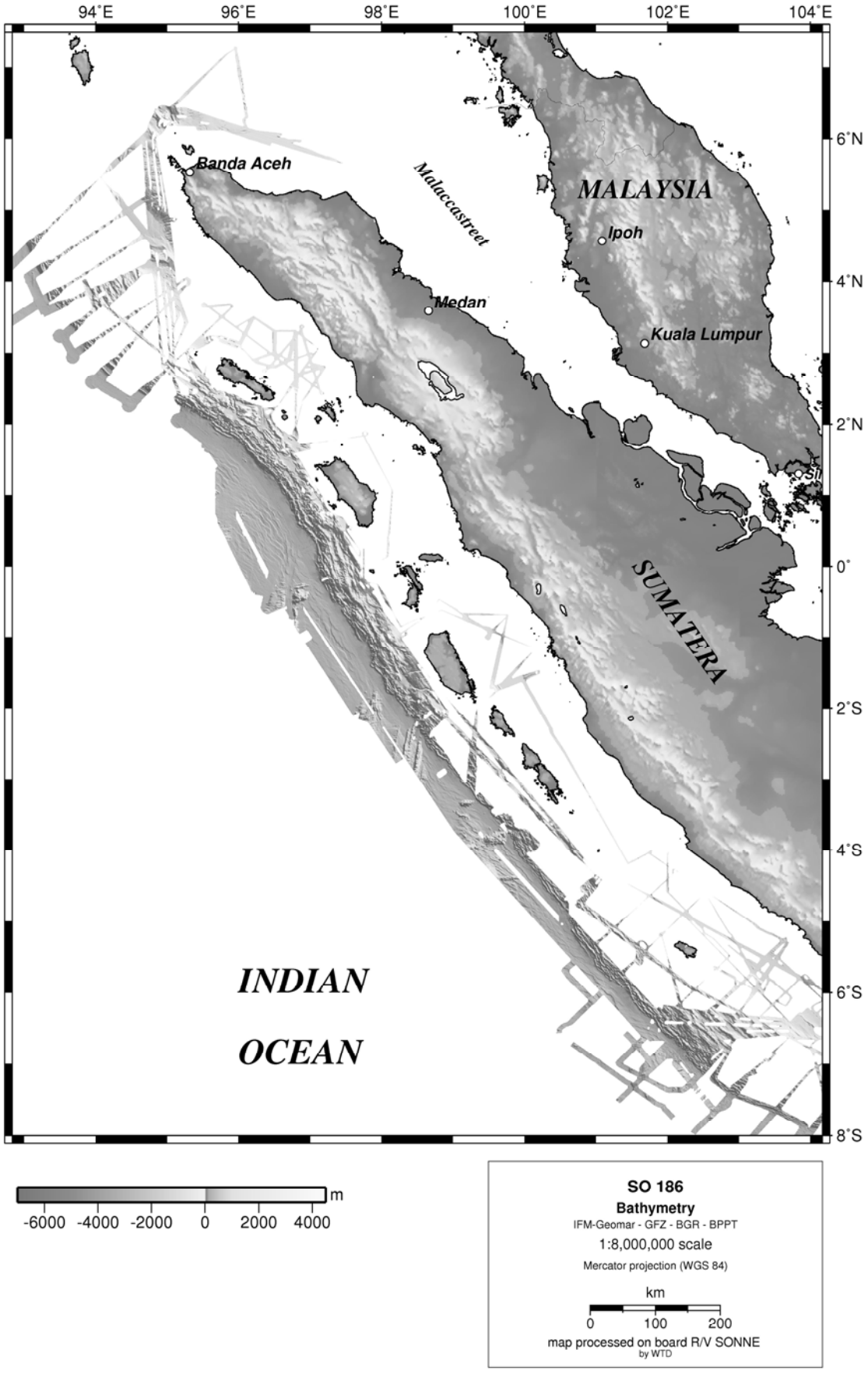

***Figure 5.1.2.2**: Swath bathymetric survey conducted offshore Sumatra.*

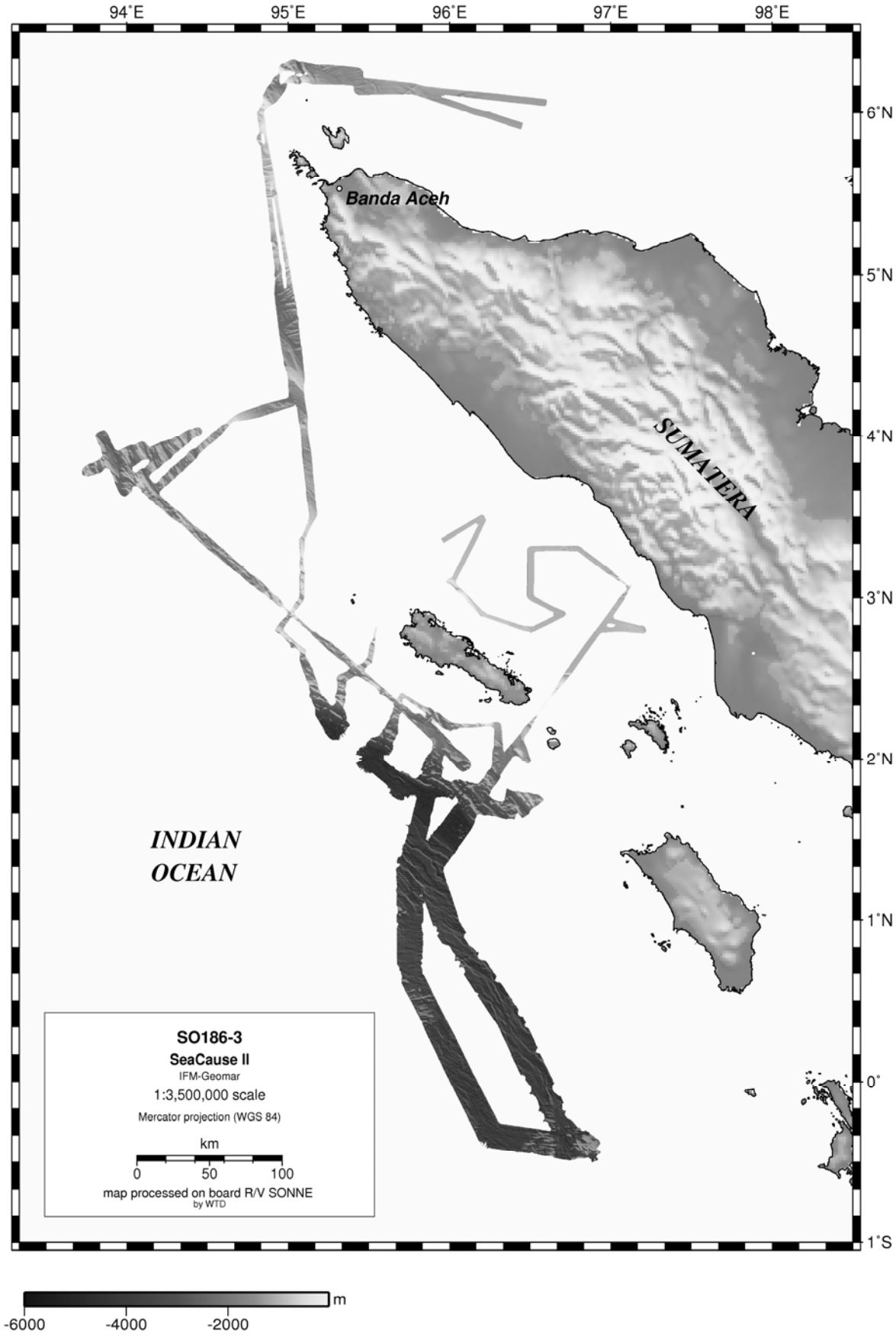

Figure 5.1.2.3: *Shaded bathymetry relief of the study area.*

5.1.3 CTD data

The CTD rosette onboard RV SONNE was deployed during cruise SO186 to measure physical oceanographic parameters (Figure 5.1.3.1.). The CTD station was run to a water depth of 1800 m at a velocity of 1 m/s measuring the sound speed in-situ continuously. The sound velocity profile is shown in Figure 5.1.3.2.

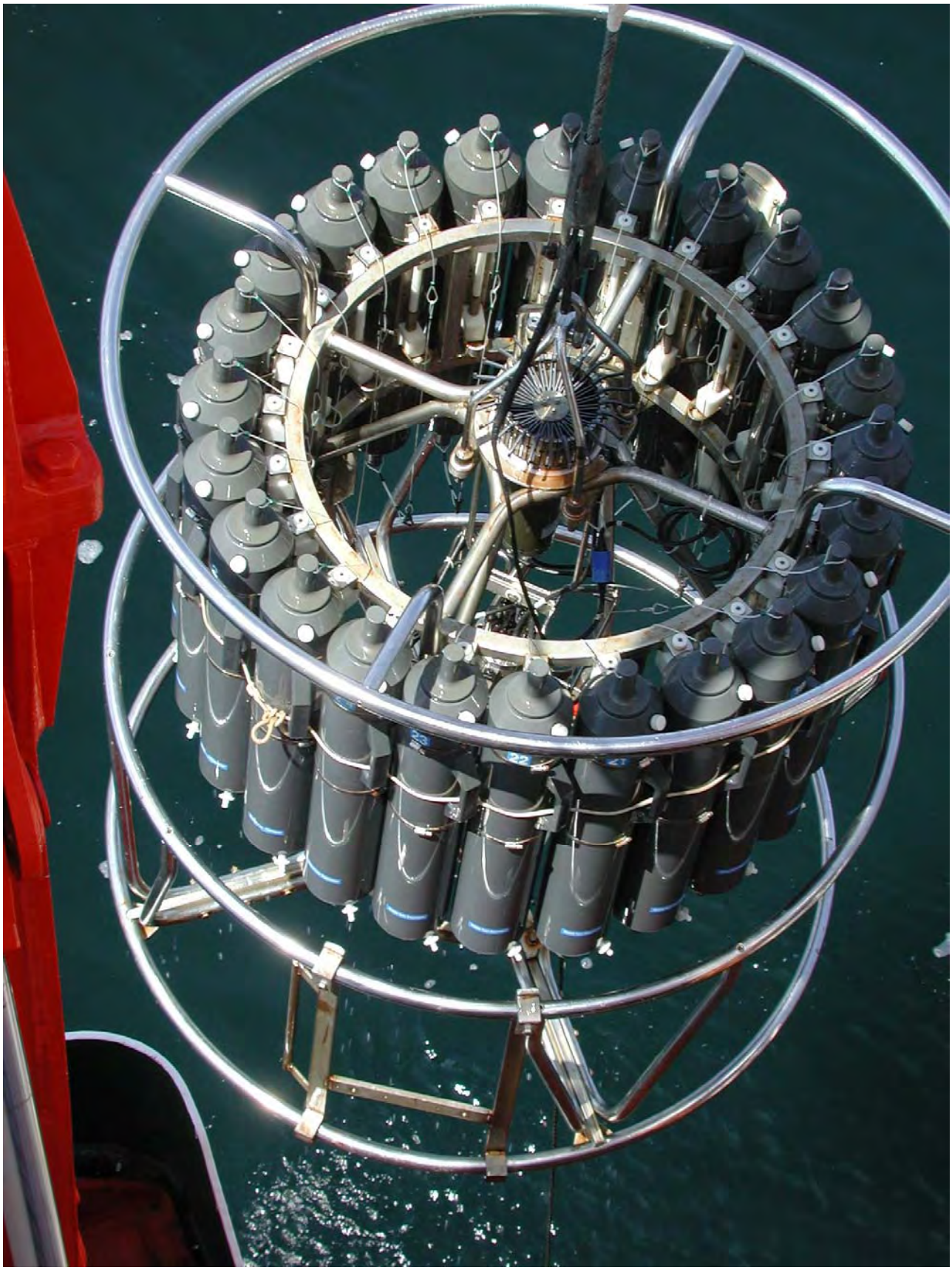

Figure 5.1.3.1: *RV SONNE's onboard CTD rosette upon deployment.*

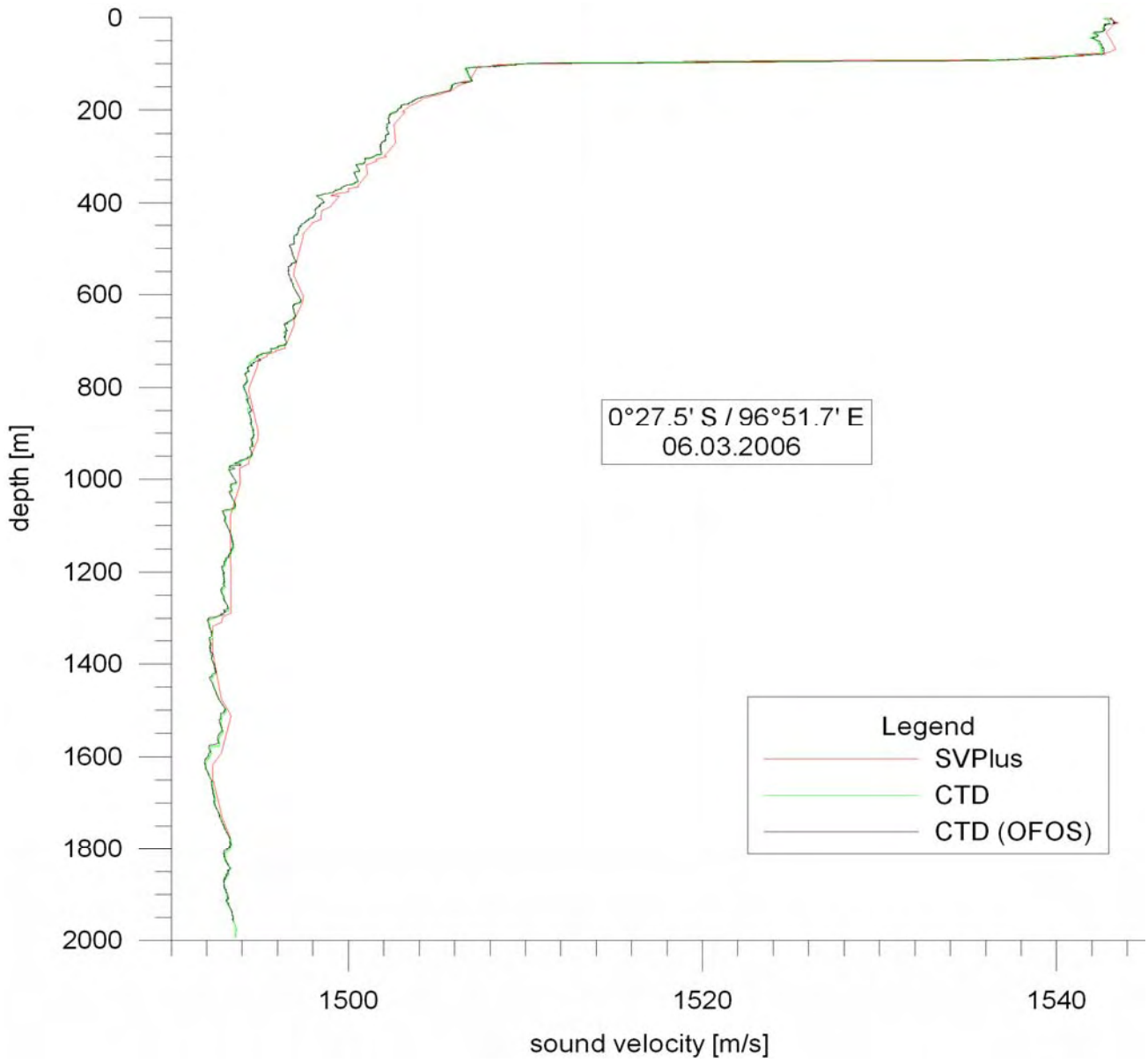

Figure 5.1.3.2: *Sound velocity profile obtained from CTD measurement during SO186.*

Accurate sound velocity profiles are needed for calibration of the water sound velocity to transfer the echo times of the bathymetric swathmapping into water depth. The velocity profile exhibits the typical curvature with similar characteristics of measurements conducted elsewhere. Sound velocity in shallow water shows a very high negative gradient in the upper 300 m of the water column, decreasing to app. 1498 m/s. Below 300 m water depth, a lesser negative gradient is observed, reaching a minimum value between 1000 m and 1200 m water depth at a sound velocity of 1487 m/s. The deeper water column is characterized by an increase in sound velocity and a positive gradient. Small excursions from the linear trend here are still observed, but less numerous and explicit as in the upper water column.

5.2 Computer facilities for bathymetry and seismic data processing

The experiments and investigations made during SO186 required special computing facilities in addition to the existing shipboard systems. For programming of ocean bottom stations, processing and interpretation of seismic data and analysis of magnetics, several workstations and a PC-laptop were installed by the wide-angle and seismology groups of IFM-GEOMAR.

Due to the large amount of data transfer IFM-GEOMAR installed a workstation cluster onboard comprising the following systems:

1	”devonia”	SUN Ultra 60	2 CPU 1 GB memory	1 TByte RAID, 150 GB disks, 2x DLT	Sun Solaris 2.6
2	”Caradoc”	AMD Duron 700 MHz	1 CPU, 128 MB memory	1 TByte RAID, 20 Gbyte disk	Linux SuSE 9.3
3	”aurinacien”	SUN Sparc 10	1 CPU, 96 MB memory	500 MByte disk	Solaris 2.6
4	”crimea”	AMD Duron 700 MHz	1 CPU, 128 MB memory	250 GByte disks, 6x PCMCIA	Windows2000, Linux SuSE 9.3
5	"pinta"	AMD Duron 700 MHz	1 CPU, 128 MB memory	250 GByte disks, 6x PCMCIA 1x DLT	Linux SuSE 9.3, Windows2000

Several laptops were used in addition to these computers. One HP Postscript Laser printer was available for plotting and printing.

The workstation cluster was placed in the Magnetics Laboratory and in the Clean Room. All computers were operated in a “stand-alone” mode. However, Caradoc’s RAID was mounted under Linux on Crimea and Pinta. The convenience of network mounted file systems has to be paid for with a heavy network load, particularly during playback of OBH-data (c.f. SO123 cruise report, Flueh et al., 1997). This required a high-performance network, which was accomplished by a switched twisted-pair ethernet. A 12-port ethernet switching-hub (3COM-SuperstackII 1000) connected all computers. This network setup showed a reliable and stable performance, and no breakdowns occurred.

5.3 OBH/OBS Seismic Instrumentation

The Ocean Bottom Hydrophone (OBH)

The first IFM-GEOMAR Ocean Bottom Hydrophone was built in 1991 and tested at sea in January 1992. This type of instrument has proved to have a high reliability; more than 3000 successful deployments were conducted since 1991. A total of 5 OBH and 30 OBS instruments were available for SO186-3. Altogether 91 sites were deployed for refraction seismic profiles during the SO186-3 cruise.
The principle design and a photograph showing the instrument upon deployment are shown in Figure 5.3.1. The design is described in detail by Flueh and Bialas (1996).

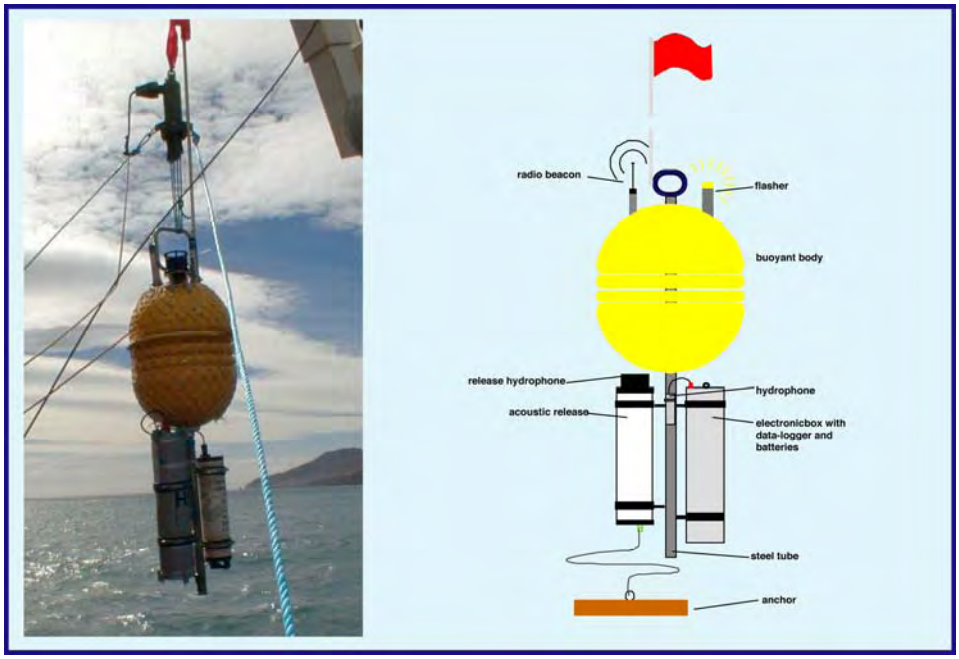

Figure 5.3.1: *Principle design of the IFM-GEOMAR OBH (right panel, after Flueh and Bialas, 1996) and the instrument upon deployment (left panel).*

The system components are mounted on a steel tube, which holds the buoyancy body on its top. The buoyancy body is made of syntactic foam and is rated, as are all other components of the system, for a water depth of 6000 m. Attached to the buoyant body are a radio beacon, a flash light, a flag and a swimming line for retrieving from aboard the vessel. The hydrophone for the acoustic release is also mounted here. The release transponder is a model *RT661CE* or *RT861* made by *MORS Technology* which recently became *IXSea*, or alternatively a *K/MT562* made by *KUM GmbH*. Communication with the instrument is possible through the ship's transducer system, and even at maximum speed and ranges of 4 to 5 miles release and range commands are successful. For anchors, we use pieces of railway tracks weighing about 40 kg each. The anchors are suspended 2 to 3 m below the instrument. The sensor is an *E-2PD* hydrophone from *OAS Inc.*, the *HTI-01-PCA* hydrophone from *HIGH TECH INC* or the *DPG* hydrophone, and the recording device is an *MBS*, *MLS* or *MTS* recorder of *SEND GmbH*, which is contained in its own pressure tube and mounted below the buoyant body opposite the release transponder (see Figure 5.3.1).

The IFM-GEOMAR Ocean Bottom Seismometer 2002

The IFM-GEOMAR Ocean Bottom Seismometer 2002 (OBS-2002) is a new design based on experiences gained with the IFM-GEOMAR Ocean Bottom Hydrophone (OBH; Flueh and Bialas, 1996) and the IFM-GEOMAR Ocean Bottom Seismometer (OBS, Bialas and Flueh, 1999). For system compatibility the acoustic release, pressure tubes, and the hydrophones are identical to those used for the OBH. Syntactic foam is used as floatation body again but this time in a less expensive cylinder shape. The entire frame can be dismounted for transportation, which allows storage of more than 50 instruments in one 20" container. Upon cruise preparation onboard all parts are screwed together within a very short time. Four main floatation cylinders are fixed within the system frame, while additional disks can be added to the sides without changes. The basic system is designed to carry a hydrophone and a small seismometer for higher frequency active seismic profiling. The sensitive seismometer is deployed between the anchor and the OBS frame, which allows good coupling with the sea floor. While the OBS sits on the seafloor, the only connection from the seismometer to the instrument is a cable and an attached wire, which retracts the seismometer during ascent to the sea surface. The three component seismometer (*KUM*) is housed in a titanium tube, modified from a package built by Tim Owen (Cambridge) earlier. Geophones of 4.5 or 15 Hz natural frequency are available. The signal of the sensors is recorded by use of the *Marine Longtime Recorder (MLS)*, and *Marine Tsunameter Seismocorder (MTS)*, which are manufactured by *SEND GmbH* and specially designed for long-time recordings of low frequency bands. The hydrophone can be replaced by a differential pressure gauge (DPG) as described by Cox et al (1984).

While deployed to the seafloor the entire system rests horizontally on the anchor frame. After releasing its anchor weight the instrument turns 90° into the vertical and ascends to the surface with the floatation on top. This ensures a maximally reduced system height and water current sensibility at the ground (during measurement). On the other hand the sensors are well protected against damage during recovery and the transponder is kept under water, allowing permanent ranging, while the instrument floats at the surface.

The Ocean Bottom Unit (OBU)

The Ocean Bottom Unit (OBU) is a modified OBS 2002 (see above), designed to adapt new sensors and acoustic devices and therefore to fulfill the requirements of the tsunami-warning buoy system. The OBU is one of the two main marine systems; the second is the tsunami buoy. The OBU is equipped with a *Güralp*-Seismometer (see below) and a Differential Pressure Gauge (DPG). Additionally, it measures pressure data with the Paroscientific depth sensor. It is the acoustic device, mounted on the OBU, that makes it different from the conventional OBS system. This acoustic device (modem) is responsible for the communication between the OBU bottom station and the surface buoy.
An additional power supply (lithium battery), which makes the OBU bigger compared to the smaller OBS, is attached to the OBU to compensate for its extra energy consumption. Four additional floats are mounted to the OBU to counterbalance the extra weight and to ensure a safe rise for recovery.

Figure 5.3.2: *Instrument setup of the Ocean Bottom Unit. In addition to the Güralp Seismometer and a Differential Pressure Gauge, an acoustic device is mounted at the OBU to communicate with the surface buoy.*

Marine Broadband Seismic Recorder (MBS)

The so-called *Marine Broadband Seismic* recorder *(MBS;* Bialas and Flueh, 1999*)*, manufactured by *SEND GmbH*, was developed based upon experience with the DAT-based recording unit Methusalem (Flueh and Bialas, 1996) over previous years. This recorder involves no mechanically driven recording media, and the PCMCIA technology enables static flash memory cards to be used as non-powered storage media. Read/write errors due to failure in tape handling operations should not occur with this system. In addition, a data compression algorithm is implemented to increase data capacity. Redesign of the electronic layout enables decreased power consumption (1.5 W) of about 25% compared to the *Methusalem* system. Depending on the sampling rate, data output could be in 16 to 18 bit signed data. Based on digital decimation filtering, the system was developed to serve a variety of seismic recording requirements. Therefore, the bandwidth reaches from 0.1 Hz for seismological observations to the 50 Hz range for refraction seismic experiments and up to 10 kHz for high resolution seismic surveys. The basic system is adapted to the required frequency range by setting up the appropriate analogue front module. Alternatively, 1, 2, 3 or

4 analogue input channels may be processed. Operational handling of the recording unit is similar to that of the *Methusalem* system, or a file can be loaded via command or automatically after power-on. The time base is based on a DTCXO with a 0.05 ppm accuracy over temperature. Setting and synchronising the time as well as monitoring the drift is carried out automatically by synchronisation signals (DCF77 format) from a GPS-based coded time signal generator. Clock synchronisation and drift are checked after recovery and compared with the original GPS units. After software pre-amplification the signals are low-pass filtered using a 5-pole Bessel filter with a -3 dB corner frequency of 10 kHz. Then each channel is digitised using a sigma-delta A/D converter at a resolution of 22 bits producing 32-bit signed digital data. After delta modulation and Huffman coding the samples are saved on PCMCIA storage cards together with timing information. Up to 4 storage cards may be used. Data compression allows increase of this capacity. Recently, technical specifications of microdrives (disk drives of PCMCIA type II technology) have been modified to operate below 10° C, therefore 2 GB drives are now available for data storage. After recording the flashcards need to be copied to a PC workstation. During this transcription the data are decompressed and data files from a maximum of four flash memories are combined into one data set and formatted according to the PASSCAL data scheme used by the *Methusalem* system. This enables full compatibility with the established processing system. While the *Methusalem* system did provide 16 bit integer data, the 18 bit data resolution of the *MBS* can be fully utilised using a 32 bit data format.

The Marine Longtime Seismograph (MLS)

For the purpose of low-frequency recordings such as seismological observations of earthquakes during long-term deployments of about one year time a new data logger, the Marine Longtime Seismograph (MLS) was developed by *SEND GmbH* with support by IFM-GEOMAR.

The MLS is again a four channel data logger whose input channels have been optimised for 3-component seismometers and one hydrophone channel. Due to the modular design of the analogue front end it can be adapted to different seismometers and hydrophones or pressure sensors. Currently front ends for the Spahr Webb, PMD and Güralp seismometers as well as for a differential pressure gauge (DPG), a pressure sensor of high sensitivity and the OAS/HTI hydrophone are available. With these sensors we are able to record events between 50 Hz and 120 s. The very low power consumption of 250 mW during recording together with a high precision internal clock (0.05 ppm drift) allows data acquisition for one year. Data storage is done on up to 12 PCMCIA type II flashcards or microdrives, now available with a capacity of up to 2 GB. The instrument can be parameterised and programmed via a RS232 interface. After low pass filtering the signals of the input channels are digitised using Sigma-Delta A/D converters. A final decimating sharp digital low-pass filter is realised in software by a Digital Signal Processor. The effective signal resolution depends on the sample rate and varies between 18.5 bit at 20 ms and 22 bits at 1 s. Playback of the data is done under the same scheme as described for the MBS above. After playback and decompression the data is provided in PASSCAL format from where it can be easily transformed into standard seismological data formats.

The Marine Tsunameter Seismocorder (MTS)

This data logger is based on the experiences with the MBS and MLS devices. The GEOLON-MTS has been developed by *SEND GmbH* and is a high precision instrument for acquisition, processing, storage of seismic signals and additionally pressure data. Like the MLS it is optimised for long time (more than 1 year) standalone operation on the ocean bottom, data storage capacity is also up to 12 PCMCIA cards. The four channel data logger is prepared for connection with a hydrophone (also different types like e.g. HTI, OAS, or the Differential Pressure Gauge, DPG) and different types of three component seismometers as described above for the MLS.
Additionally a digital absolute pressure gauge can be connected to the auxiliary connector. During SO186 the *Paroscientific* digital pressure sensor was deployed for the first time.
Playback of the data is done according to the scheme described for the MBS and MLS above. After playback and decompression the data is provided in PASSCAL format.

The METS (Capsum) Methane sensor

The detector is a semi-conductor. Adsorption of hydrocarbons on the active layer leads to electron exchange with oxygen and thus to modification of the conductivity of the active layer, which the electronic converts into a voltage. A membrane desorbs dissolved gasses of the surrounding water into the gas phase containing the detectors. The diffusion is driven by Henry's Law. The direction is conditioned to the concentration gradient between water and gas phase, and within the membrane itself. The sensor is calibrated at relative humidity of 100%. Operational temperature range: -2°C to +60°C, calibration range 2 – 20°C; Methane: 50 nanomol/l – 10 µmol/l Response: Reaction time: 1 to 3 sec. t90-time: 5 to 30 min dependent on turbulences. Typical range limits are concentrations between 50 nmol/l and 10 µmol/l, and temperatures between 2 and 20°C.
The data logger is different to those of the seismic and pressure recorders. Therefore the methane sensors are mounted on separate OBS instruments, which are deployed close to OBS collecting seismic and/or pressure data. The configuration of the data logger and the download management is run under Windows-based software. For data storage, a 512 MB Secure Digital Card (SD-Card) is used. The logging interval is the time between two records of data on the SD-card. It can be set between 1 and 90 min, and between 1 and 24 hours. The acquisition time is the time within the logging interval during which measurement values are acquired and averaged.

The Paroscientific Pressure Sensor

The Pressure or Depth sensor consists of a pressure transducer and a serial interface board in a rugged waterproof package. Commands are sent and measurement data are received via one RS-232 and one RS-485 serial port. Measurement data are provided directly in user-selectable engineering units with a typical accuracy of 0.01% or better over a wide temperature range. Pressure measurements are fully temperature compensated using a precision quartz crystal temperature sensor. Each intelligent depth sensor is pre-programmed with calibration coefficients for full plug-in interchangeability.
The device can be switched to a low power "sleep" state after a user-defined period of serial inactivity to conserve power. After serial activity, the unit will "awaken", allowing normal operation.
The IFM-GEOMAR OBS and OBU systems can be equipped with MTS data loggers and these pressure sensors. The MTS data loggers (see above) are especially designed to read out the pressure data (the accuracy is 0.1 mBar) in addition to the conventional 4C recordings.

The Güralp Seismometer (CMG-OBS40T)

The OBS40T is a low-power, true broadband ocean bottom seismometer system consisting of three sensor housed in a *Nautilus* "Vitrovex" glass sphere 150mm in diameter.
The spherical gimbal is mounted in a stainless steel base. This mount has a number of holes in it, to allow water to flow.
Once the seismometer has come to rest on the sea bed, it is supplied with power causing it to level itself automatically after a delay of 30 seconds. This procedure is supervised by an on-board microcontroller and consists of several stages. 1. The gimbal's brake mechanism is released, allowing the sensors to swing freely, 2. After 45 seconds, once the sensors have come to rest, the brakes are re-applied, 3. The microcontroller measures the mass positions and compares them with the satisfactory values, 4. If mass positions are significantly off-center, steps 1-3 are repeated until they improve, or to a maximum of 3 levelling attempts. Additionally, the levelling routine can be repeated at any time, depending on the configuration parameters.

Airgun System

T. Behrens, D. Franke, J. Sievers, & E. Surburg

The BGR's G-Gun airgun array was used for signal generation during the cruise.
The G-Gun array is subdivided into two sub-arrays with eight guns each (Figure 5.3.3). Each sub-array consists of four two-gun clusters. The volumes of the individual guns of the port array range between 380 in^3, 250 in^3, 180 in^3 and 100 in^3 whereas in the starboard array volumes vary between 250 in^3, 200 in^3 120 in^3 and 70 in^3. Each sub-array is equipped with two near field hydrophones. The maximum total volume used was 3,100 in^3 (50.8 l) and the towing depth was 6 m throughout the survey. Each sub-array has a total length of 15.56 m. The offset between the ship's antenna and the center of the airgun array was 107.4 m. The center of the array had an offset of 48 m to the stern.
The working pressure was 2,100 psi (145 bar). Triggering and synchronisation was controlled by a SYNTRON GSC-90 system. It is capable of controlling up to 32 airguns.

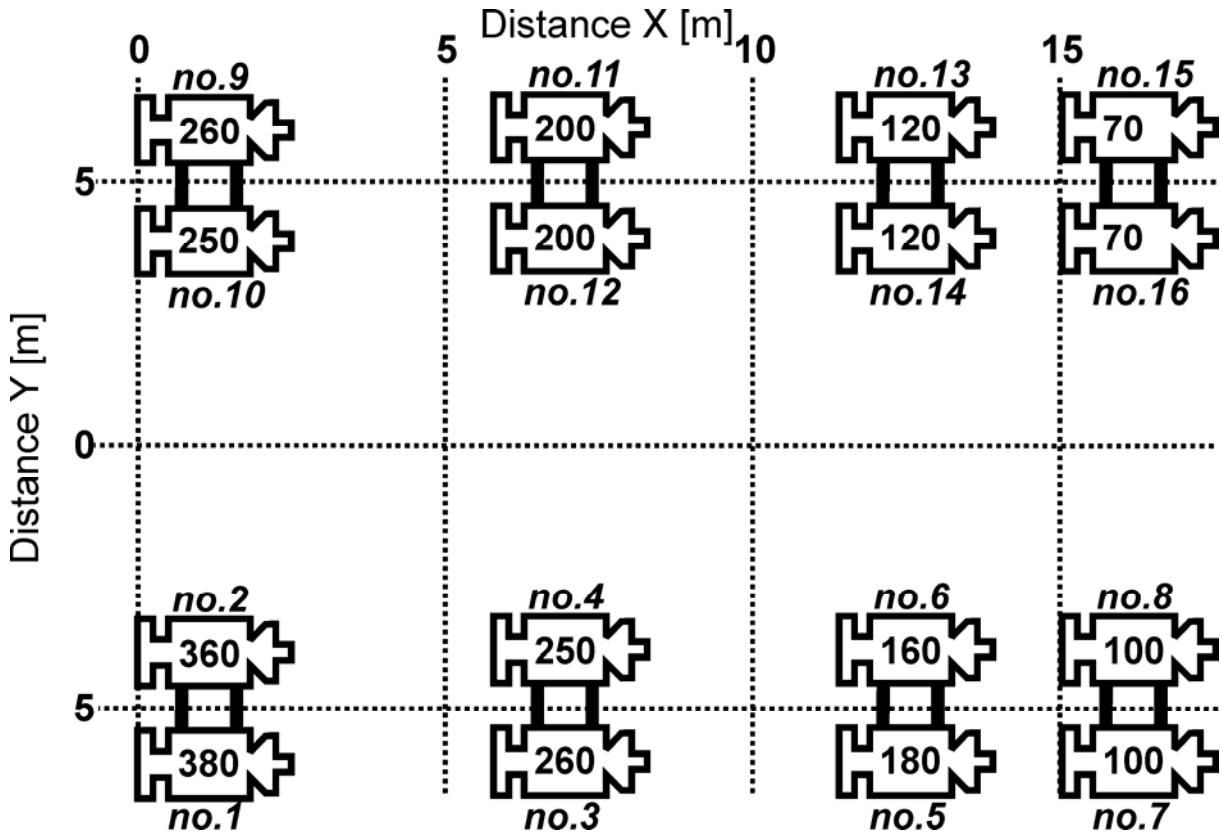

Figure 5.3.3: *Configuration of BGR's airgun system during cruise SO186-3.*

The shot time interval was generated on the Master PC with an interface card for triggering the airgun array via the SYNTRAK 960 system and the Syntron shot trigger device GCS 90. To correlate between shot numbers and position a trigger pulse was transmitted to the positioning system to archive the corresponding coordinates for each shot.
A summary of the airgun configuration, number of shots and navigation for each line is given in Appendix 9.2.

Refraction seismic line SO186-3-01 was shot along reflection seismic line BGR06-135 with a shot interval of 60 s. Lines SO186-3-02-05 were shot perpendicular to reflection seismic line BGR06-119 with varying shot intervals and gun configurations, and lines SO186-3-06-12 were shot perpendicular to line BGR06-109 with a shot interval of 30 s. The lines SO186-3-13-19 were shot along a part of line BGR06-109, also with a shot interval of 30 s.

During the measurements the G-Guns proved to be very reliable. Minor gun maintenance had to be done during the cruise. Line SO186-3-01 was shot without problems but one air hose broke (sb gun no.8 SP 247) while shooting lines SO186-3-02-05. This problem still persisted when line SO186-3-03 was shot. Lines SO186-3-04 and -05 were shot without problems.
From shotpoint 490 of line SO186-06 on gun 6 at the port side had to be switched off due to problems with the air supply. This problem was tackled before the start of profile SO186-13.

6. Work Completed and Preliminary Scientific Results
6.1. Seismic Processing of OBH/OBS Wide-Angle Data

- **The processing scheme**

The OBH/S data recorded in continuous mode on the MLS, MBS, and MTS units have to be converted into standard trace-based SEG-Y format for further processing. The necessary program structure was mainly taken from the existing REFTEK routines and modified for the OBH requirements and IFM-GEOMAR´s hardware platforms.
The flow chart shown in Figure 6.1.1 illustrates the processing scheme applied to the raw data. A detailed description of the main programs follows below:

send2pas
For the PC-cards used with the MBS, MLS, and MTS recorders, data expansion and format conversion into REFTEK data format is performed using a DOS/Windows based PC. The program send2pas reads data from the flashcards used during recording. Decompressed data are written onto the PC's hard disk using PASSCAL data format. Either 16 or 32 bit storage is available. After ftp transmission to a SUN workstation, ref2segy and all other software can be used to handle and process the data files and store them as SEG-Y traces.

While processing the MLS/MTS recordings many time slips of one sampling interval were detected by the send2pas software, typically at a rate of one time slip every 1-2 hours. The time slips are caused by mismatch of the actual sampling rate of the MLS/MTS recorder compared to the desired sampling rate. This mismatch arises because the clock rate of the crystal oscillator in the MLS/MTS recorder is temperature dependent (Klaus Schleisiek, SEND GmbH, pers. comm.). The temperature dependence is known and corrected for in the determination of the system time, but for performance reasons the sampling pulses are directly generated from the oscillator signal without any time correction. The send2pas routine detects when the accumulated inaccuracies of the sample rate cause an effective timing error of one sample, but it only reports and does not correct the "time slip".
The resulting total time error was on average 200 to 400 ms for the wide-angle profiles and up to several tens of seconds for the seismology network, showing clearly the necessity of a special time slip correction for the MLS/MTS data. A correction for the time slips is applied with the “unslip” routine.

ref2segy
The ref2segy program converts the output of send2pas to a pseudo SEG-Y trace consisting of one header and a continuous data trace containing all samples, as used by the PASSCAL suite of seismic utility programs. For each channel (normally pressure, vertical velocity, and velocity along two mutually perpendicular horizontal directions for OBS; pressure for OBH) one file is created with the name derived from the start time, the serial number of the Methusalem system, and the channel number. The file size of the pseudo-SEGY file is directly related to the recording time. For instance, a recording time of one hour sampled at 200 Hz (16 Bit) will produce a file size of 1.44 MB per channel. A record with two channels and a recording time of two days will produce a total data volume of 70 MB.

send2x
Alternatively to the Windows-based PC routine (send2pas), send2x operates under Linux.

Although data of all recorders (MBS, MLS, and MTS) can be read out with send2x, only the mts-routine was used during SO186-3. The Windows-based PC routines do not handle the new format of the MTS data loggers. The program library SEND2X converts the compressed recordings of GEOLON-MTS into different formats. The current version allows the conversion of raw data into a binary file, an audio-wave file, or into the SEG-Y format if an appropriate shot file is available.

mtsread
mtsread has to be used to convert raw data acquired by the GEOLON-MTS/MTS-M data logger. At first, the raw data of all PCMCIA cards belonging to one recording session as well as the corresponding MLS.SYS file must be copied to a directory using e.g. the cp command. Then mtsread is used to decompress and convert the raw seismic data into the internal send2x format. The raw data of the absolute pressure gauge will be converted into ASCII format and stored in a separate file. The name of this file will be generated automatically with the extension **.pressure**

resample
Data recorded with the GEOLON-MLS and GEOLONON-MTS or MTS-M may show so-called "time slips" (see above), due to differences between the long term stabilization of the internal clock and the sample frequency clock. Thus, within a given sample period, less or more samples than required are recorded, e.g. 99 samples instead of 100. If this misalignment of sample periods and samples actually collected is influencing the precision of your experiment, you can correct the data using RESAMPLE. RESAMPLE does not correct time slips for other GEOLON Data Loggers, but may be for correction of filter influences and adjusting skew times.

seg-ywrite
seg-ywrite converts the data stored in s2x format to standard SEG-Y format. The option --reftek is used for a pseudo SEG-Y output format and allows optional 16bit or 32bit output.

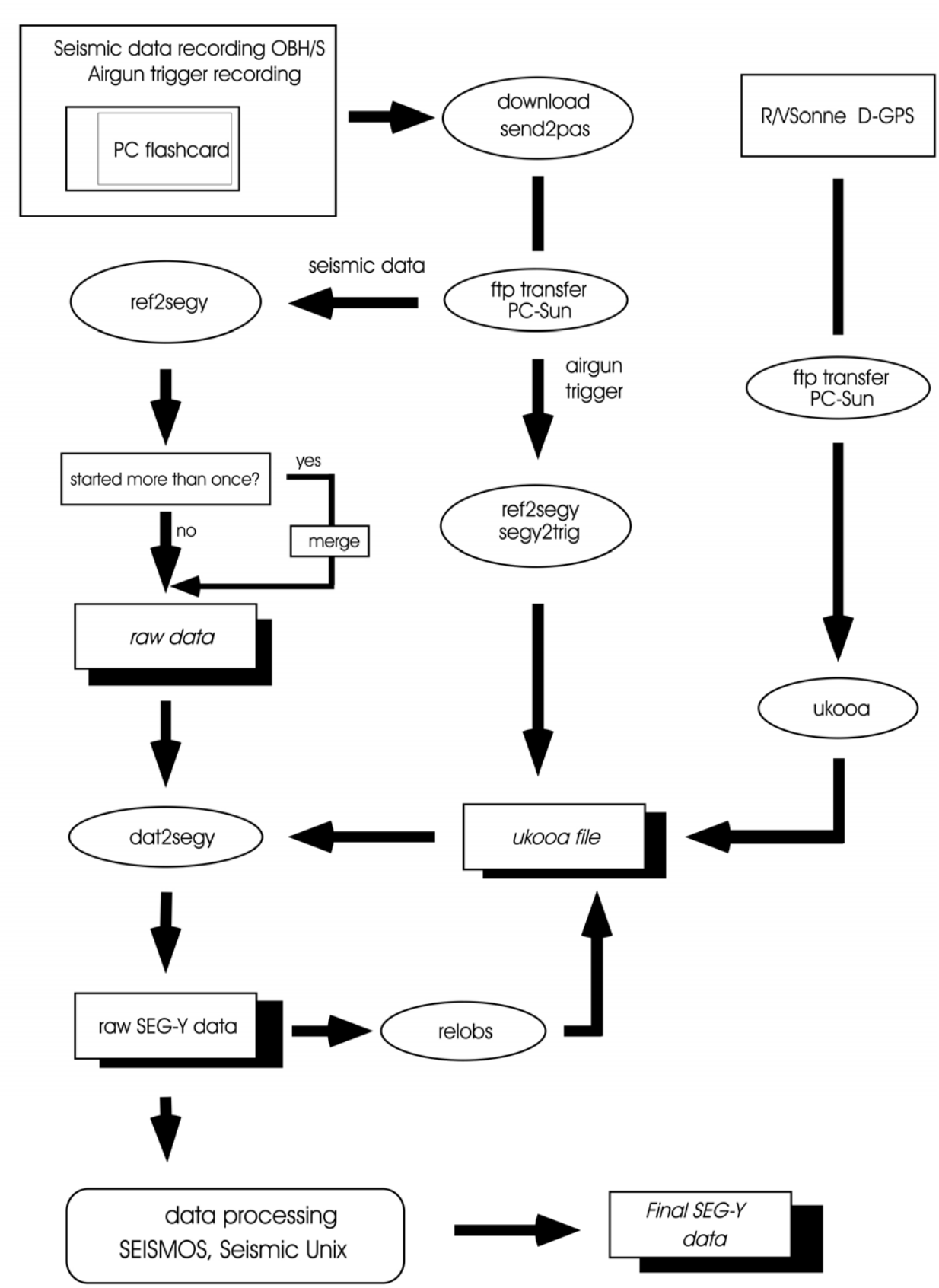

Figure 6.1.1: *Processing flow of seismic refraction data (OBS/OBH) from raw data to SEG-Y records.*

merge
If an error occurs during the download process, the ref2segy program has to be restarted. This may lead to several data files with different start times. Merging these files into a single file is performed by the merge program. Gaps between the last sample and the first sample of the consecutive data traces are filled with zeros. Overlapping parts are cut out.

pql
pql (Passcal Quick Look) is a simple display program for continuous seismic data. Its interactive zooming capability allows a rapid inspection of data quality.

segy2trig
The trigger signal, provided by the airgun control system, is recorded on an additional MBS unit during the shooting period. The trigger data are treated similarly to regular seismic data and are downloaded to the hard disk via the send2pas and ref2segy programs. Then, the segy2trig program detects the shot times in the data stream by identifying the trigger signal through a given slope steepness, duration and threshold of the trigger pulse. The output is an ASCII table consisting of the shot number and the shot time. Accuracy of the shot time is one of the most crucial matters in seismic wide-angle work, and must be reproduced with a precision of a few ms. Due to this demand the shot times have to be corrected with the shift of the internal recorder clock. Additionally, the trigger file contains the profile number, the start/end time of the profile and the trigger recording. The shot times are part of the ukooa file, which links them with the source coordinates.

apc
The apc program is used to establish the geometric database by calculating the positions of sources at any given shot time and offset from the ship. The source is placed on the ship track using simple degree/meter conversions and then written to a file in UKOOA-P84/1 format. Corrections for offsets between antenna and airguns as well as consistency checks are included. This file will be used when creating a SEG-Y section via the dat2segy program. The program requires the trigger file to contain the shot times, navigation, and a Parameter file containing information for the UKOOA file header as basic input information.

dat2segy
The dat2segy program produces standard SEG-Y records either in a 16 or 32 bit integer format by cutting the single SEG-Y trace (the ref2segy/seg-ywrite output) into traces with a defined time length based on the geometry and shooting time information in the ukooa file. In addition, the user can set several parameters for controlling the output. These parameters are information about the profile and the receiver station, number of shots to be used, trace length, time offset of the trace and reduction velocity (to determine the time of the first sample within a record). Also the clock drift of the recorder (skew) is taken into account and corrected for. For the MLS data the total time error resulting from the observed time slips described above was subtracted from the clock drift value. The final SEG-Y format consists of the file header followed by the traces. Each trace is built up by a trace header followed by the data samples. The output of the dat2segy program can be used as input for further processing with SEISMOS or Seismic Unix (SU).

relobs
Because of drifting of the OBH and OBS instruments during deployment and inaccuracies in the ship's GPS navigation system, the OBH positions may be mislocated by up to several 100 m.

Since this error leads to asymmetry and incorrect traveltime information in the record section, it has to be corrected. This is accomplished with the program relobs.
For input, the assumed OBH location, shot locations and the picked traveltimes of the direct wave near to its apex are needed. To simplify the picking a static correction with a hyperbolic equation was performed to flatten the direct wave. This yields a much more coherent direct arrival which would normally suffer from strong spatial aliasing in the uncorrected section making it difficult to track. By shifting the OBH position, relobs minimizes the deviation between computed and real travel times using a least mean square fitting algorithm (assuming a constant water velocity). The source offset, i.e. the distance from the research vessel's GPS position to the center of the airgun array, was determined to 90 m.
Besides these main programs for the regular processing sometimes additional features are needed for special handling of the raw data:

segyhdr
The routine segyhdr prints all the header values of the raw data on the screen.

segyshift
Segyshift modifies the time of the first sample, allowing the whole raw data trace to be shifted by a given value. This is very useful when shifting the time base from Middle European Time to Greenwich Mean Time or any local time. Because of recording problems, the data sometimes show a constant time shift, which can be corrected as well with segyshift.

- **OBH/OBS data analysis and processing**

Frequency filter analysis: To determine the frequencies of the seismic energy, filter panels with narrow frequency band passes for the offset range of 0-16 km are shown in Figure 6.1.2. The amplitude spectra of the used Ormsby frequency filter operators are characterized by linear slopes. The filter is described by four corner frequencies, i.e. lower stop/pass band boundary and upper pass/stop boundary. The main energy of the phase between 3 and 5 s is between 3-38 Hz and for the direct wave it reaches up to 55 Hz. As a broad frequency range is contained in the data, time and offset dependent filtering was applied (see below).

Deconvolution analysis: To improve the temporal resolution of the seismic data a deconvolution is applied to compress the basic seismic wavelet. The recorded wavelet has many components, including the source signature, recording filter, and hydrophone/geophone response. Ideally, deconvolution should compress the wavelet components and leaving only the earth's reflectivity in the seismic trace. We applied Wiener deconvolution in successive trace segments, based on the following assumptions:

1. The earth's reflectivity is 'white'.
2. The wavelet shows the minimum-delay phase behavior.

As in these wide-angle data the amplitude spectra of the seismic traces vary with time and offset (e.g. reflected, refracted pp phases and reflected ps and ss phases), the deconvolution must be able to follow these time and offset variations. To improve especially the spatial resolution of the seismic data a multi-trace deconvolution also called rollalong deconvolution, which uses autocorrelograms averaged over a number of traces, is performed to compress the basic seismic wavelet. Here, each trace is divided into 3-s data gates with 1-s overlaps, in which time invariant deconvolution operators are computed from the average autocorrelation function of 51 traces.

The operator is recalculated for every trace in each data segment and applied. The overall deconvolved trace results from a weighted merging of the independently deconvolved gates.

Raw data are input for the deconvolution process. As several recordings were influenced by a DC shift, a 1-3-Hz high-pass minimum delay Kaiser frequency filter with 60 dB attenuation between the pass and reject zone was applied prior to deconvolution in order to center the amplitudes around zero.
The deconvolution test panels are shown in Figure 6.1.3 for the offset ranges 0-16 km (upper panel) and 20-32 km (lower panel). Constant operator lengths of 300 ms and 800 ms (predictive lag excluded) with a variation of the prediction lag from 4 to 120 ms are displayed for a multi-trace deconvolution (avere=51). The best compromise between temporal resolution and signal-to-noise ratio is obtained for an operator length of 300 ms including a predictive length of 80 ms which was chosen for the processing of the data sets of this cruise. After deconvolution, an offset- and time-variant Ormsby filter with zero-phase characteristic was applied. As the seafloor depth changes along the seismic lines, each trace was statically corrected to a fixed seafloor travel time of 11 s based on the water depth before filtering. This information is available in the trace headers. After this filter was applied, the data were shifted back to their original travel times.

Processed data: Comparison of the preprocessed data in Figure 6.1.4 (upper panel) to the unprocessed data in Figure 6.1.4 (lower panel) shows a clear compression of the wavelet signal and an increase in signal-to-noise ratio, especially in the far offset range. For the picking of events and model building by raytracing both sections were used to keep all available seismic information.

Final processing sequence

- Input: SEGY-data, 4 ms or 5ms sampling rate with complete geometry information
- Tapering the first 0.5 s to zero to reduce the response of the debias filter operator
- Kaiser highpass (debias)
- Gated Wiener deconvolution: gate length 3 s, overlap 1 s, length of merge region 1 s, operator length 300 ms (prediction interval included), prediction interval 80 ms
- Static correction to a fixed seafloor traveltime of 11 s
- Time and offset-dependent Ormsby frequency filter

On time-shifted traces with a reduced time scale of 8 km/s the following filter parameters were used:

lower stop/pass	upper pass/stop (Hz)	offset(m)	beginfull(s)	endfull(s)
3/5	65/85	0	0	12.8
		8000	0	12.6
		48000	0	0
2/4	45/60	0	13.7	14.3
		8800	13.5	14.4
		13200	13.0	13.9
		52000	2.0	4.7
		107000	0.5	1.0
1/3	30/40	0	15.3	16.8
		11700	15.1	16.6
		19200	14.8	16.3
		61700	7.0	10.1
		114000	2.0	3.0
		152000	1.5	2.4
1/3	20/30	0	19.0	trace length
		20000	18.4	trace length
		130000	3.5	trace length

• **Data archiving**

Data recorded with the MBS/MLS and MTS recorder on flash discs were transferred via a PC to a SUN workstation. On the workstation they were transformed into a so-called PSEUDO-SEGY format. After navigation data had been merged and SEGY formatted traces with the appropriate header words had been created, the data were also archived. Finally, a third set was stored and archived after the shipboard processing, as described above, had been applied. All final processed SEGY data were archived on tapes.

• **Data exchange**

For the exchange of the OBH/OBS data, the SEGY-format on disk with a Sun tar-format was chosen. The raw segy data are in Integer2 format with trailer bytes between the record structure of SEGY. The processed data are in IBM-floating point without trailer bytes between the records.
For UTM transformation into Cartesian coordinates use: WGS84 spheroid, central meridian 95 0. 0. E, northern hemisphere.

This is the definition of the segy trace header for the IFM-GEOMAR OBS wide-angle reflection data. The extension of the standard SEGY header from 181 to 240 byte is a layout in order to process the data on the SEISMOS software system. Reading bytes directly into this header will allow access to all of the fields.

BytePos	Bytes	Information	Comments (note: not all headers available in processed data)
1-8	(2x4)	lineSeq, reelSeq;	/* Sequence numbers within line and reel, resp.*/
			/* here station and shot number Def: 1, 1 */
9-12	(4)	profNumber;	/* Original field record number */
			/* Here profile number */
13-16	(4)	traceNumber;	/* Trace number within the original field record.*/
			/* Here station (receiver) Number */
17-20	(4)	energySourcePt;	/* Energy source (shot) point numbe */
			/* Def: 0 */
21-24	(4)	cdpEns;	/* CDP ensemble number: shot number */
			/* Def: 0 */
25-28	(4)	traceInEnsemble;	/* Trace number within CDP ensemble */
			/* Here azimuth in seconds of arc for unprocessed data*/
29-30	(2)	traceID;	/* Trace identification code:
			1=seismic data (Def) 4=time break 7=timing
			2=dead 5=uphole 8=water break
			3=dummy 6=sweep 9..., optional use */
31-34	(2x2)	vertSum, horSum;	/* Def: 1, 1 */
35-36	(2)	dataUse;	/* 1=production (Def), 2=test */
37-40	(4)	sourceToRecDist;	/* Distance in (m) */
41-44	(4)	recElevation;	/* Elevation in (m), Def: 0 */
45-48	(4)	sourceSurfaceElevation;	/* Def: 0 (m) */
49-52	(4)	sourceDepth;	/* Def: 0 (m) */
53-60	(2x4)	datumElevRec, datumElemSource;	/* Def: 0, 0 (m) */
61-68	(2x4)	sourceWaterDepth, recWaterDepth;	/* Def: 0, 0 (m) */
69-70	(2)	elevationScale;	/* Scale elevations Def: 0 (10**0) */
71-72	(2)	coordScale;	/* Scale coordinates
			Def: -2, means coordinates multiplied
			by 10**(-2) to get real value for unprocessed data.
			NOTE: for processed data -100 means to divide by 100

to get the real value */

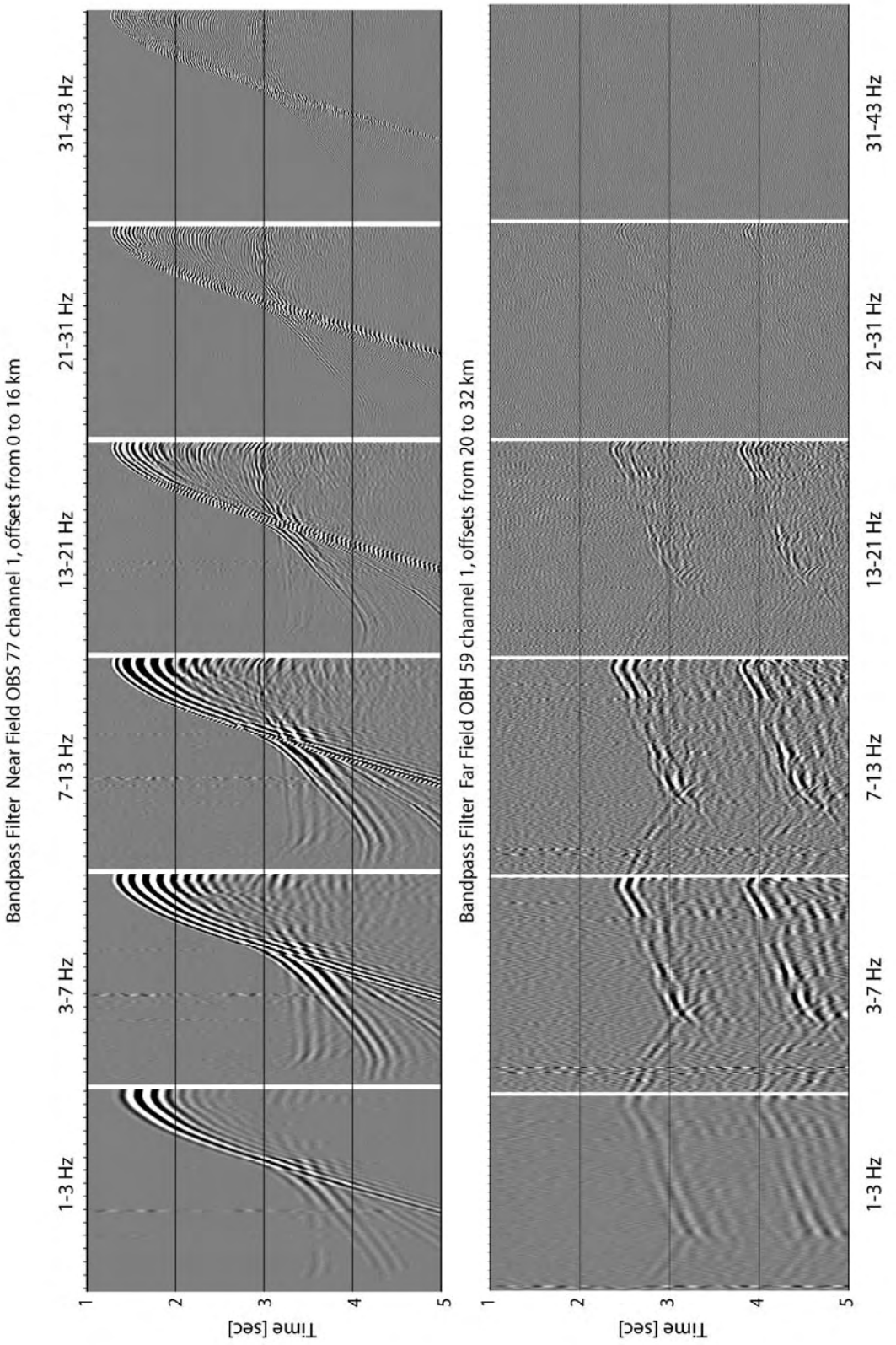

Figure 6.1.2: Testpanels for optimizing the Bandpass Filter parameters for Near- and Far-Field arrivals

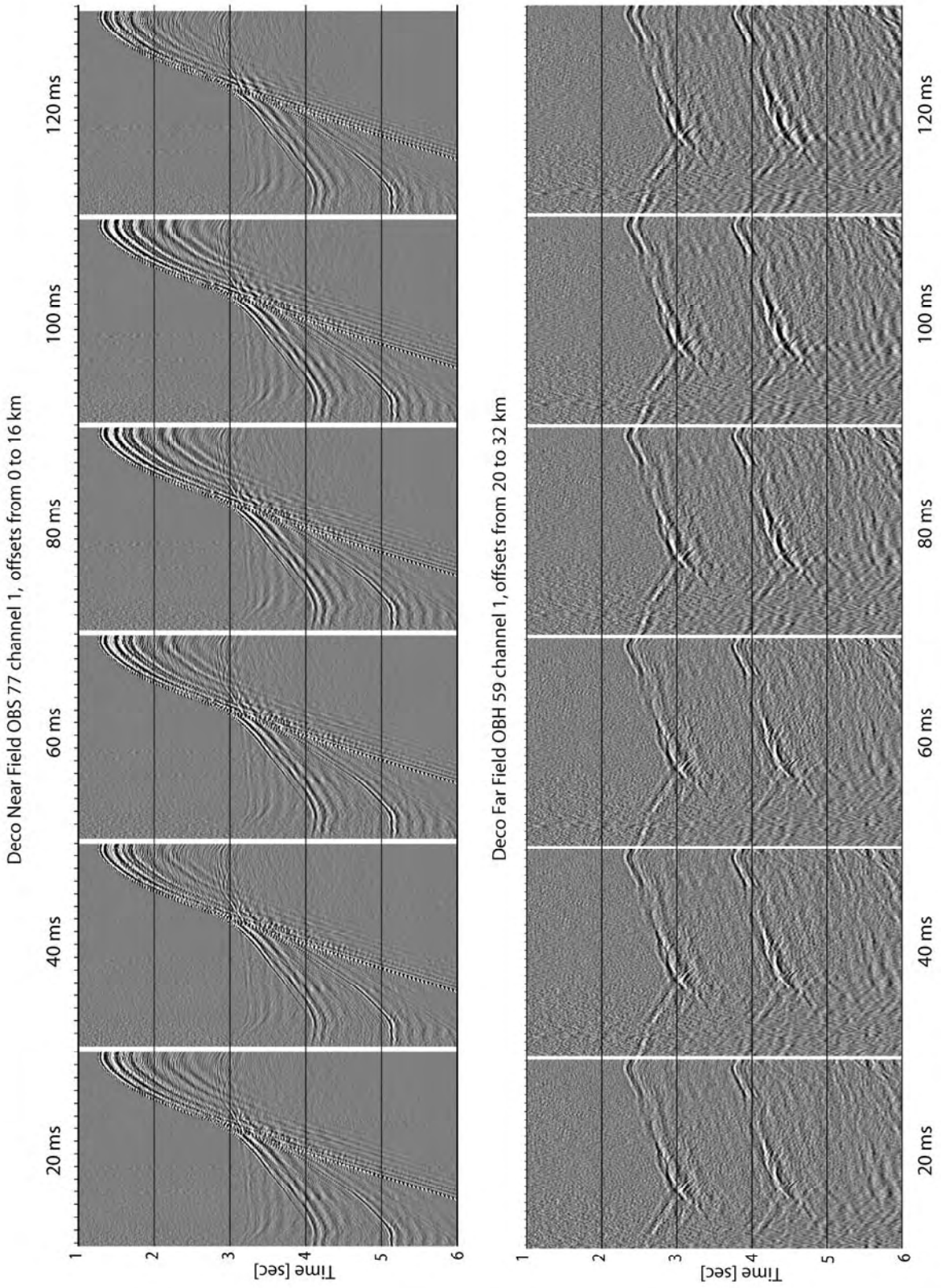

Figure 6.1.3: Testpanels for optimizing the deconvolution parameters for Near- and Far-Field arrivals

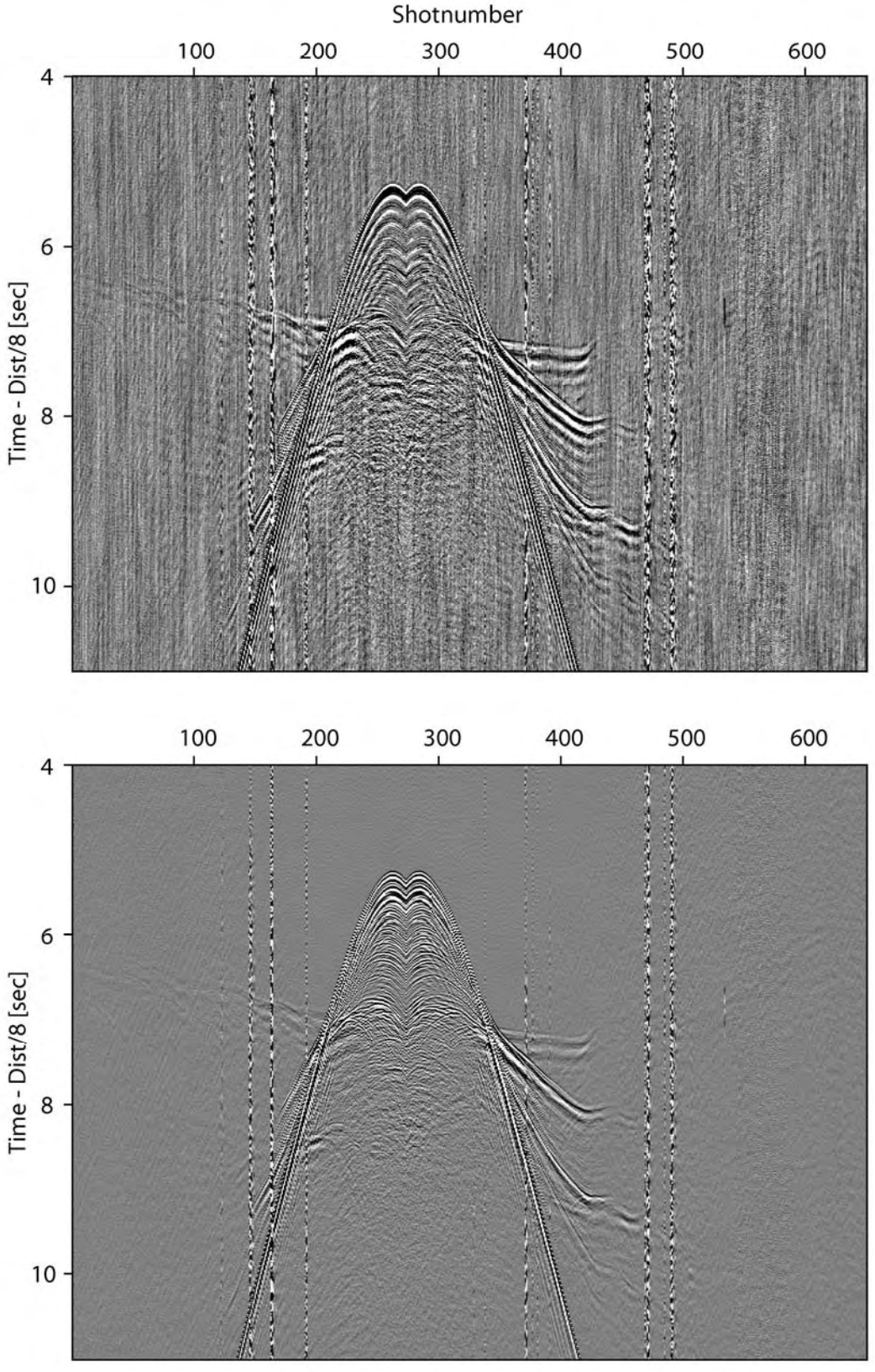

Figure 6.1.4: Seismic section of obs77 before (upper panel) and after (lower panel) processing

6.2 Seismological Observations

6.2.1 Processing of Earthquake Data

The initial data processing of earthquake data is identical to the processing sequence for wide angle data described above. Later, however, the processing of the PASSCAL SEGY files differs from the processing of the active source data. To generate more manageable files sizes used to apply time correction and search automatically for seismic events the PASSCAL SEGY are cut into 25 hours records with one hour overlap between adjacent records, such that each record generally begins at 0:00:01.

For all stations timing errors of the internal clock against GPS time were corrected. In addition, for instruments which were operated over the changing years of 2005 and 2006 we had to correct for a shift of 1000 ms in UTC time that occurred at January 01 at 0:00 am.

To detect automatically seismic events in the daily records a short-term-average versus a long-term-average (STA/LTA) trigger algorithm was applied. The trigger parameters were the length of the short term (s) and long term (l) time window, the mean removal window length (m), the trigger (t) and detrigger ratio (d), minimum number of stations (S) and the network trigger time window length (M). The trigger parameters used for shipboard processing shown in Table 6.2.1.1 were applied to unfiltered hydrophone data of good quality. To test the trigger parameters, a continuous 24 hours data stream of all stations was visually checked. Moreover, we tested the parameters for two days and transferred the data in the SEISAN package used to analyse and locate the local earthquakes. Applying these trigger parameters we obtained less than ~10% false triggers and lost only those events that were recorded only on a few stations, while all major events were triggered. Most false triggers were caused by the seismic coda of earthquakes with magnitudes of M>4 that were not only recorded on the local SNET (for Simeulue seismic network) but also on the Global Seismic Network (GSN) as reported by the National Geophysical Earthquake Information Center (NEIC) in Boulder, Colorado, USA. In addition, distant events often triggered twice due to the large separation in time between *P*-wave and *S*-wave arrivals.

Table 6.2.1: *Trigger parameters as defined in the text to search the continuous recordings for seismic events.*

Parameter	s	l	m	t	d	S	M
Value	0.5 s	60 s	200 s	3.0	1.8	6	20 s

After finding event triggers the events were cut from the 25 hours files and stored into subdirectories, one per event. Because we were investigating local earthquakes the appropriate time window length for the events was 3 minutes, starting 60 s prior to trigger time. The SEGY traces in the event directories were converted first into SAC, and then into SEISAN waveform format, which made it possible to store all traces associated with an event into a single waveform file. After conversion the data were registered in the SEISAN database (Havskov and Ottemöller, 2001). *P*-wave and *S*-wave arrival times were picked and events were preliminarily located with the program HYP, which employed an iterative solution to the nonlinear localization problem (Lienert and Havskov, 1995). Travel times were calculated using a 1-D velocity model. The velocity model consisted of four layers with a velocity of 5.0 km/s in the uppermost 16 km, 6.4 km/s down to 20 km, 7.1 km/s between 20 to 28 km, and

8.1 km/s down to 50 km depth. A test of several velocity models indicated that the epicentres were reasonably robust, while the depth changed significantly for different models, indicating that a refined velocity model was needed for the post-cruise data analysis.

6.2.2 First results

During the first two weeks of the deployment (15 October to 30 October 2005) we located 125 seismic events. In addition, we studied a number of days in December, including December 18, when an event with magnitude (Mw) 5.7 occurred. Figure 6.2.1 shows the waveforms from this event recorded on OBS15 at a distance of 117 km from the epicentre. Due to the different amplification factor for the hydrophone and geophone channels the hydrophone was generally overloaded by most stations within 100 km off the source location, while the lower amplification of the geophone allowed for identification of secondary arrivals like *S*-waves.

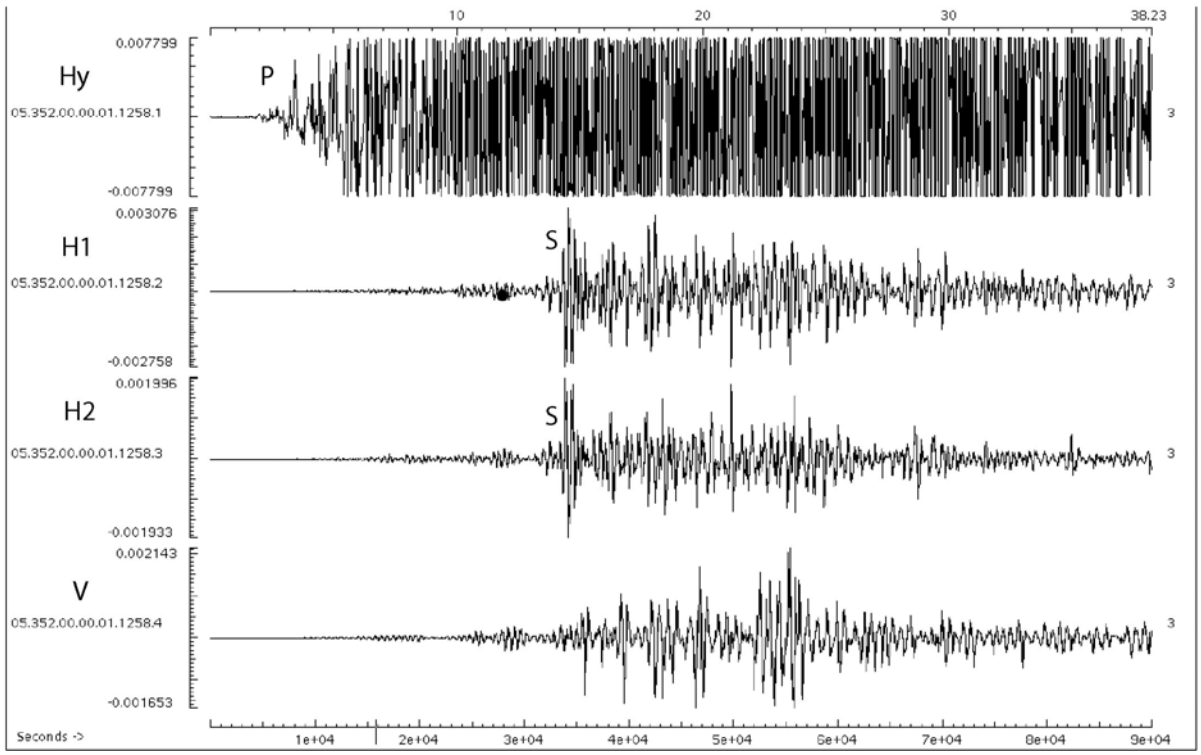

Figure 6.2.1: *Waveforms for a Mw=5.7 event recorded on OBS15 on December 18, 2005.*

Figures 6.2.2 to 6.2.3 show the distribution of epicentres in the vicinity of the island Simeulue. The seismic front (onset of seismicity in the megathrust fault) was located roughly 50 km from the trench axis, and earthquakes occurred ~150 km landwards away from the seismic front. Only a few earthquakes were located farther landwards. This may indicate that the properties in the megathrust fault change from unstable stick-slip (seismogenic slip) to stable aseismic sliding. In Figure 6.2.4 we show the depth distribution of the October events projected on a crustal model derived from gravity modelling across the nucleation point of the December 26, 2004 megathrust earthquake to the north of Simeulue (Grevemeyer and Tiwari, 2006). Although the hypocentres have to be considered as preliminary and may change when

a more appropriate velocity model is chosen for the location procedure, we could derive a few

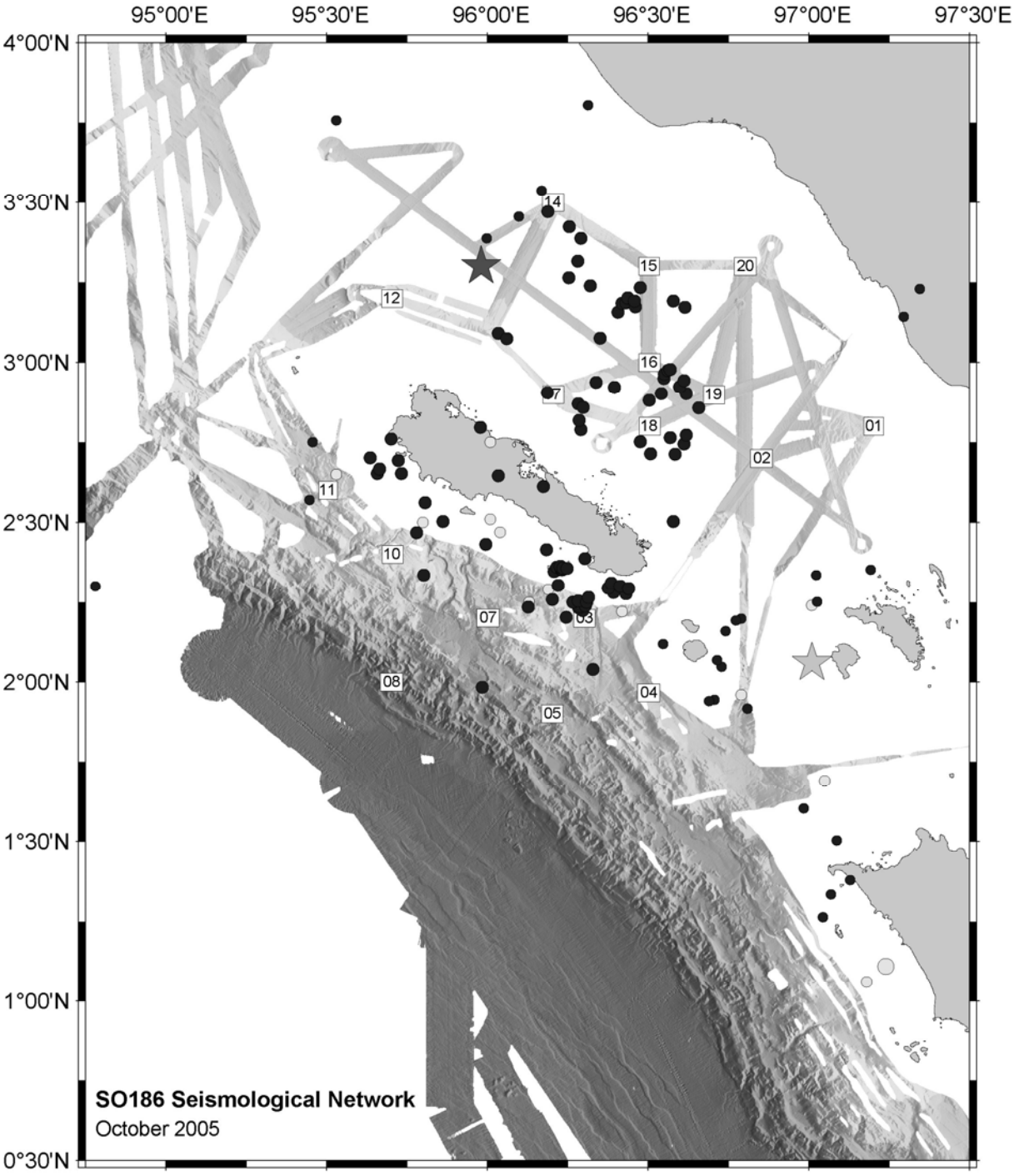

Figure 6.2.2: *Epicentres of the events located in October 2005 (black dots) and NEIC epicentres (light grey dots) for the same time period. Black star marks the nucleation point of the December, 26, 2004 tsunami earthquake and grey star the epicentre of the March, 28, 2005 event.*

features: a number of earthquakes occurring roughly along a band within the downgoing ocean crust (though earthquakes occurring within the crust may be actually interface events that are mislocated by a few kilometers in depth). No events occurred landward of the

intersection of the forearc Moho with the downgoing plate. This limit may be explained by aseismic hydrous minerals present in the mantle wedge. During subduction the downgoing plate experiences higher pressures and temperatures. Water trapped in crust and mantle is gradually forced out, infiltrating the overlying forearc mantle, forming serpentinite and brucite, and changing the strong, dry rocks into weak, hydrous rocks. These fragile rocks do

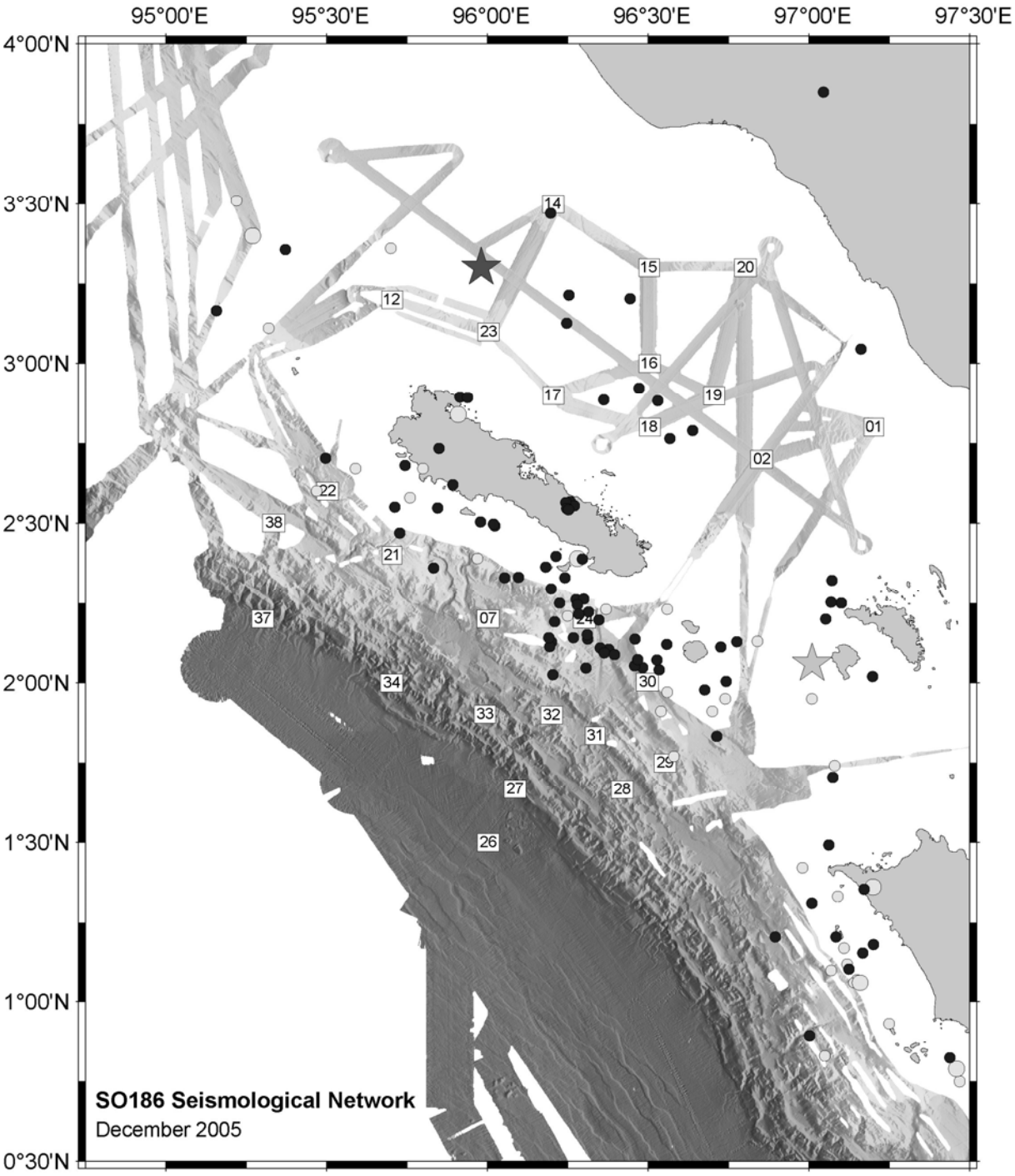

Figure 6.2.3: *Epicentres of the events located in December 2005 (black dots) and NEIC epicentres (light grey dots) for the same time period.*

not support seismogenic slip and thus may suggest that the mantle wedge is serpentinized (Hyndman and Peacock, 2003).

In addition, we used the events located in December to compare the epicentres reported by the National Geophysical Earthquake Information Center (NEIC) in its PDE catalogue with our locations. The PDE epicentres are mislocated with respect to our assessment by 3 to 48 km (Figure 6.2.5). Most events, however, are only mislocated by ~10 km and hence within the formal error reported by NEIC.

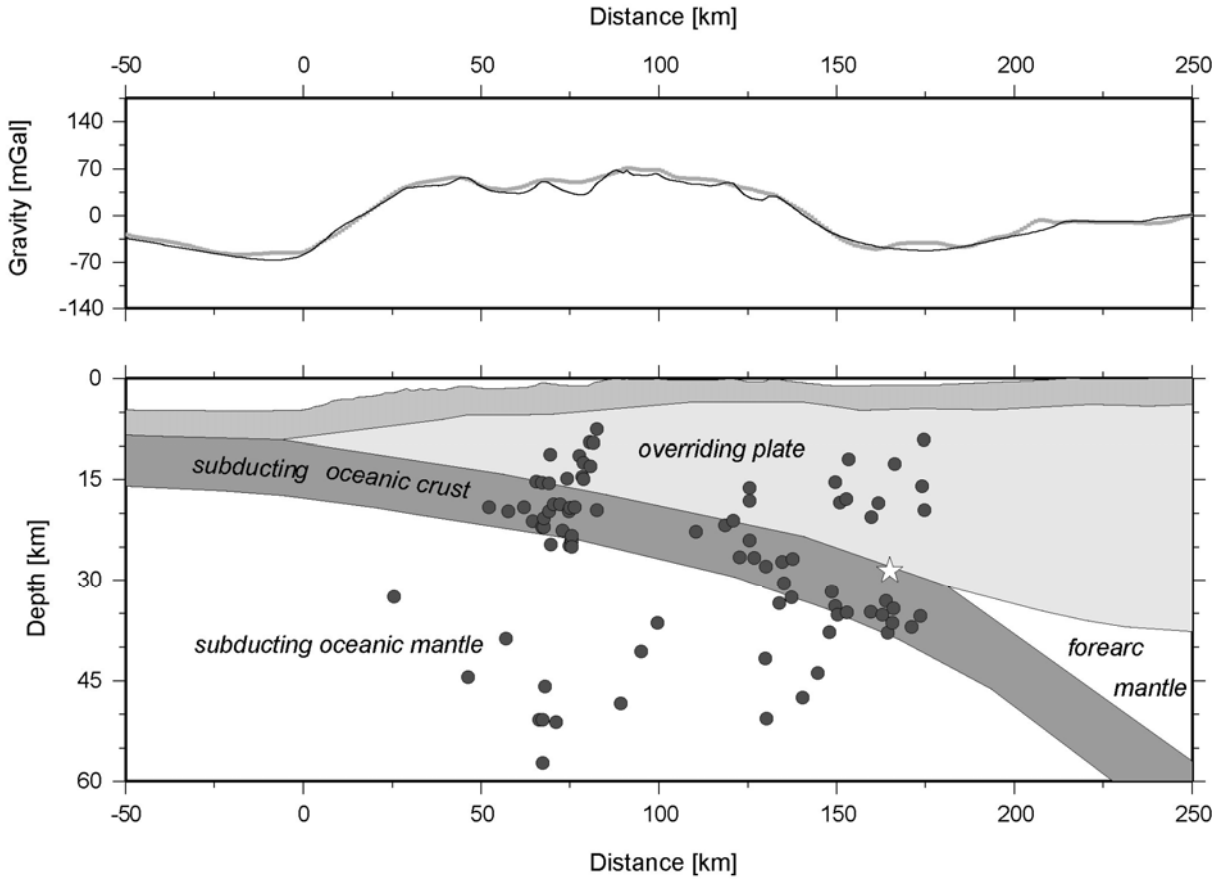

Figure 6.2.4: *Crustal model north of Simeulue derived from gravity modelling and hypocentres (black dots) for October 2005.*

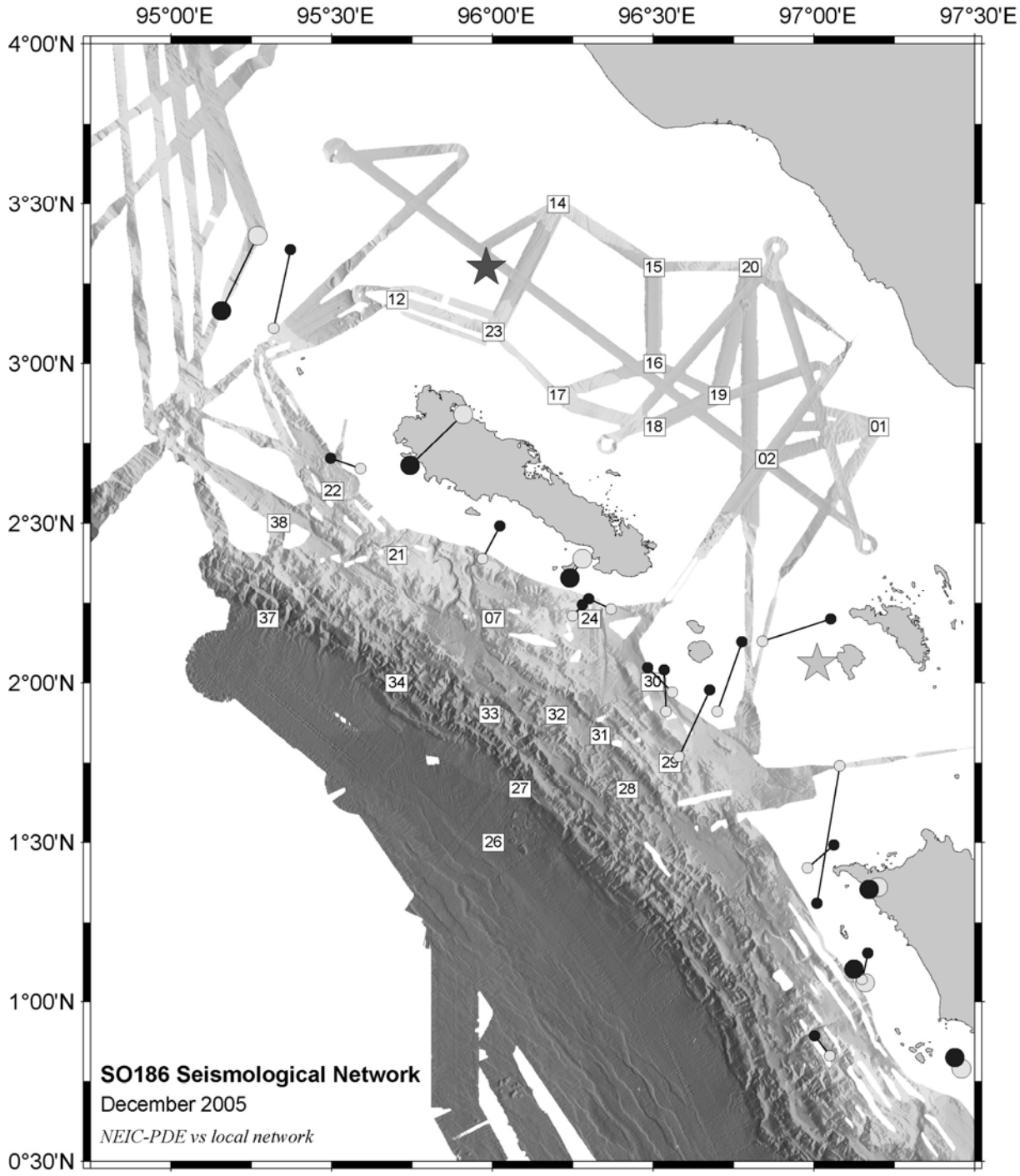

Figure 6.2.5: *Pairs of the epicentres for the same events located in December 2005 (black dots) and NEIC epicentres (light grey dots).*

6.3 Profile SO186-3-01

This profile was shot from 03 March 06:00 to 04 March 17:00 at an average speed of 4 kn and a trigger interval of 60 sec resulting in an average shot spacing of 120 meters. Along the profile 25 Ocean Bottom stations were deployed, and in addition 6 instruments of the seismological network were still in operation (see Figure 6.3.1 for an overview and Appendix 9.1 for details on instrumentation). During the previous leg MCS data had been collected along this profile by our colleagues from BGR. A preliminary line drawing is reproduced in Figure 6.3.2 (from Gaedicke et al, 2006).
All data were played back following the procedure outlined in section 6.1, and the record sections are shown in Figures 6.3.3 to 6.3.36. The collected data are of high quality.

A preliminary interpretation was attempted on board. 2D ray tracing was used to obtain a geologic model and a velocity-depth model. The resulting model is displayed in Figure 6.3.37. For the starting model the water depth was obtained from the bathymetric measurements and used as seafloor. The wave propagation velocity in the water is constant with 1.5 km/s. The thickness of the sedimentary layers was implemented using the seismic MCS section BGR06-135 obtained from the previous cruise leg (Figure 6.3.2). The sediment thickness is relatively thin (about some 100 m) on top of the oceanic crust in the south-west of the profile, and increases up to 2 km thickness in the trench with seismic P-wave velocities of 1.7 km/s. There are sediment basins of up to 2.5 km thickness (e.g. region between OBS 64 and 02) with recently deposited undisturbed sediment layers along the continental slope with P-wave velocities of 1.7 km/s. The seismic P-wave velocity below the uppermost sediment layers takes values of 2.8 km/s to 4.2 km/s along the continental margin indicating older sediments.

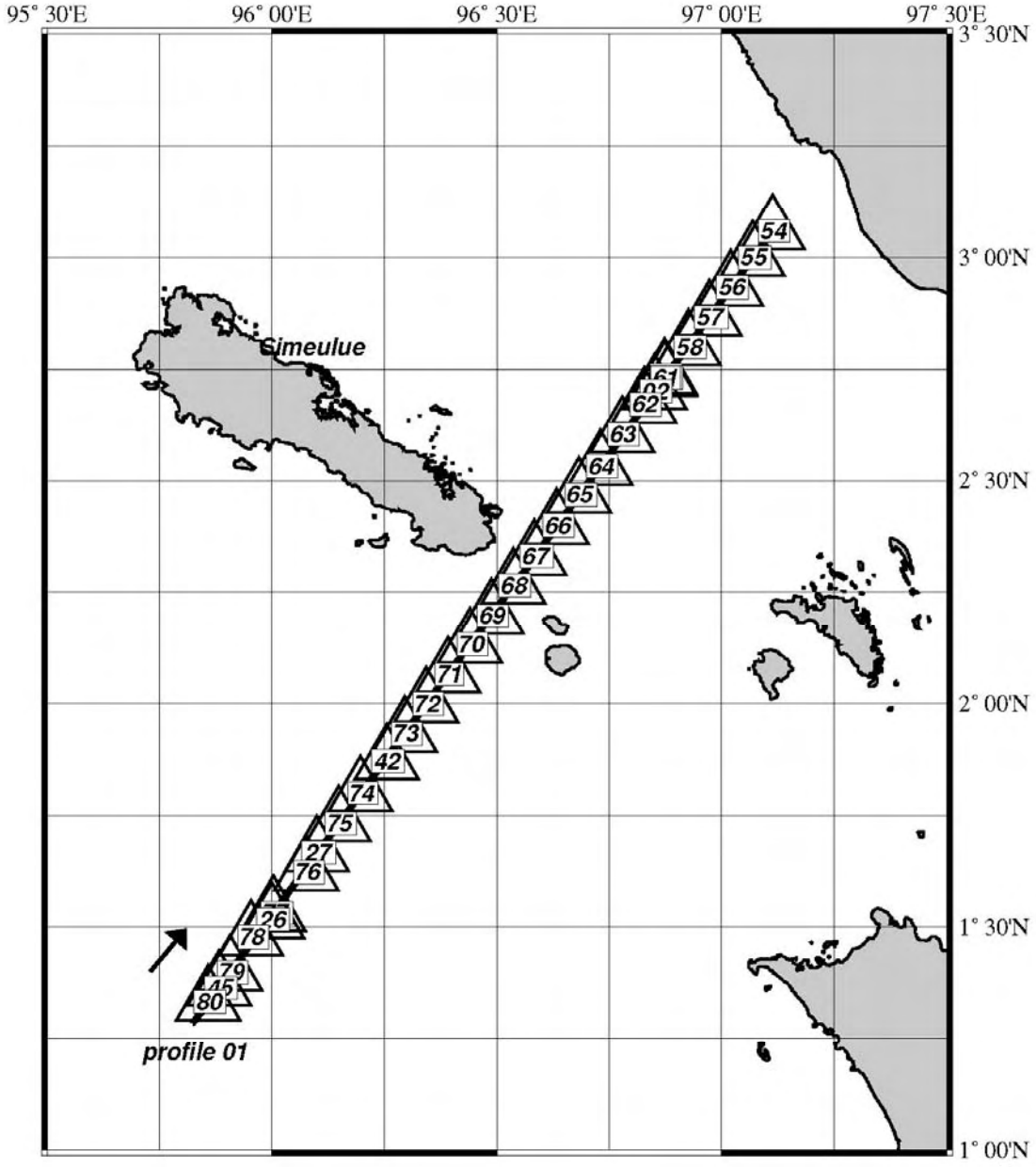

Figure 6.3.1: Location Map

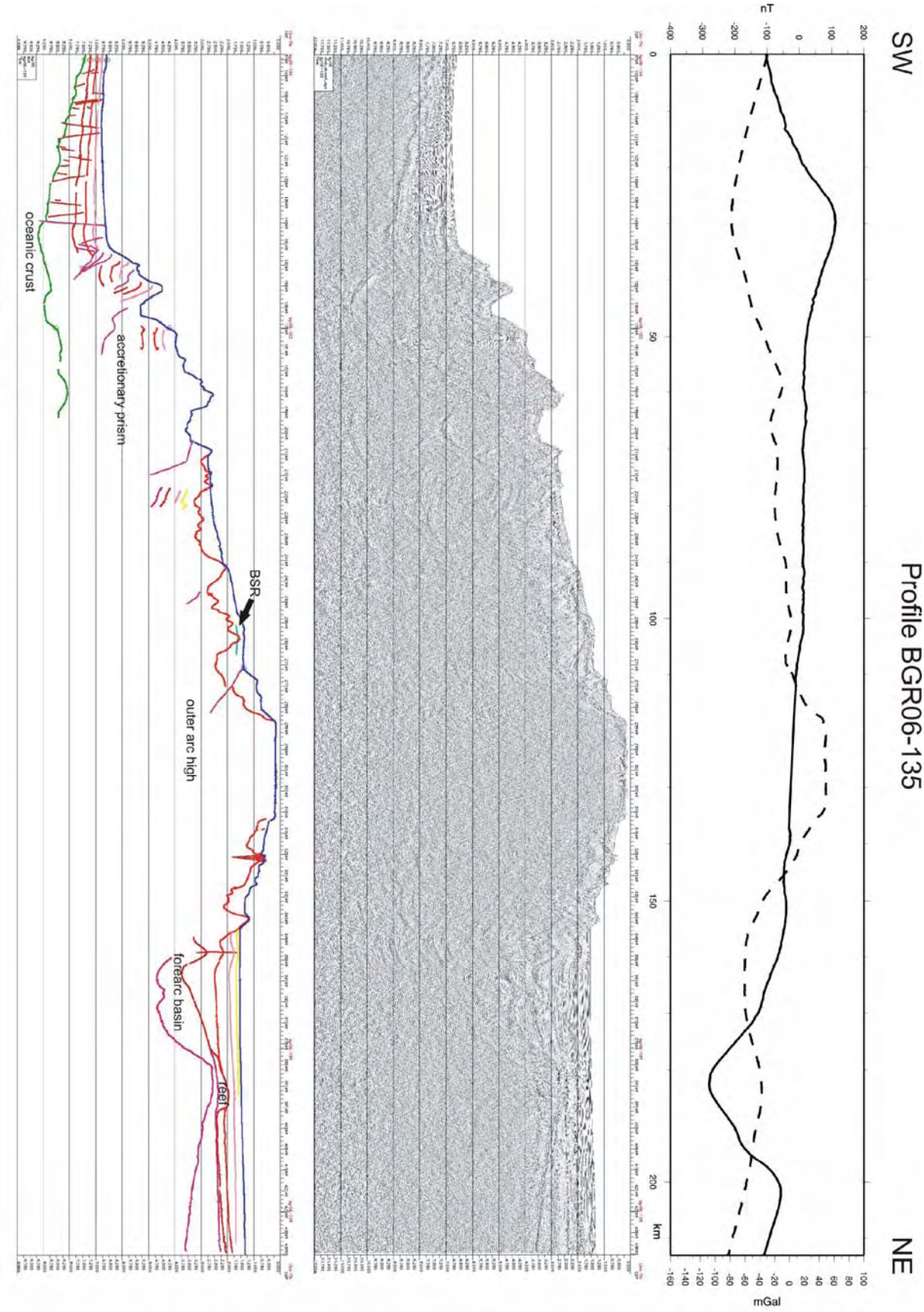

Figure 6.3.2: Line drawing of BGR Profile 06-135, OBS refraction Profile 01.

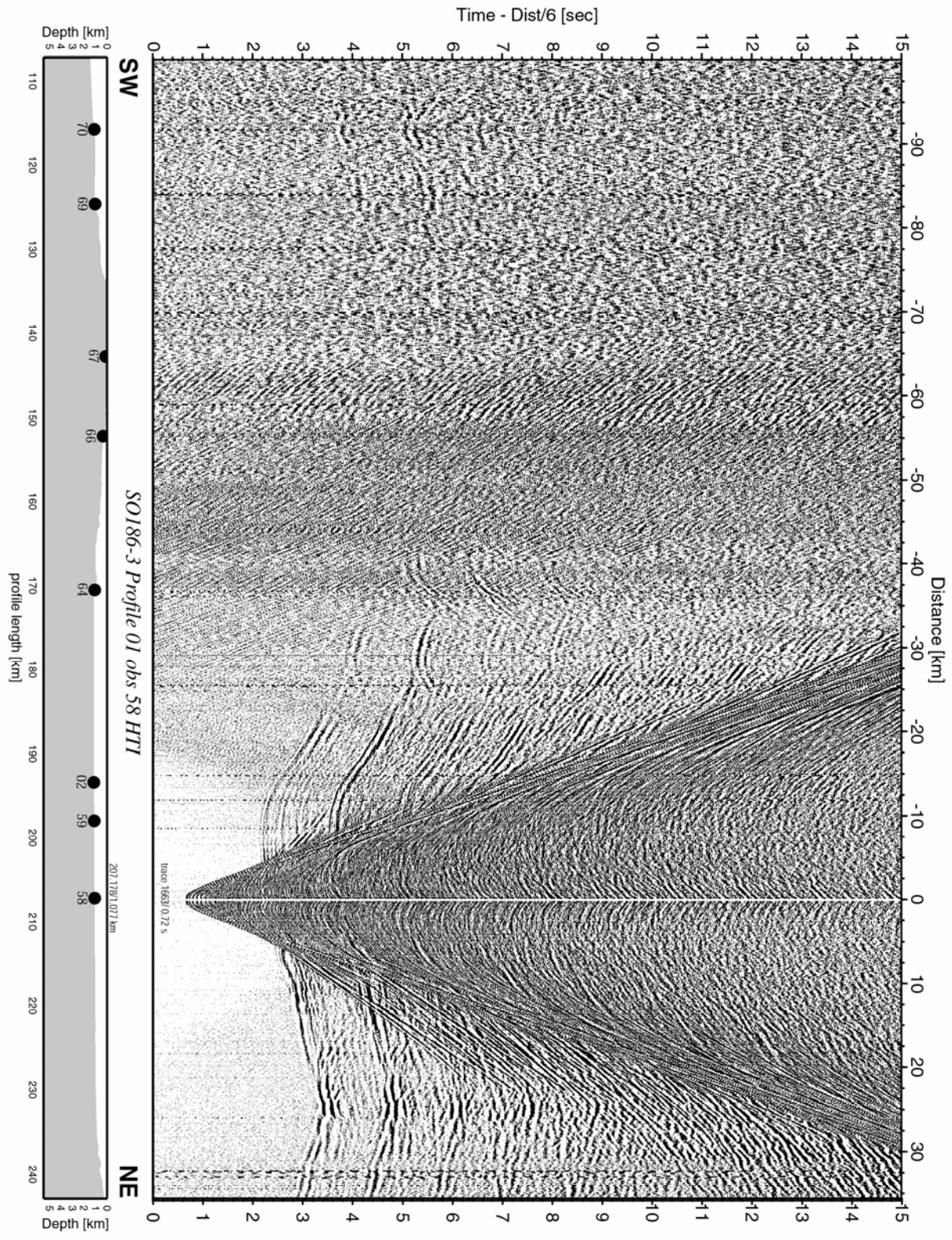

Figure 6.3.3: Record section from obs 58 HTI, Profile 01.

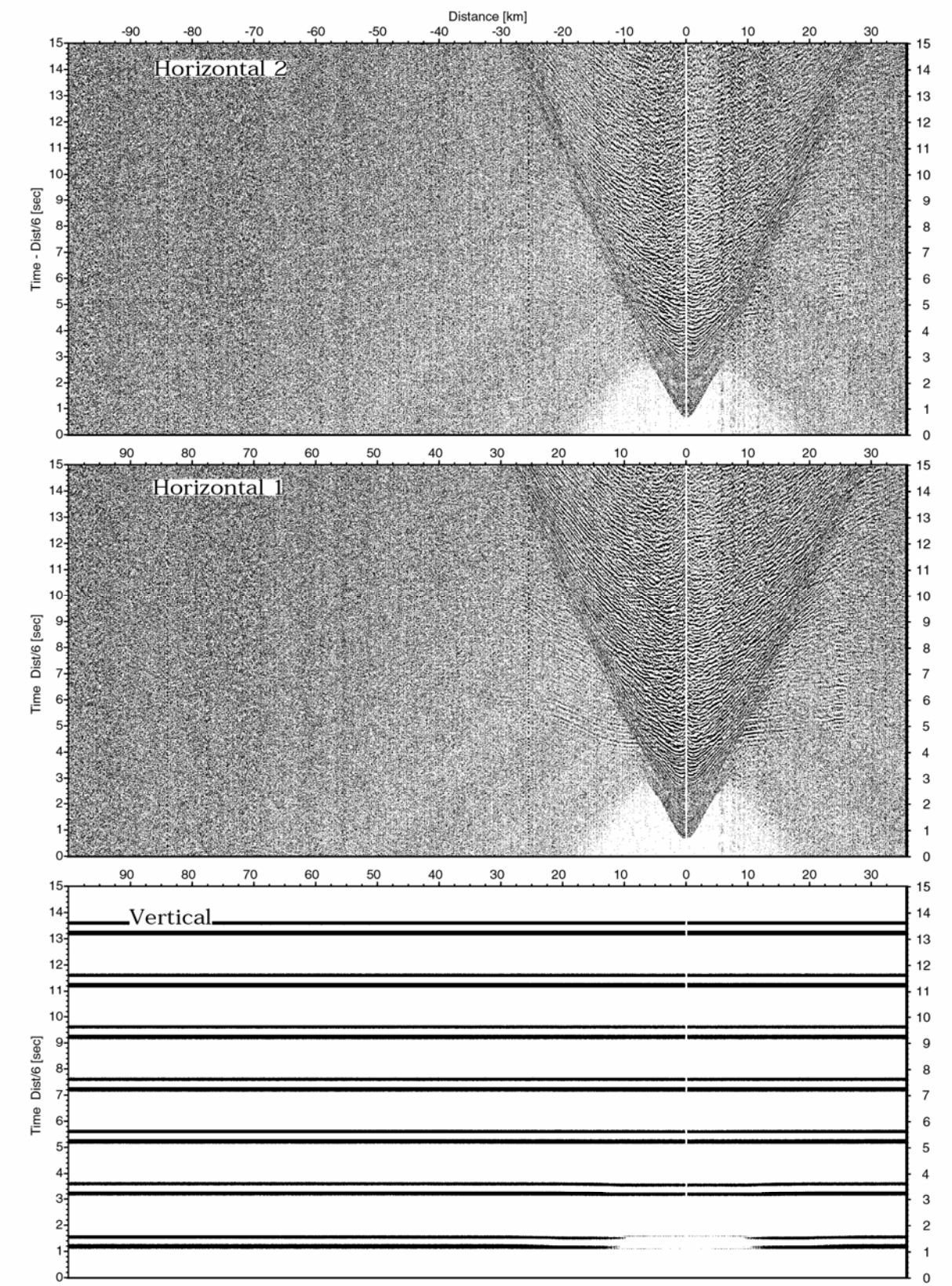

Figure 6.3.4: Record sections from obs 58 HTI/Owen4.5Hz, SO1863 Profile 01.

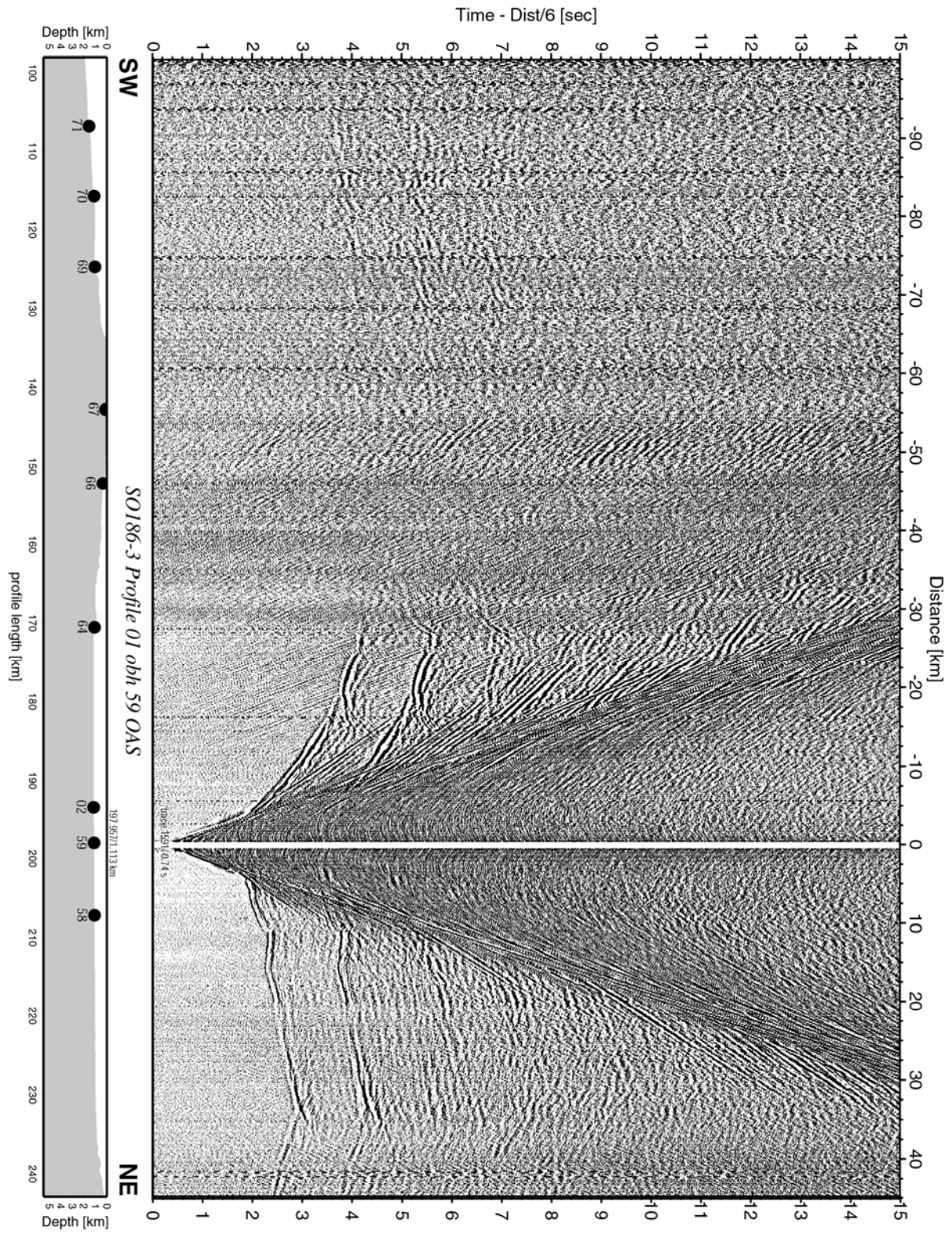

Figure 6.3.5: Record section from obh 59 OAS, Profile 01.

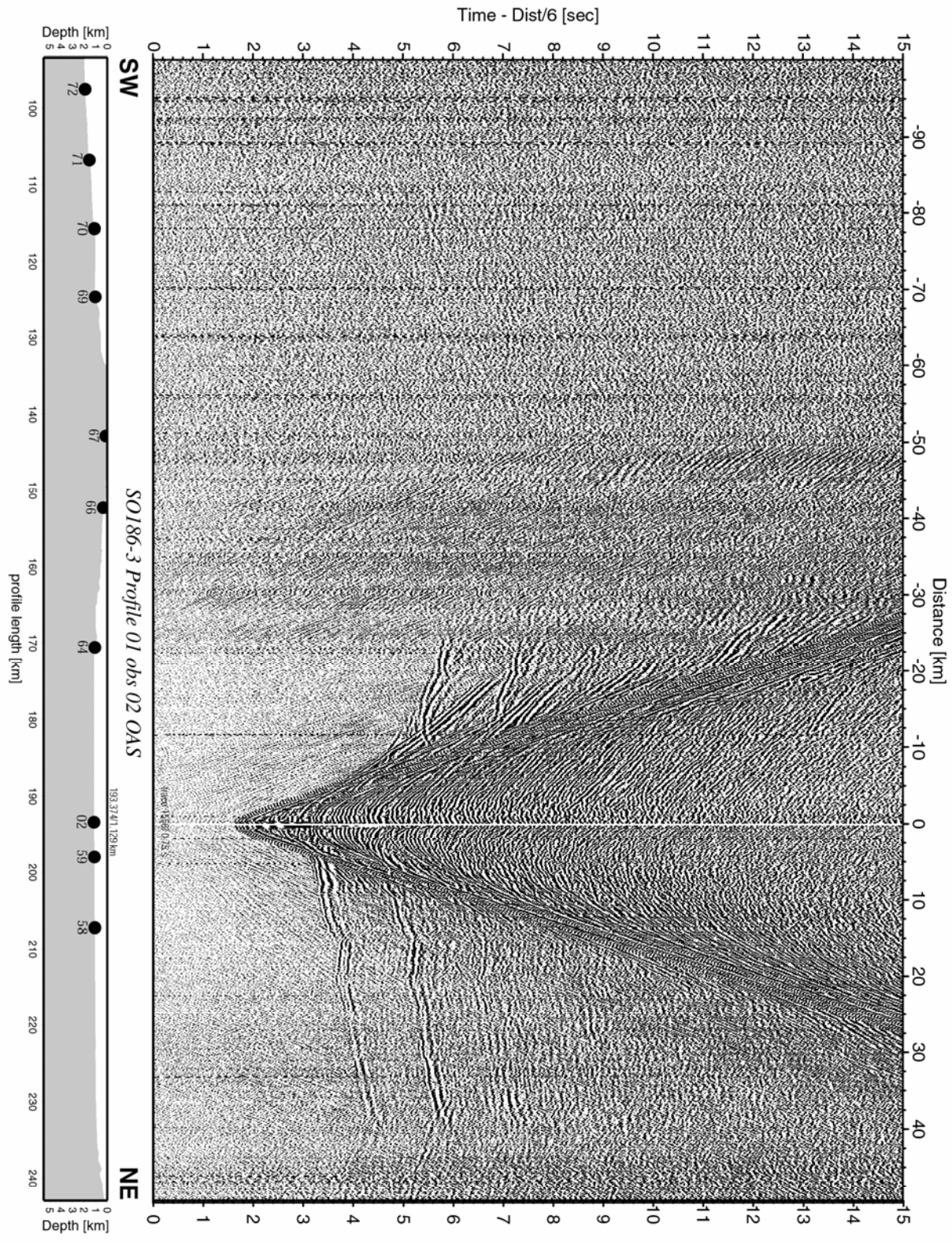

Figure 6.3.6: Record section from obs 02 OAS, Profile 01.

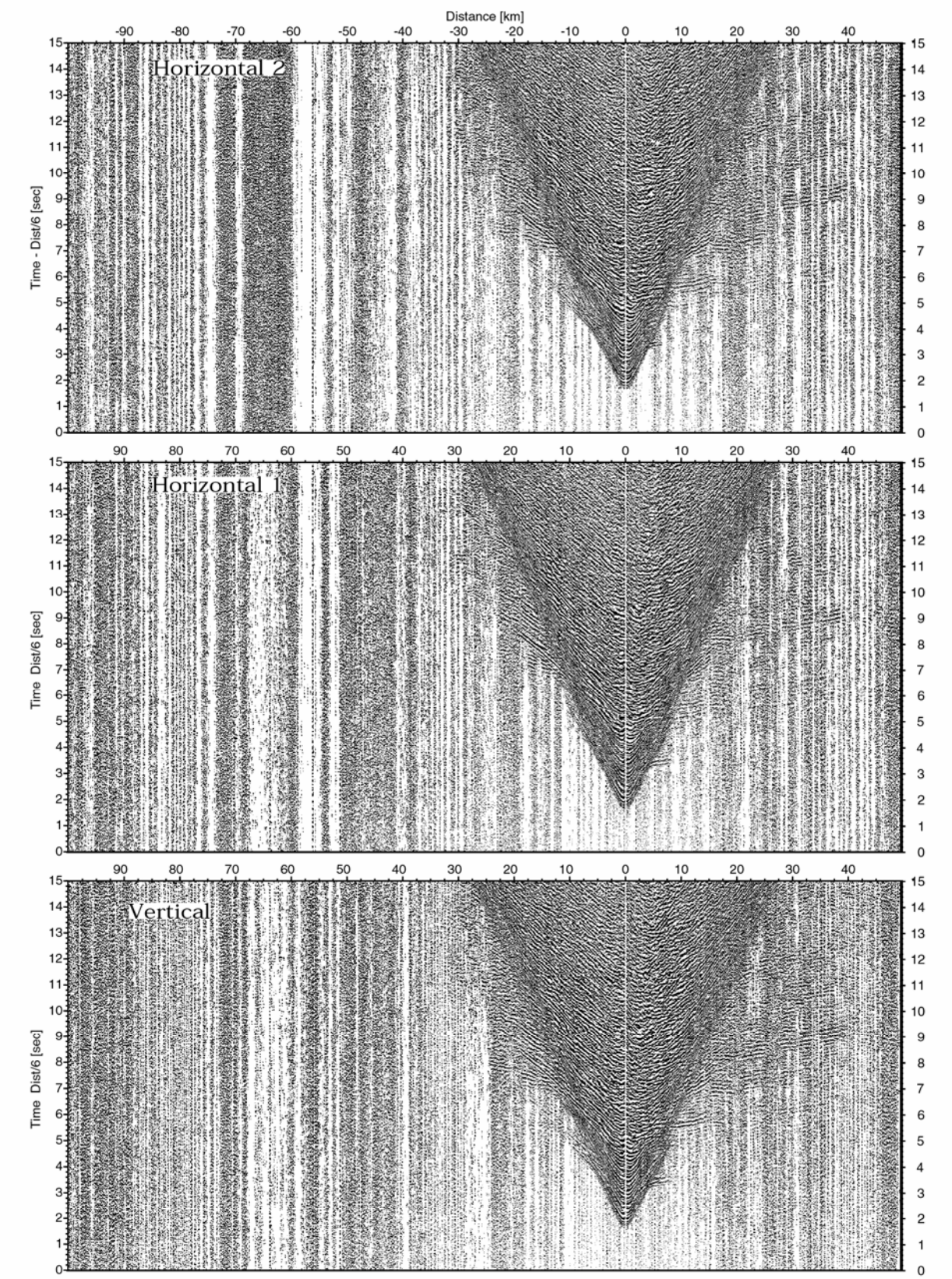

Figure 6.3.7: Record sections from obs 02 OAS/Owen4.5Hz, SO1863 Profile 01.

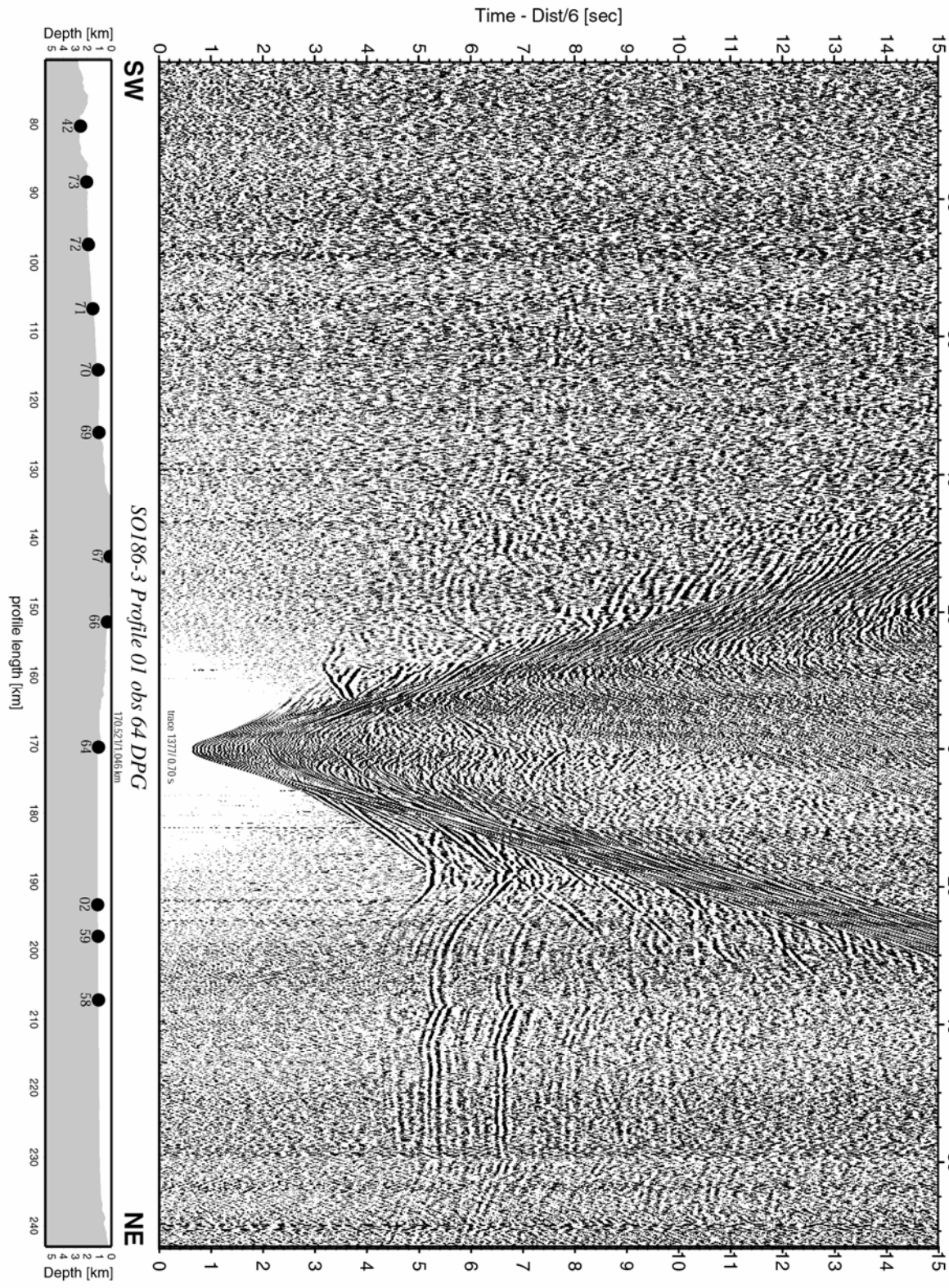

Figure 6.3.8: Record section from obs 64 DPG, Profile 01.

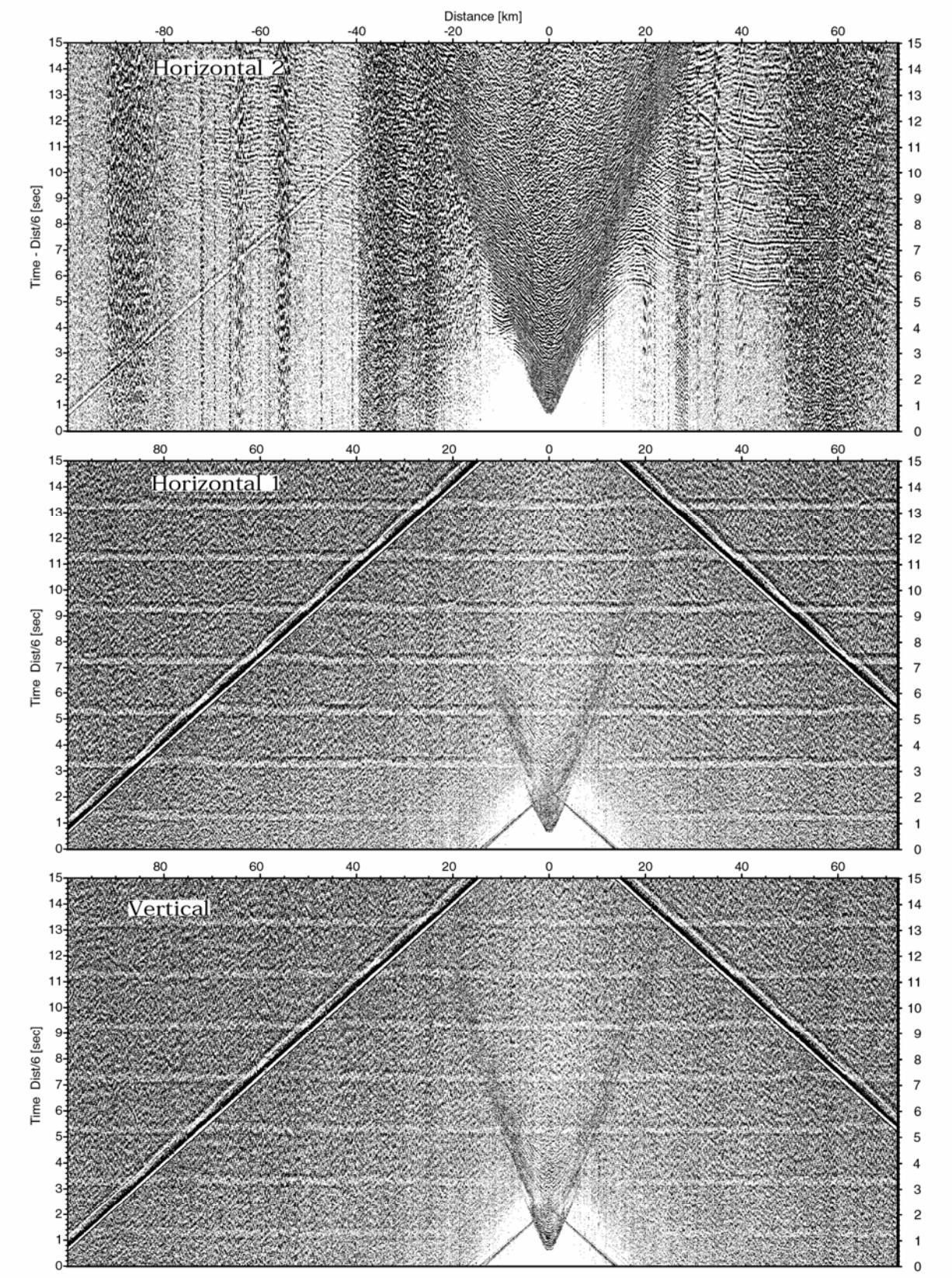

Figure 6.3.9: Record sections from obs 64 DPG/Owen4.5Hz, SO1863 Profile 01.

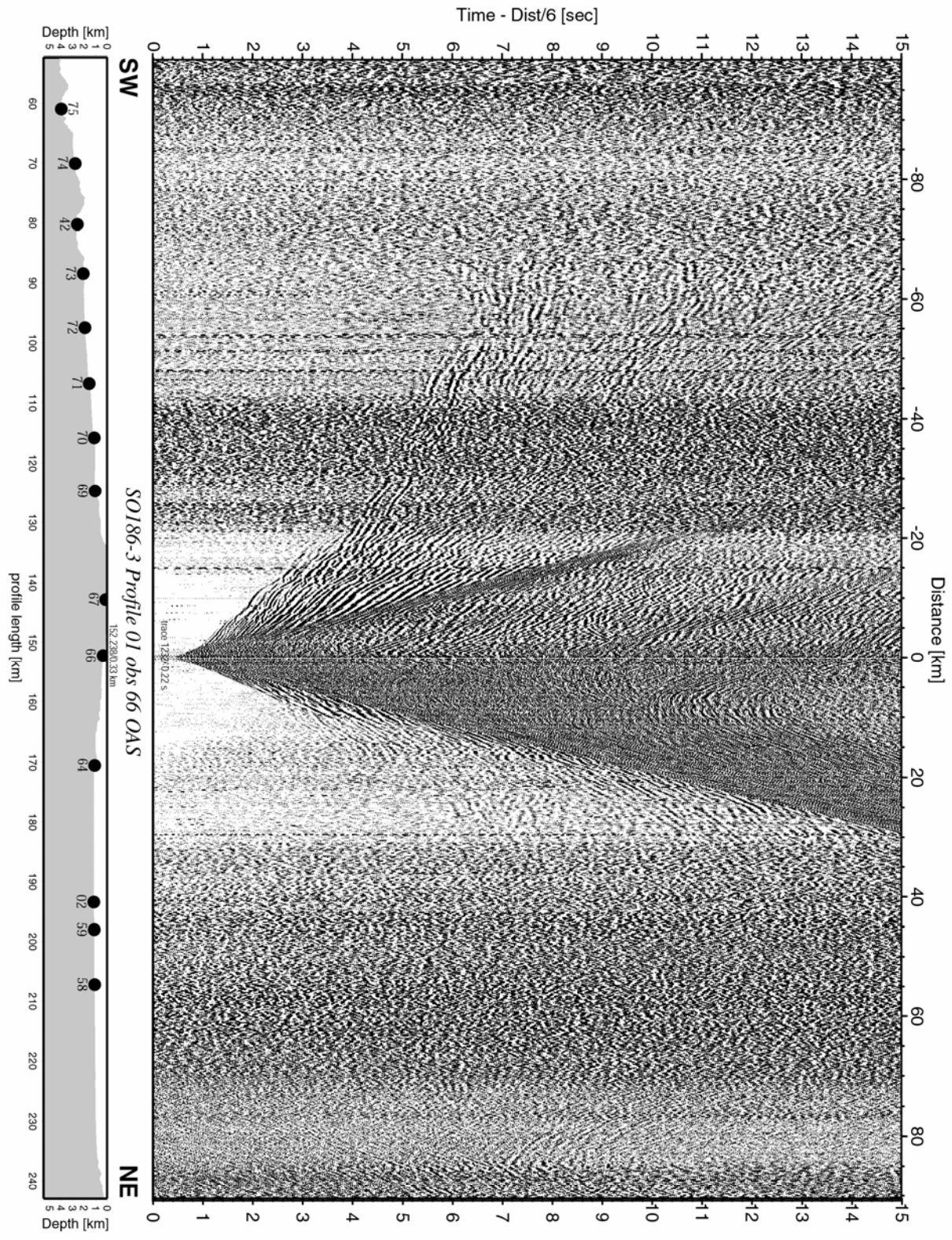

Figure 6.3.10: Record section from obs 66 OAS, Profile 01.

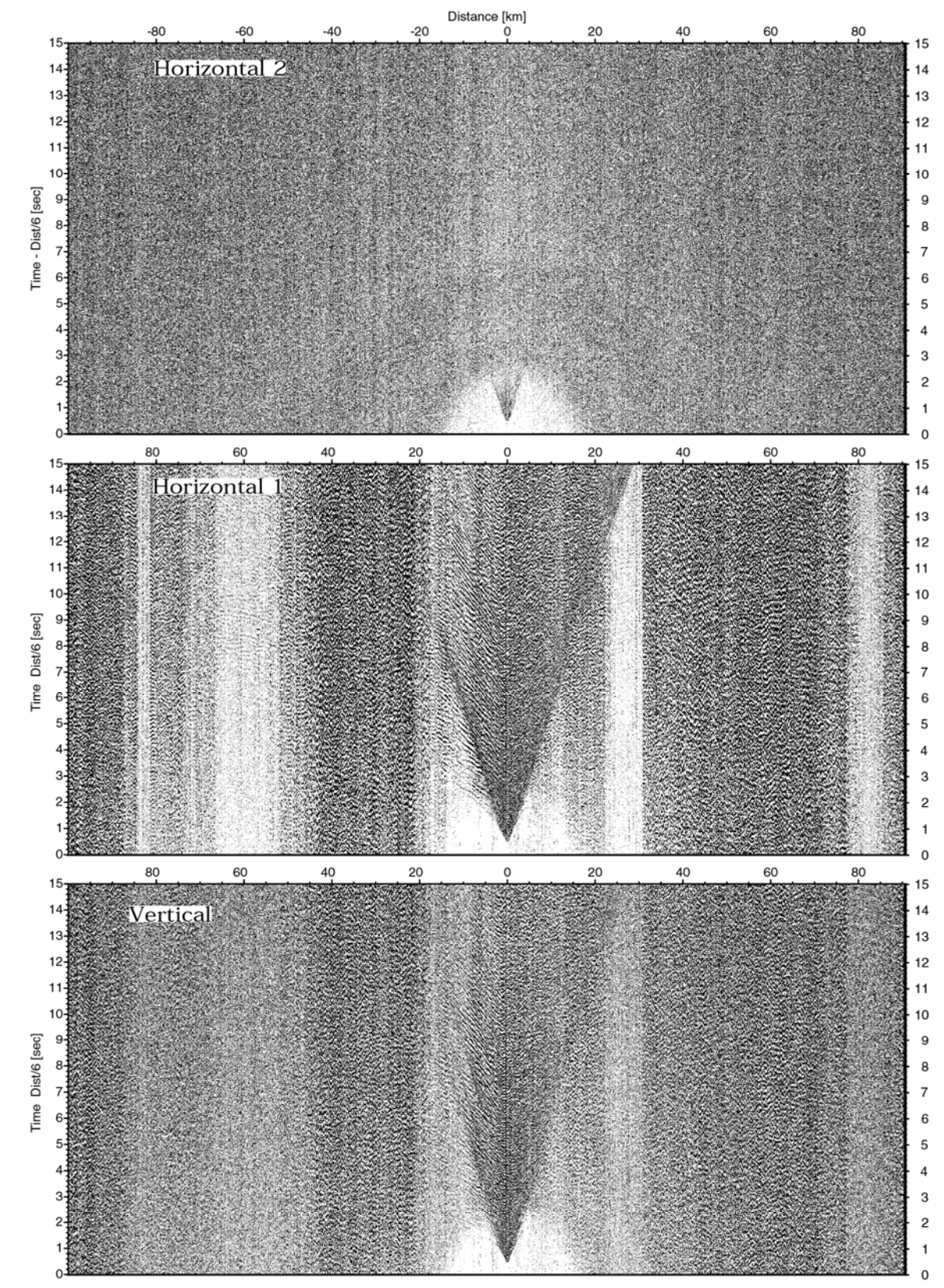

Figure 6.3.11: Record sections from obs 66 OAS/Owen4.5Hz, SO1863 Profile 01.

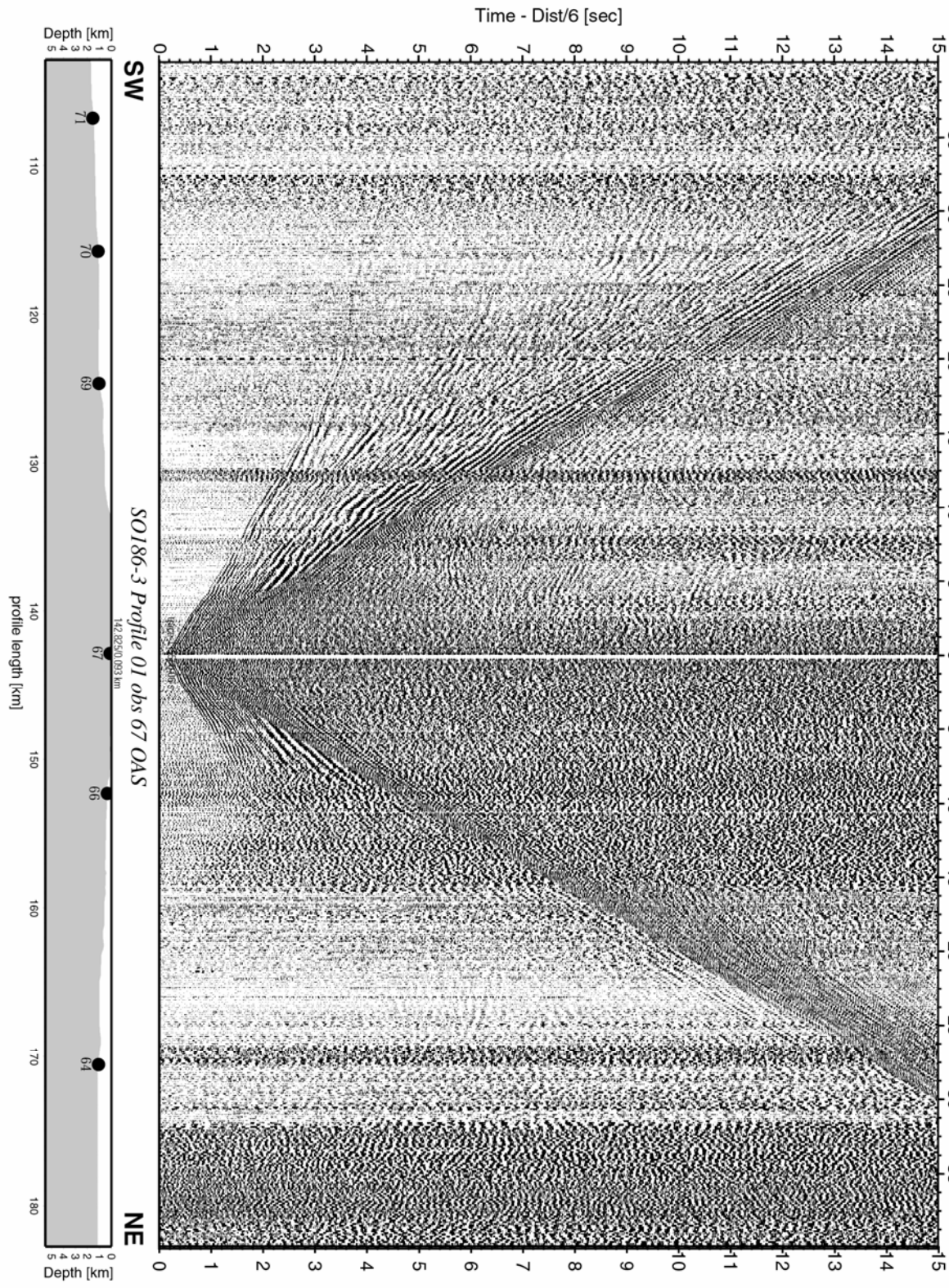

Figure 6.3.12: Record section from obs 67 OAS, Profile 01.

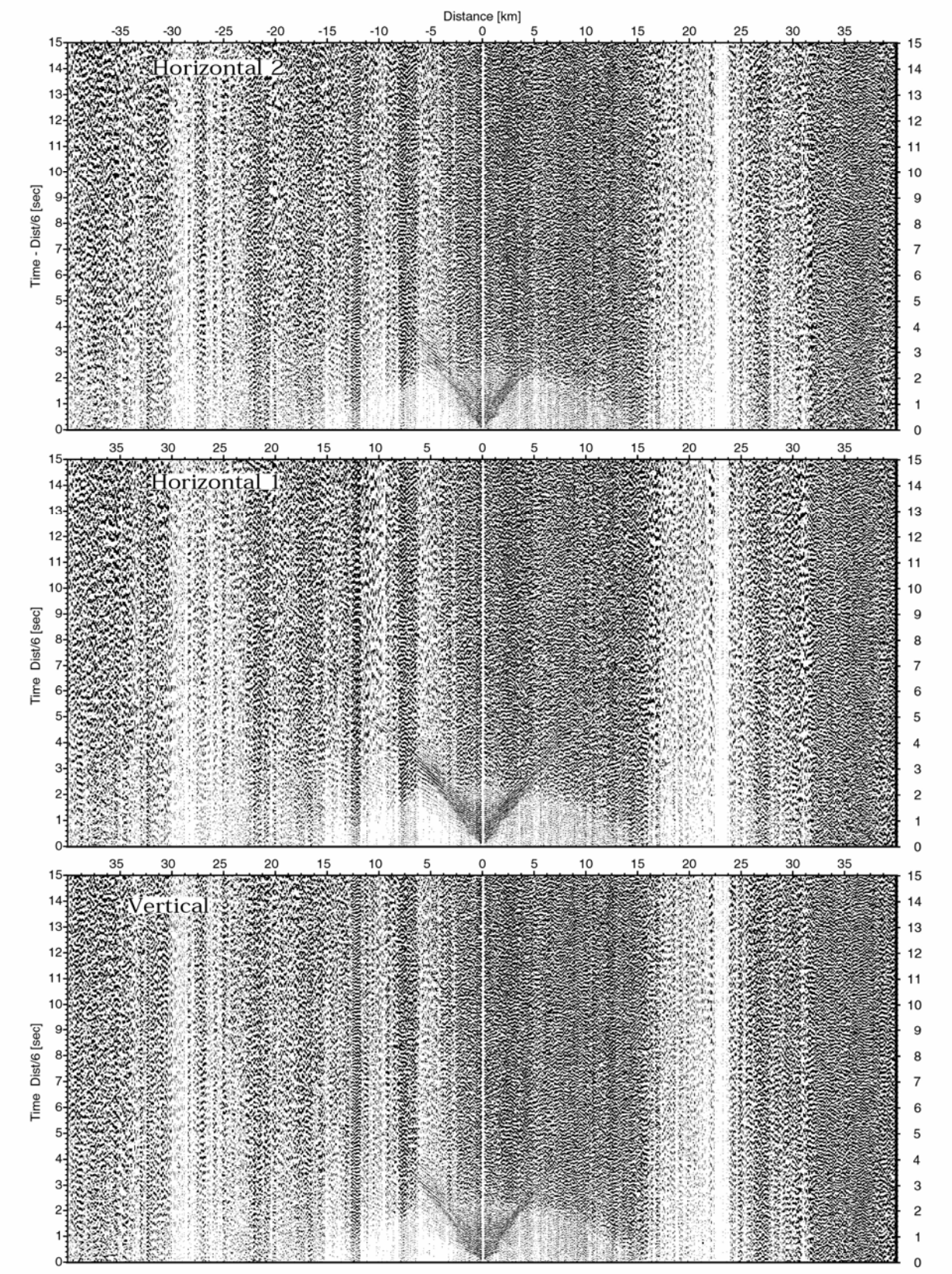

Figure 6.3.13: Record sections from obs 67 OAS/Owen4.5Hz, SO1863 Profile 01.

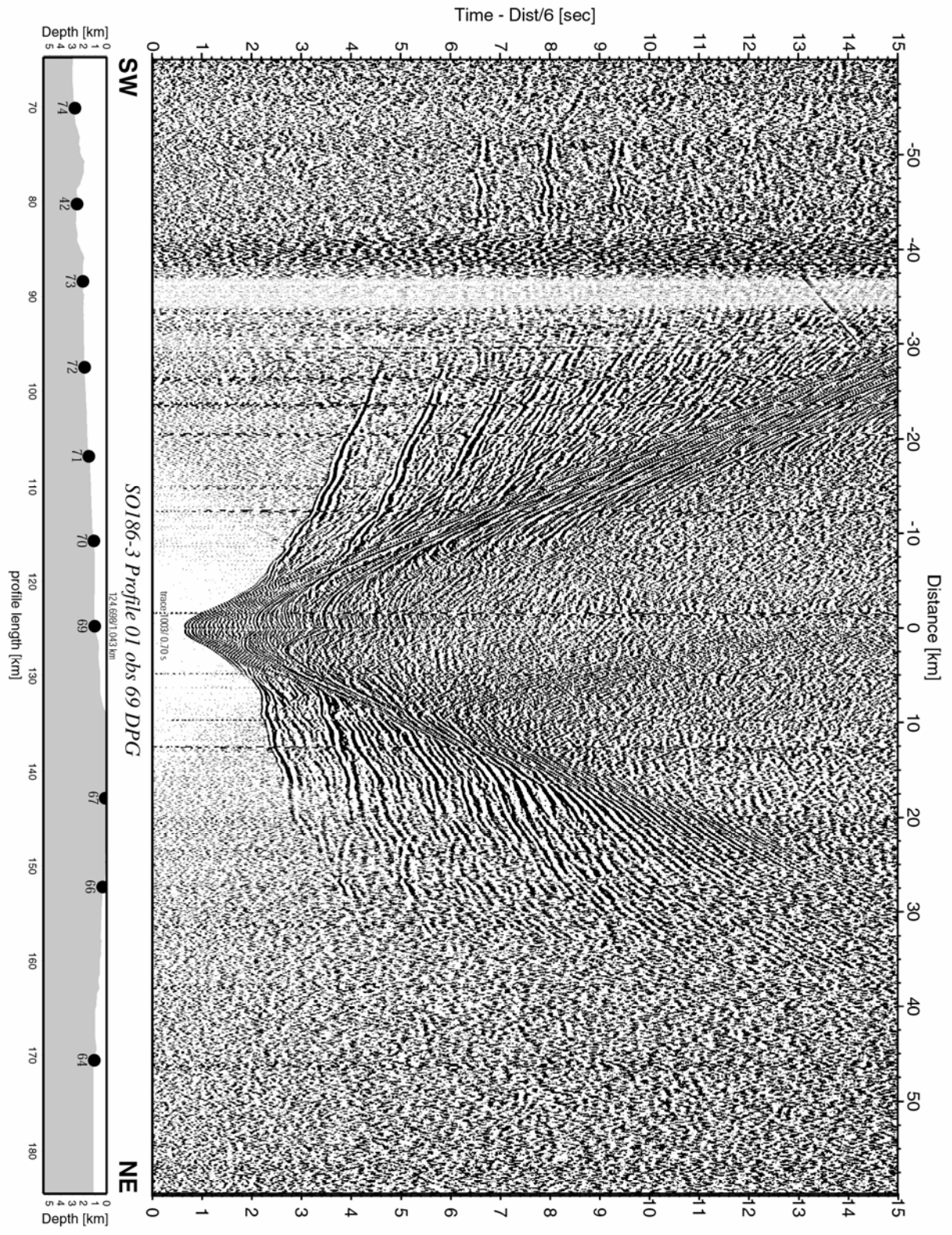

Figure 6.3.14: Record section from obs 69 DPG, Profile 01.

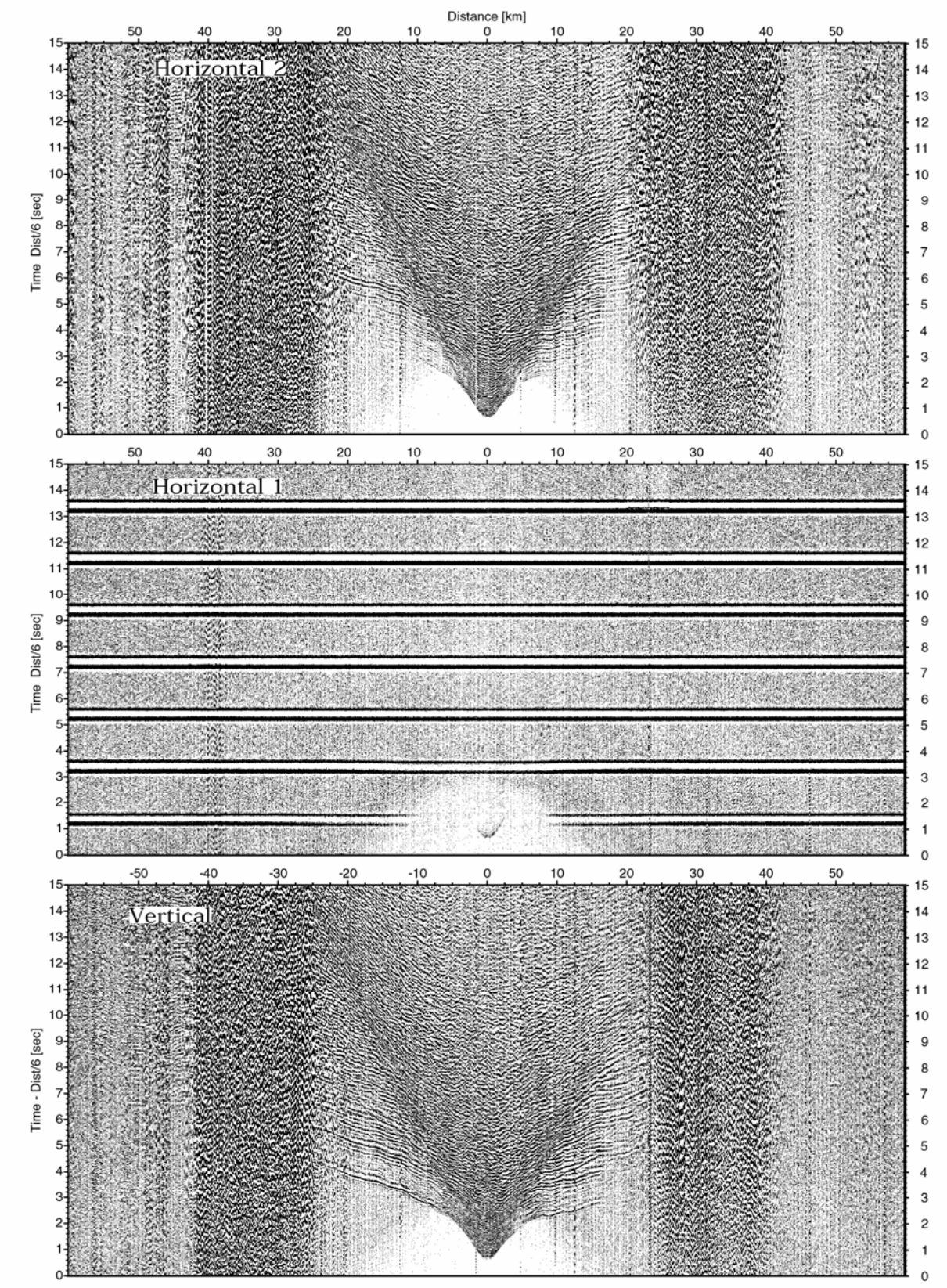

Figure 6.3.15: Record sections from obs 69 DPG/Guralp, SO1863 Profile 01.

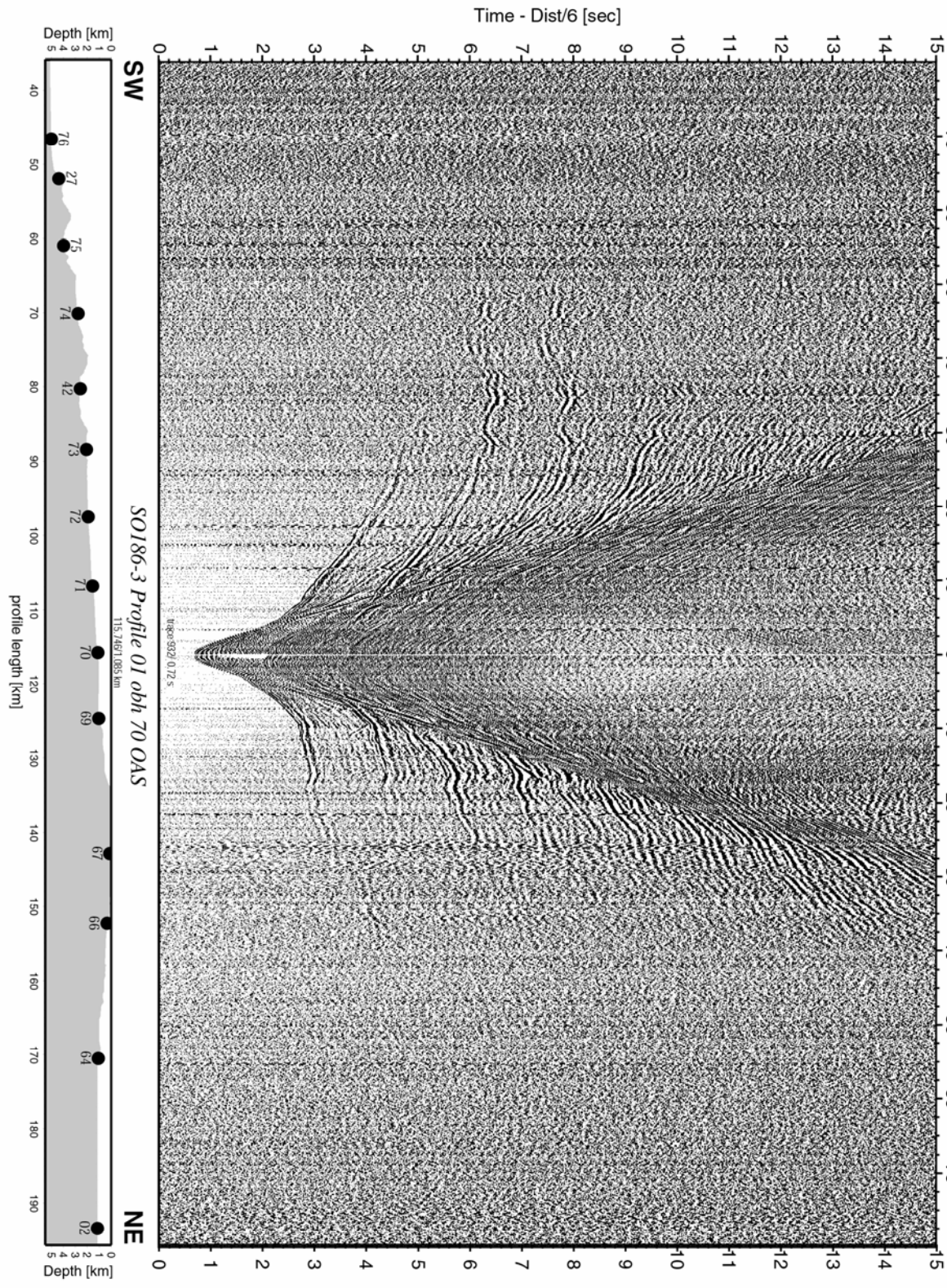

Figure 6.3.16: Record section from obh 70 OAS, Profile 01.

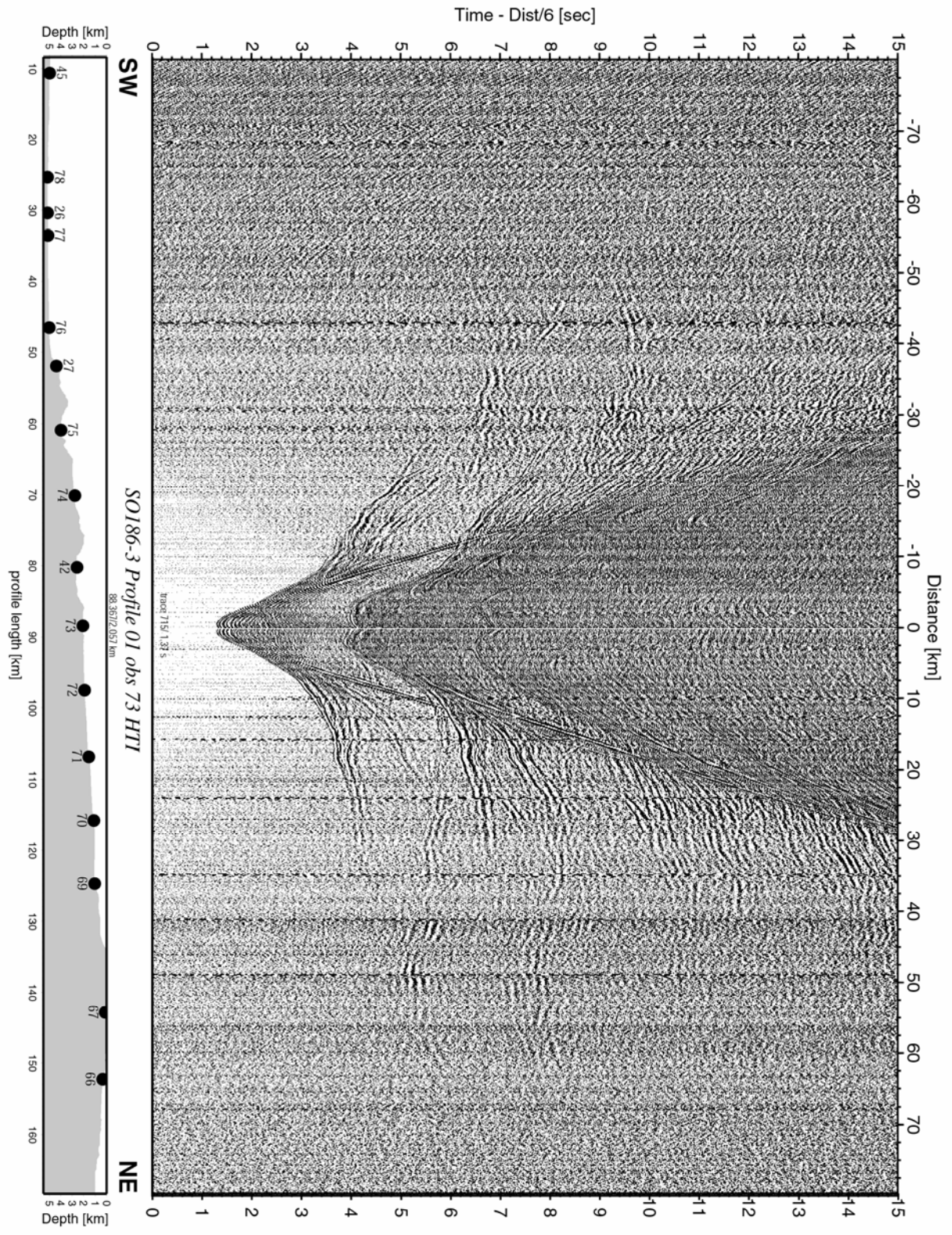

Figure 6.3.17: Record section from obs 73 HTI, Profile 01.

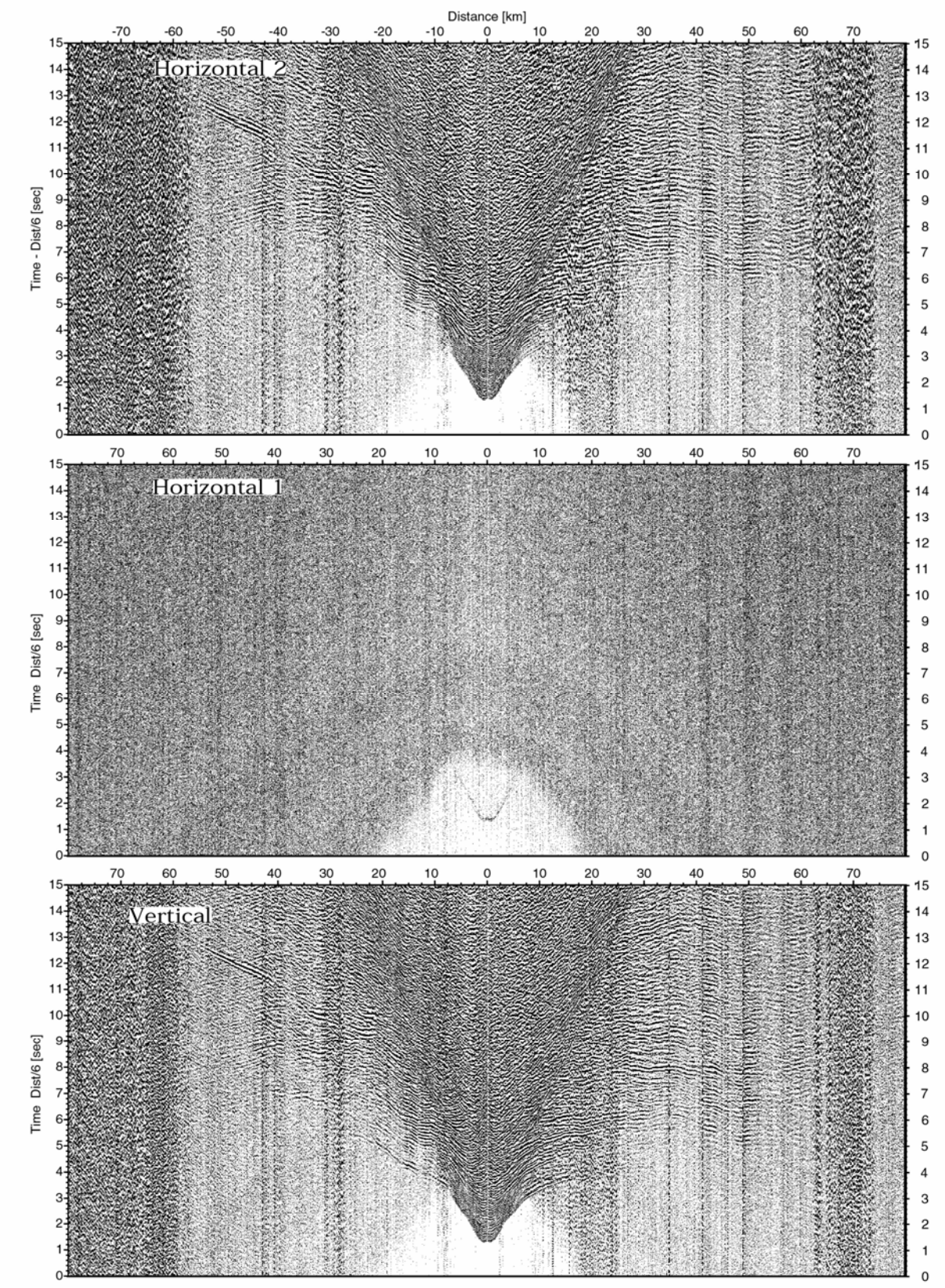

Figure 6.3.18: Record sections from obs 73 HTI/Owen4.5Hz, SO1863 Profile 01.

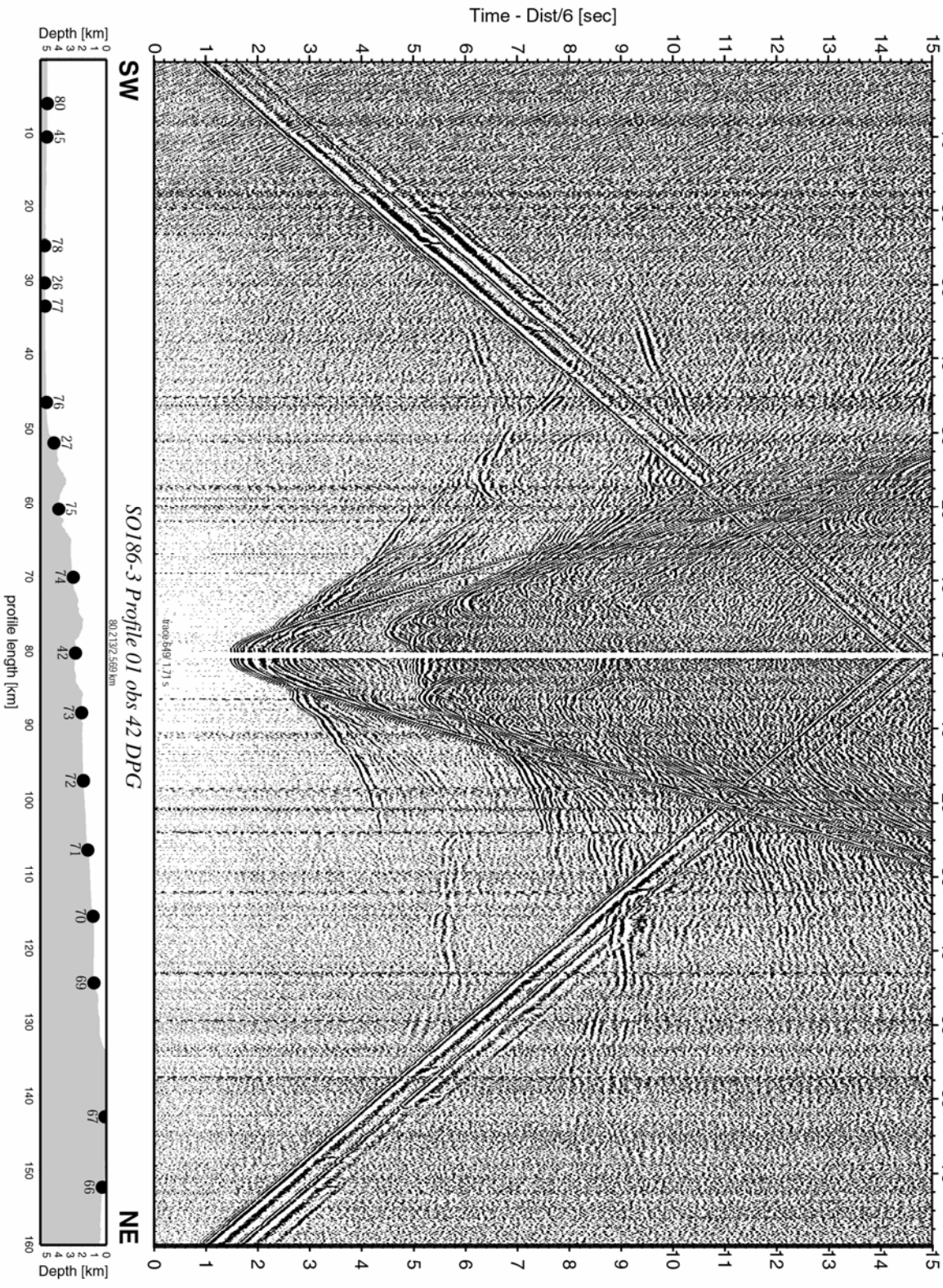

Figure 6.3.19: Record section from obs 42 DPG, Profile 01.

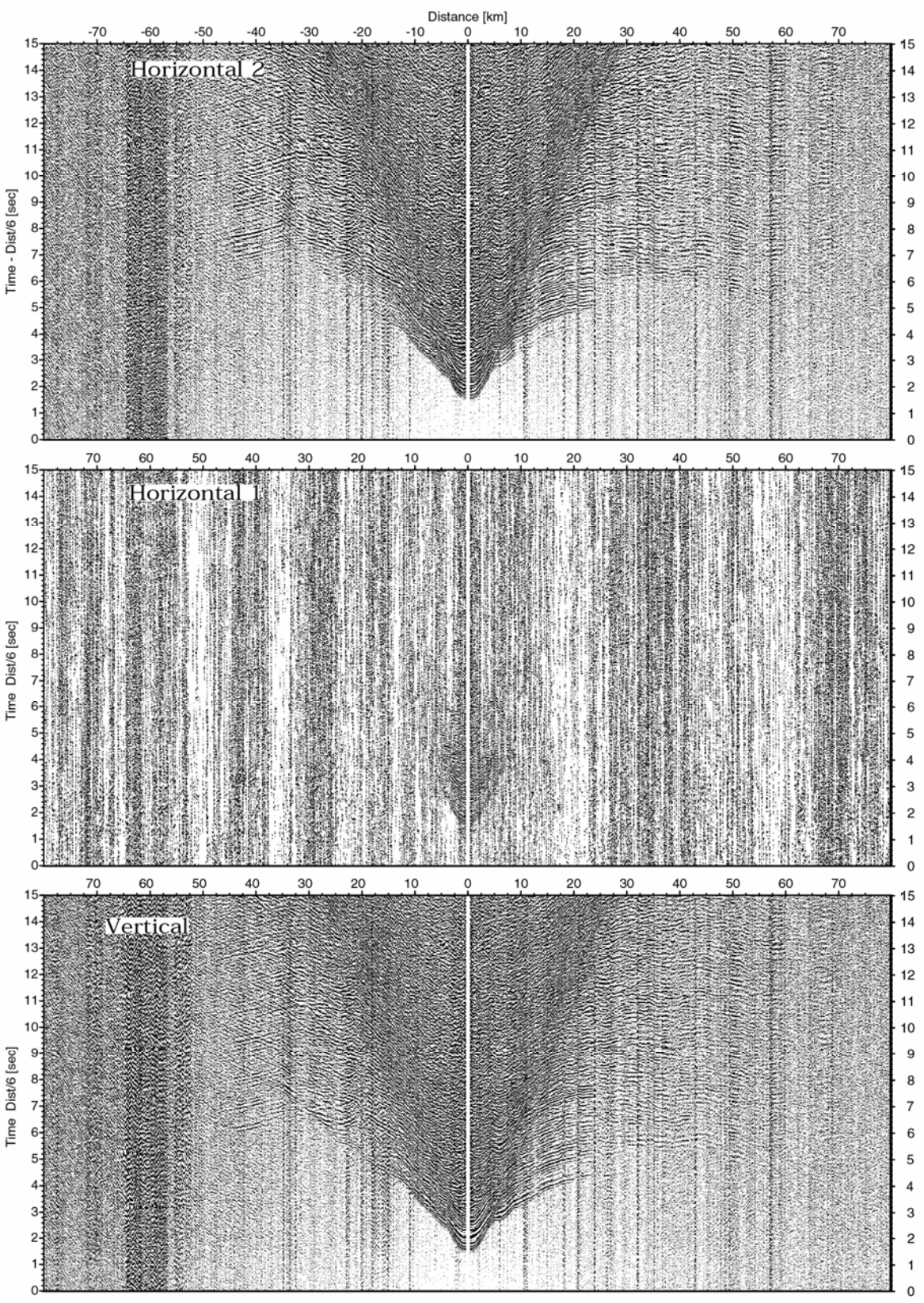

Figure 6.3.20: Record sections from obs 42 DPG/Owen4.5Hz, SO1863 Profile 01.

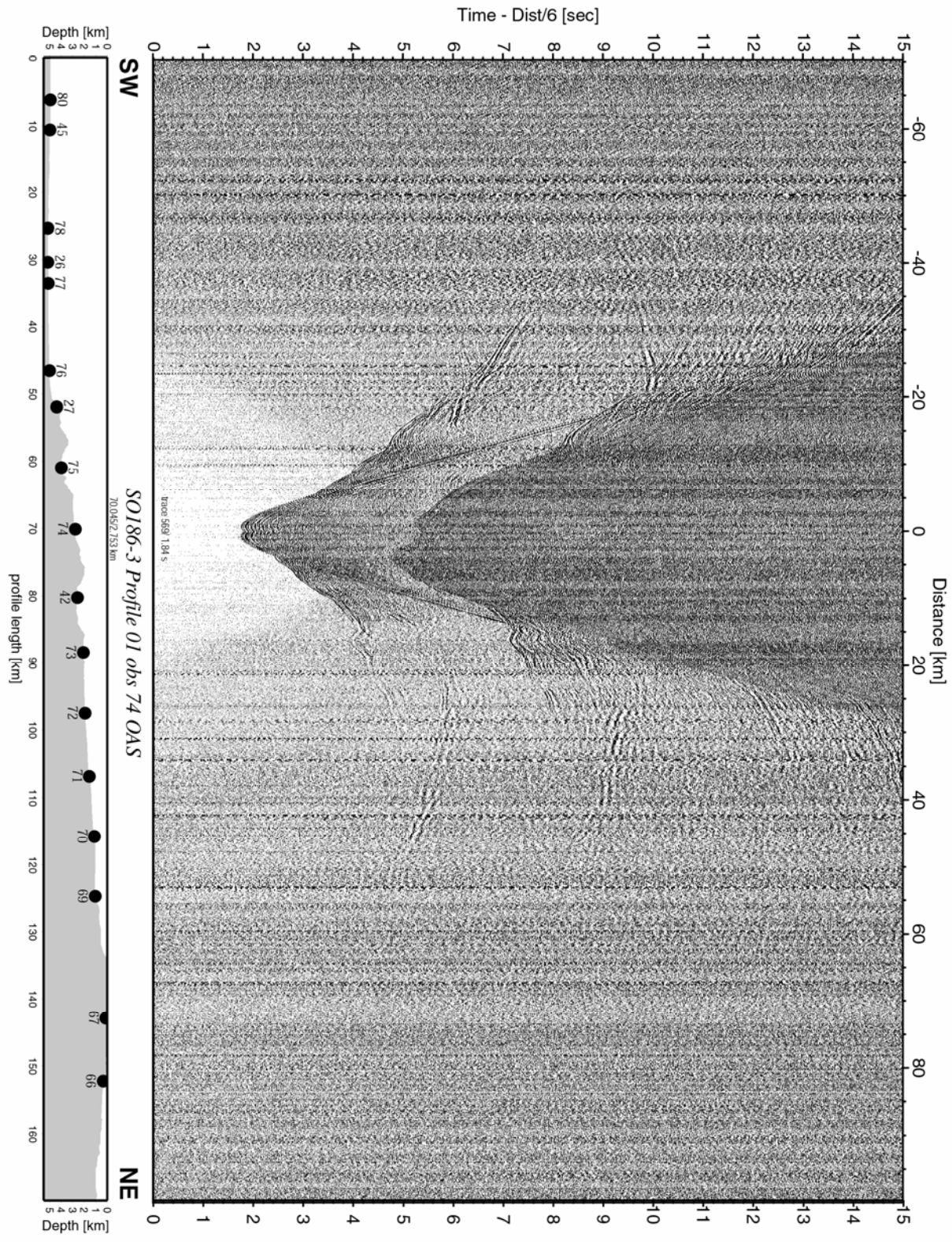

Figure 6.3.21: Record section from obs 74 OAS, Profile 01.

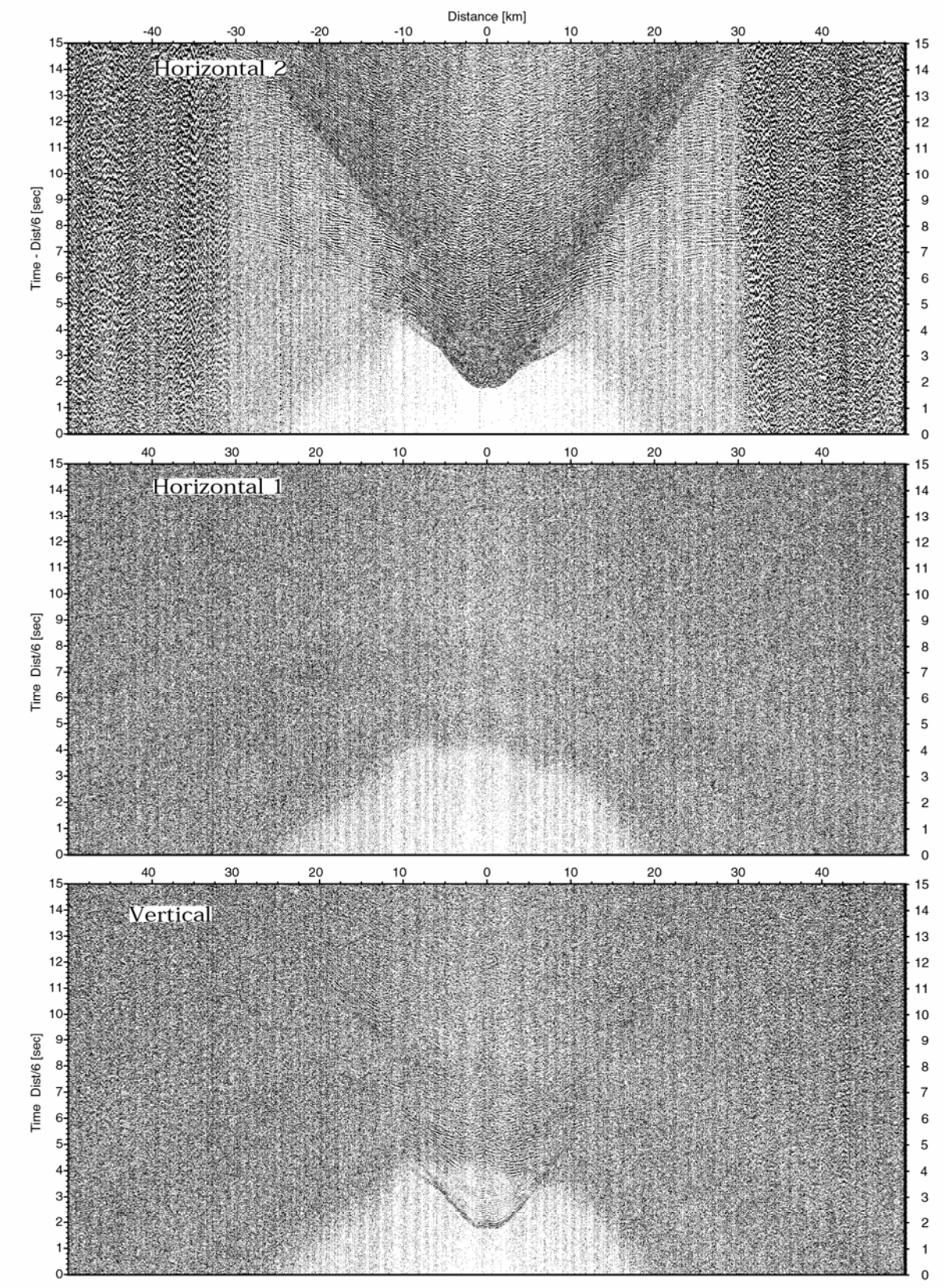

Figure 6.3.22: Record sections from obs 74 OAS/Owen4.5Hz, SO1863 Profile 01.

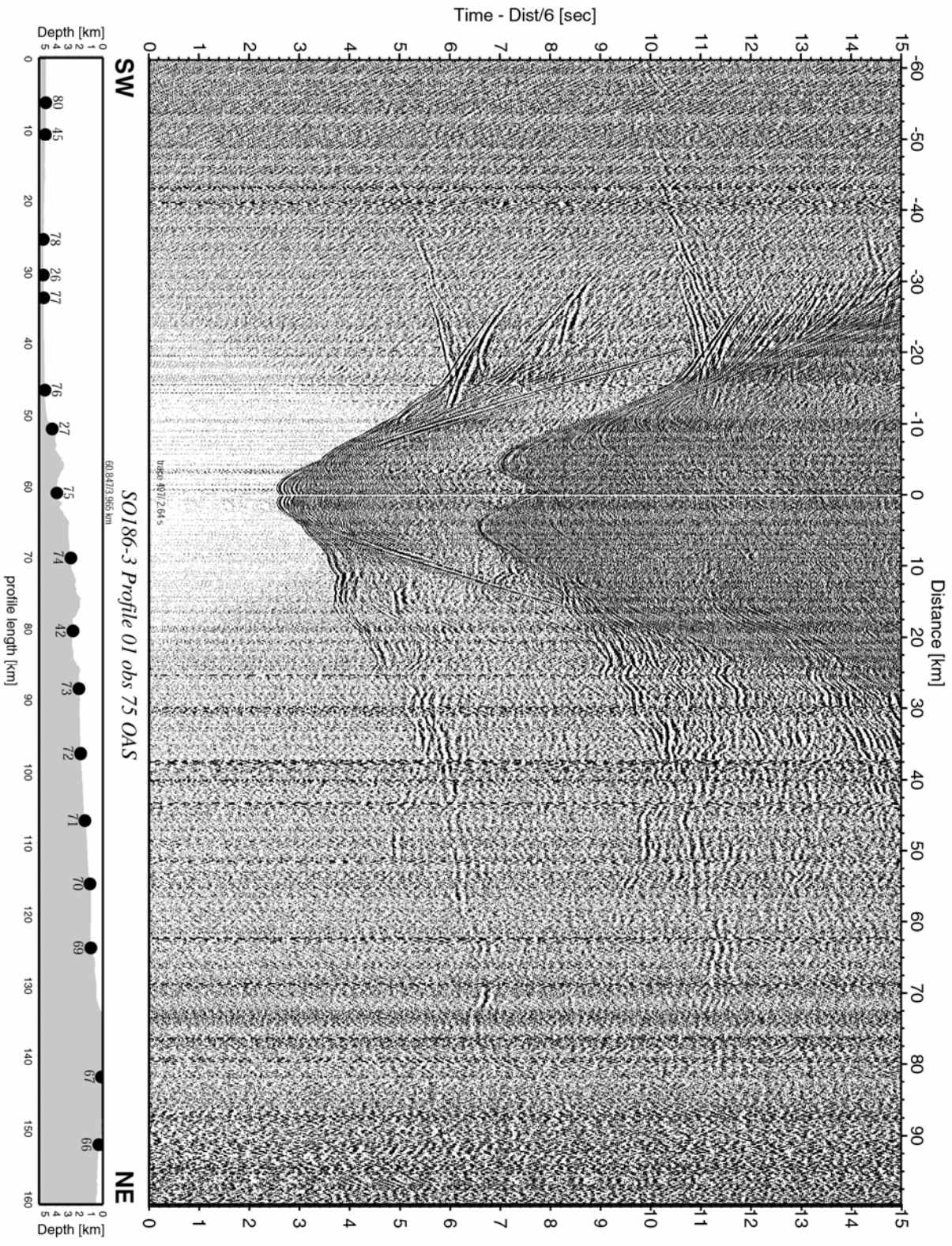

Figure 6.3.23: Record section from obs 75 OAS, Profile 01.

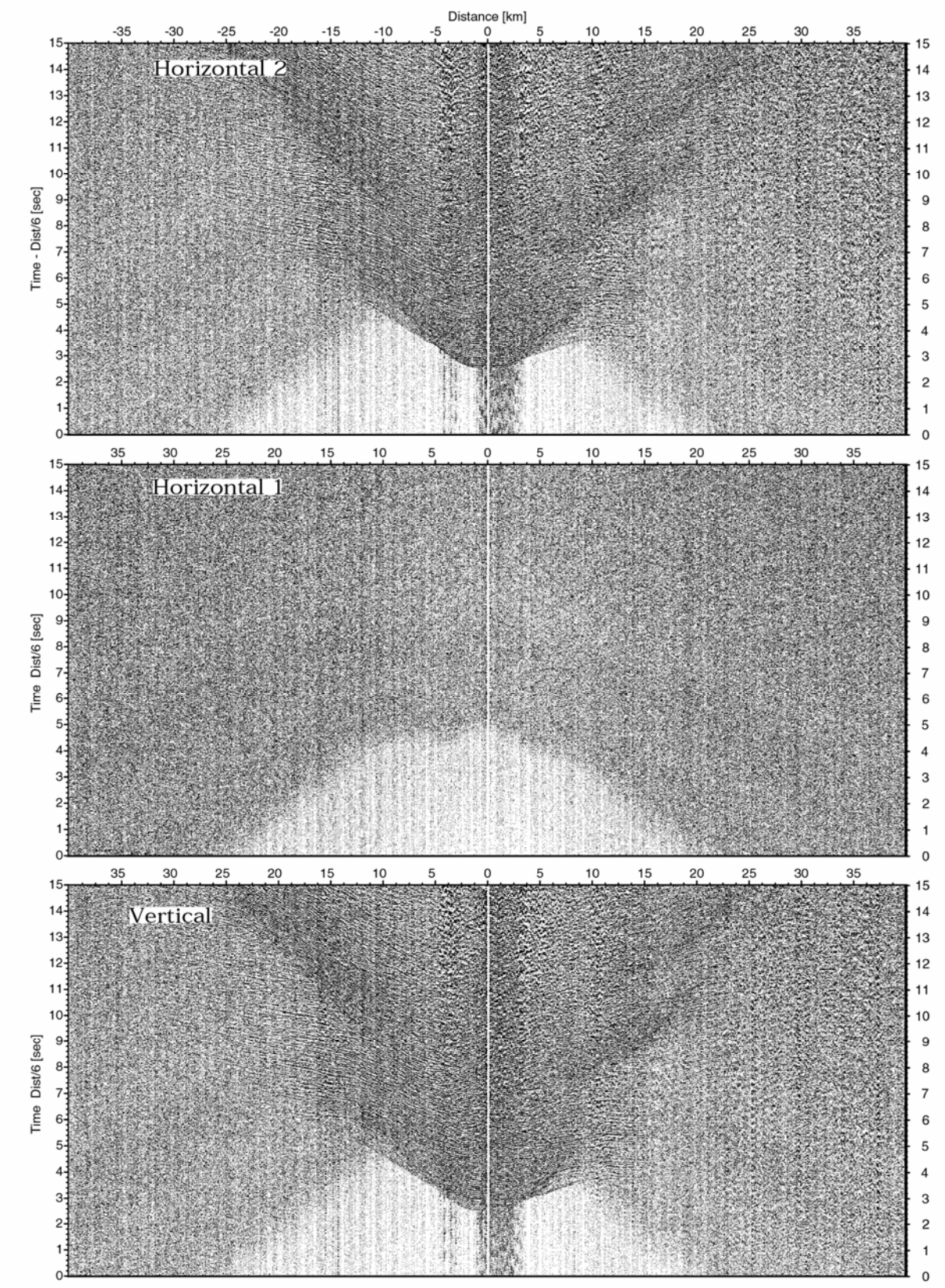

Figure 6.3.24: Record sections from obs 75 OAS/Owen4.5Hz, SO1863 Profile 01.

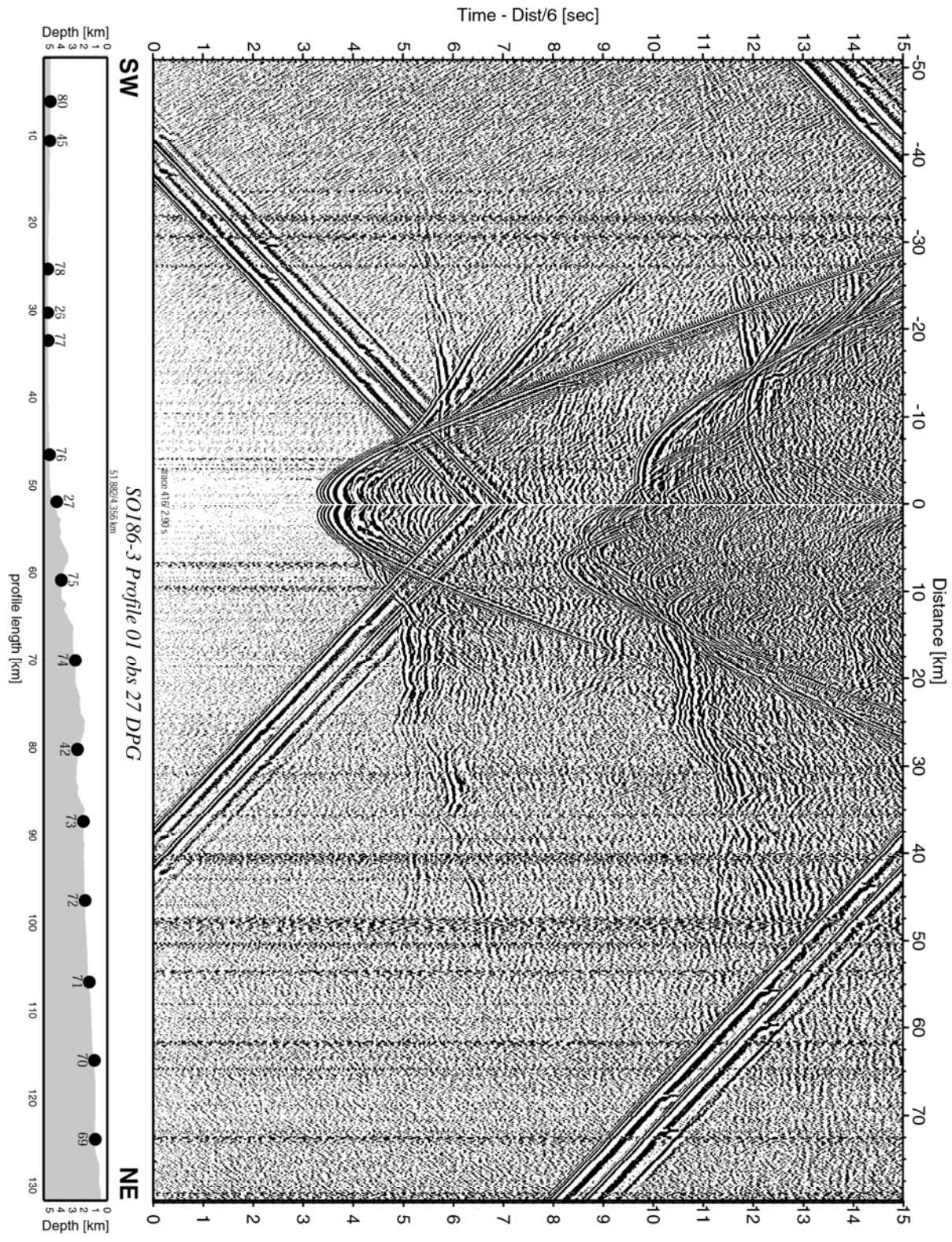

Figure 6.3.25: Record section from obs 27 DPG, Profile 01.

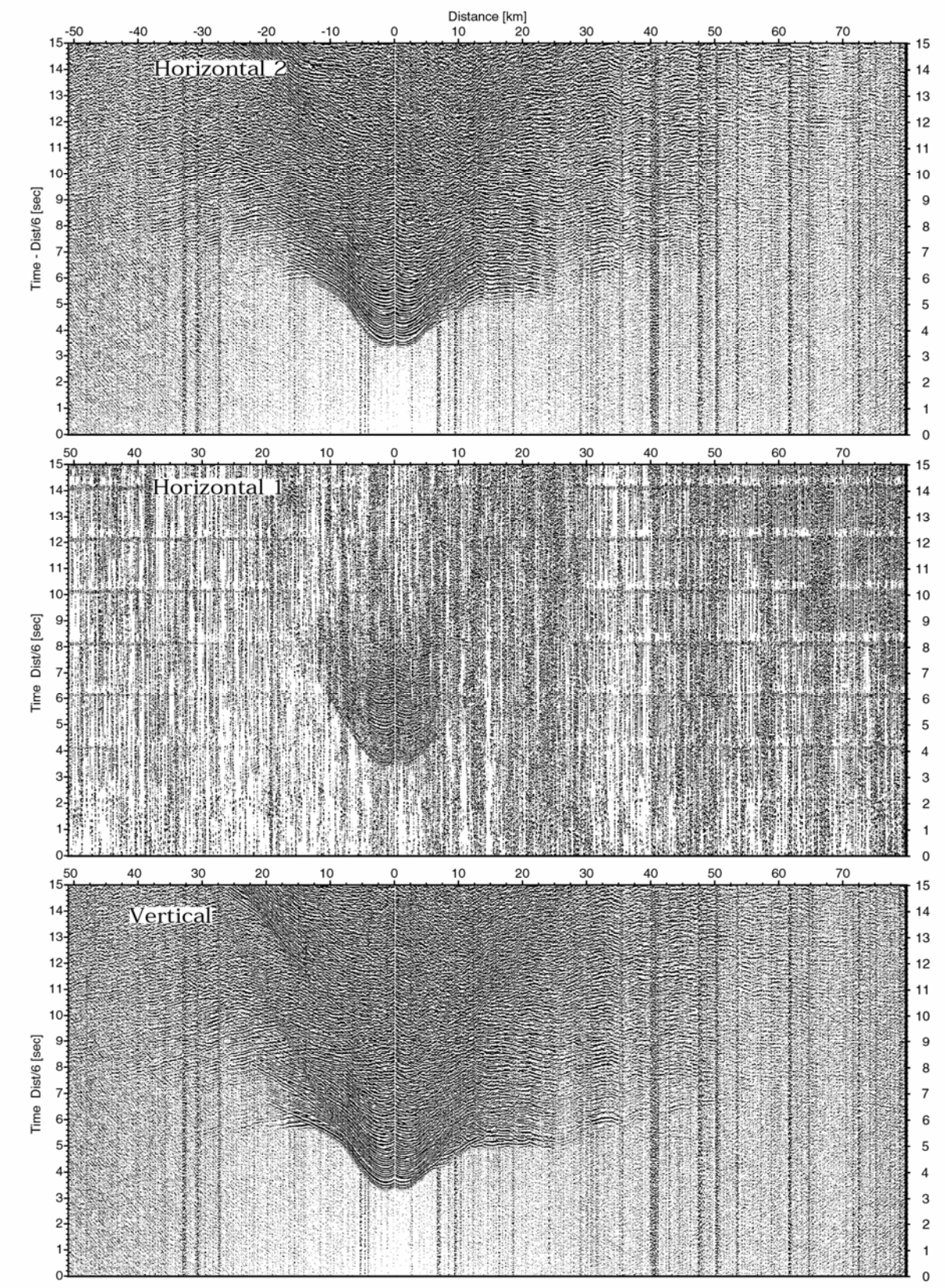

Figure 6.3.26: Record sections from obs 27 DPG/Owen4.5Hz, SO1863 Profile 01.

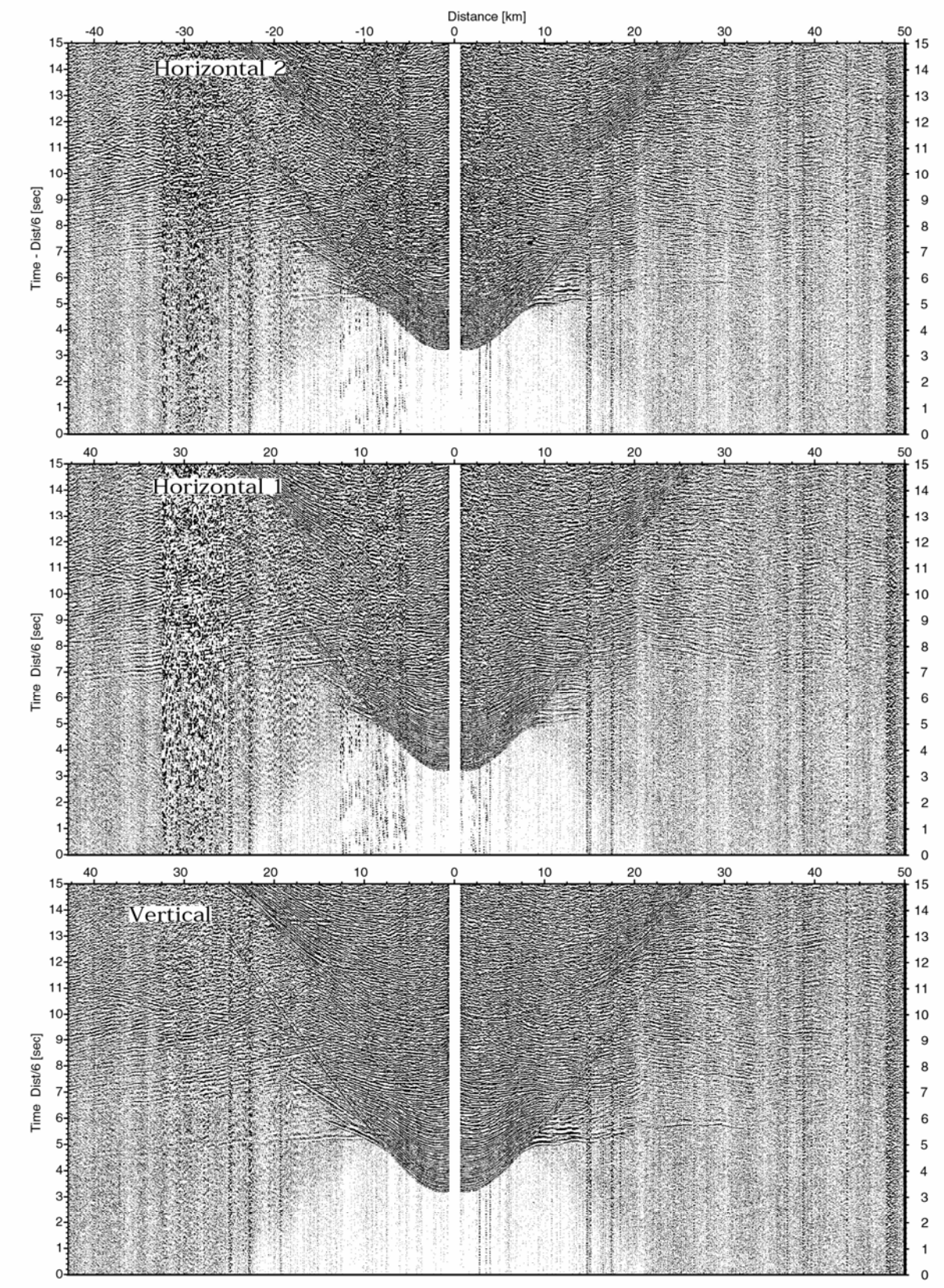

Figure 6.3.27: Record sections from obs 76 OAS/Owen4.5Hz, SO1863 Profile 01.

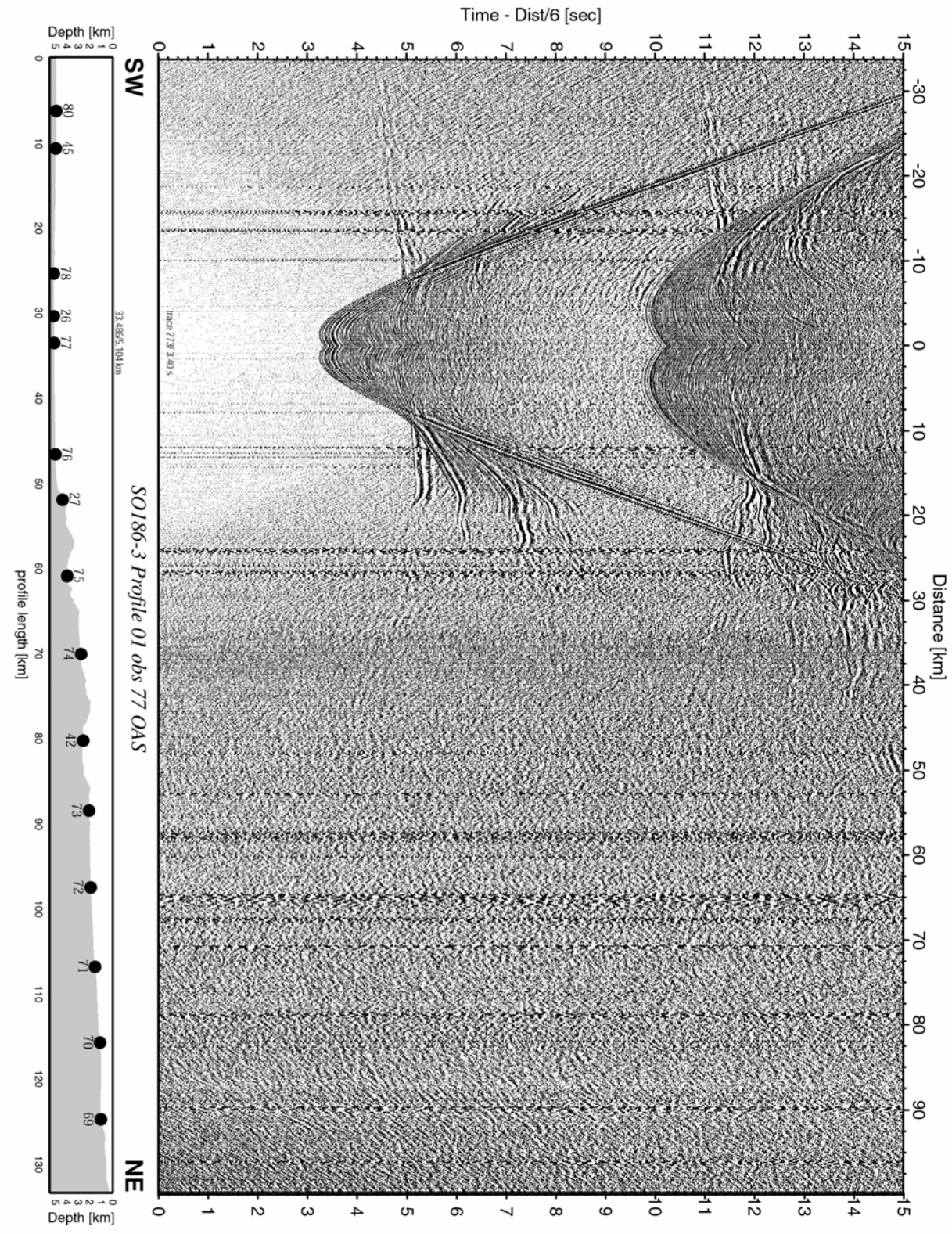

Figure 6.3.28: Record section from obs 77 OAS, Profile 01.

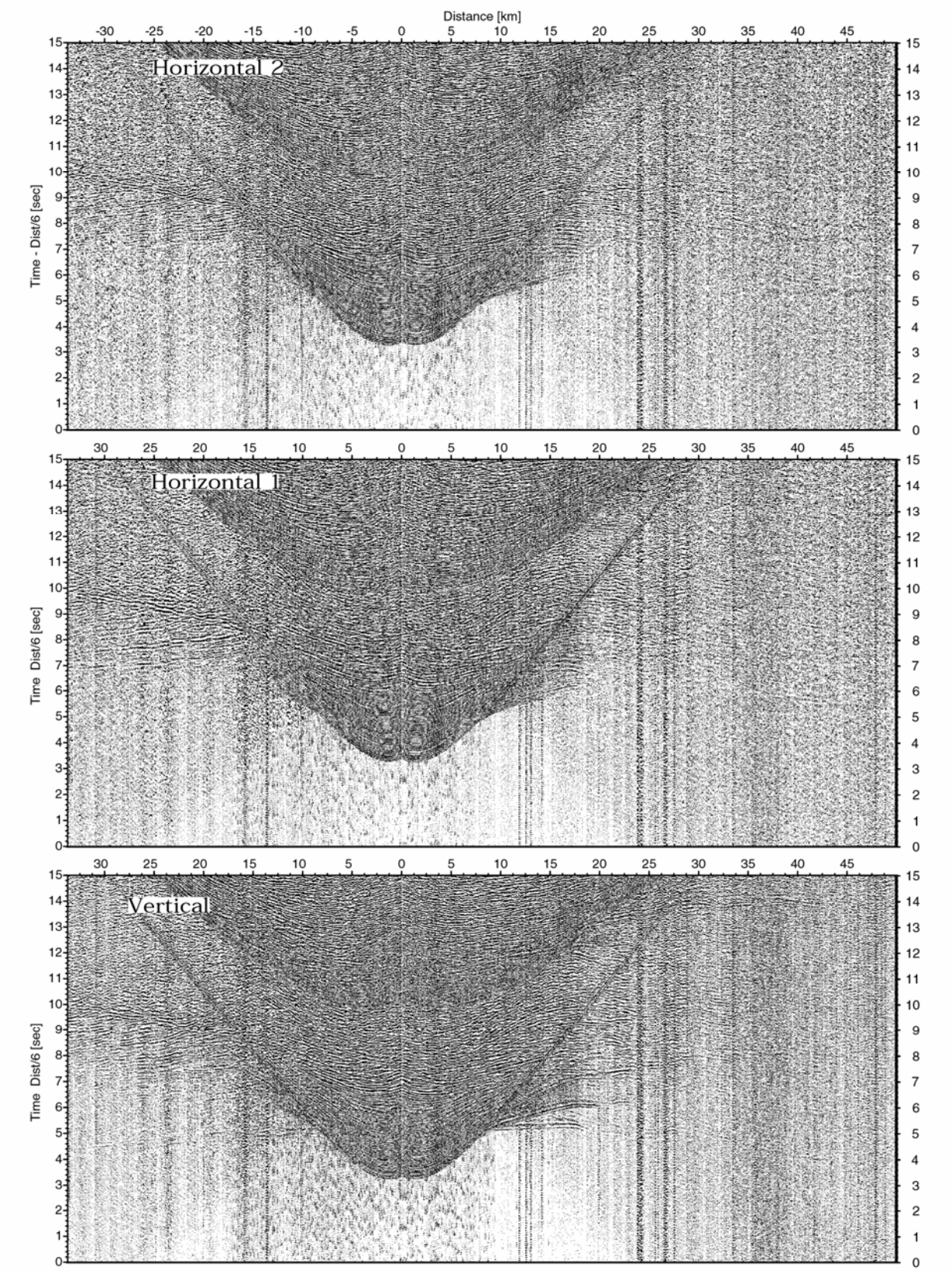

Figure 6.3.29: Record sections from obs 77 OAS/Owen4.5Hz, SO1863 Profile 01.

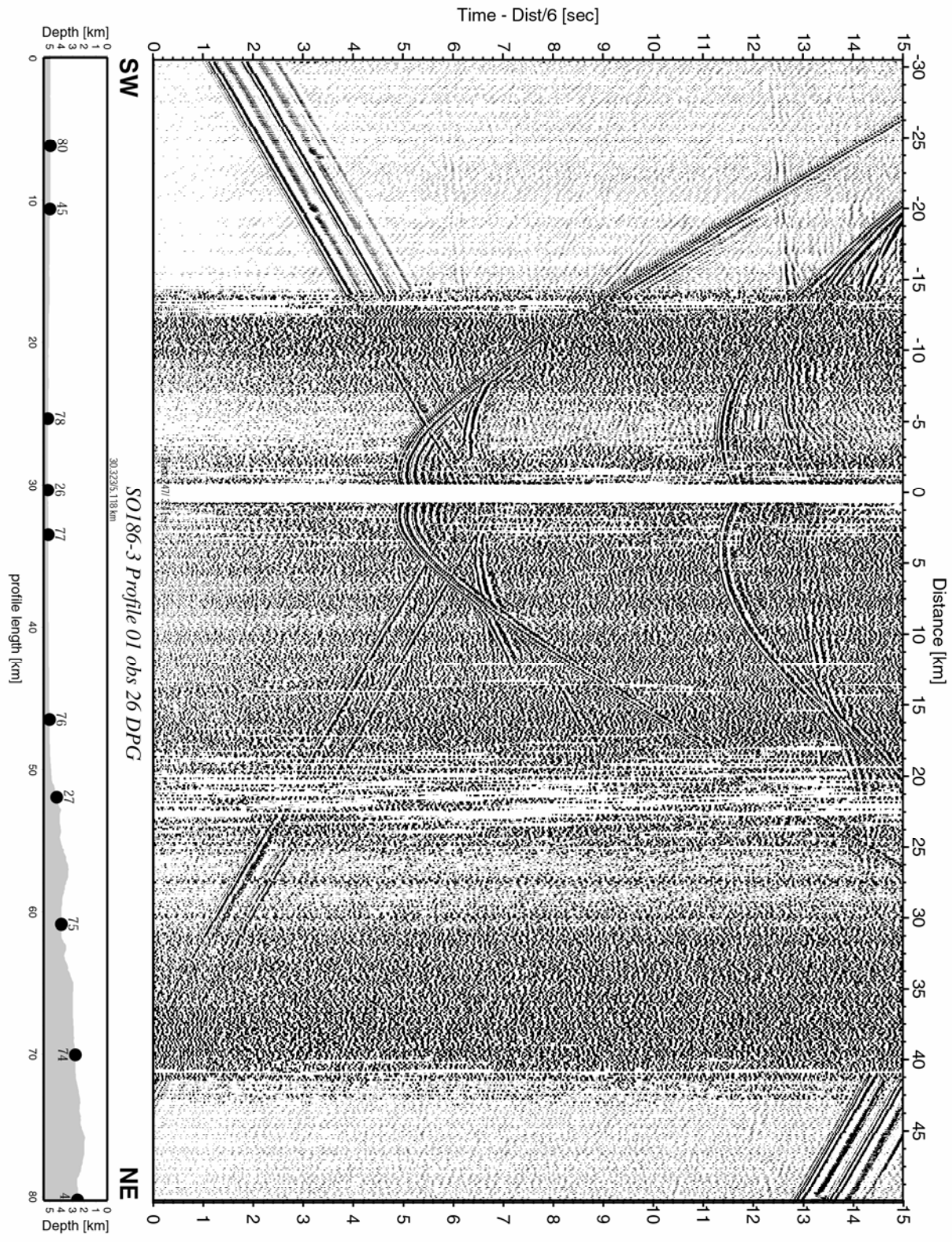

Figure 6.3.30: Record section from obs 26 DPG, Profile 01.

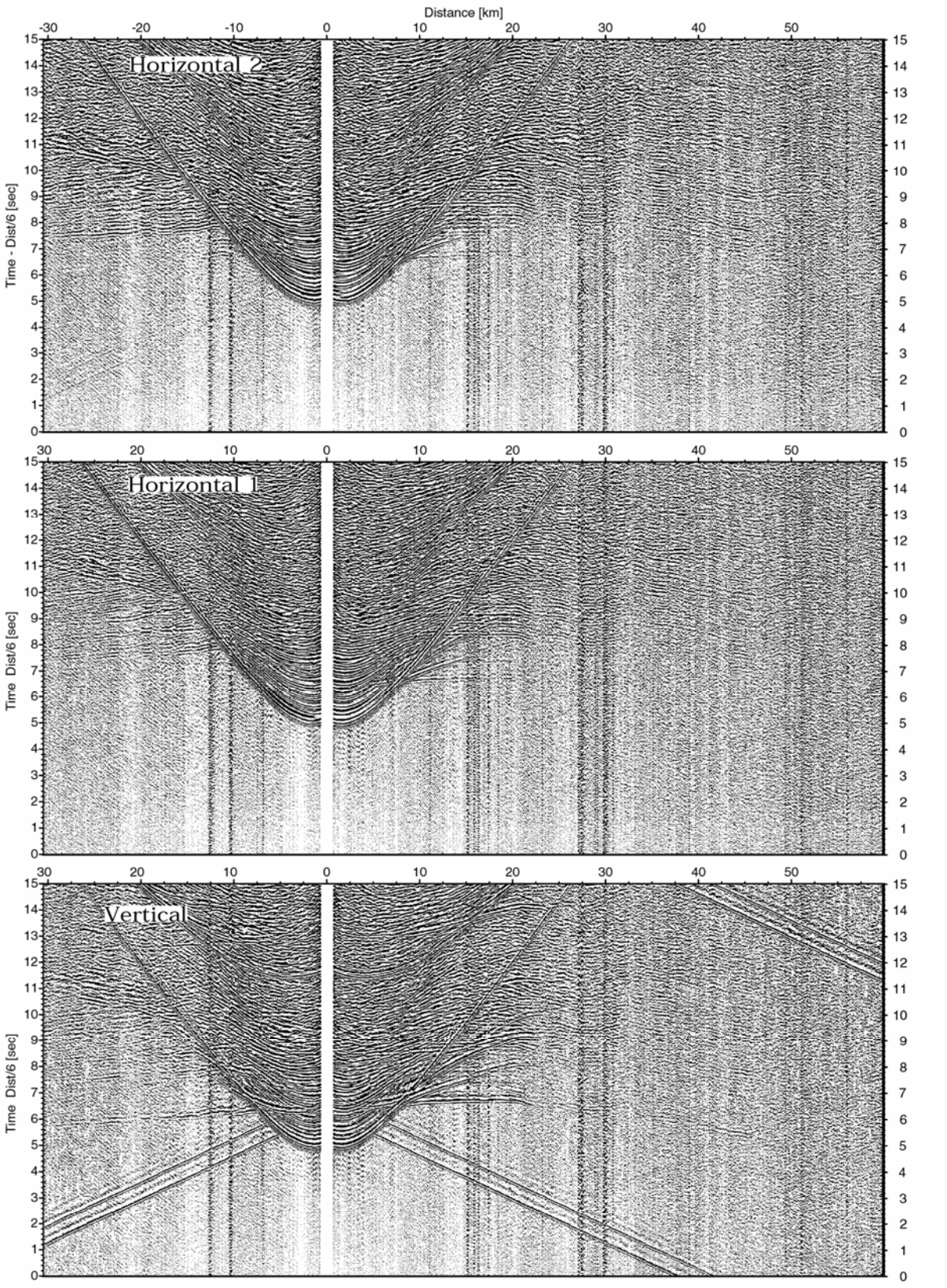

Figure 6.3.31: Record sections from obs 26 DPG/Owen4.5Hz, SO1863 Profile 01.

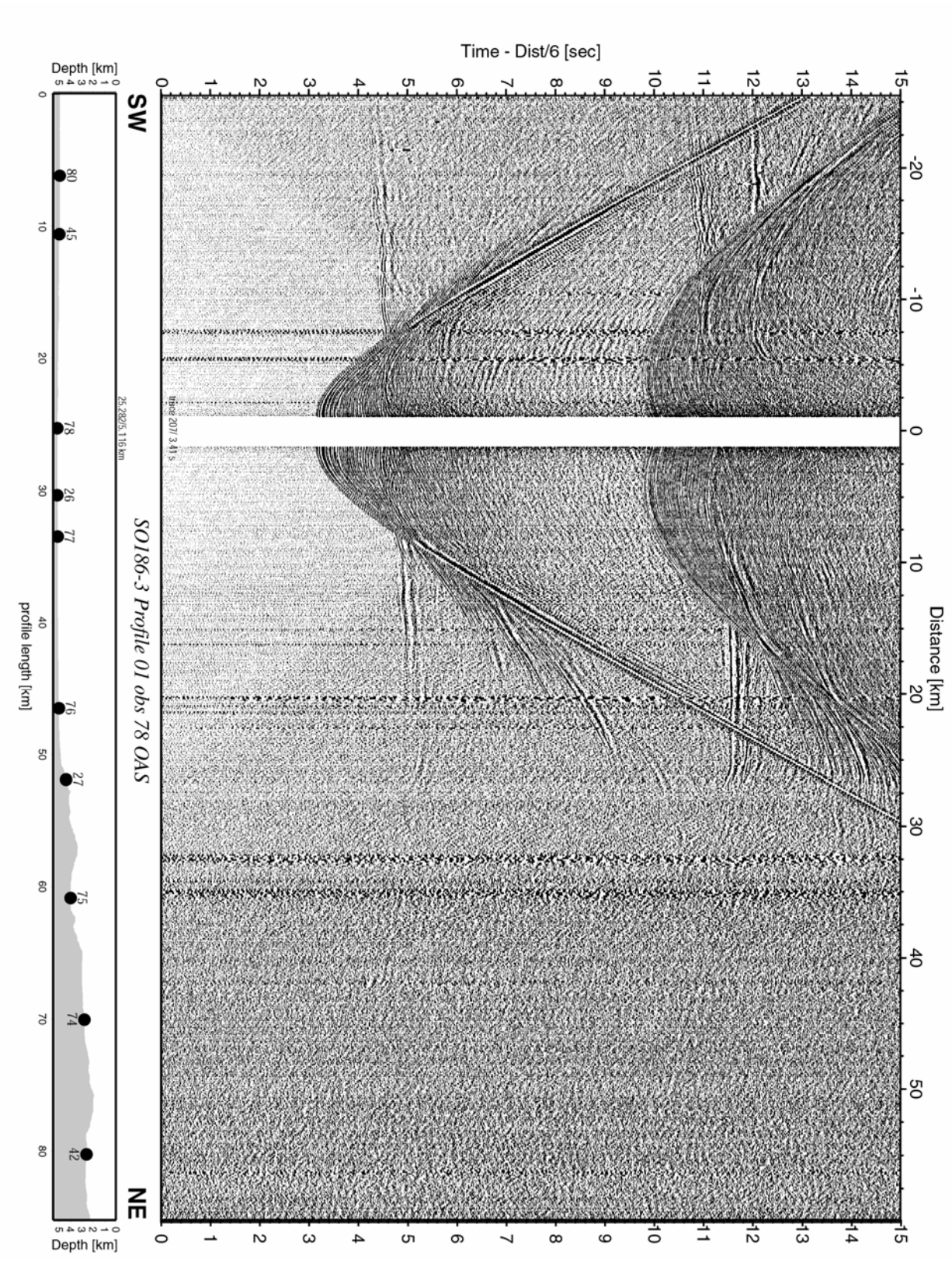

Figure 6.3.32: Record section from obs 78 OAS, Profile 01.

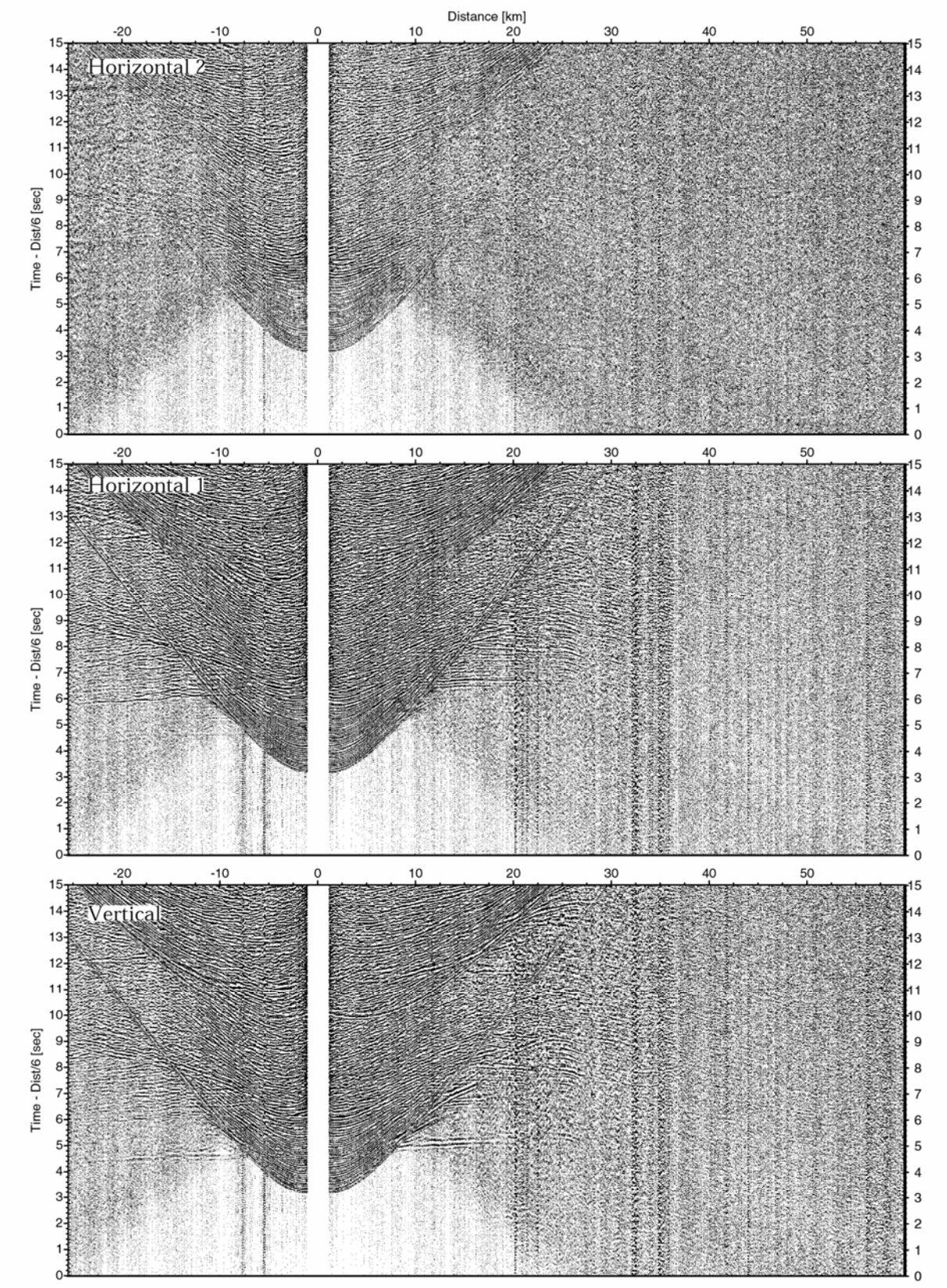

Figure 6.3.33: Record sections from obs 78 OAS/Owen-4.5Hz, SO186-3 Profile 01.

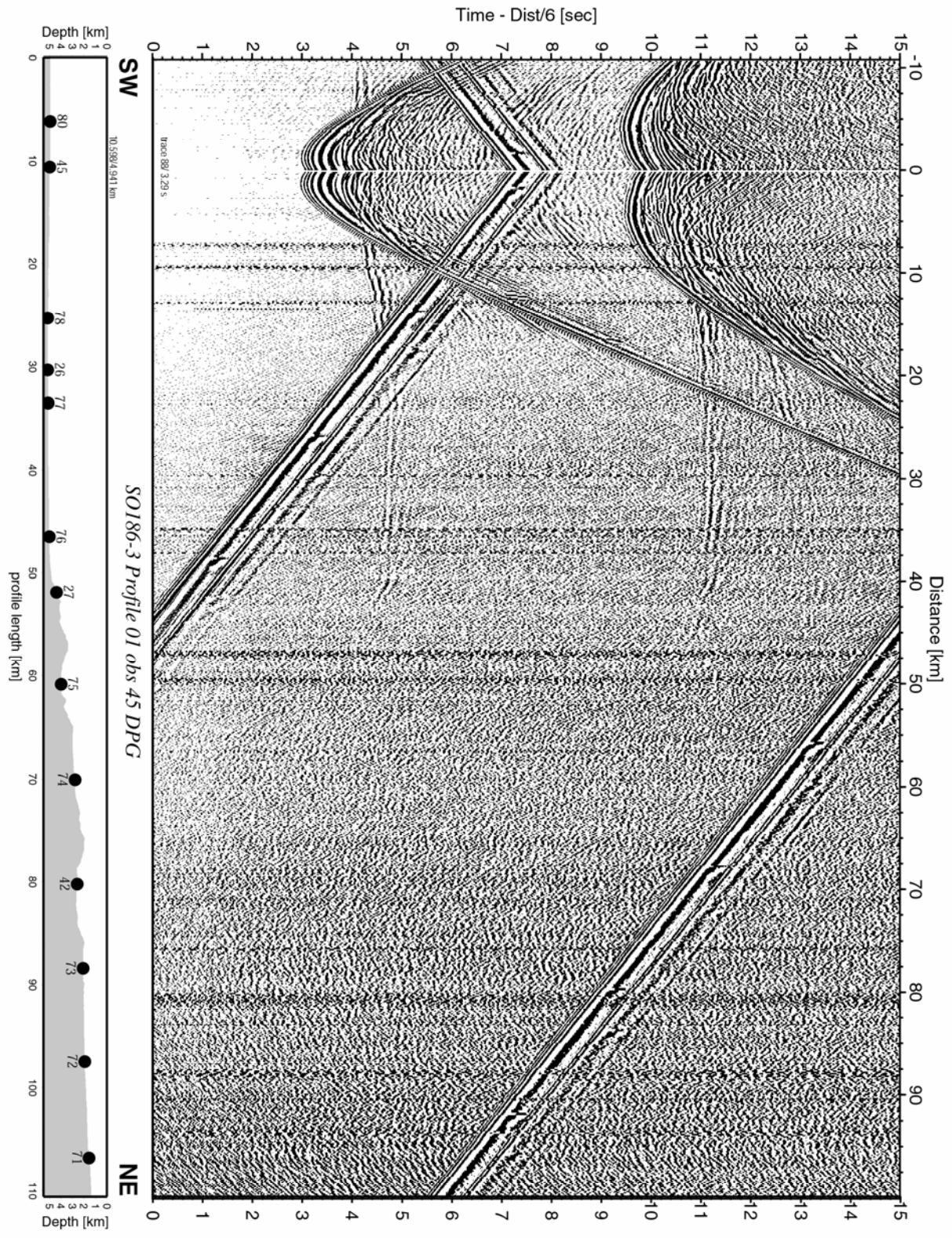

Figure 6.3.34: Record section from obs 45 DPG, Profile 01.

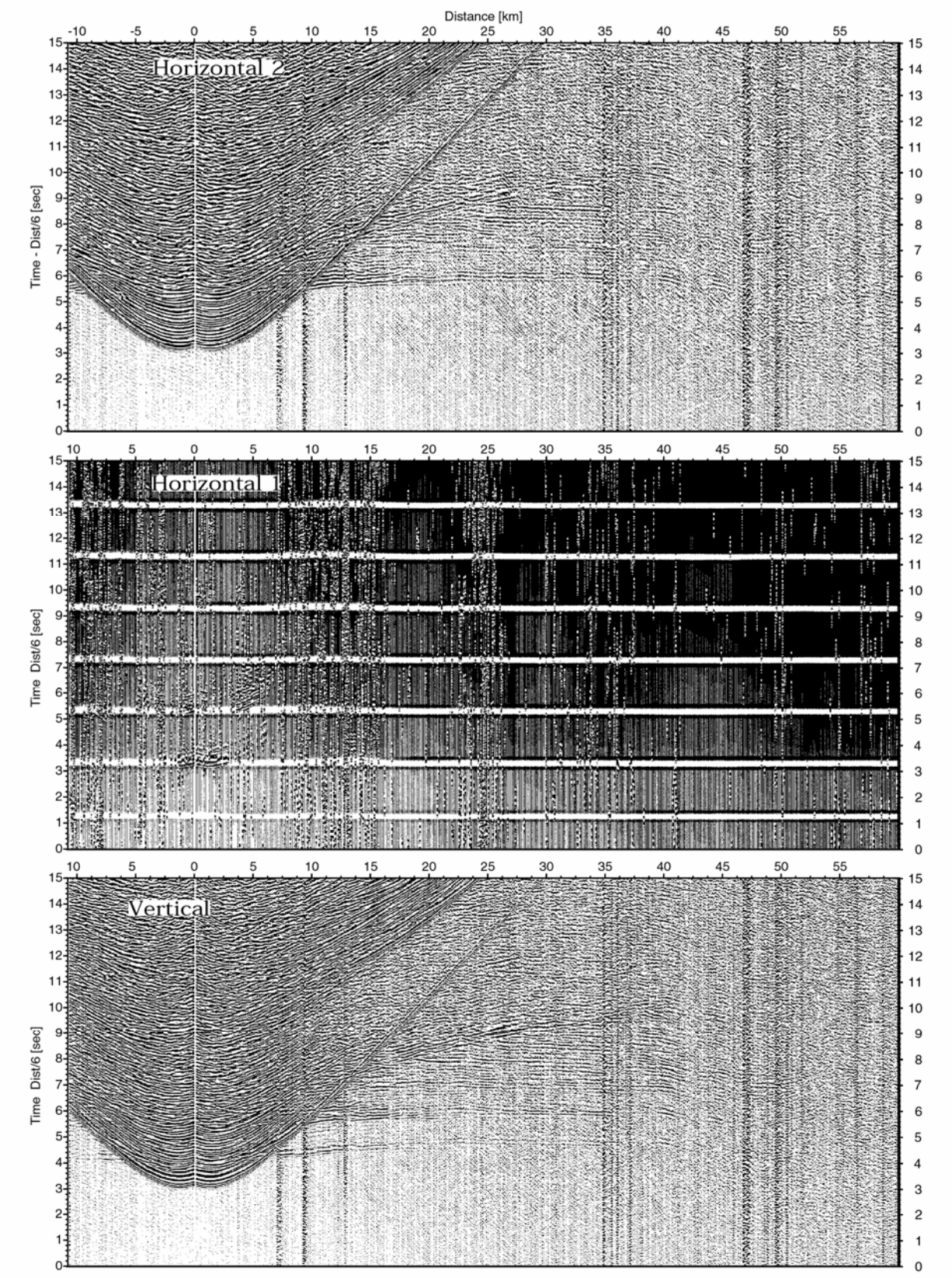

Figure 6.3.35: Record sections from obs 45 DPG/Owen4.5Hz, SO1863 Profile 01.

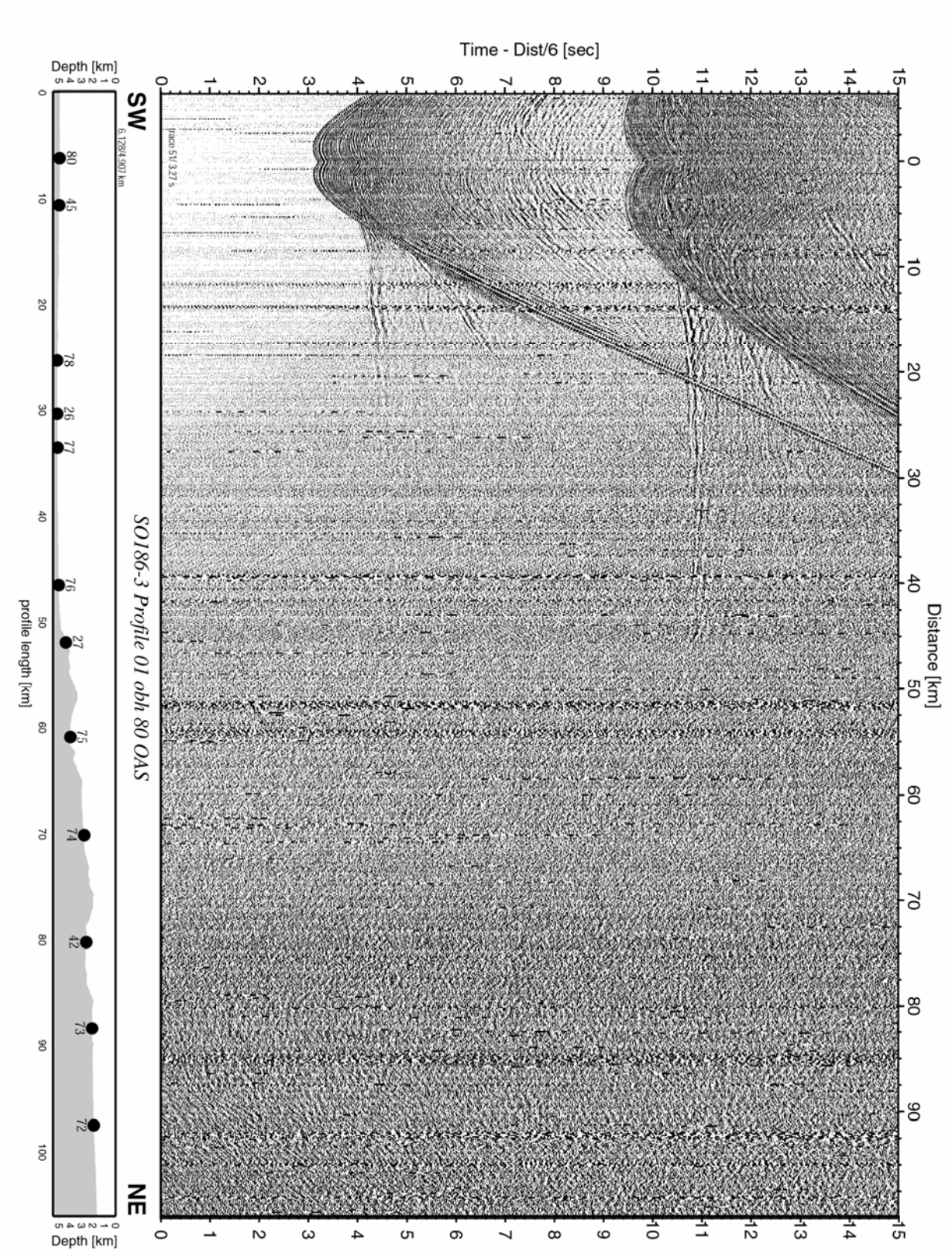

Figure 6.3.36: Record section from obh 80 OAS, Profile 01.

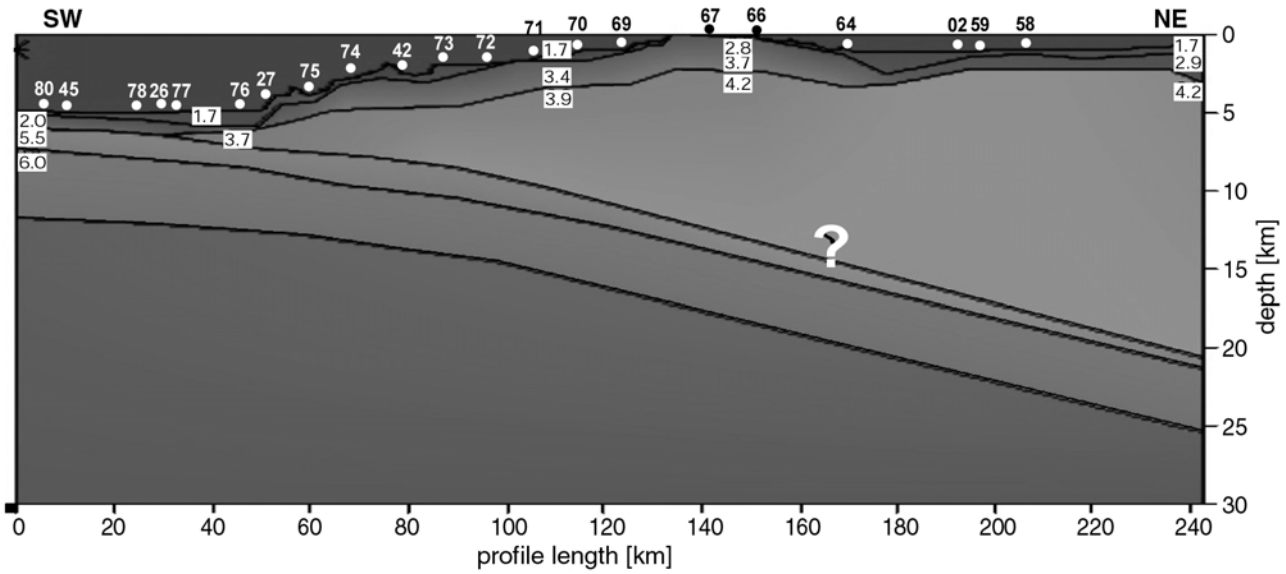

Figure 6.3.37: *Initial velocity model of profile 01, velocities are annotated in km/s. The steepness of the slab has not yet been calculated. Positions of the stations used for producing the model are indicated with dots and annotated in the model.*

6.4 Profile SO186-3-02/05

In this working area a total of 20 OBS and one OBH with a 500 m long anchor cable were deployed at an average spacing of 0.1 miles. The aim was a detailed investigation of the plate boundary that was identified on MCS data collected by our colleagues from BGR during the previous leg (Profile BGR-119). Across this 2 nm long array of Ocean bottom instruments four 20 nm long profiles were shot with different airgun configurations and trigger intervals (one or two arrays, 40 or 60 sec trigger). Ship speed was 4 kn.
Instrument deployment started at 05:00 on March 07, and by midday March 08 all instruments were back on board for data inspection. A location map is shown in Figure 6.4.1. All data were played back following the procedure as outlined in 6.1, record sections are shown in Figures 6.4.2 to 6.4.25.
A preliminary interpretation was attempted on board.

The hydrophone raw data of OBS station 92 are shown in Figure 6.4.26 (upper figure). The station was positioned at the sea floor at a water depth of 2186 m, and the air gun array was towed at a depth of 7-9 m below the sea surface. The traveltime curve of the direct wave shows that the sound wave propagates in the water column with an average velocity of (1500+/-5) m/s. This result coincides with results of CTD measurements, which indicate an average velocity of 1495 m/s.

The first cycle of the airgun signal has a duration of approximately 50 milliseconds, which corresponds to a main frequency of 20 Hz. The upper end of the frequency range is at 60 Hz. The oscillating air bubble generates a signal with several cycles. The signal is filtered to decrease the duration of the direct wave, which interferes with the seismic reflections (f-k filter, velocity filter, fan filter). A time shift is applied to the data with the traveltime of the direct wave (Figure 6.4.27, upper figure). A 2D Fourier transformation is applied to this seismogram section, and a boxcar filter is applied in the transform domain to remove the direct wave and the bubble effect. The data are back-transformed and the first cycle of the direct wave is added again (Figure 6.4.27, lower figure). The reflection signals now have similar shape on neighbouring seismic traces, which was not the case in the raw data section. Finally the time shift is applied again with negative sign. The filtered section is displayed in Figure 6.4.26 (lower figure). This filtering procedure improves the signal shape of the direct wave, but not the shape of the reflection signals. Alternatively a Wiener shaping filter deconvolution could be applied based on the signal, which was recorded with a hydrophone in the water column.

Shear waves are generated by conversion from P to S during reflection at interfaces in the subsurface, while conversion during transmission at the sea floor is too small to generate S-waves. The shear waves are recorded by the horizontal seismometer components. The orientation of the seismometer at the sea floor can be determined from the data. The two components are rotated so that one component points in the direction of the vertical projection of the shot point to the sea floor. The second component, which is perpendicular, has no energy after rotation, if all reflectors are horizontal. The S-wave velocity in marine sediments is much lower than the P-wave velocity. It follows from Snell's law that the S-waves propagate nearly vertically after reflection. Therefore the 2D filter is applied only to the P-waves in the 0.4 s interval after the first arrival. The horizontal component of OBS 90 after rotation is shown in Figure 6.4.28. In the rotated seismogram section the shear waves have the same phase along the profile, while the direct P-wave and the PP-reflections change the sign of

the signal for positive and negative offsets. One shear wave arrives with 0.4 s zero-offset traveltime after the direct wave, and another stronger shear wave arrives 0.25 s later. The S-wave signals have a longer time duration than the P-wave signals, which is caused by strong S-wave attenuation during transmission in the sediments, which constitute a porous medium, i.e. a mixture of solid material and water.

A 1D P-wave velocity-depth model is constructed by using reflections from horizontal interfaces. Theoretical reflection traveltimes for this model are computed and a corresponding time shift is applied to the data. The results for the first reflector below OBS station 95 and for a deeper reflector are shown in Figure 6.4.29. In the same way a 1D S-wave velocity-depth function is obtained computing traveltimes of PS-reflections. The layer thicknesses and P-wave velocities for the downward propagating wave are already known from the P-wave modelling, so that only the S-wave velocity is varied. The seismograms are time shifted and the horizontal component of OBS 90 is displayed in Figure 6.4.30. 1D P-wave and S-wave velocity-depth functions are shown in Figure 6.4.31. The P-wave velocity increases by 500 m/s in the first 500 m below the sea floor. The S-wave velocity takes a value of 210 m/s in the first 80 m below the seafloor and 350 m/s in the next 70 m.

Kirchhoff depth migration is applied to the seismogram sections of OBS stations 90, 92 and 95 using the smooth gradient P-wave velocity model shown in Figure 6.4.31 (dashed line). The resulting images are displayed in Figures 6.4.32 and 6.4.33. The images show a sequence of parallel layers with a maximum thickness of 900 m. Below the sediments the plate boundary is imaged.

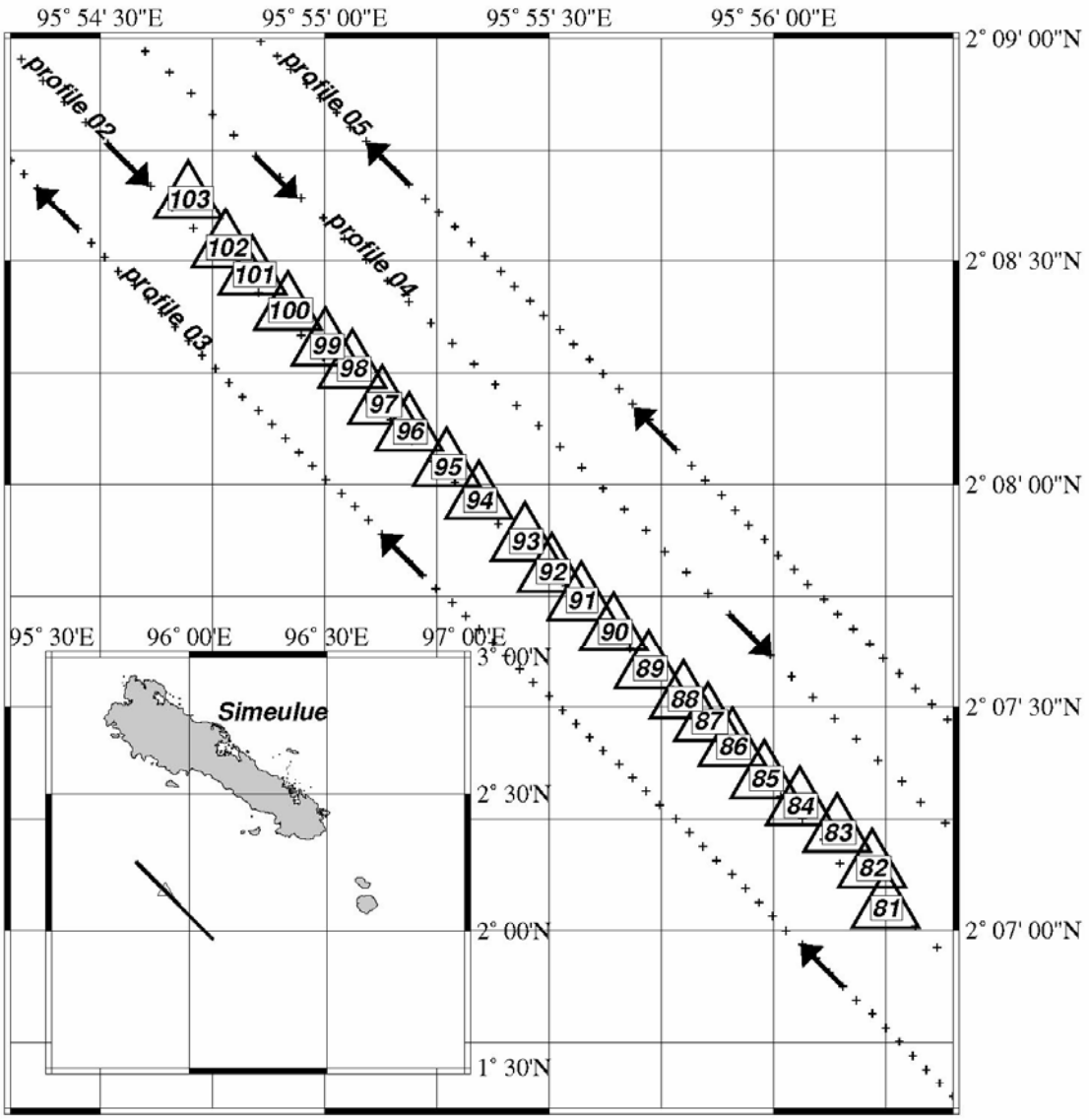

Figure 6.4.1: Location Map

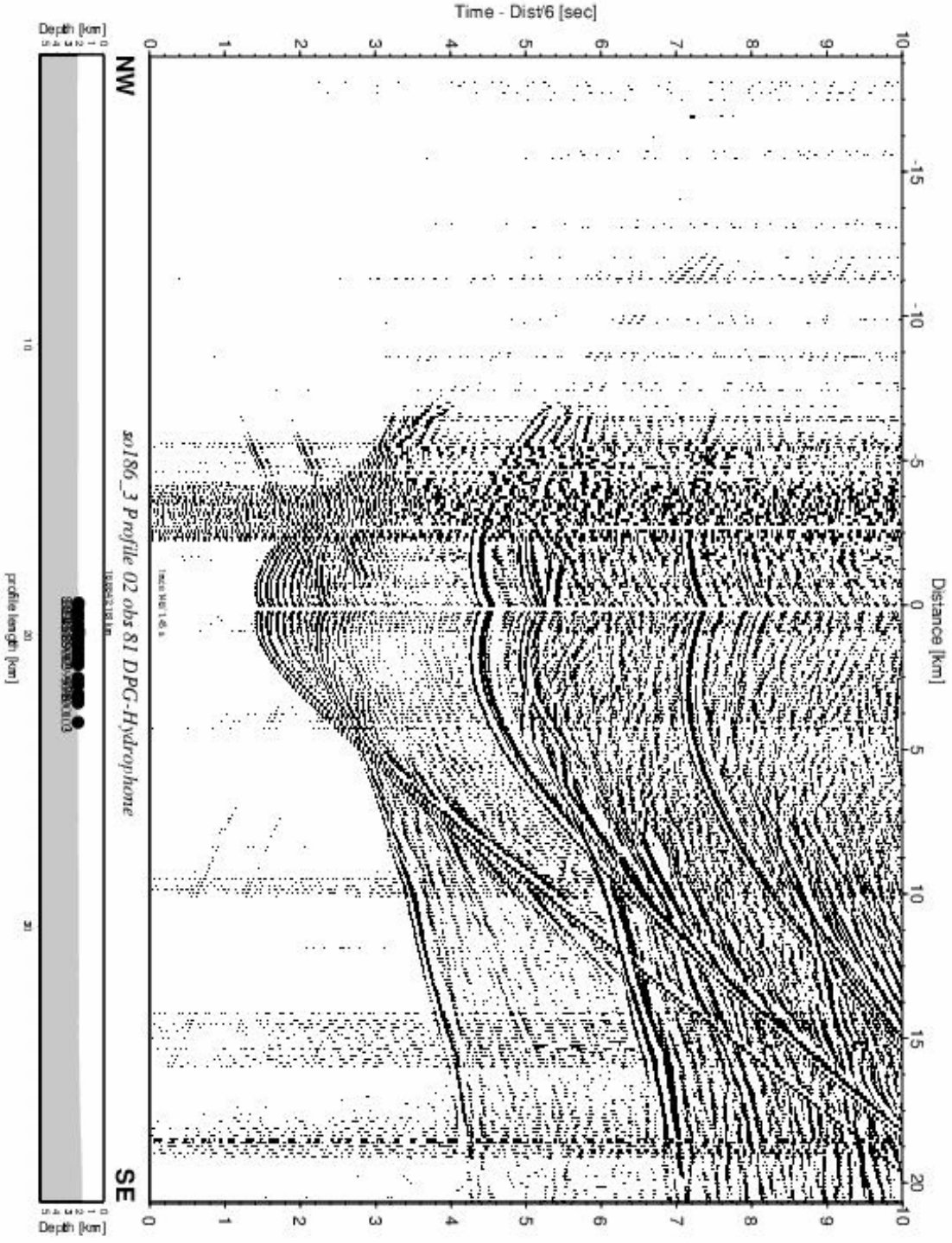

Figure 6.4.2: Record section from obs 81 DPG-Hydrophone, Profile 02.

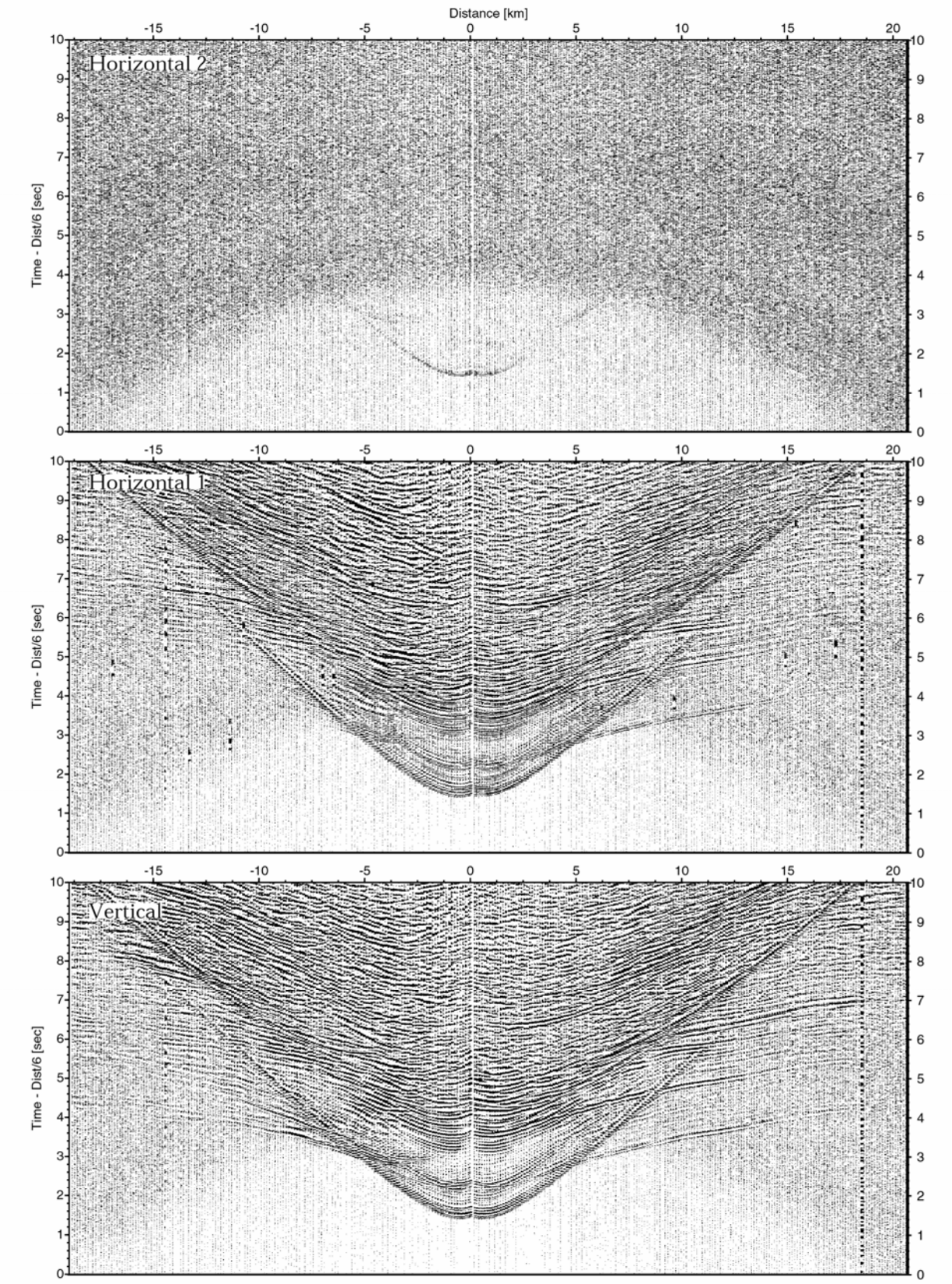

Figure 6.4.3: Record sections from obs 81 DPG/4.5Hz, so186_3 Profile 02.

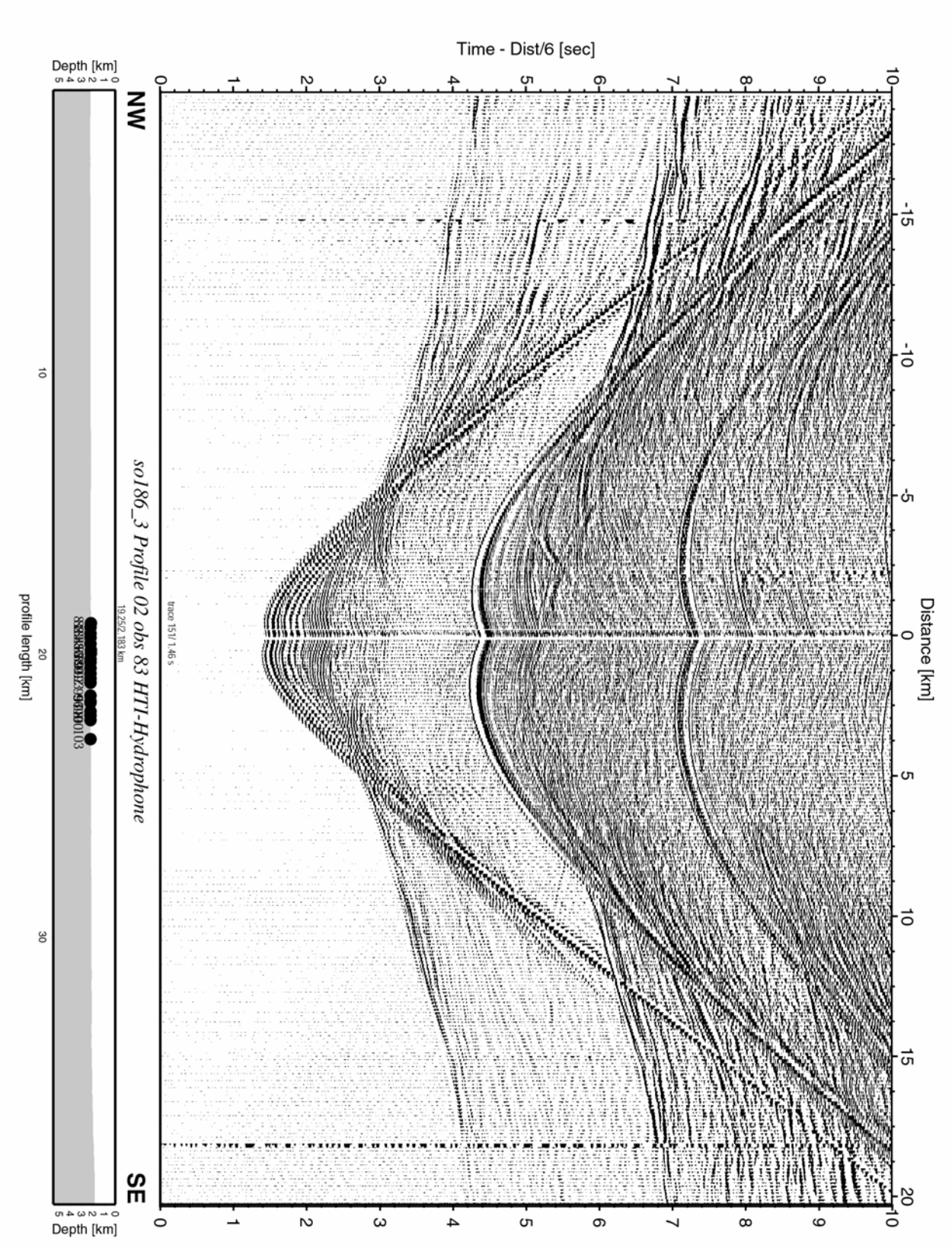

Figure 6.4.4: Record section from obs 83 HTI-Hydrophone, Profile 02.

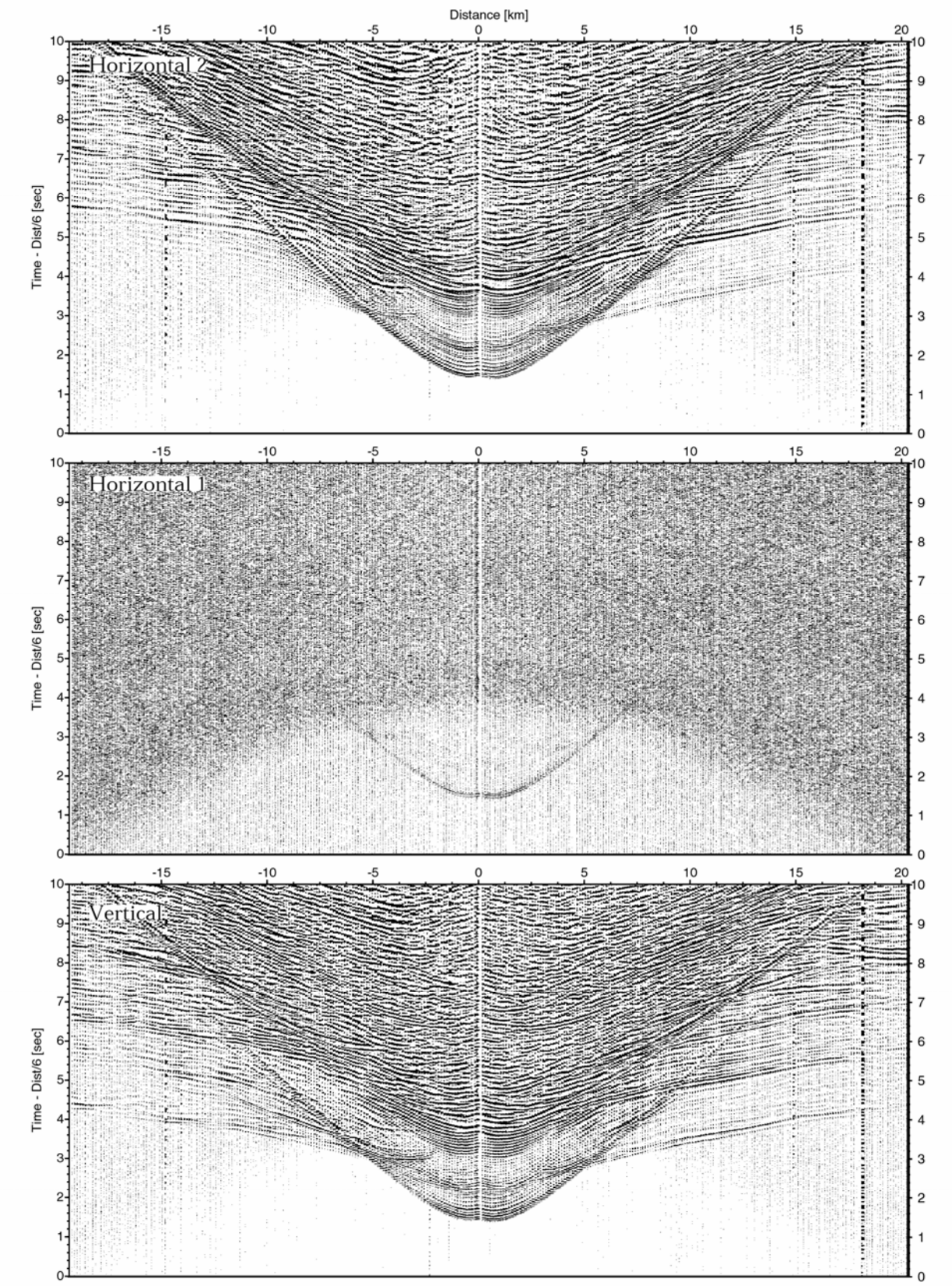

Figure 6.4.5: Record sections from obs 83 HTI/4.5Hz, so186_3 Profile 02.

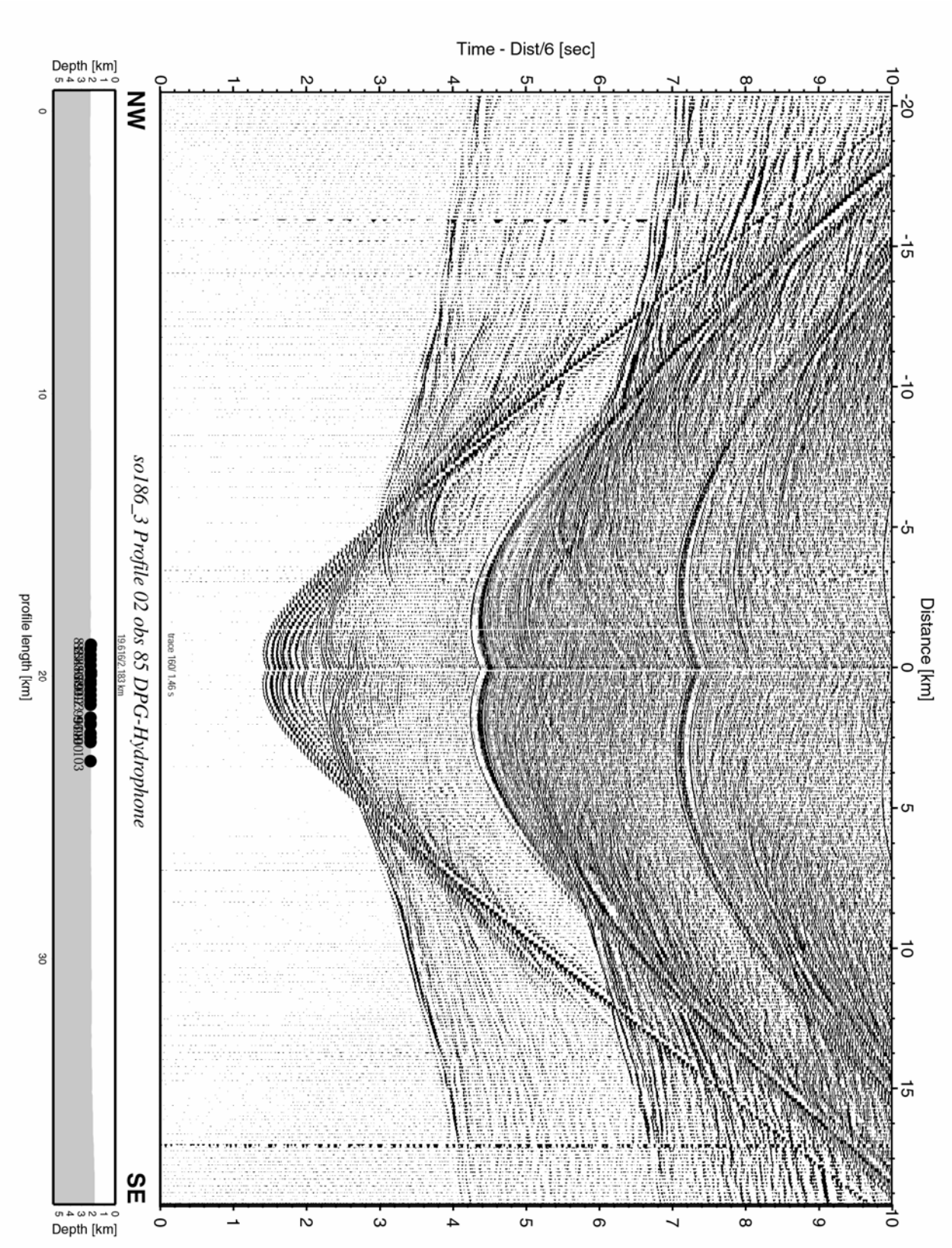

Figure 6.4.6: Record section from obs 85 DPG-Hydrophone, Profile 02.

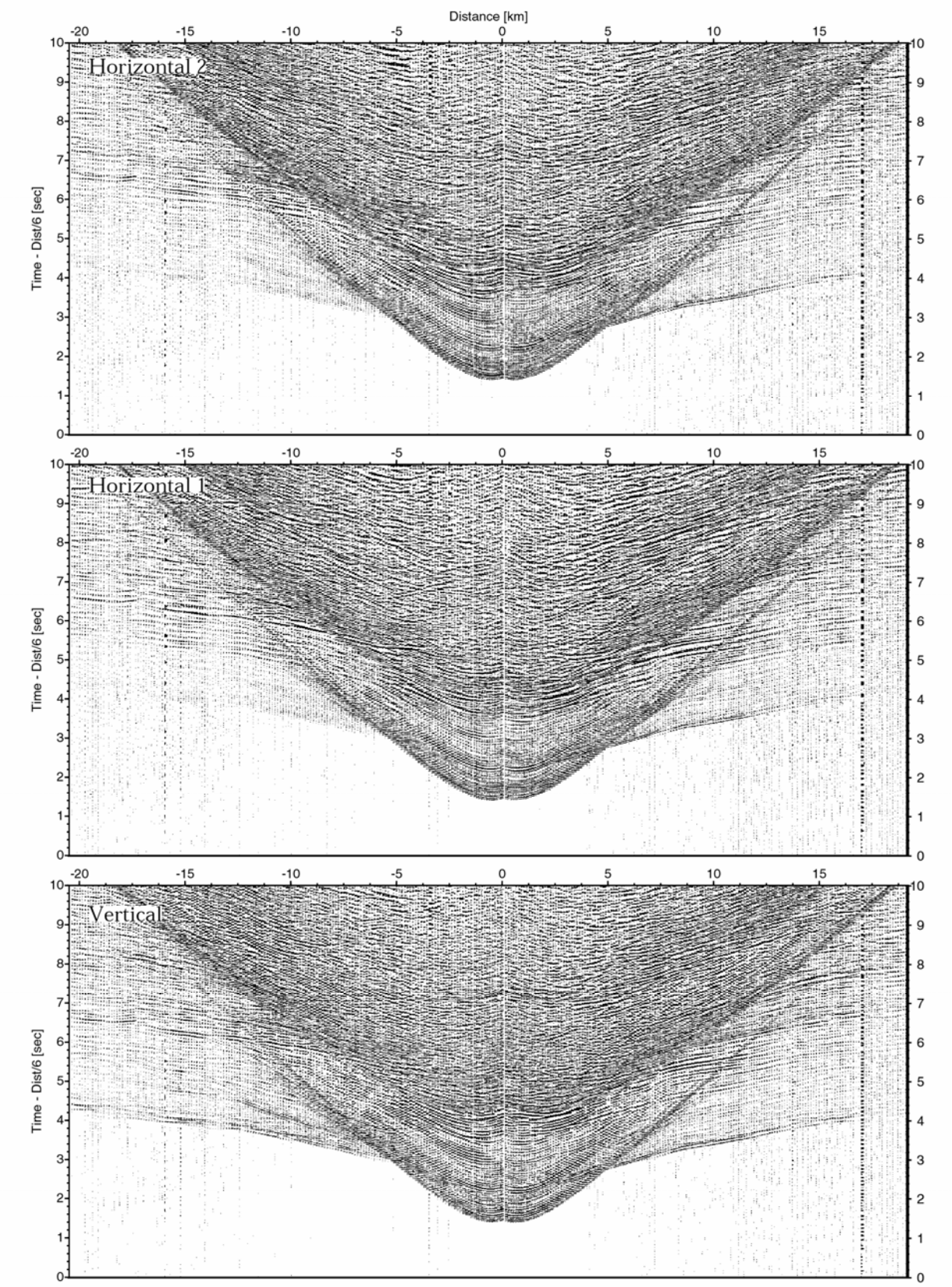

Figure 6.4.7: Record sections from obs 85 OAS/4.5Hz, so186_3 Profile 02.

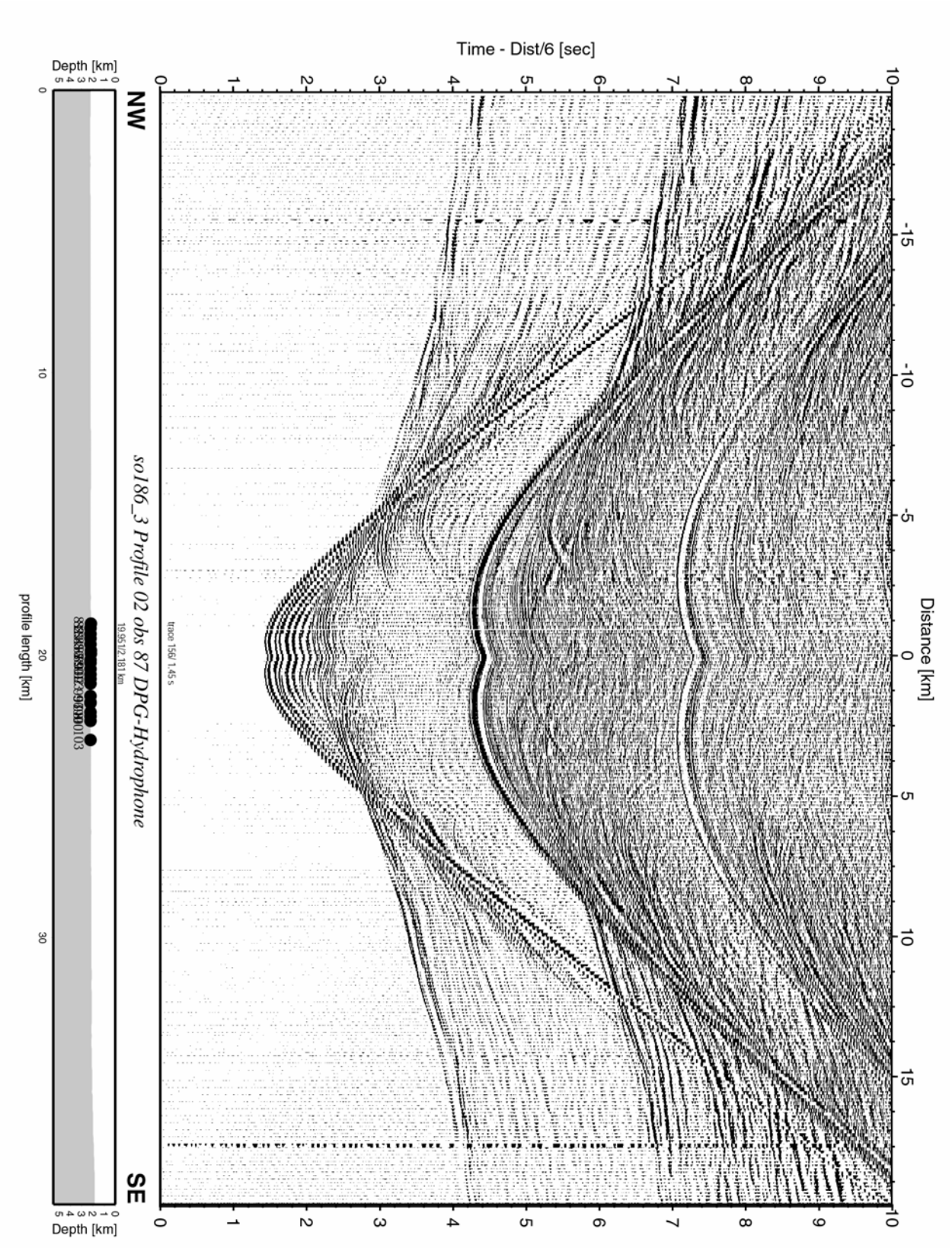

Figure 6.4.8: Record section from obs 87 DPG-Hydrophone, Profile 02.

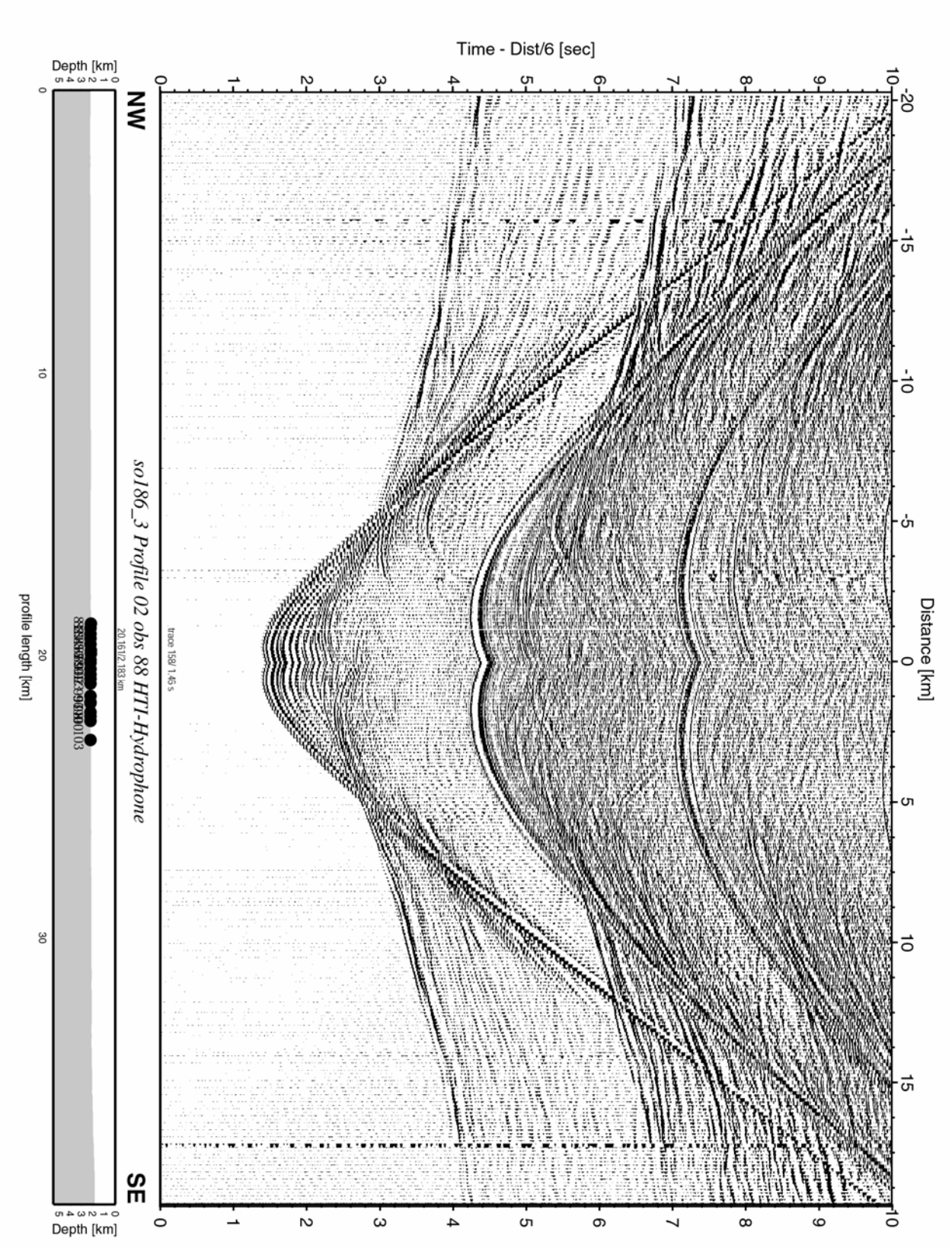

Figure 6.4.9: Record section from obs 88 HTI-Hydrophone, Profile 02.

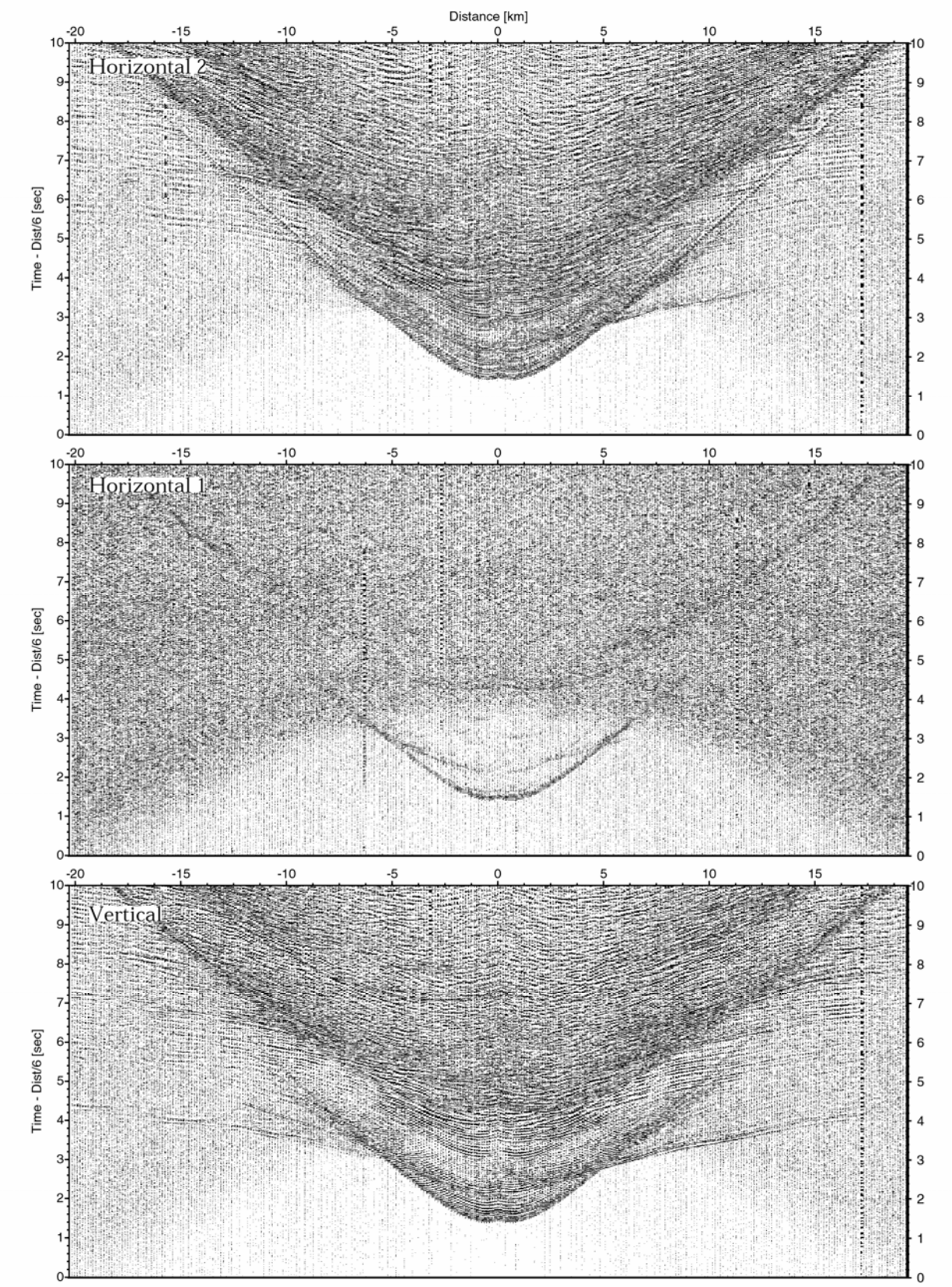

Figure 6.4.10: Record sections from obs 88 HTI/4.5Hz, so186_3 Profile 02.

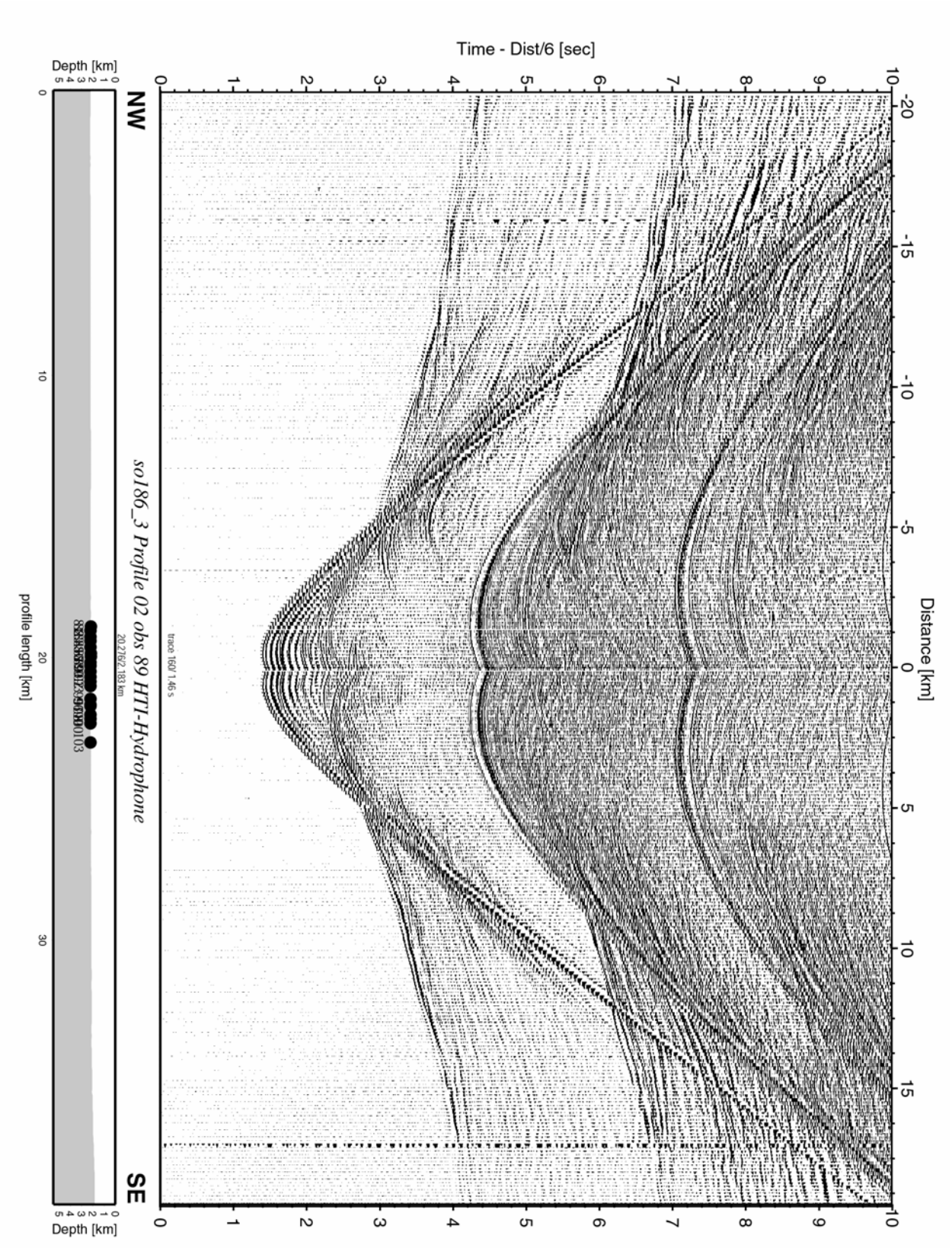

Figure 6.4.11: Record section from obs 89 HTI-Hydrophone, Profile 02.

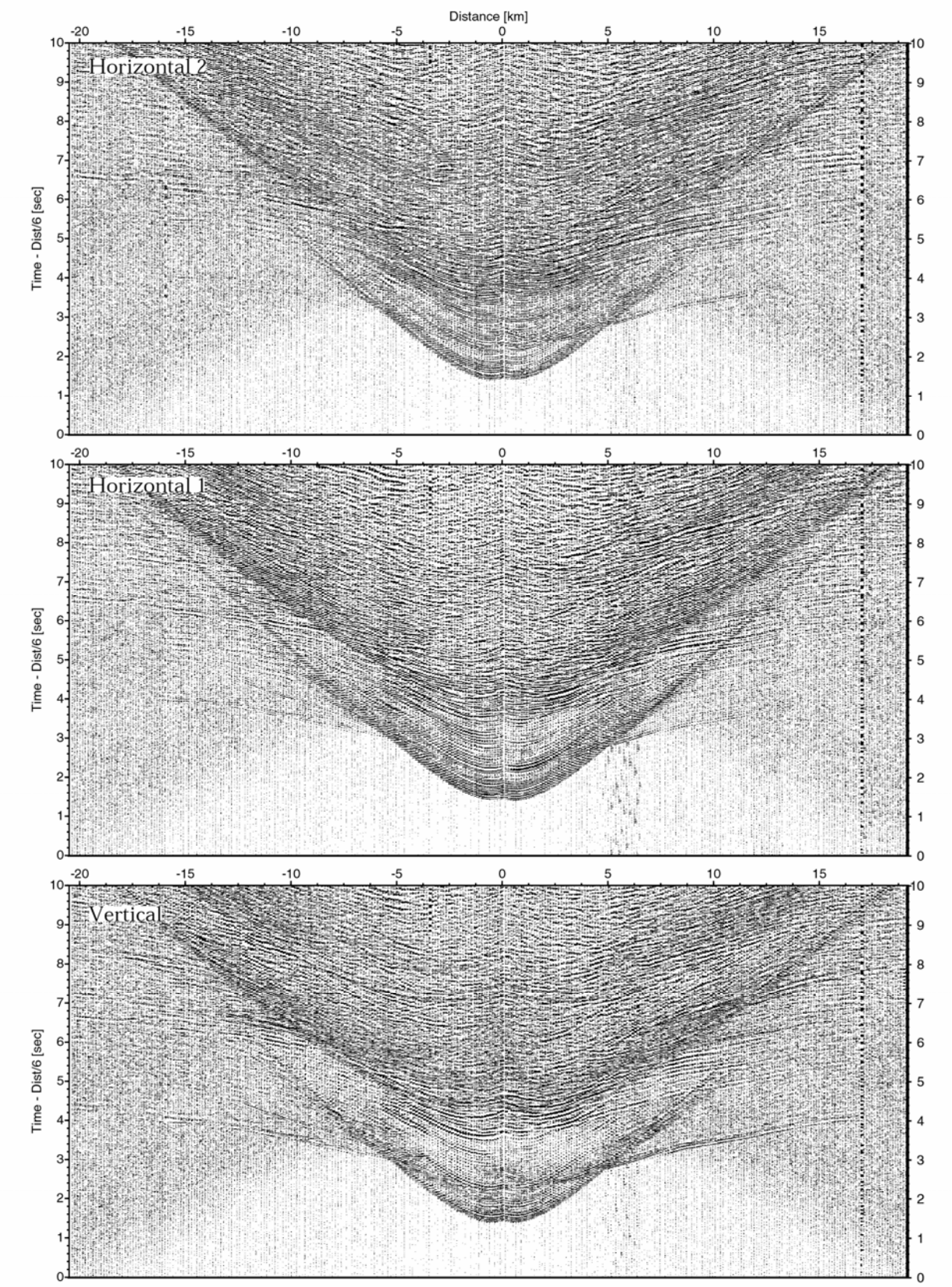

Figure 6.4.12: Record sections from obs 89 HTI/4.5Hz, so186_3 Profile 02.

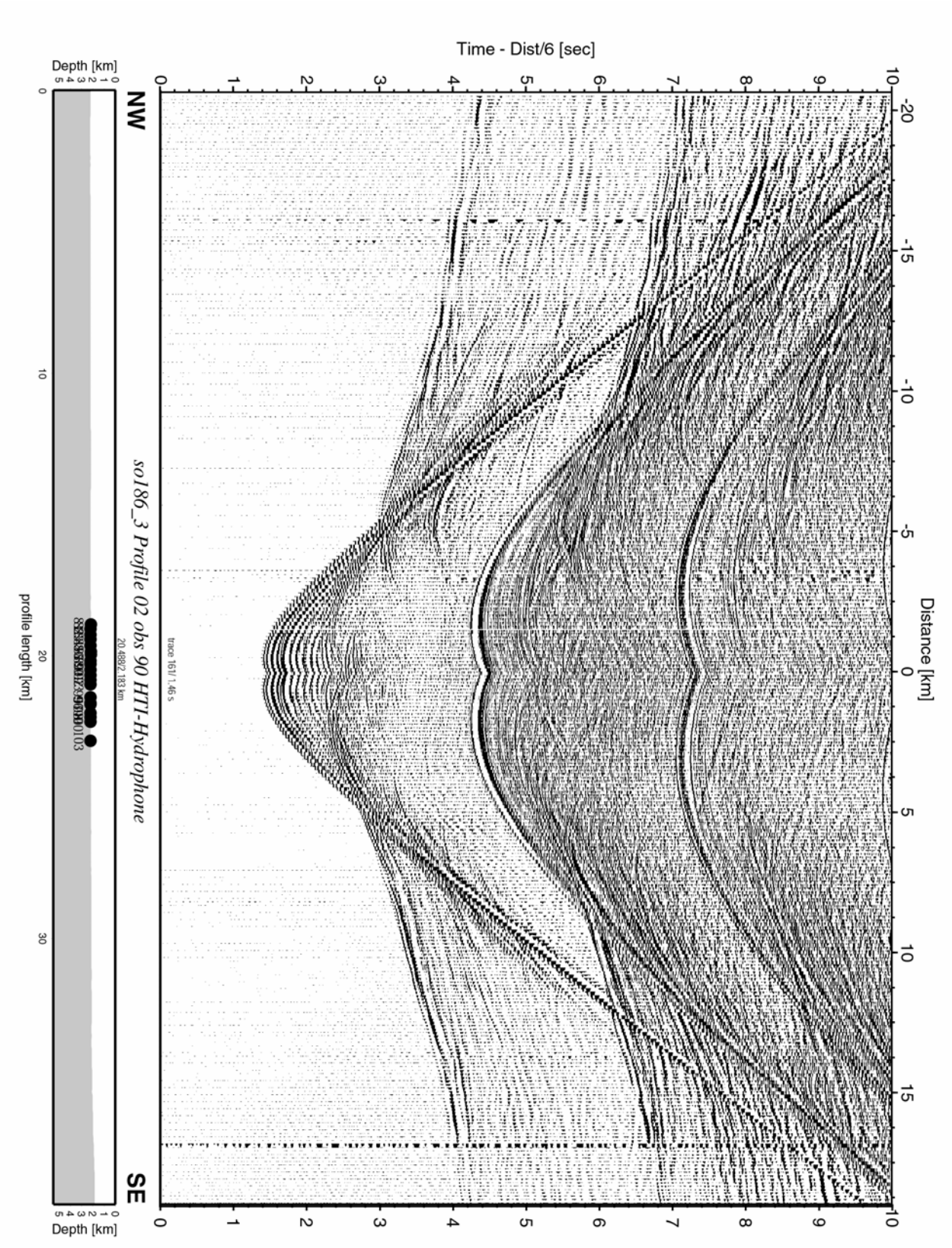

Figure 6.4.13: Record section from obs 90 HTI-Hydrophone, Profile 02.

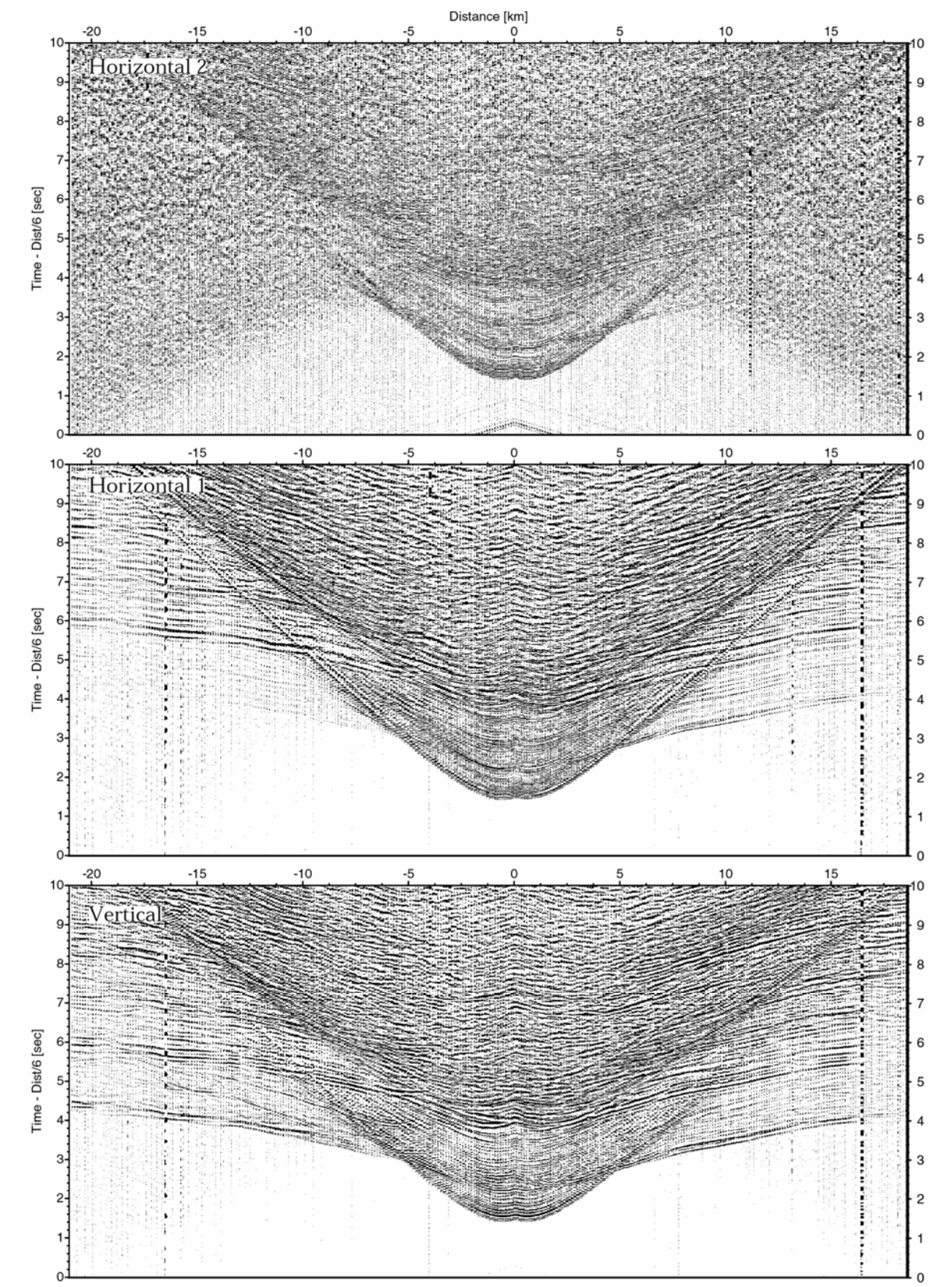

Figure 6.4.14: Record sections from obs 91 DPG/4.5Hz, so186_3 Profile 02.

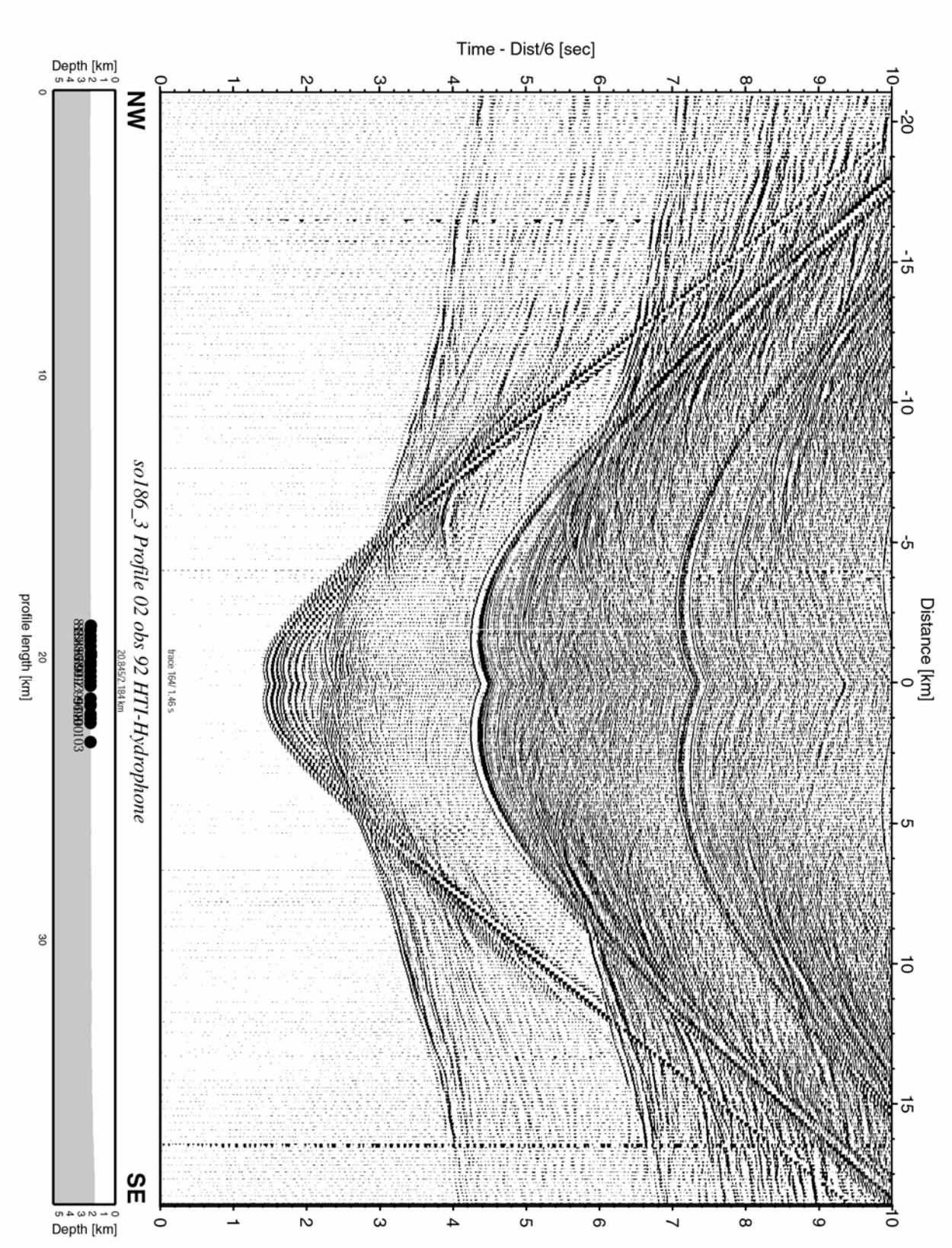

Figure 6.4.15: Record section from obs 92 HTI-Hydrophone, Profile 02.

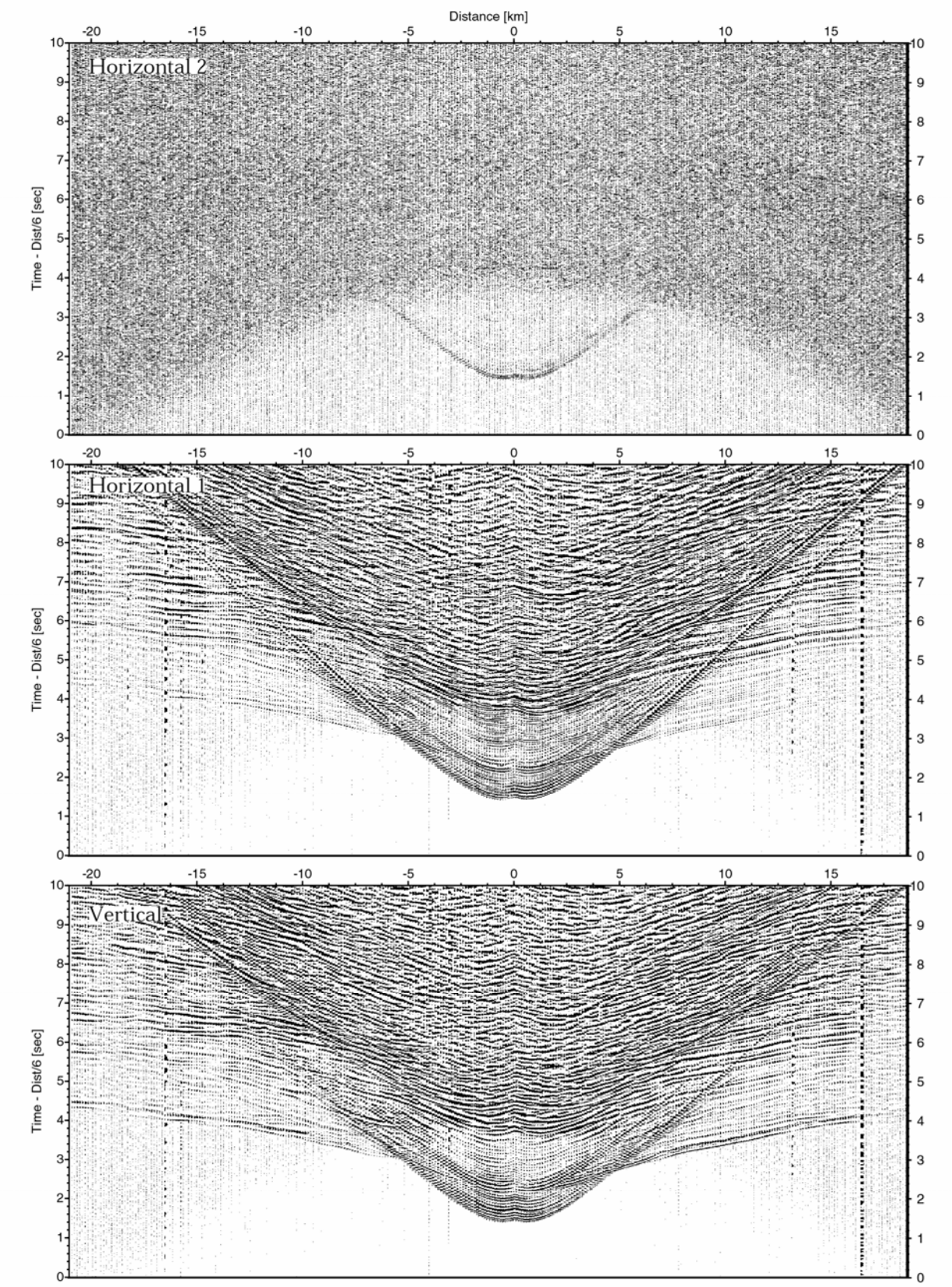

Figure 6.4.16: Record sections from obs 92 HTI/4.5Hz, so186_3 Profile 02.

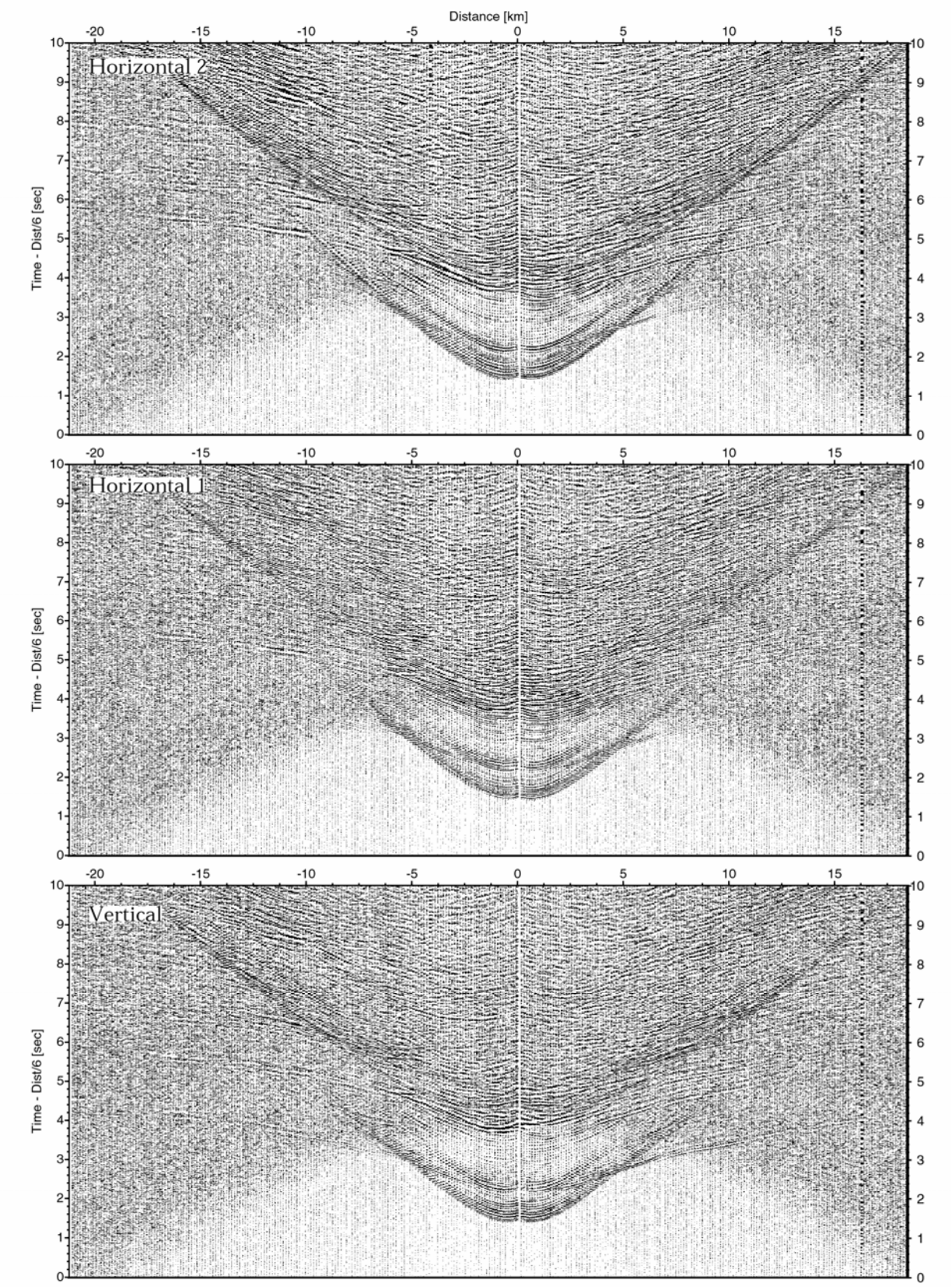

Figure 6.4.17: Record sections from obs 93 HTI/4.5Hz, so186_3 Profile 02.

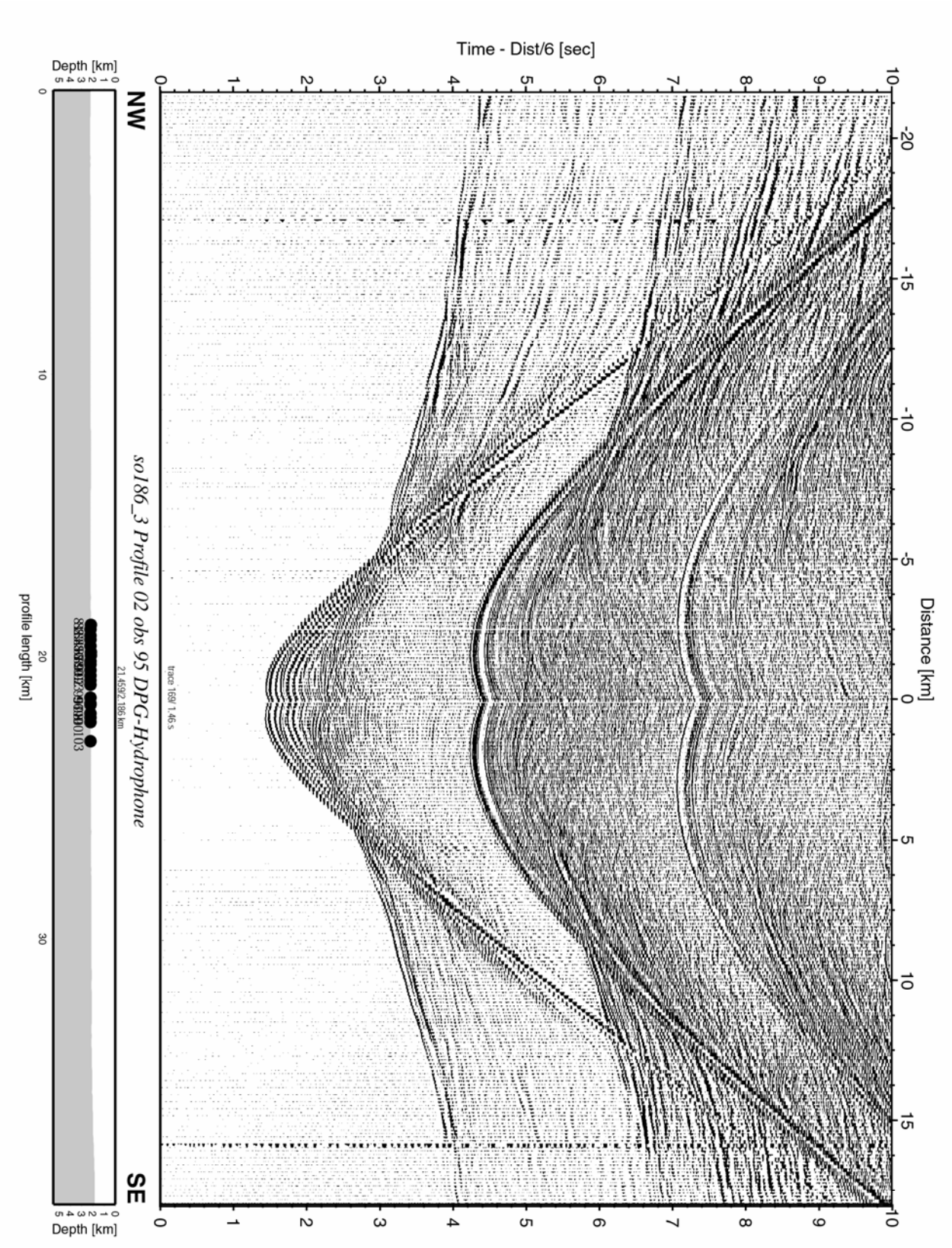

Figure 6.4.18: Record section from obs 95 DPG-Hydrophone, Profile 02.

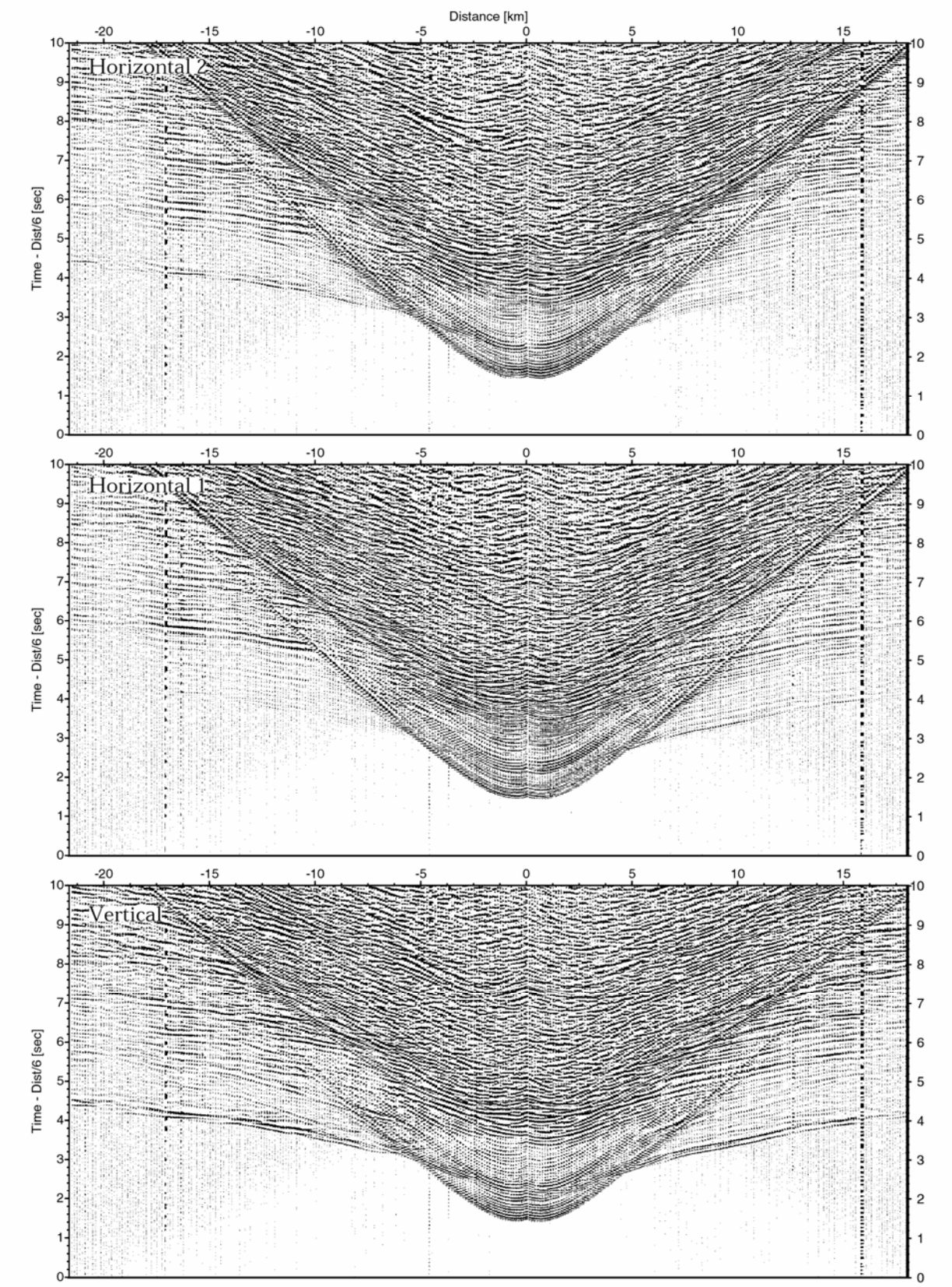

Figure 6.4.19: Record sections from obs 95 OAS/4.5Hz, so186_3 Profile 02.

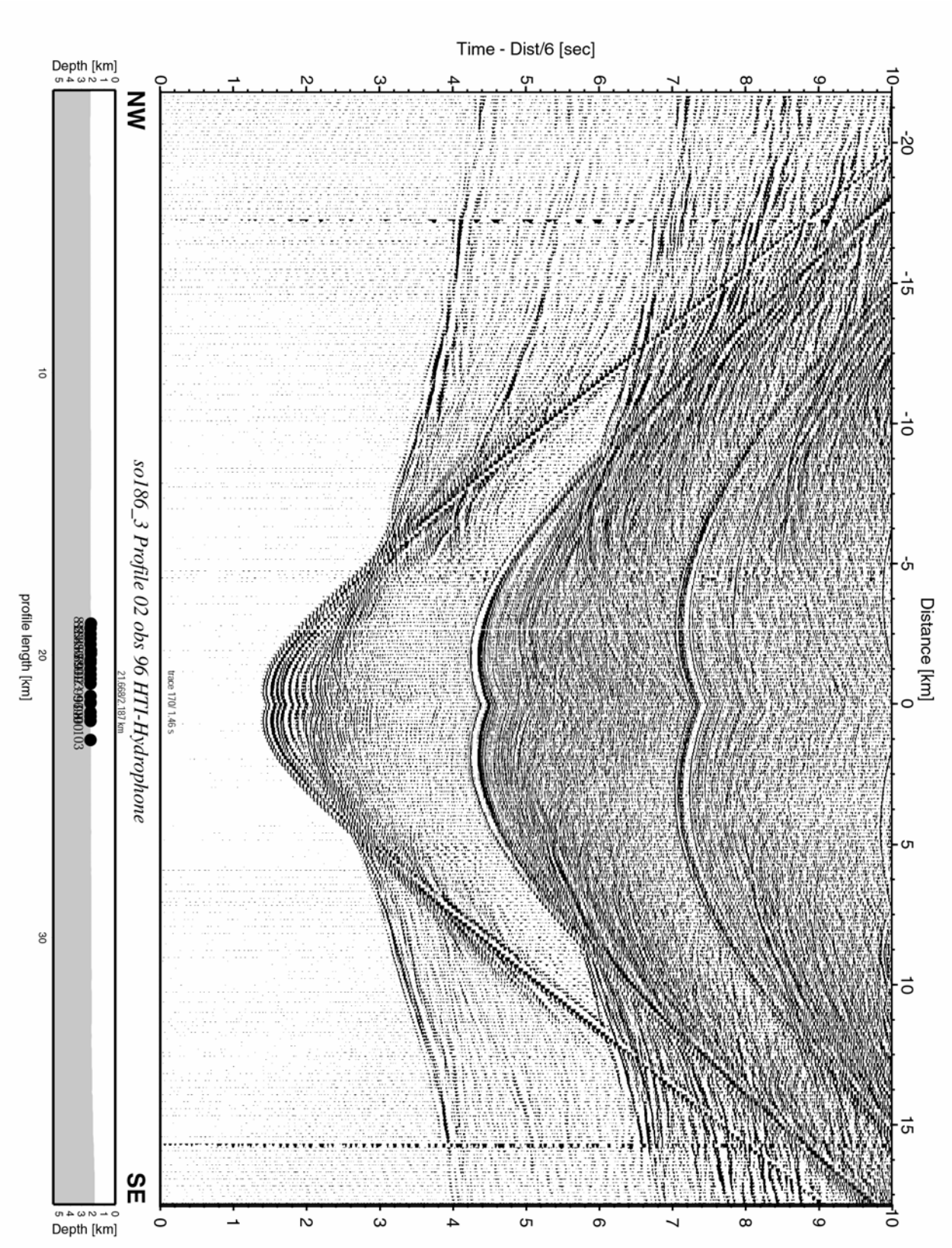

Figure 6.4.20: Record section from obs 96 HTI-Hydrophone, Profile 02.

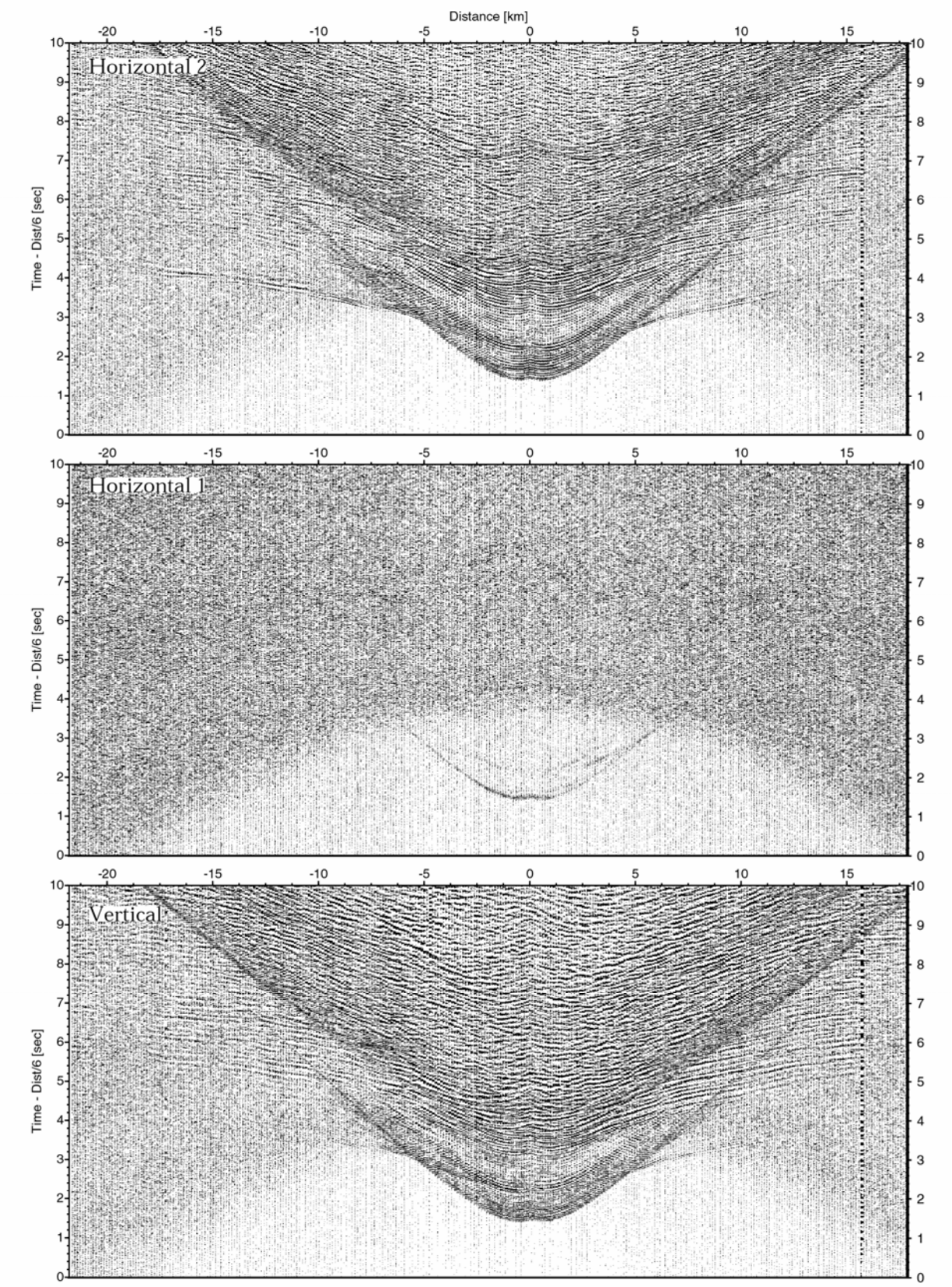

Figure 6.4.21: Record sections from obs 96 HTI/4.5Hz, so186_3 Profile 02.

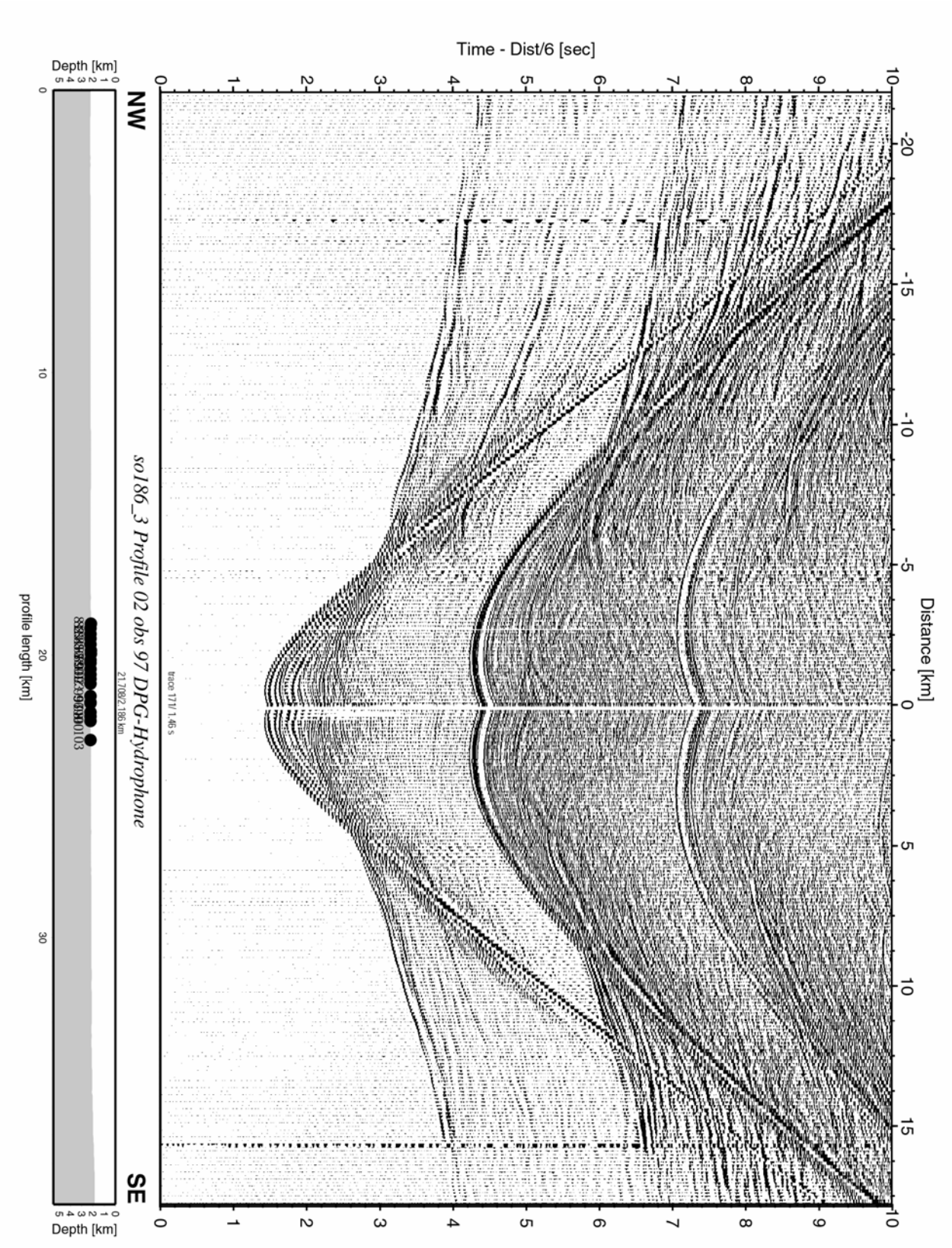

Figure 6.4.22: Record section from obs 97 DPG-Hydrophone, Profile 02.

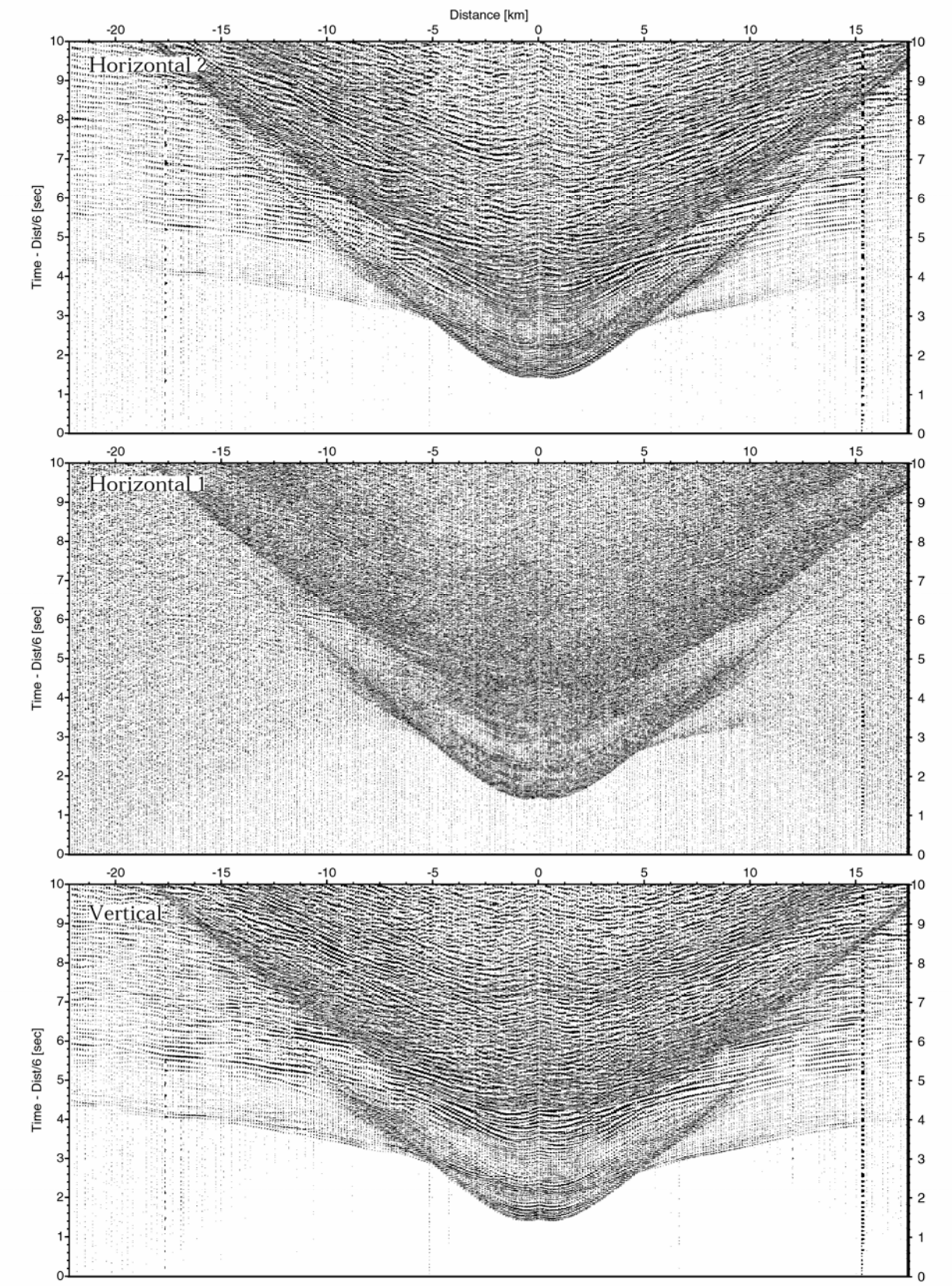

Figure 6.4.23: Record sections from obs 98 OAS/4.5Hz, so186_3 Profile 02.

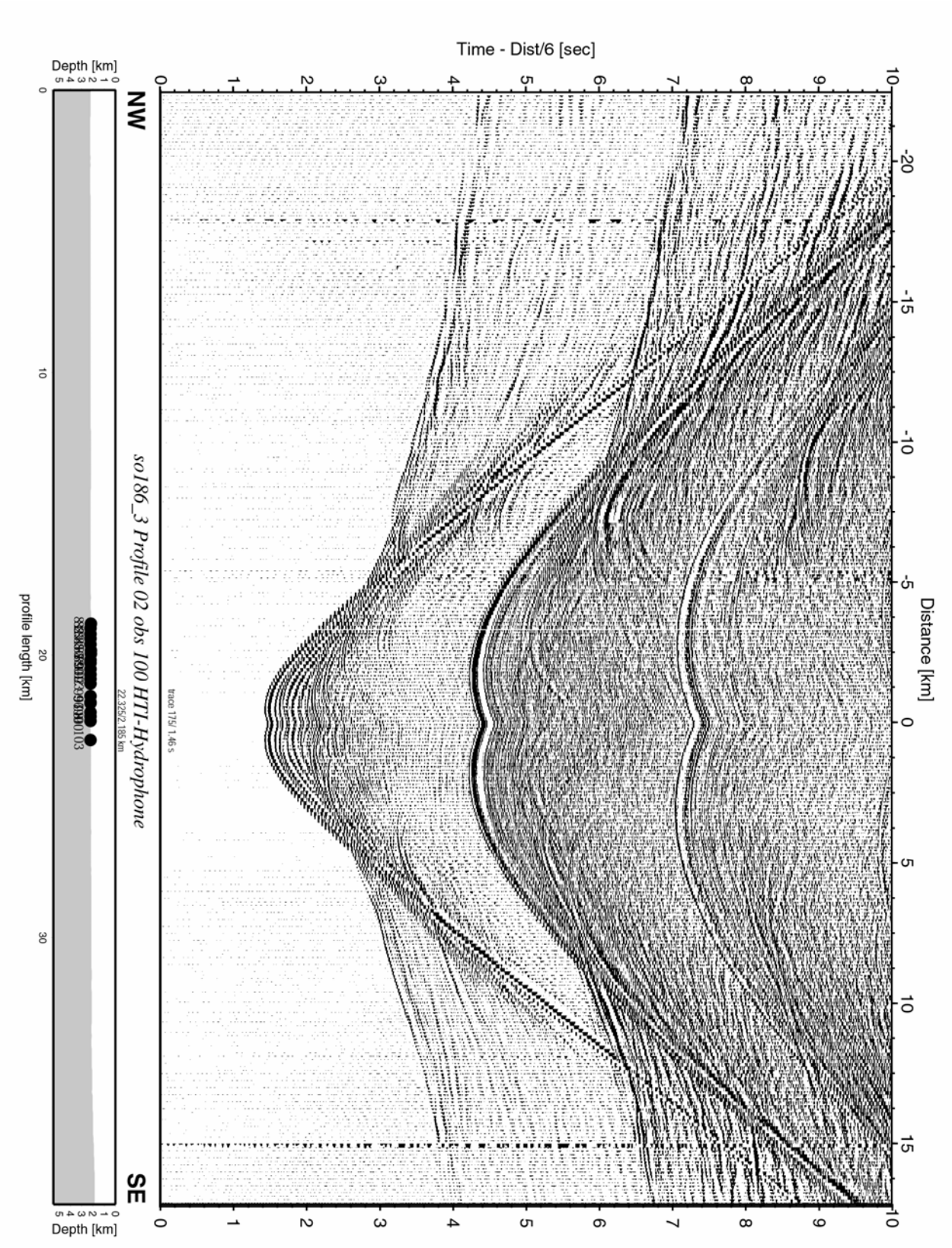

Figure 6.4.24: Record section from obs 100 HTI-Hydrophone, Profile 02.

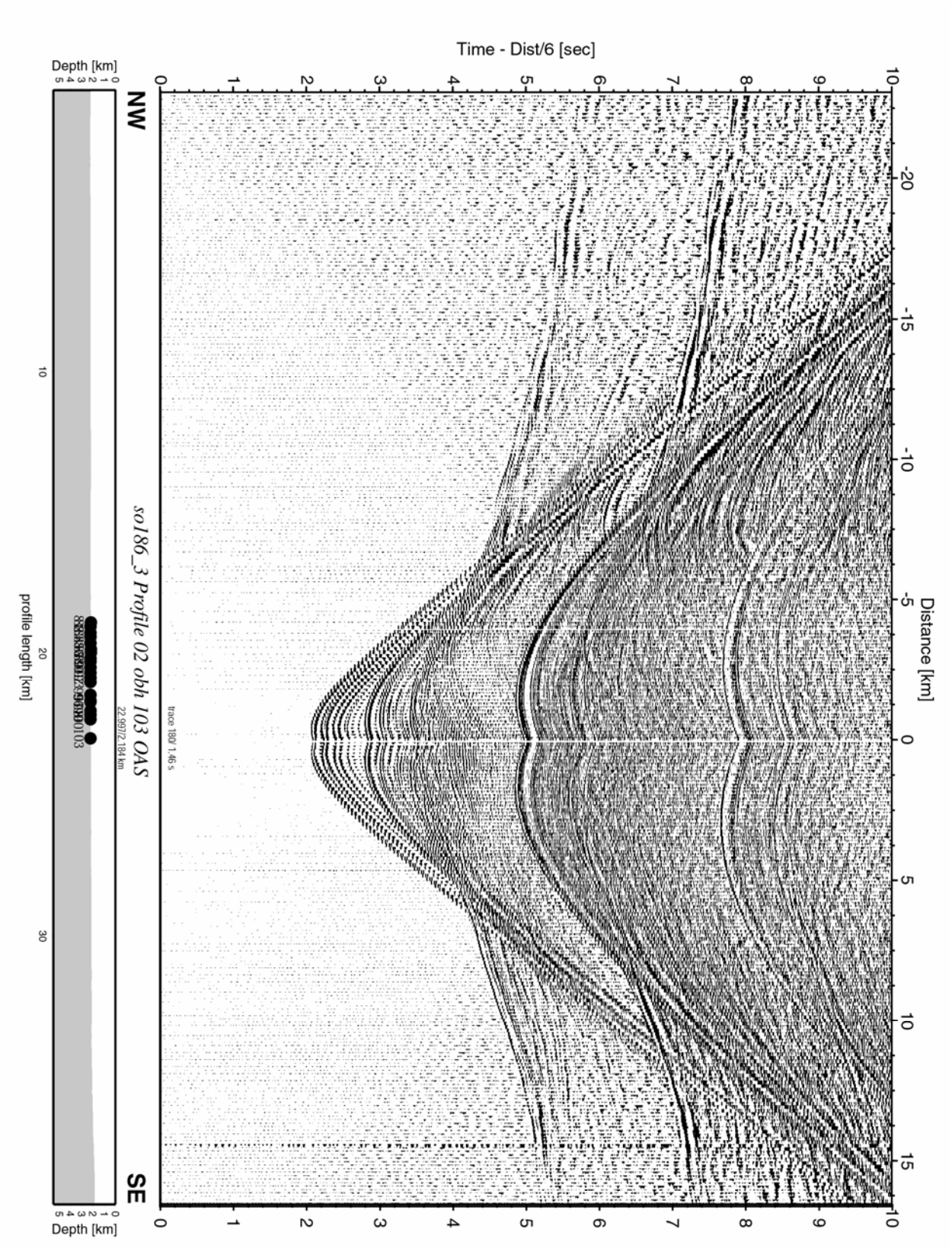

Figure 6.4.25: Record section from obh 103 OAS, Profile 02.

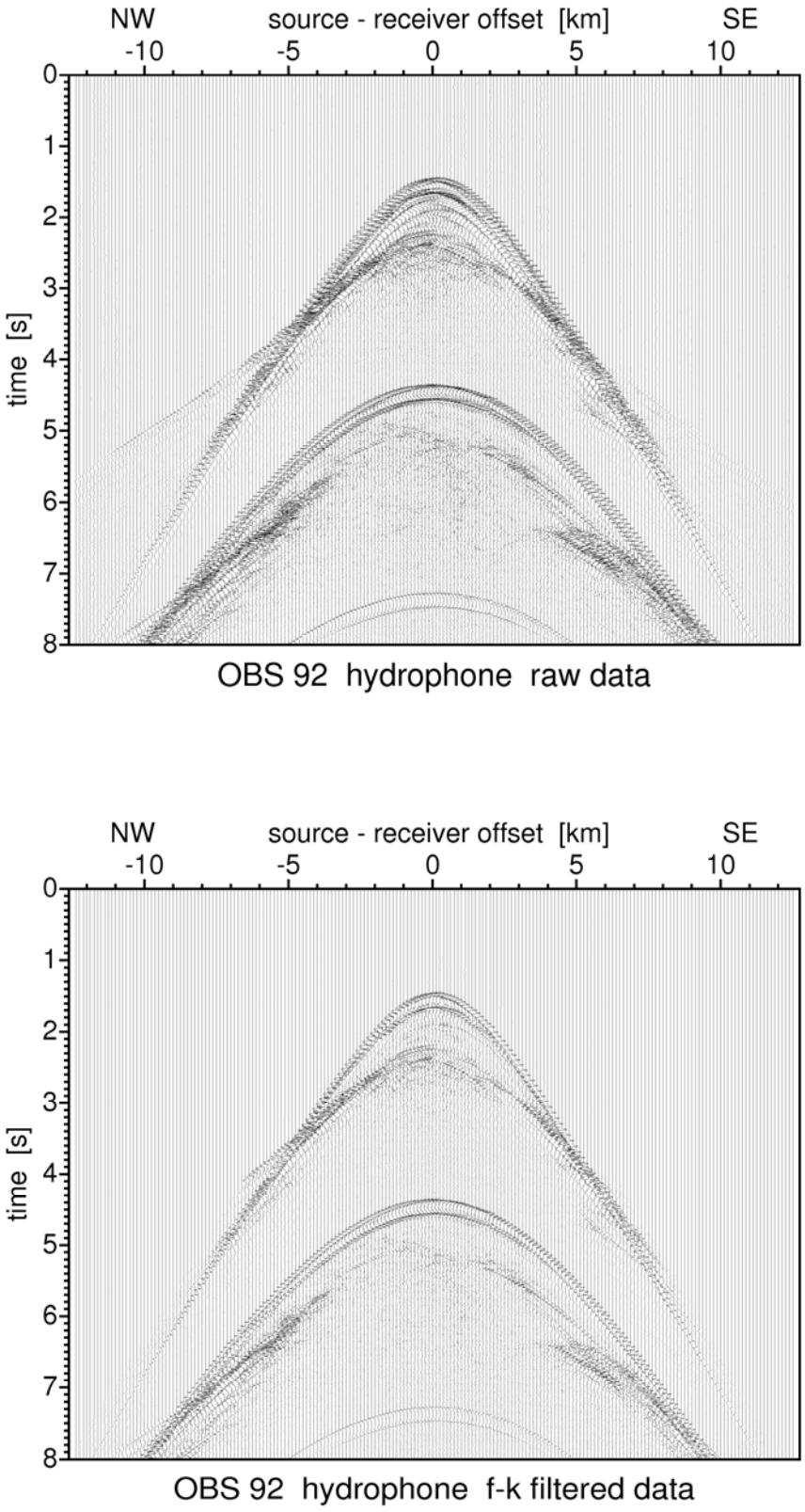

Figure 6.4.26: P-waves of shot profile 2 recorded with the hydrophone at OBS station 92.

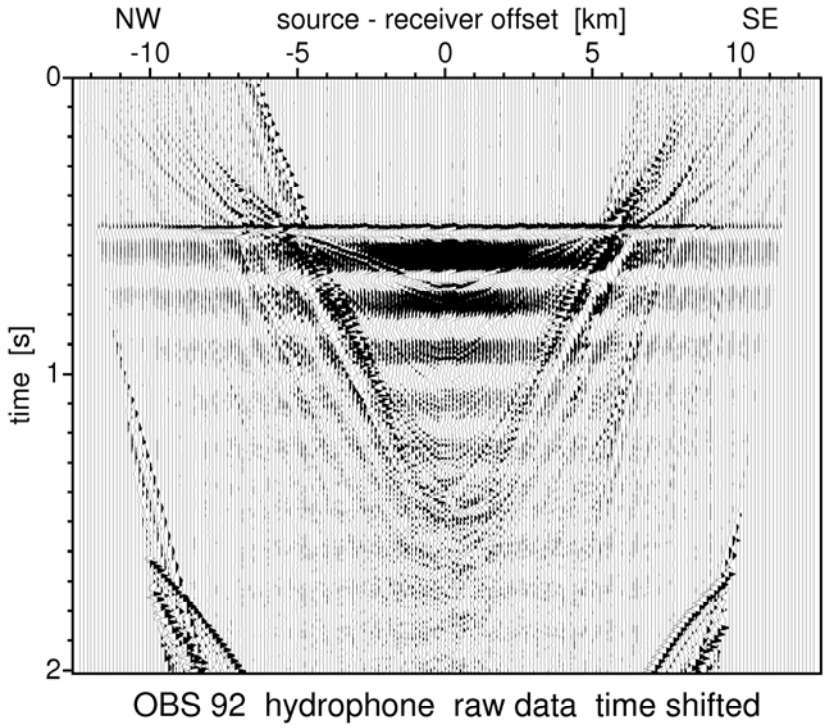

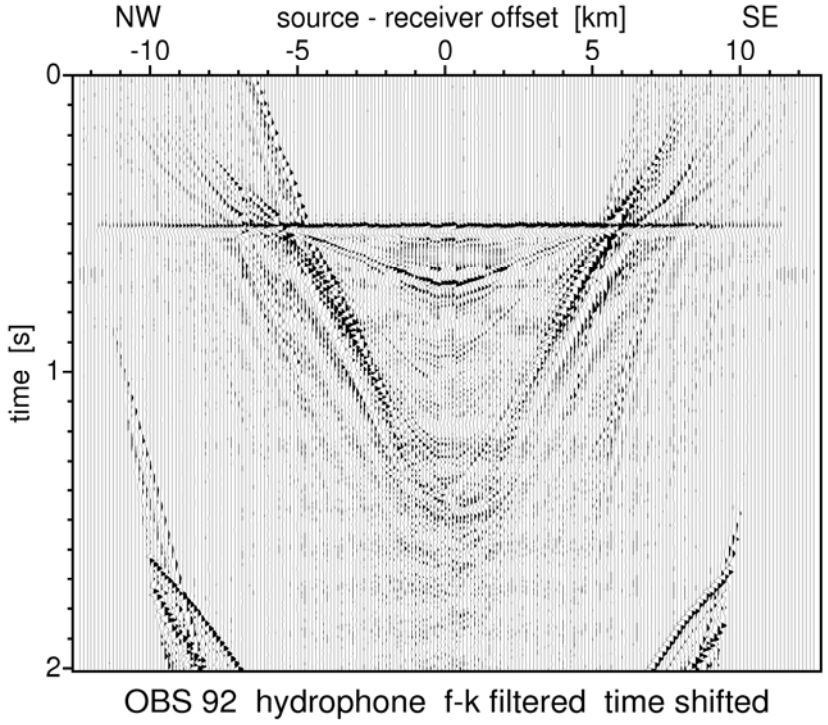

Figure 6.4.27: *The wave field is time shifted with the traveltime of the direct wave in the water column. A 2D Fourier transformation is applied and the bubble of the direct wave is eliminated with a boxcar filter in the transform domain.*

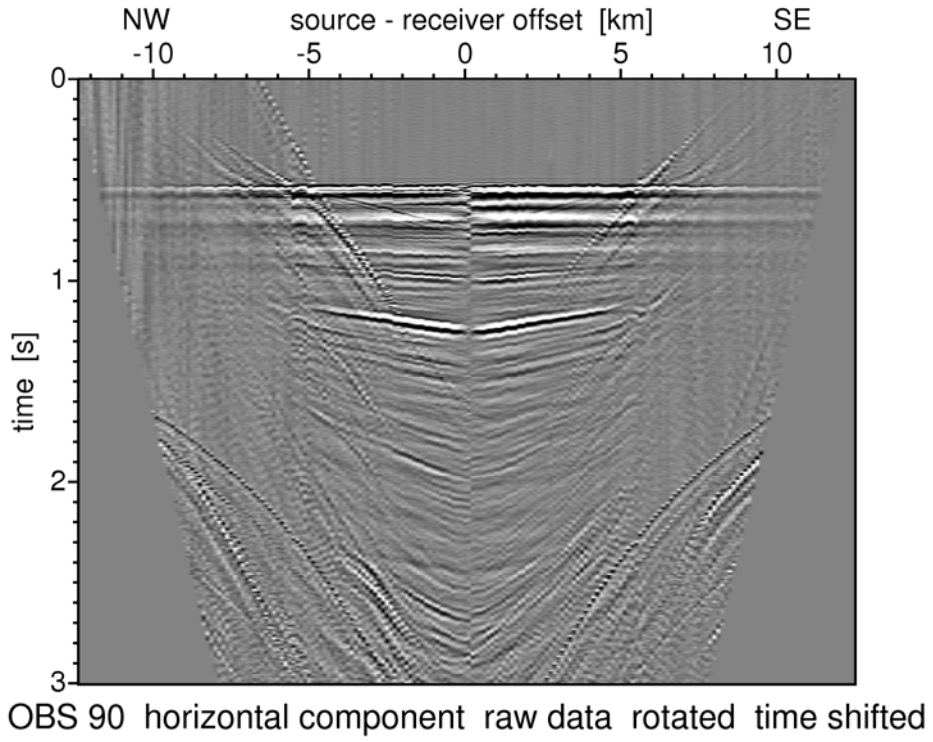

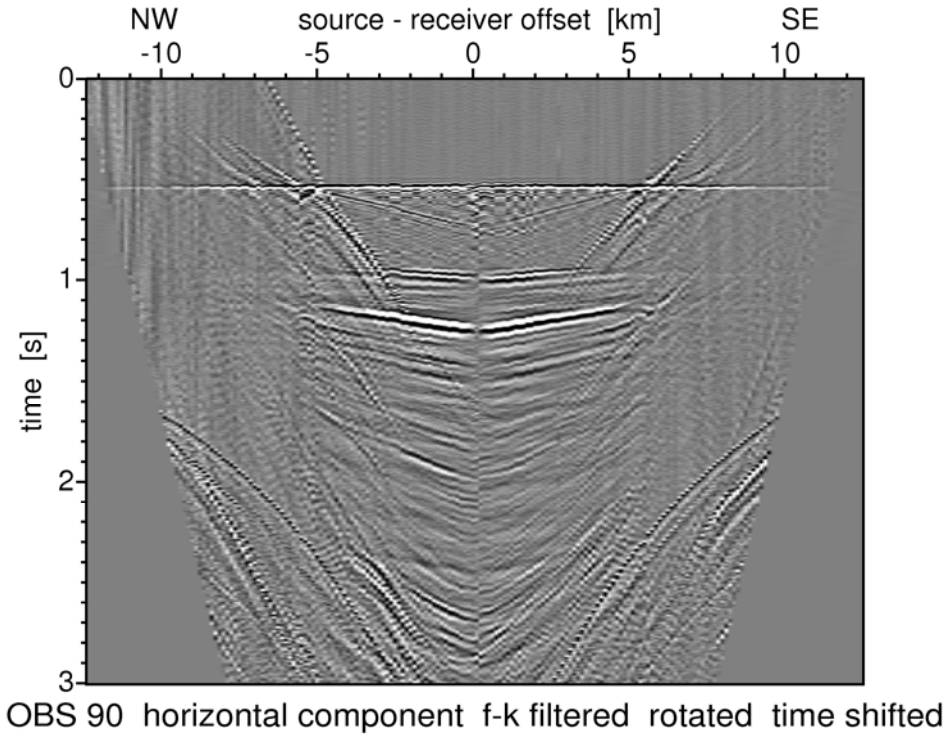

Figure 6.4.28: *S-waves recorded by the horizontal seismometer components of OBS station 90.*

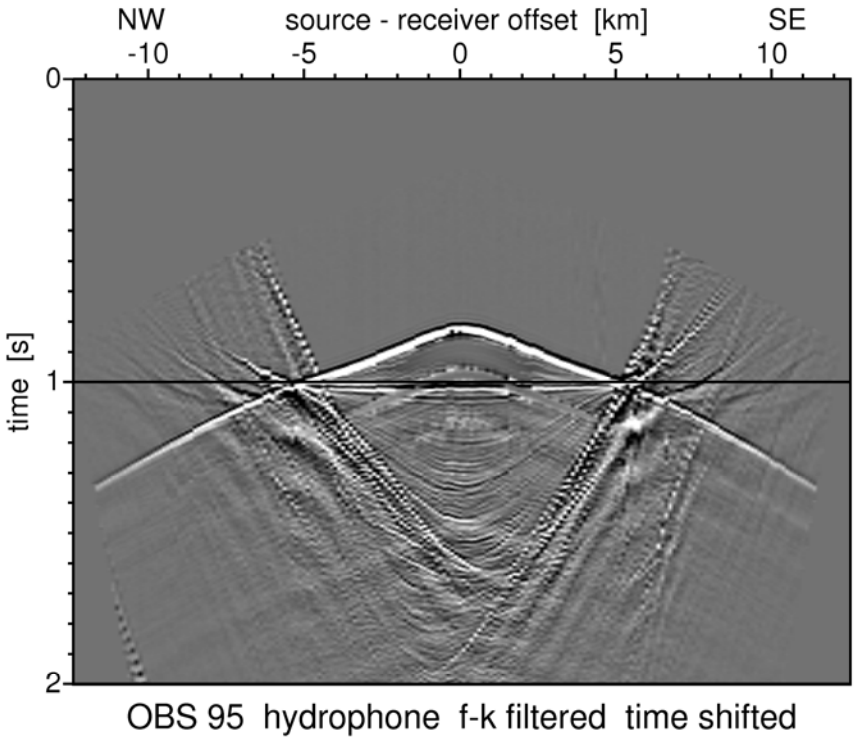

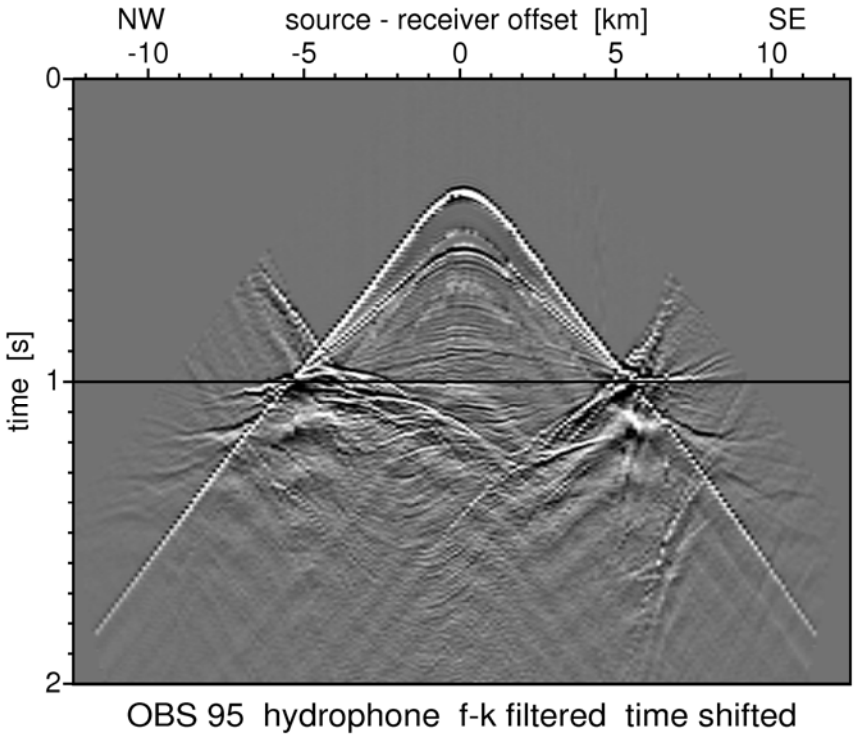

Figure 6.4.29 *The travetime of a PP reflected wave is computed by 1D ray tracing. The data are time shifted to check the parameters in the model, i.e. layer thickness and P-wave velocity.*

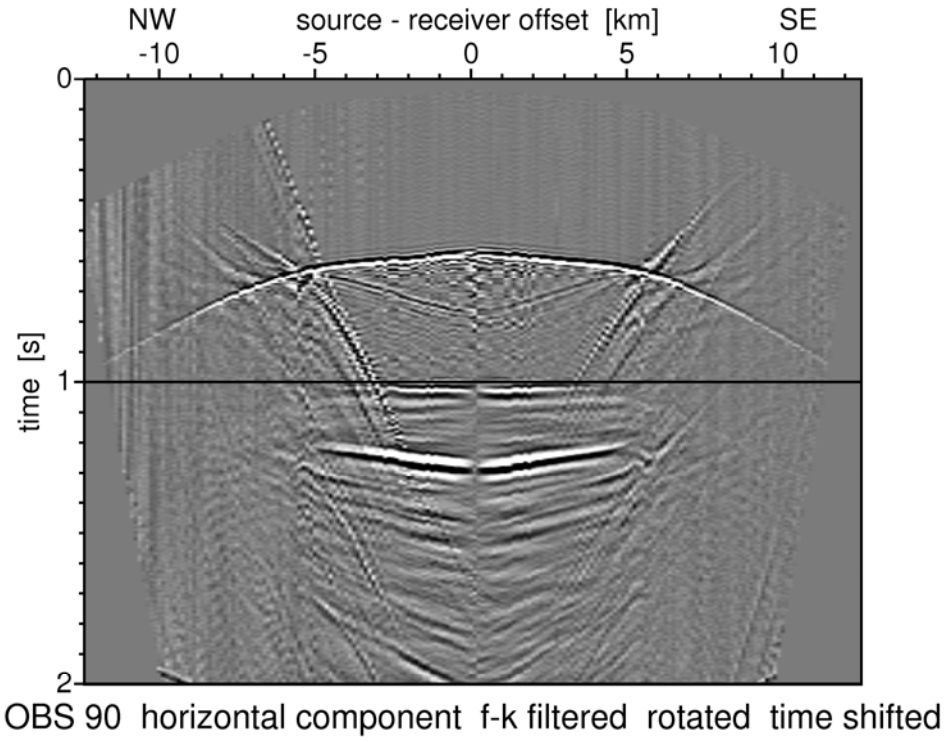

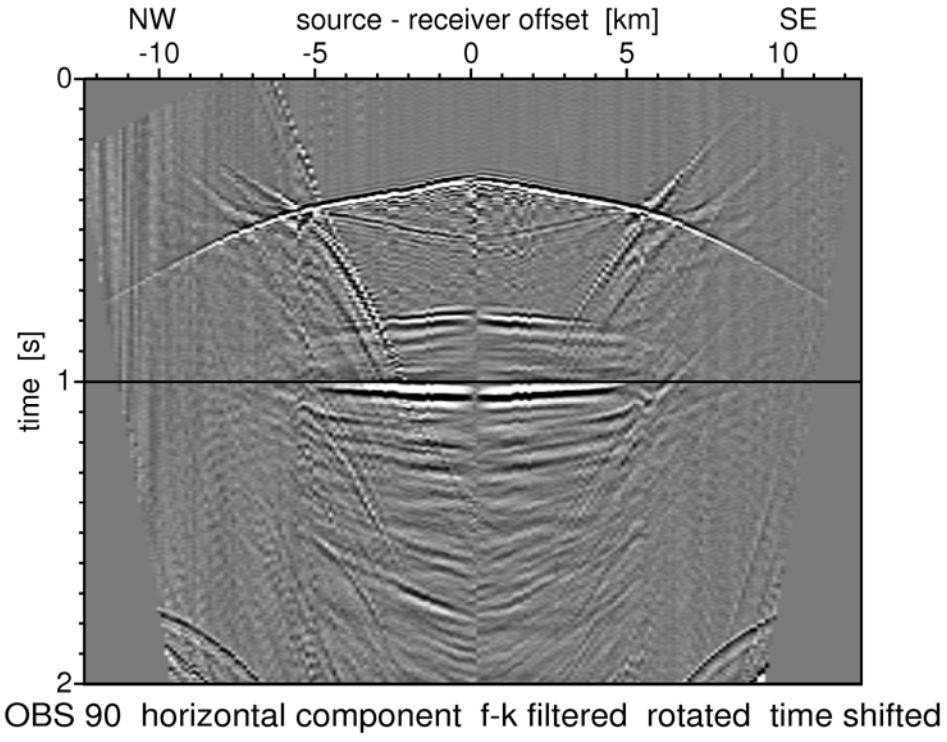

Figure 6.4.30: *The traveltime of a PS-reflected wave is computed by 1D ray tracing. The data are time shifted to determine the S-wave velocity. The layer thickness is known from previous P-wave modelling.*

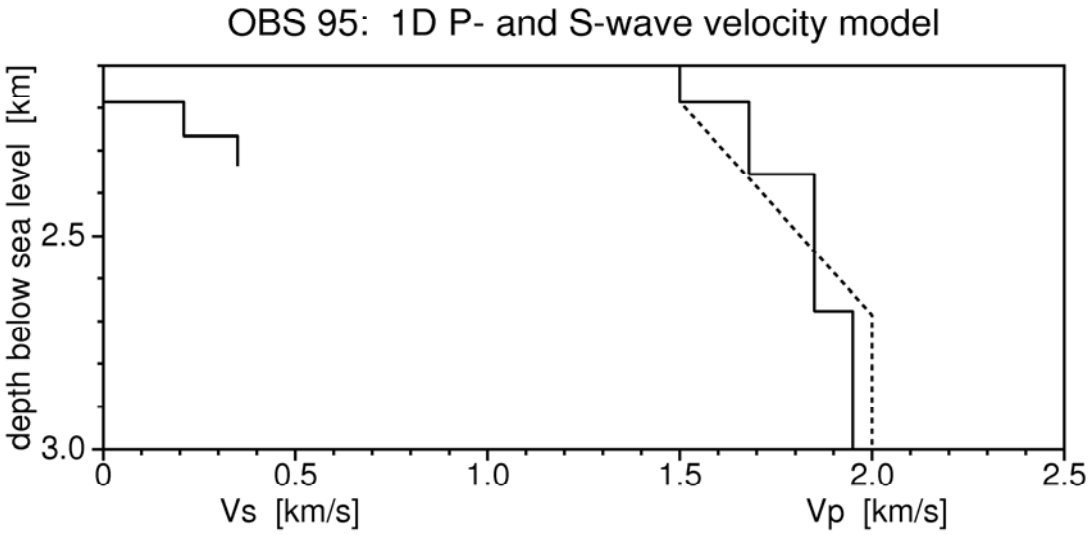

Figure 6.4.31: *P- and S-wave velocity-depth functions obtained by 1D ray tracing (solid lines). A smooth approximation to the P-wave velocity is used to migrate the data (dashed line).*

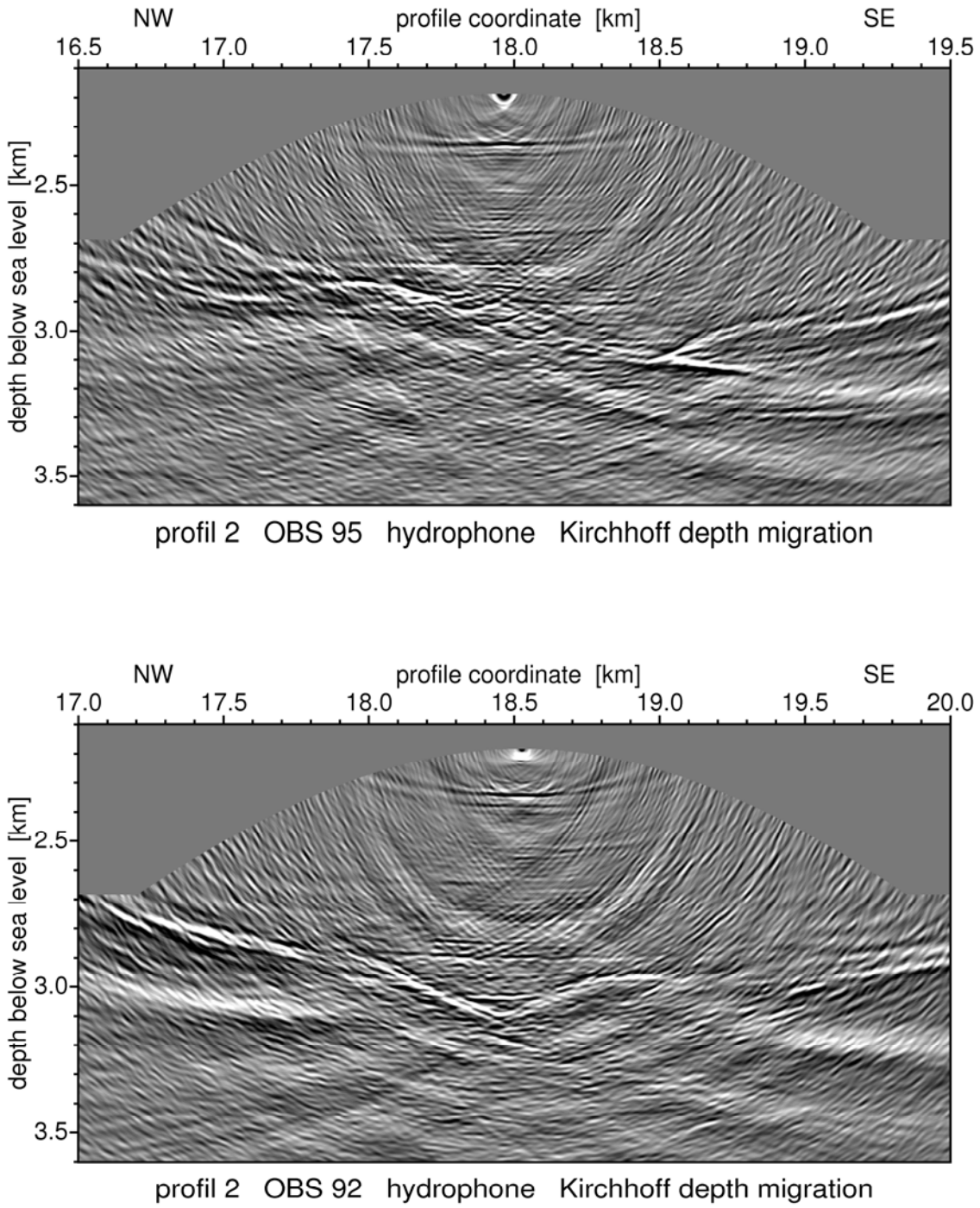

Figure 6.4.32: *Images obtained by Kirchhoff migration of the reflected P-waves at OBS stations 92 and 95.*

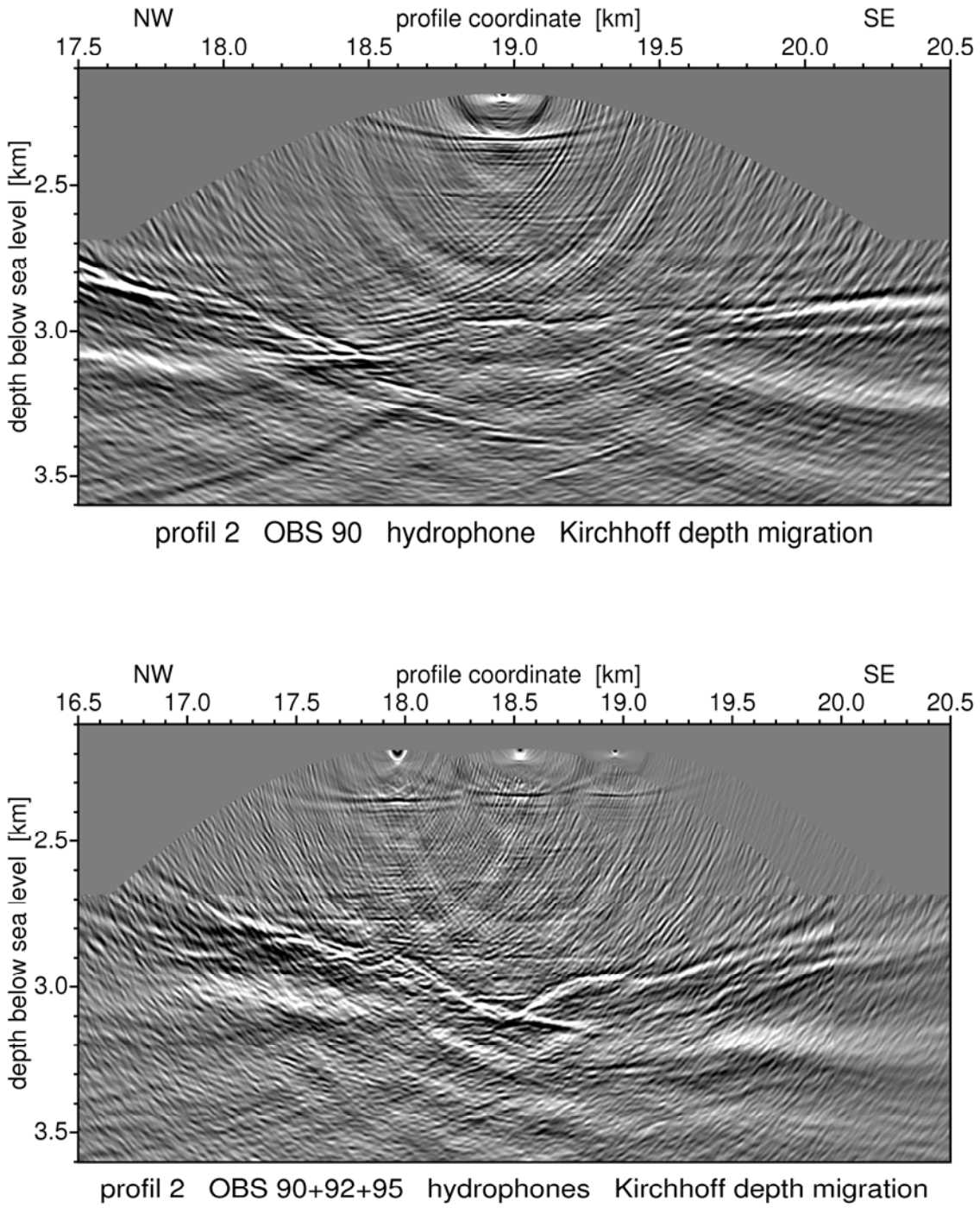

Figure 6.4.33: *Image at OBS station 90 and superposition of the three images of stations 90, 92 and 95.*

6.5 Profile SO186-3-06/19

In this working area a total of 20 OBS and one OBH with a 1000 m long anchor cable were first deployed at an average spacing of 0.1 miles parallel to the trench. The aim was a detailed investigation of the plate boundary that was identified on MCS data collected by our colleagues from BGR during the previous leg (Profile BGR06-109). Across this 2 nm long array of ocean bottom instruments six 20 nm long profiles were shot with both airgun arrays and the trigger interval set to 30 sec. Ship speed was 4 kn, and thus the shot spacing was about 60 m.
Instrument deployment started at midnight on March 09, and after shooting six profiles (p06 to p11) 11 instruments were recovered and redeployed perpendicular to the previous array, with nine instruments remaining in their position. Subsequently, on March 10 and 11 six profiles with identical parameters as before were shot across the array (p13 to p18).
A location map is shown in Figure 6.5.1. All data were played back following the procedure as outlined in 6.1, record sections are shown in Figures 6.5.2 to 6.5.35. All data are of excellent quality.

The OBS114 (Figure 6.5.1) was placed in the junction of both sets of profiles. For this reason it was chosen for 1-D modelling with MacRay using refractions but also reflections. Figure 6.5.36 shows the resulting velocity model. The data at this station and at the most of the others in this area are of good quality independent of the direction of the profile, across or along the trench. Mostly differences in the roughness of topography affect the data. The profiles are situated at the forearc side in an area of smooth topography with water depths at around 2470 m.
The sediment thickness is very high. A layer of loose very young sediments is estimated to about 500 m by a constant velocity of 1700 m/s. Beneath these several layers of older sediments follow with slightly rising velocities caused by compaction and pressure increase. These velocities increase to 5.4 km/s at a depth of 15 km. At this depth the velocities increase to > 6.2 km/s, typical for oceanic crust that is subducted here.

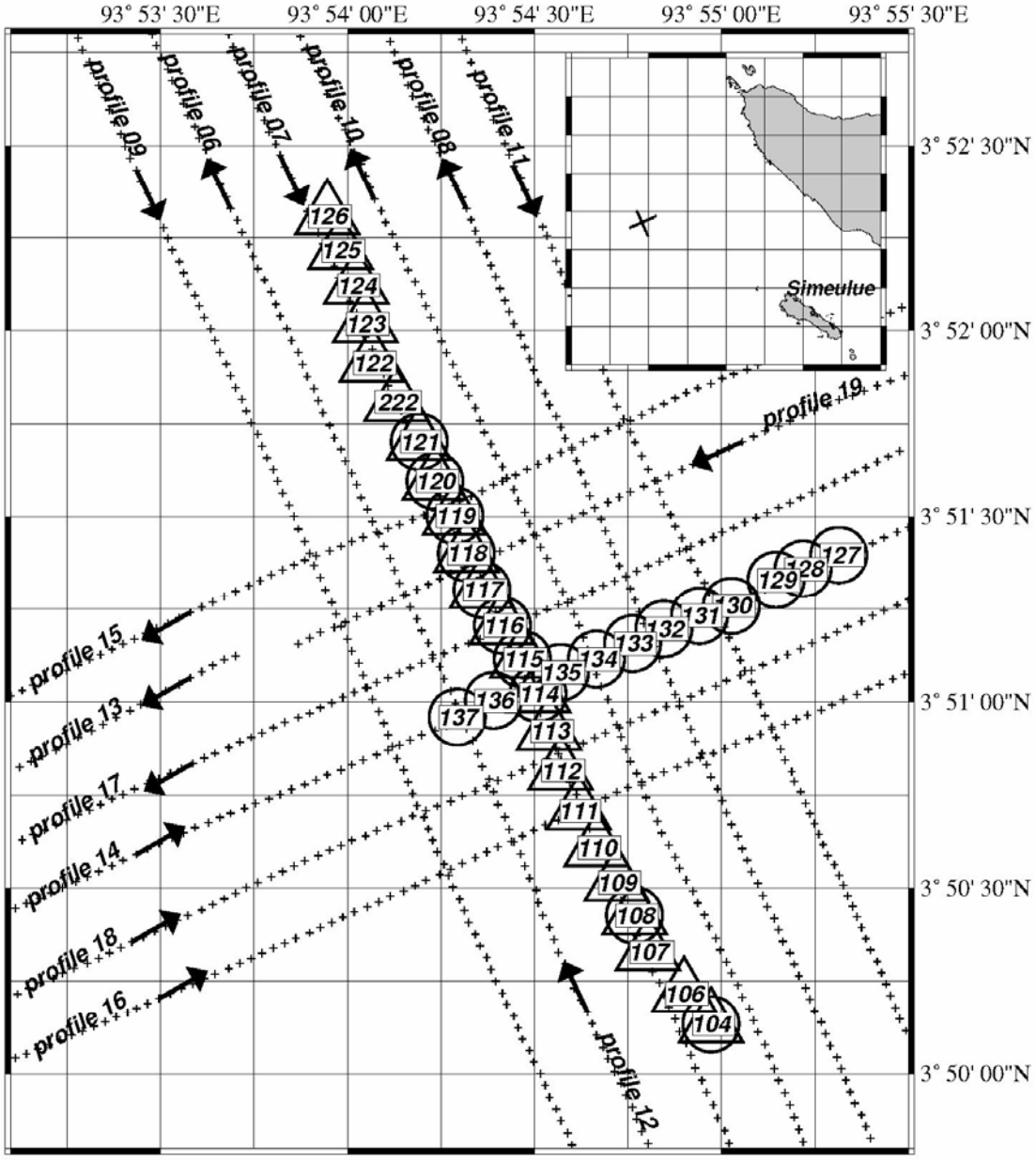

Figure 6.5.1: Location Map

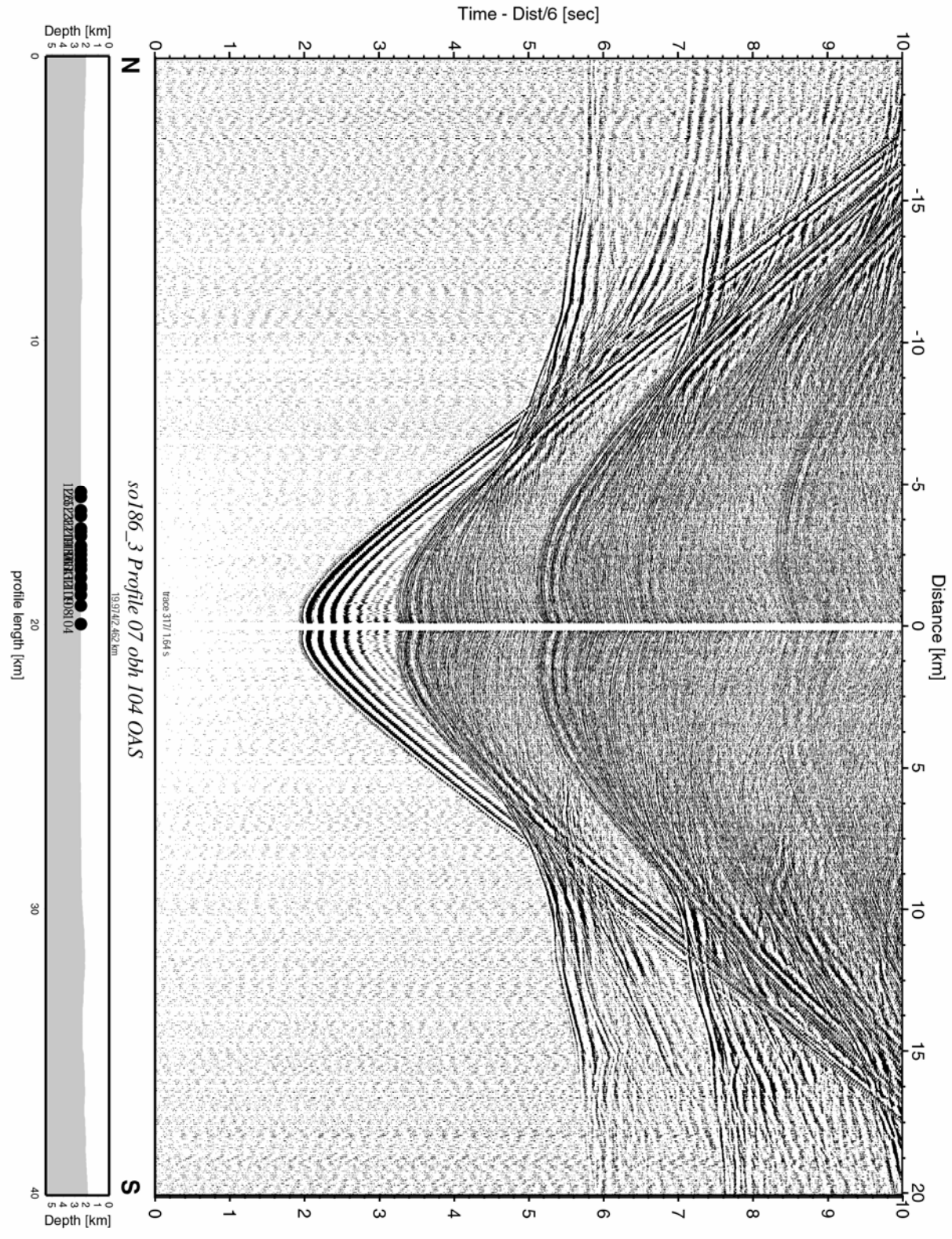

Figure 6.5.2: Record section from obh 104 OAS, Profile 07.

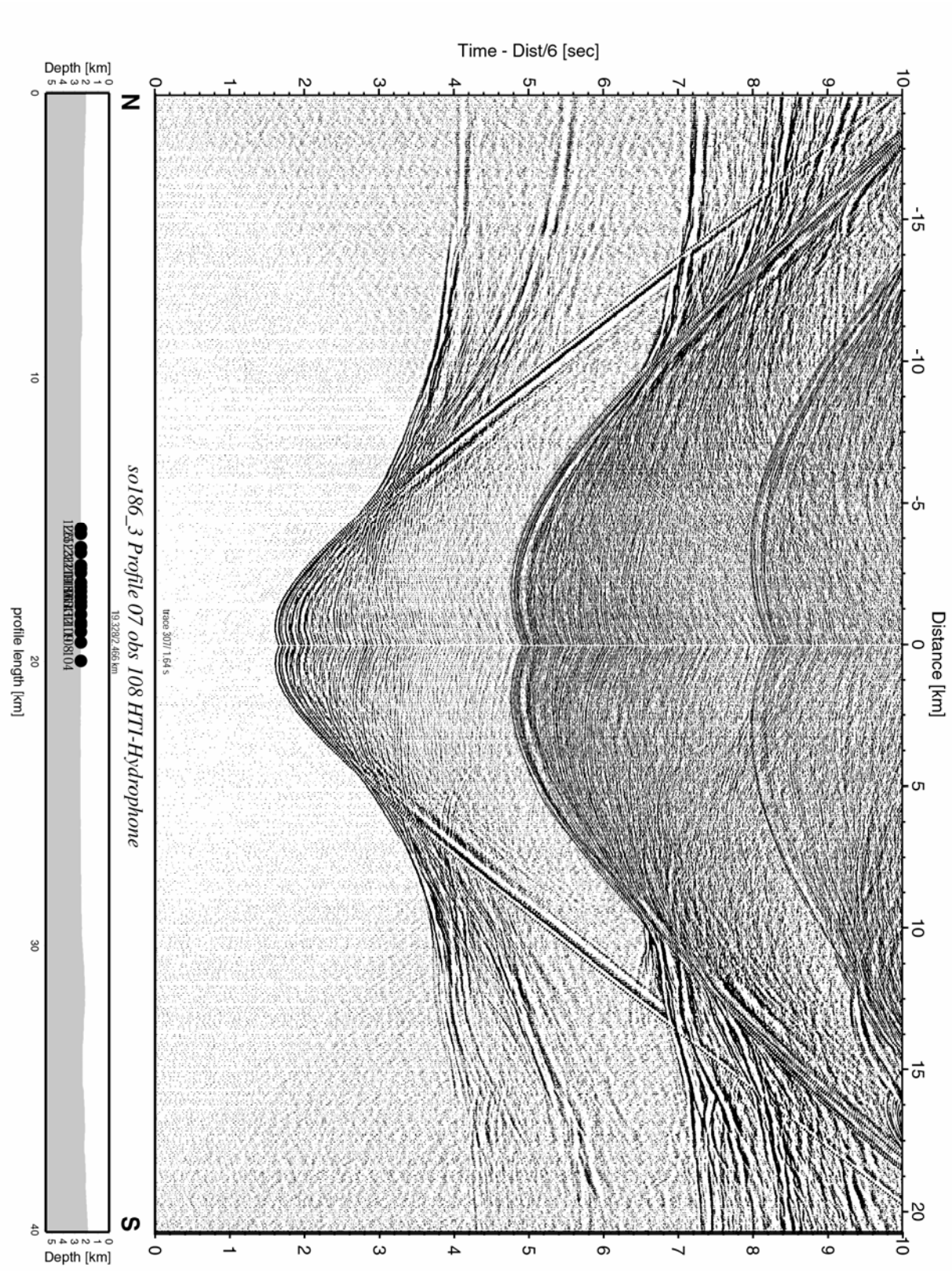

Figure 6.5.3: Record section from obs 108 HTI-Hydrophone, Profile 07.

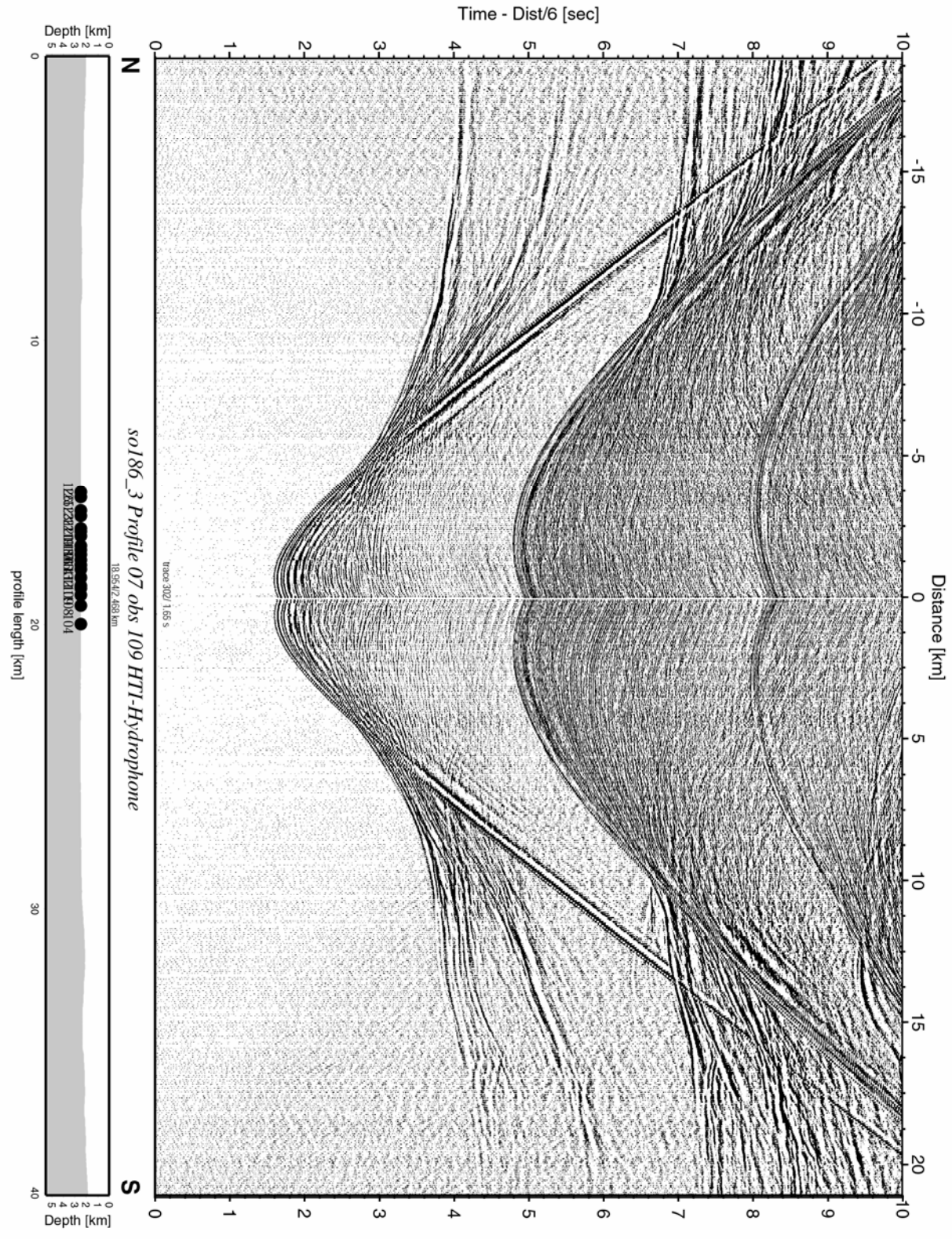

Figure 6.5.4: Record section from obs 109 HTI-Hydrophone, Profile 07.

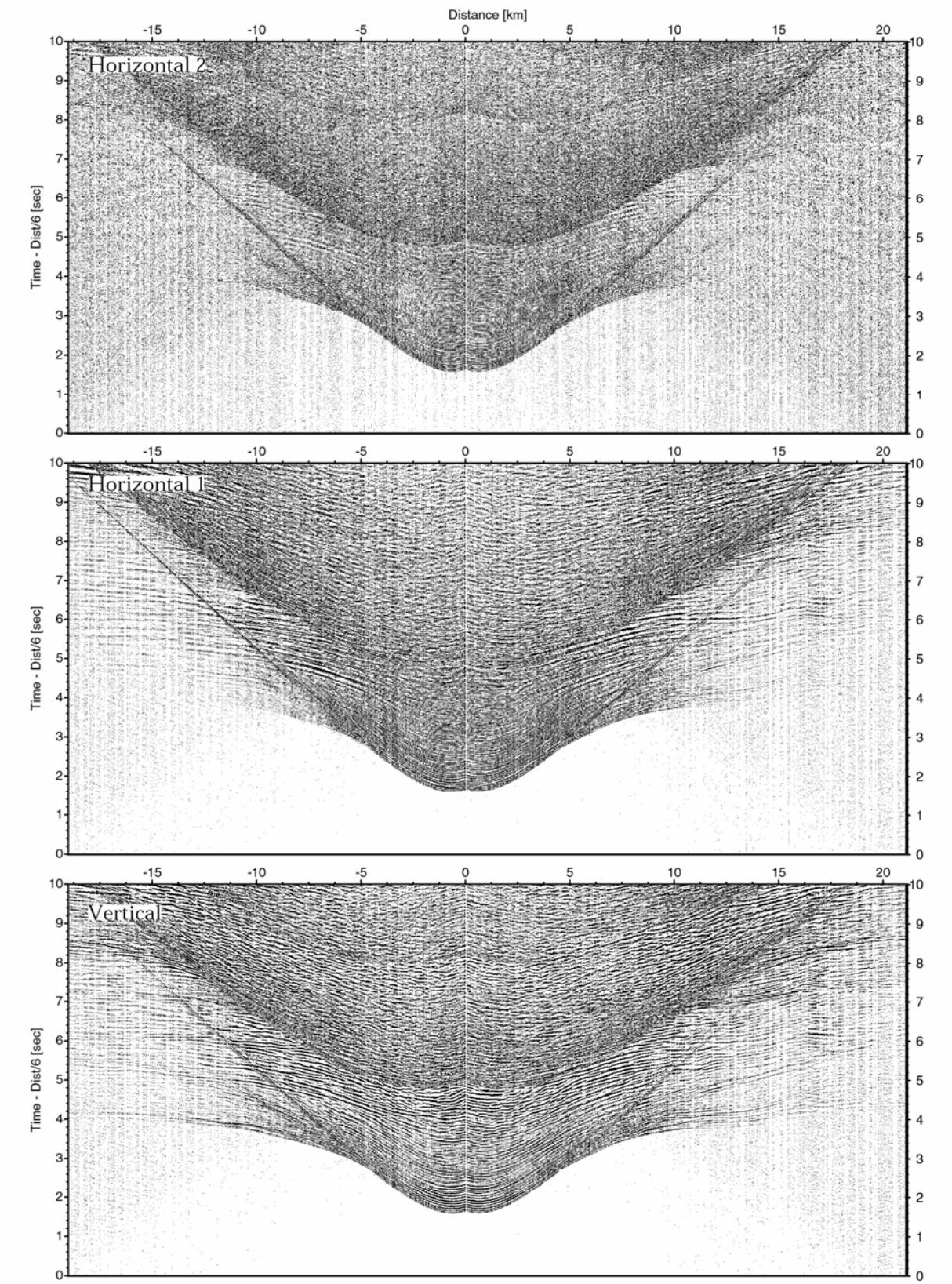

Figure 6.5.5: Record sections from obs 109 HTI/4.5Hz, so186_3 Profile 07.

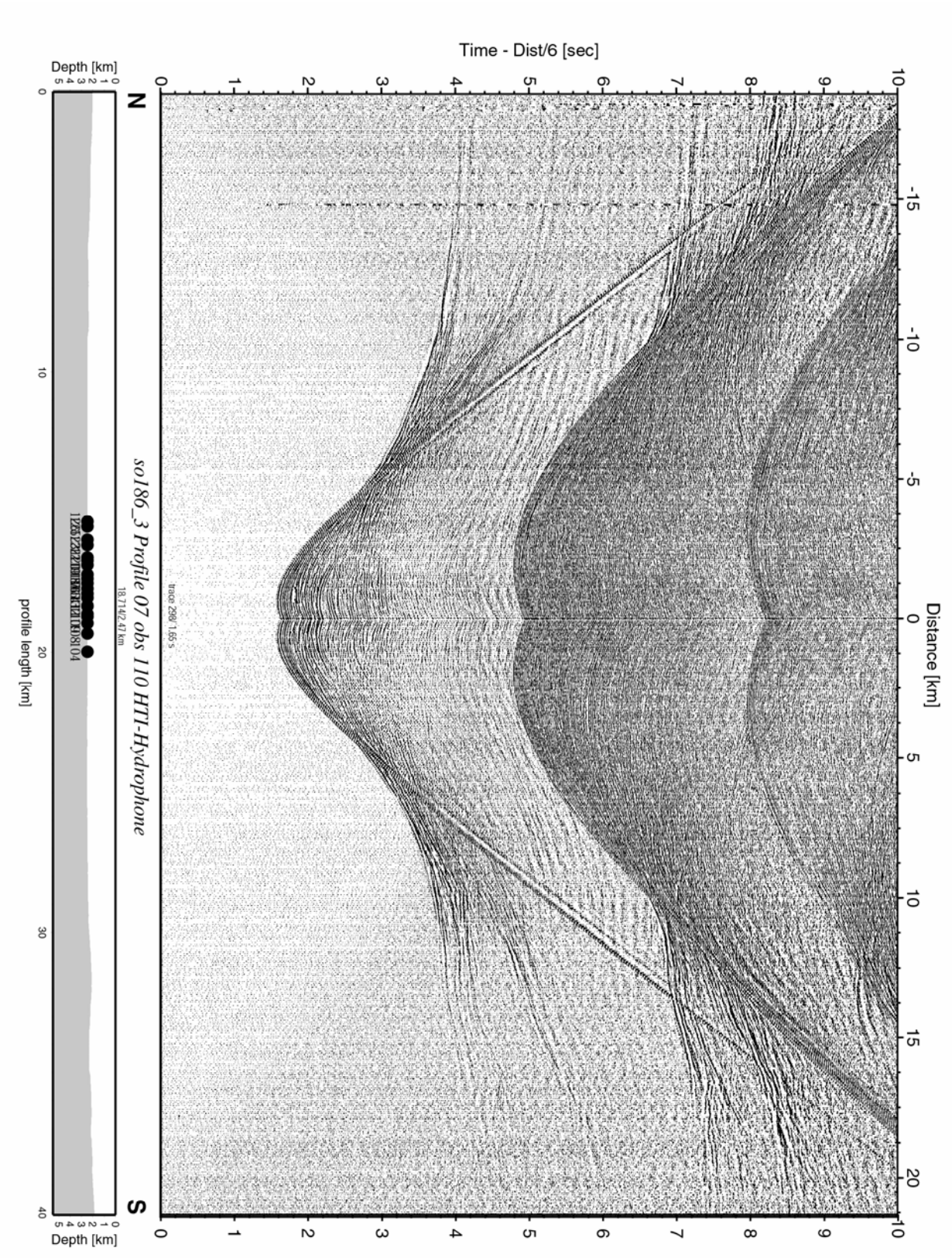

Figure 6.5.6: Record section from obs 110 HTI-Hydrophone, Profile 07.

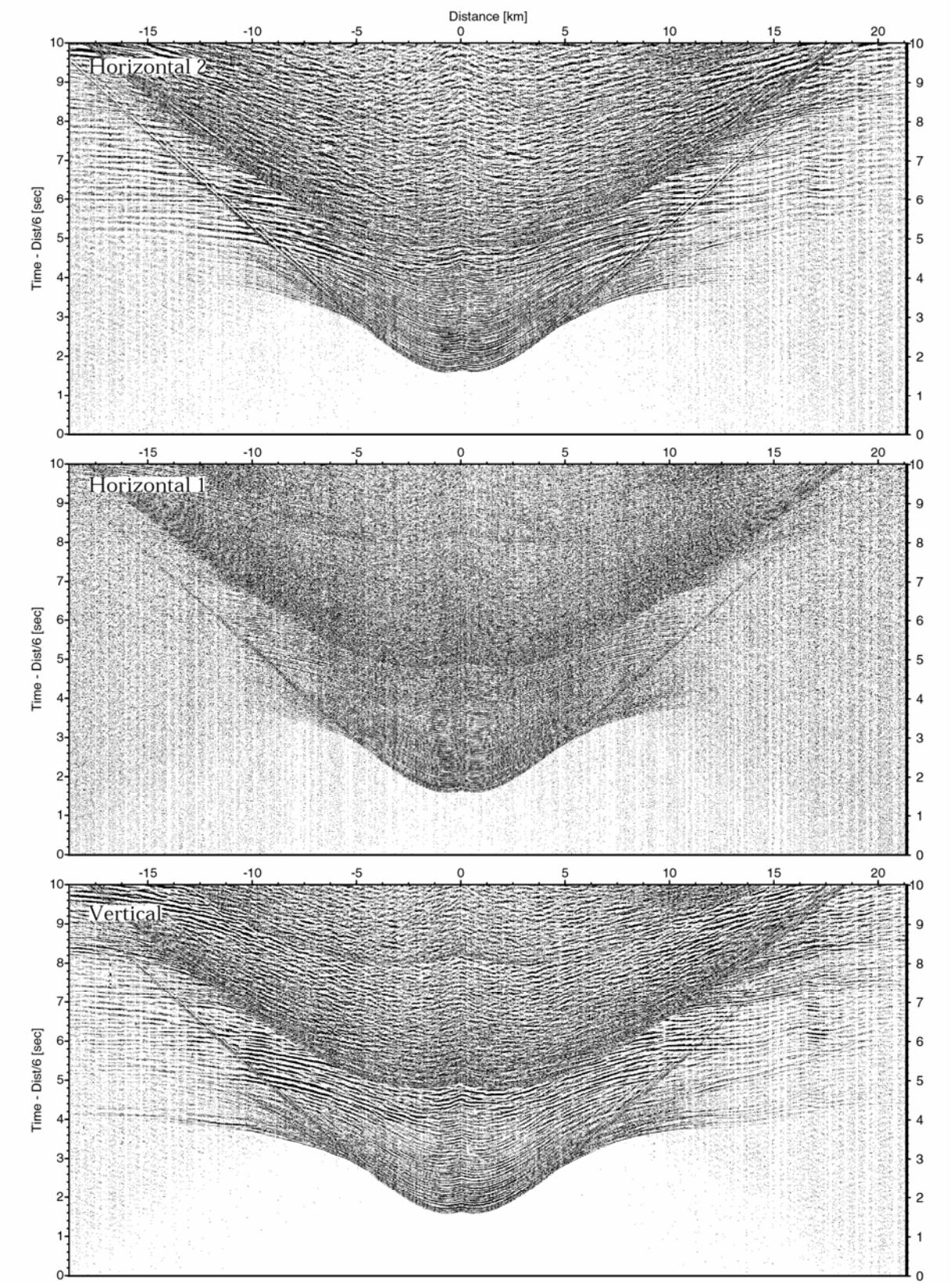

Figure 6.5.7: Record sections from obs 110 HTI/4.5Hz, so186_3 Profile 07.

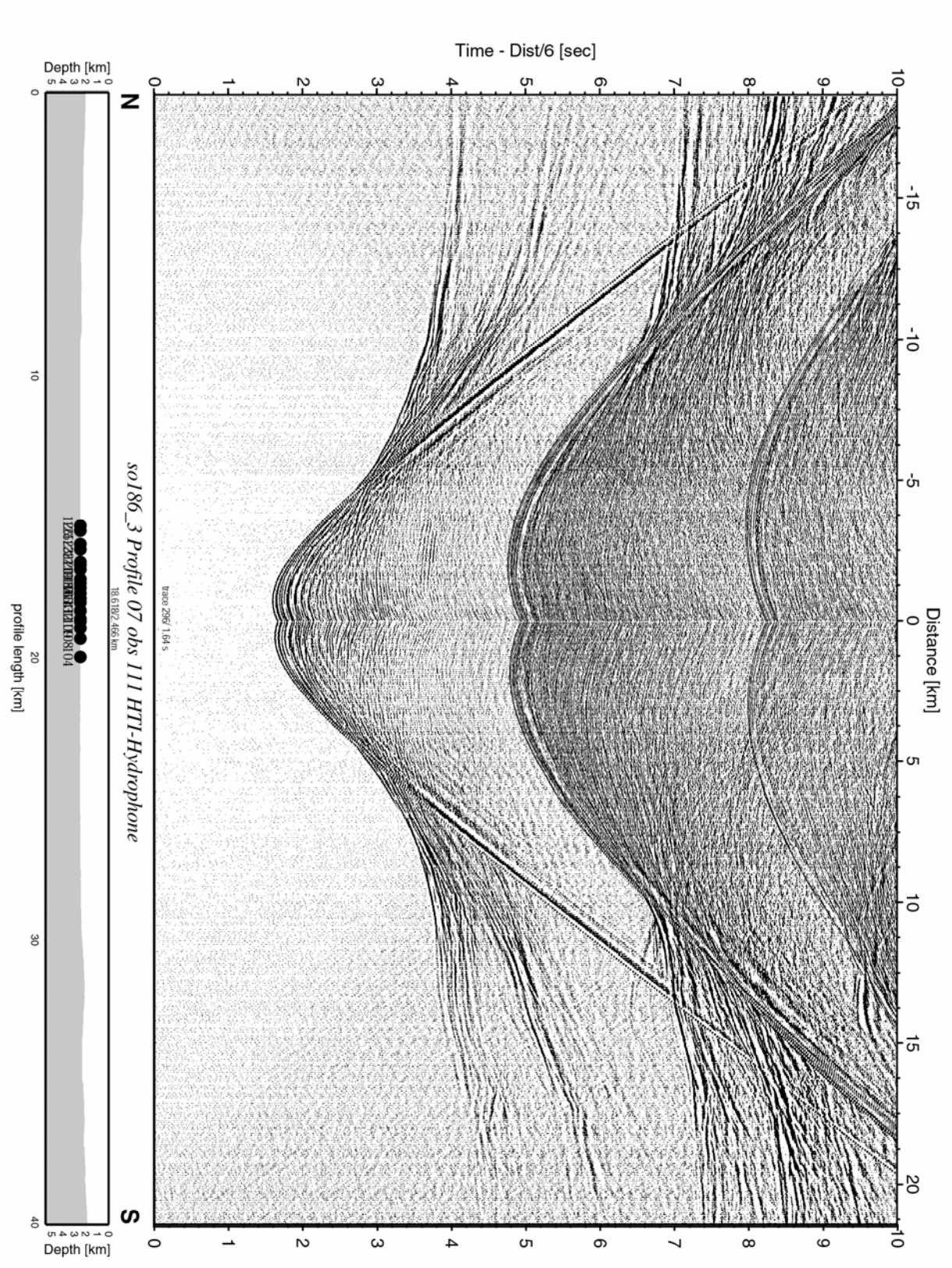

Figure 6.5.8: Record section from obs 111 HTI-Hydrophone, Profile 07.

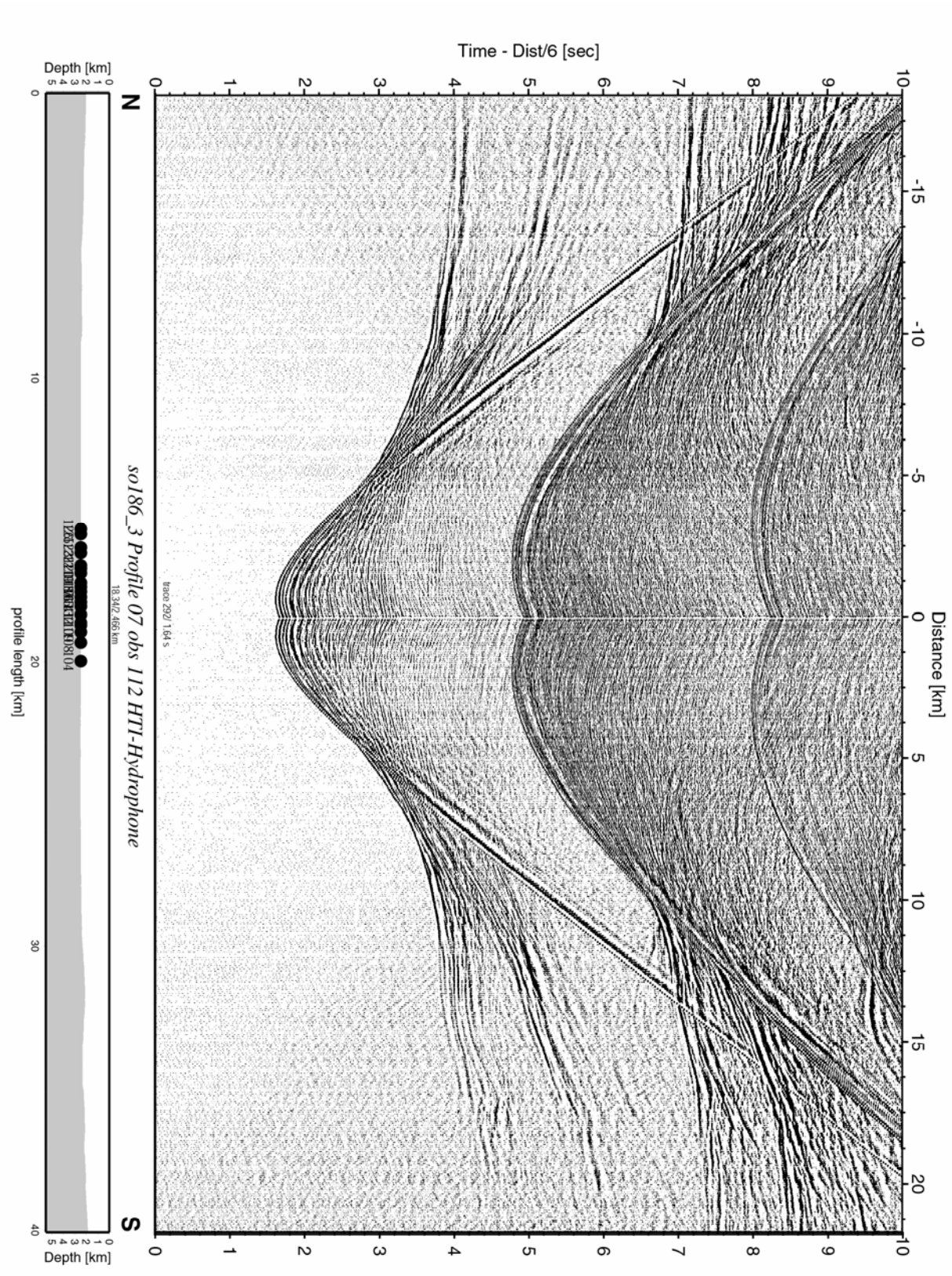

Figure 6.5.9: Record section from obs 112 HTI-Hydrophone, Profile 07.

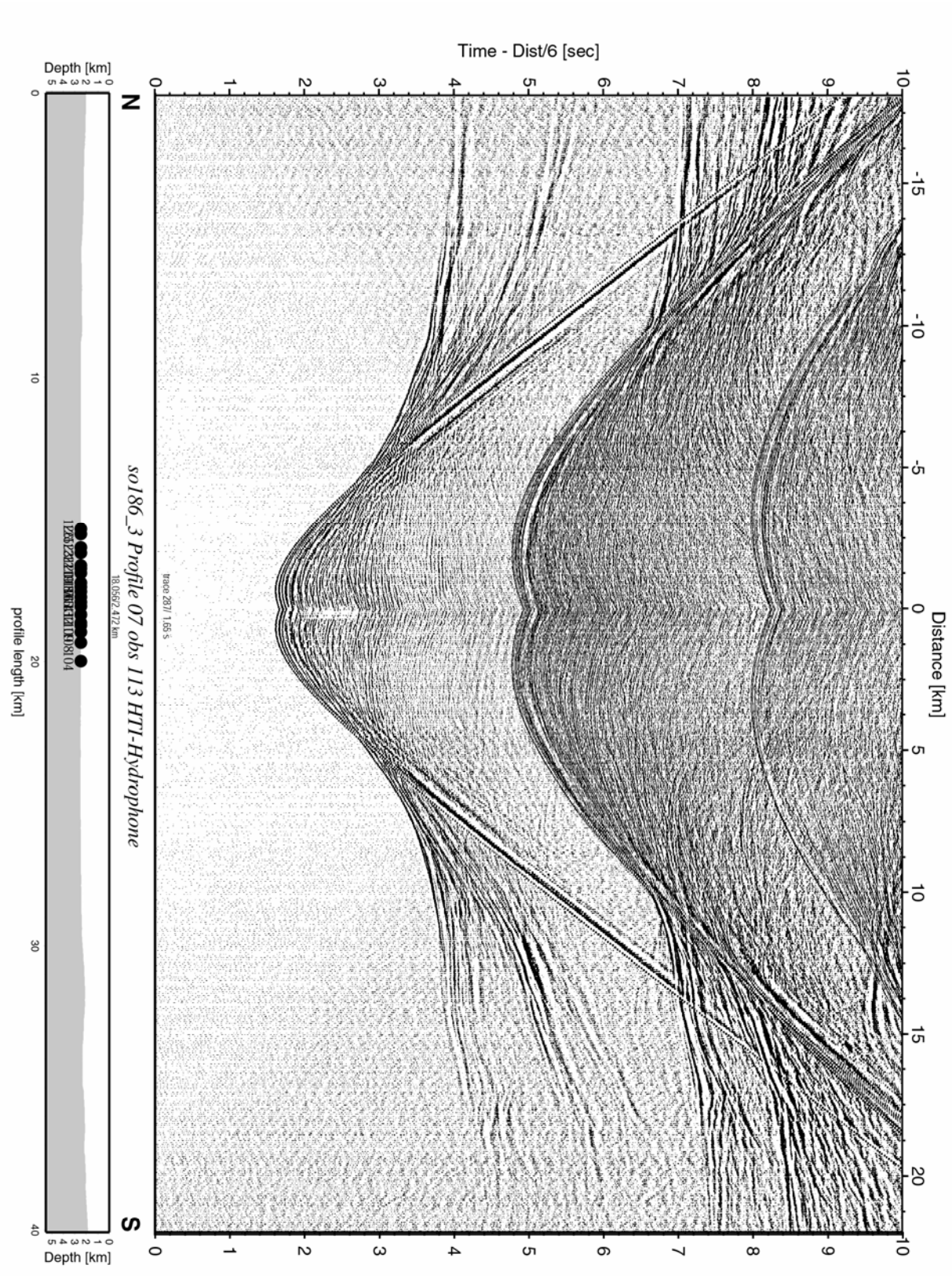

Figure 6.5.10: Record section from obs 113 HTI-Hydrophone, Profile 07.

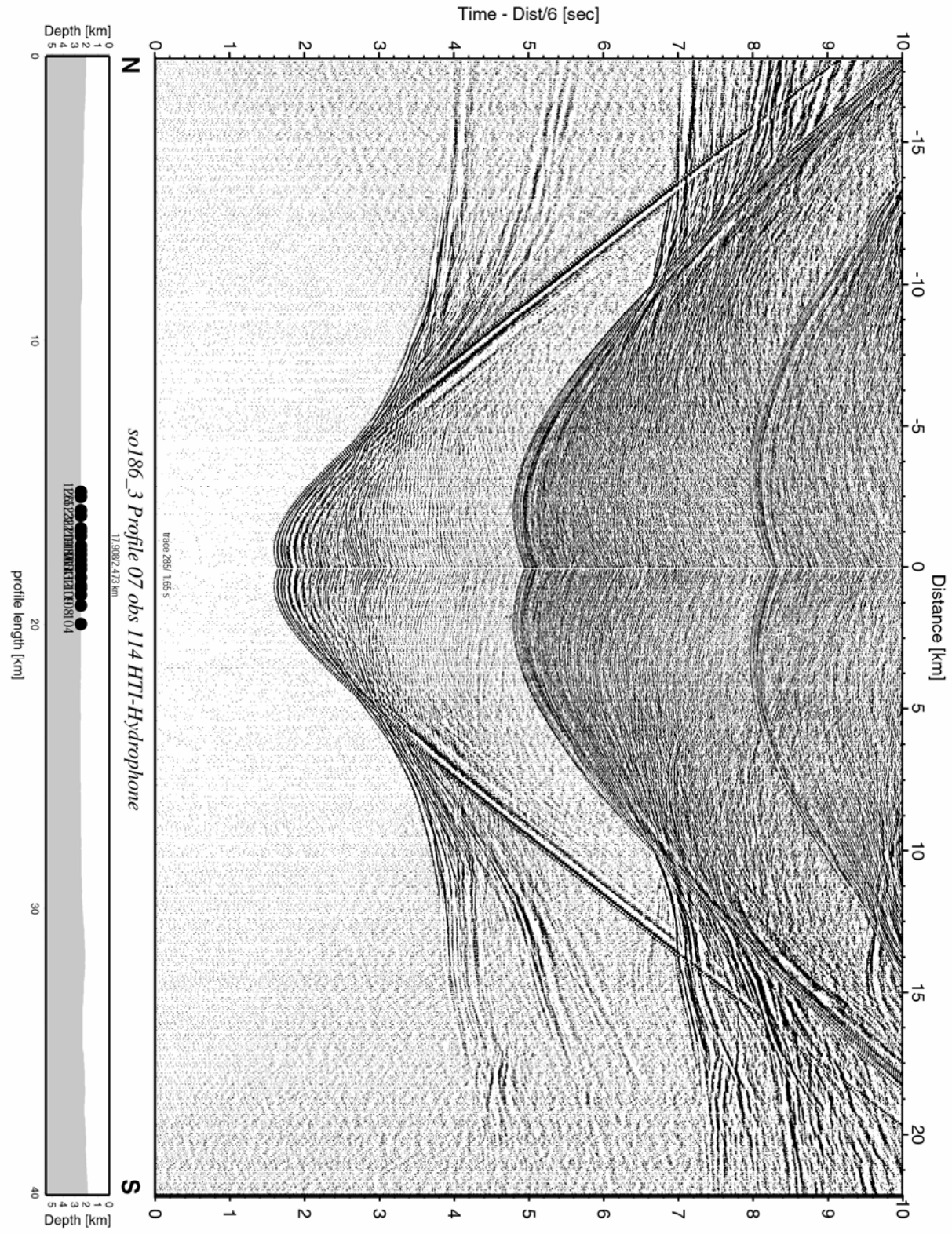

Figure 6.5.11: Record section from obs 114 HTI-Hydrophone, Profile 07.

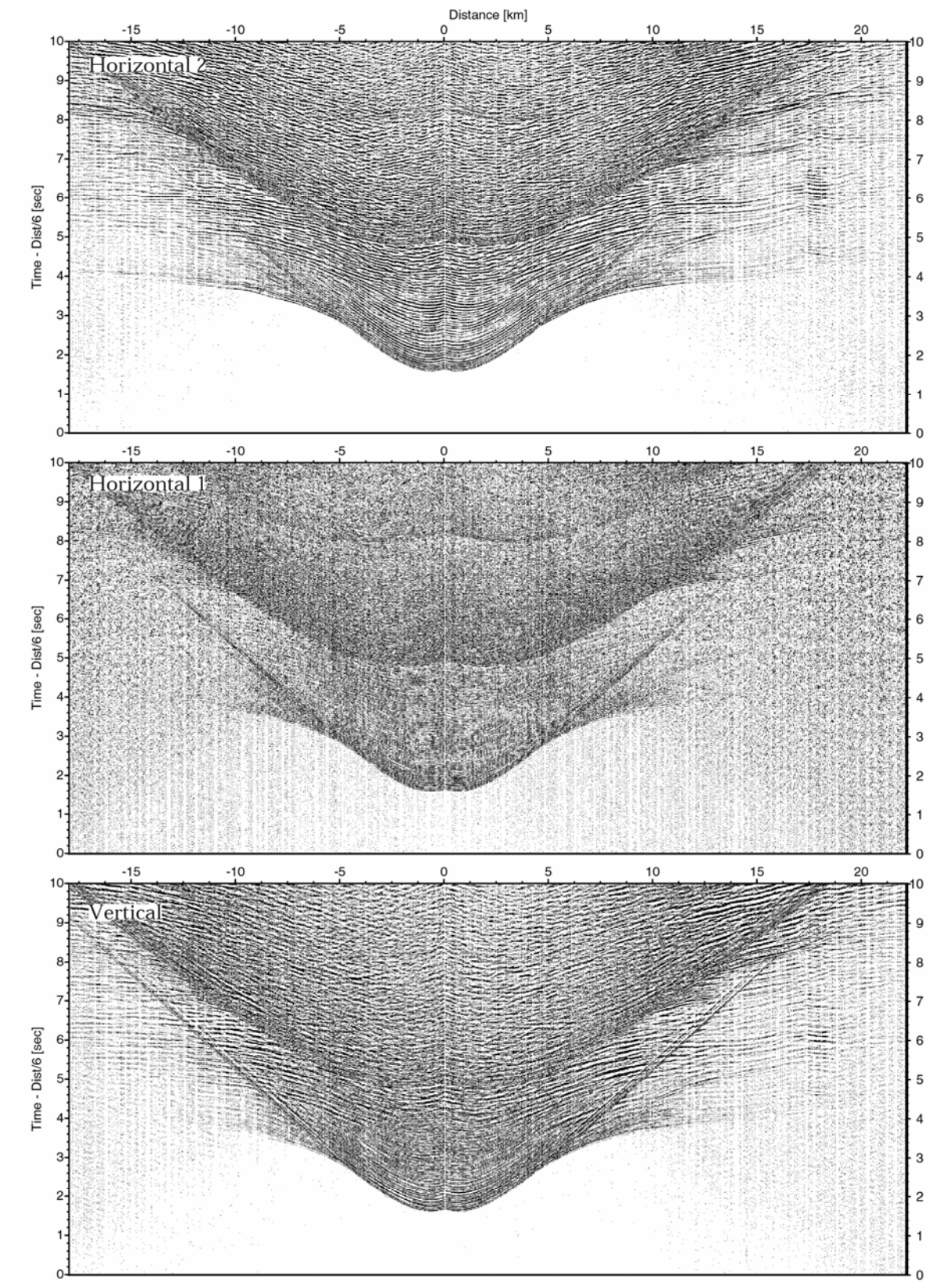

Figure 6.5.12: Record sections from obs 114 HTI/4.5Hz, so186_3 Profile 07.

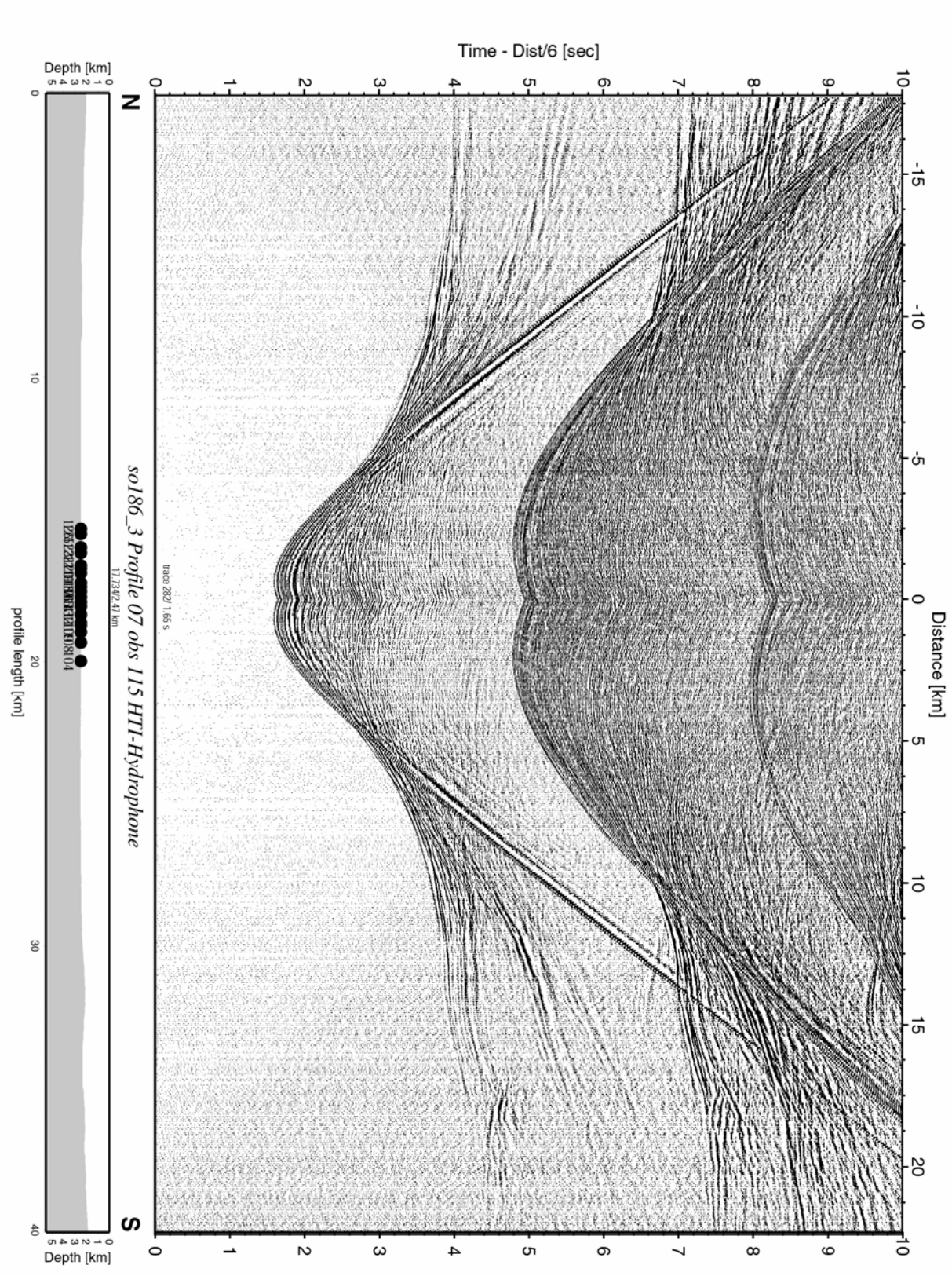

Figure 6.5.13: Record section from obs 115 HTI-Hydrophone, Profile 07.

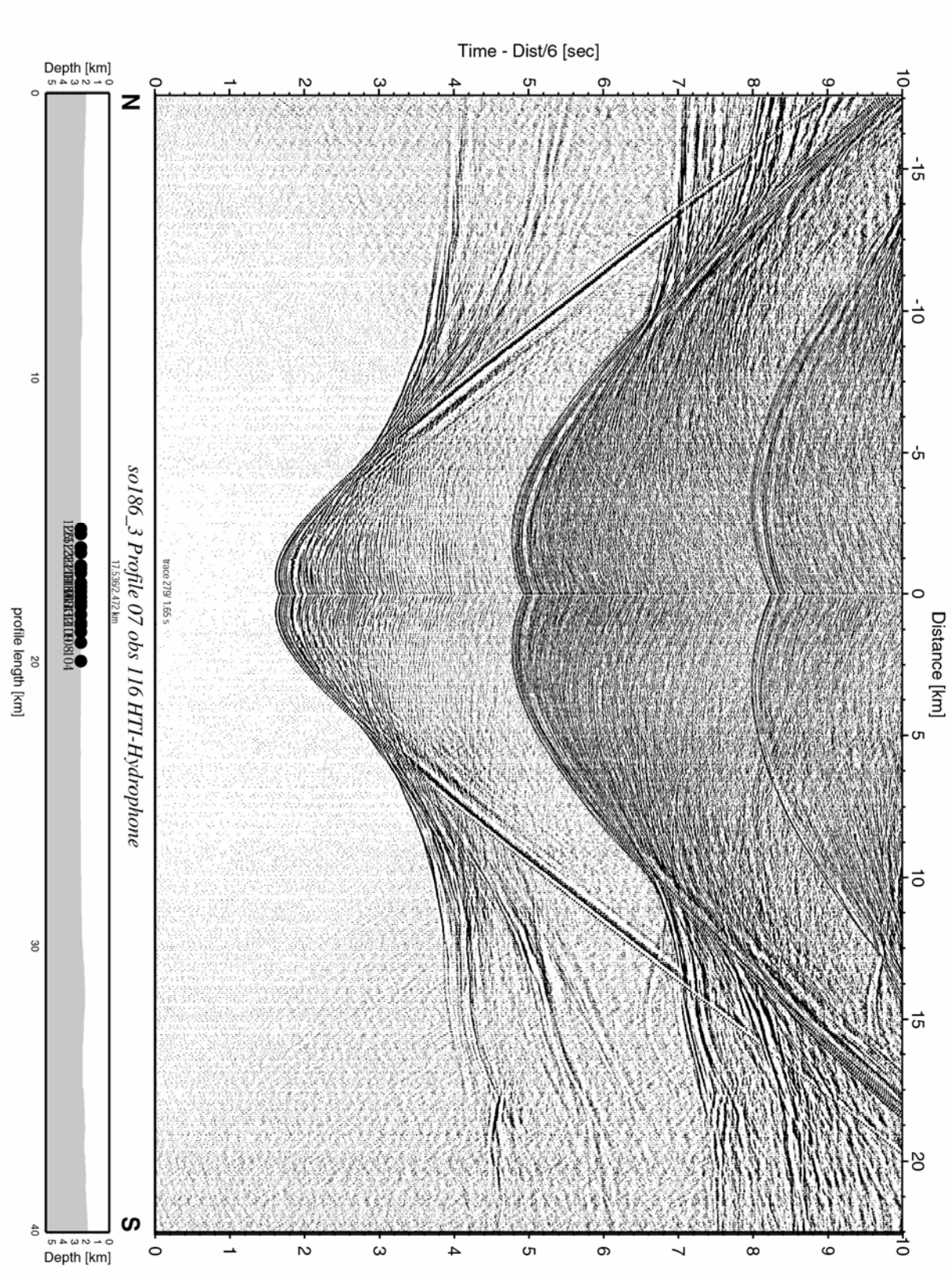

Figure 6.5.14: Record section from obs 116 HTI-Hydrophone, Profile 07.

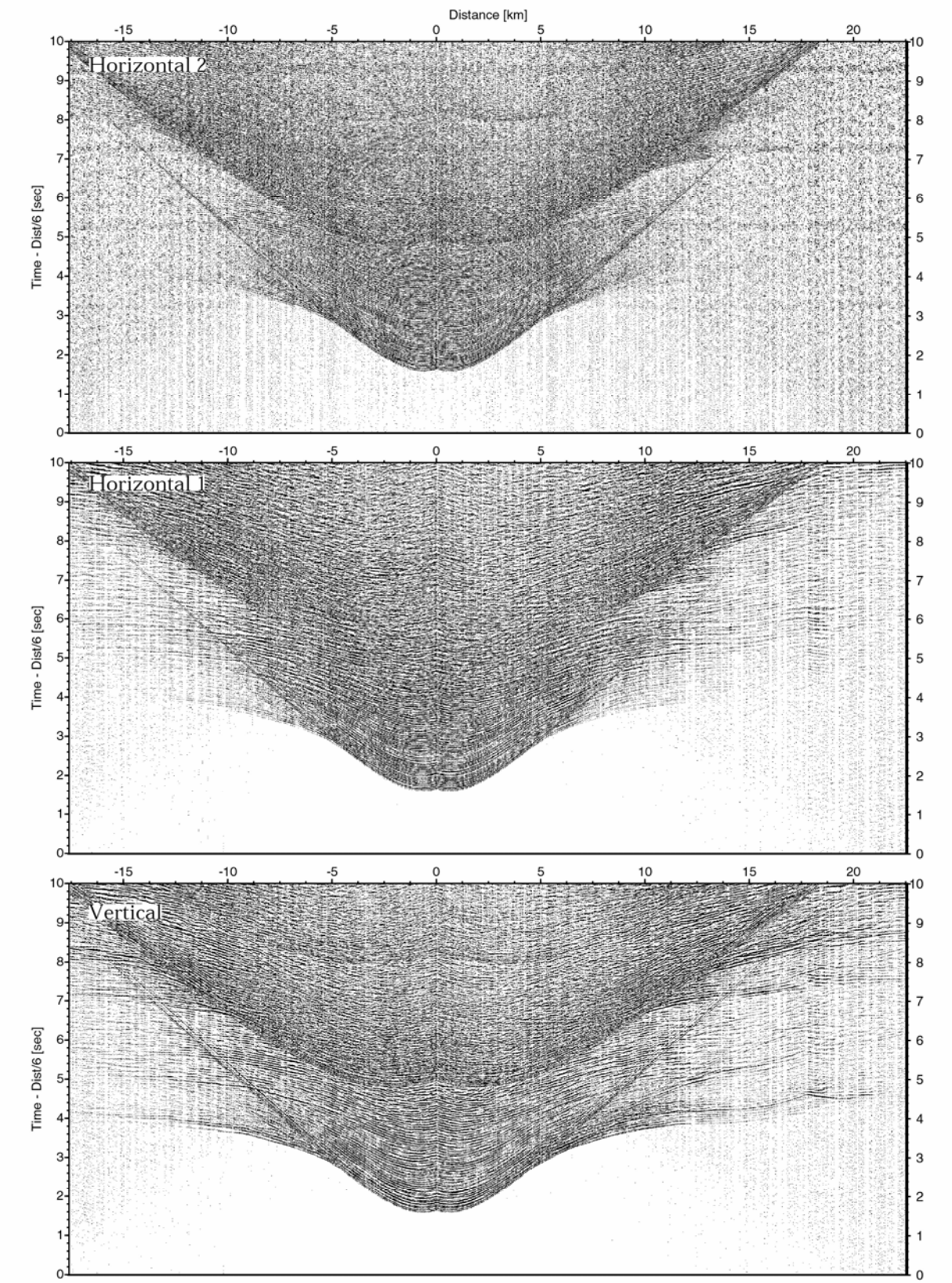

Figure 6.5.15: Record sections from obs 116 HTI/4.5Hz, so186_3 Profile 07.

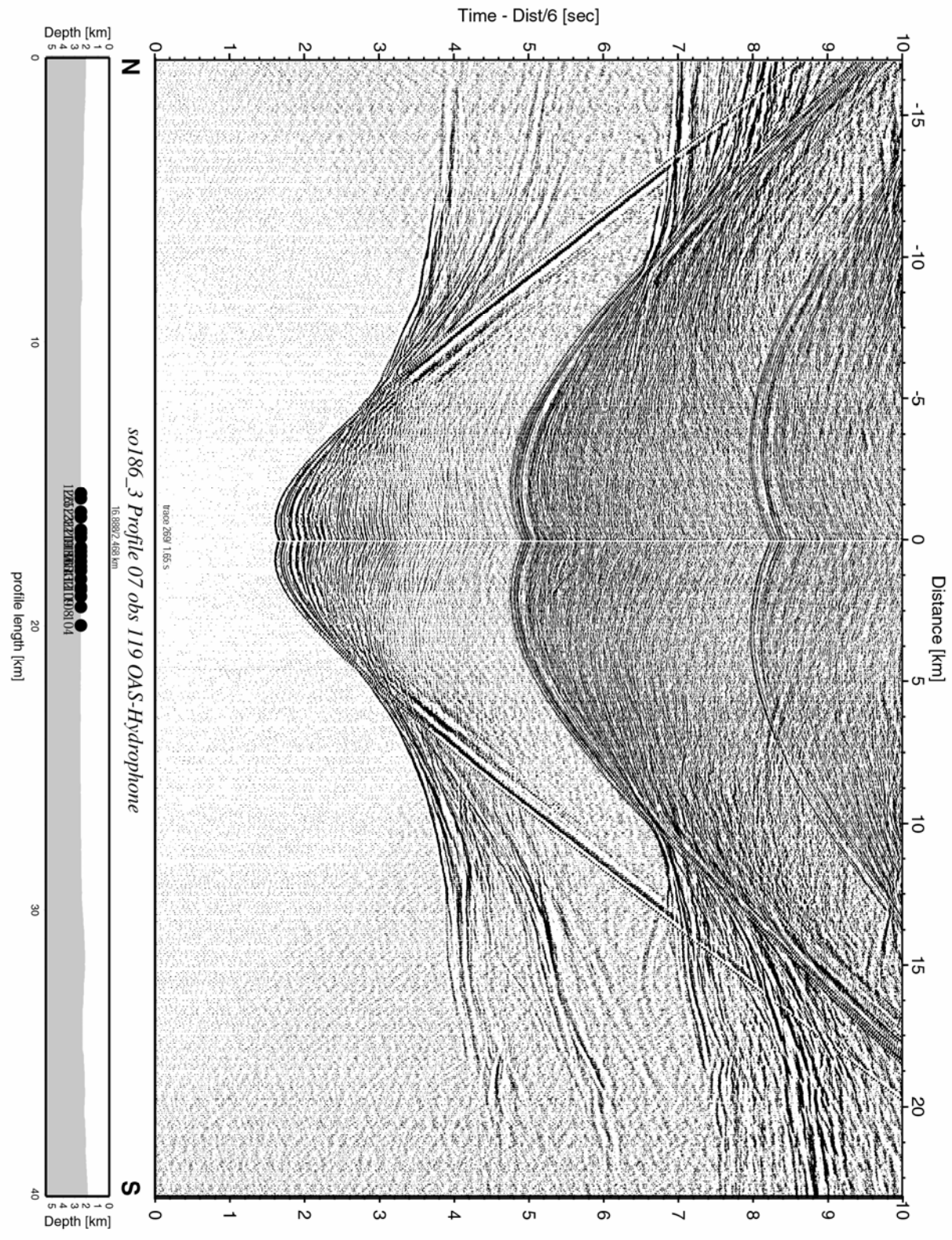

Figure 6.5.16: Record section from obs 119 OAS-Hydrophone, Profile 07.

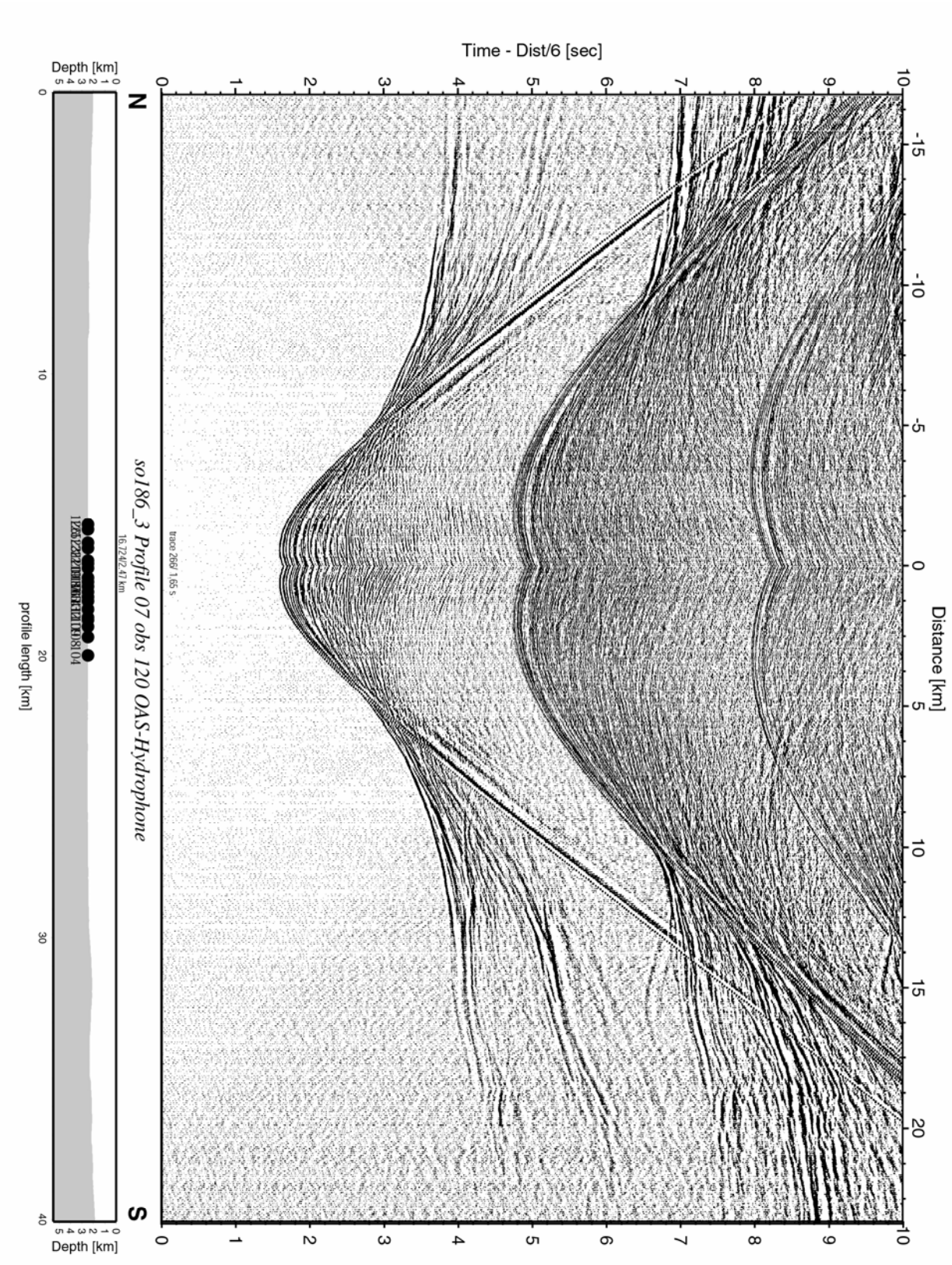

Figure 6.5.17: Record section from obs 120 OAS-Hydrophone, Profile 07.

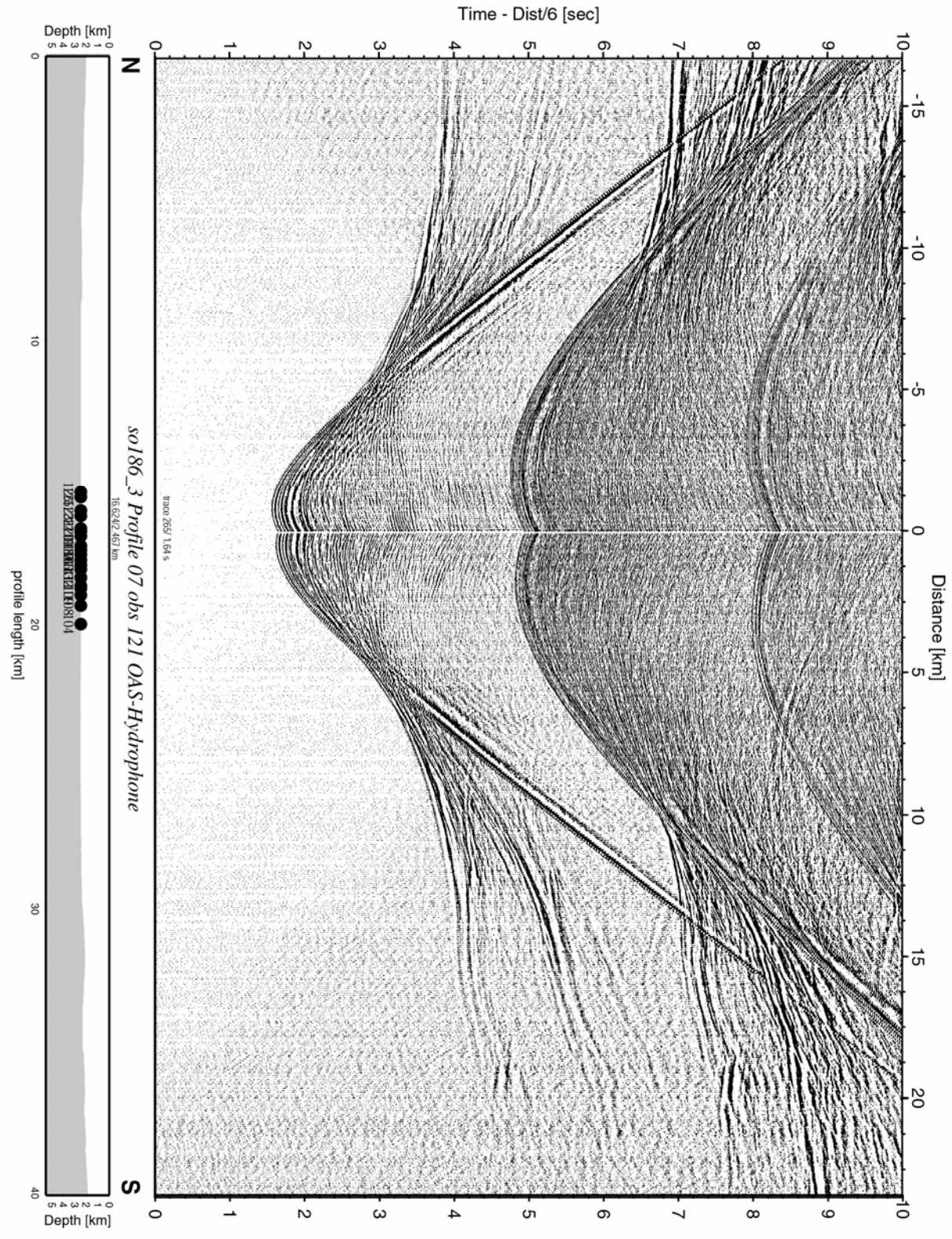

Figure 6.5.18: Record section from obs 121 OAS-Hydrophone, Profile 07.

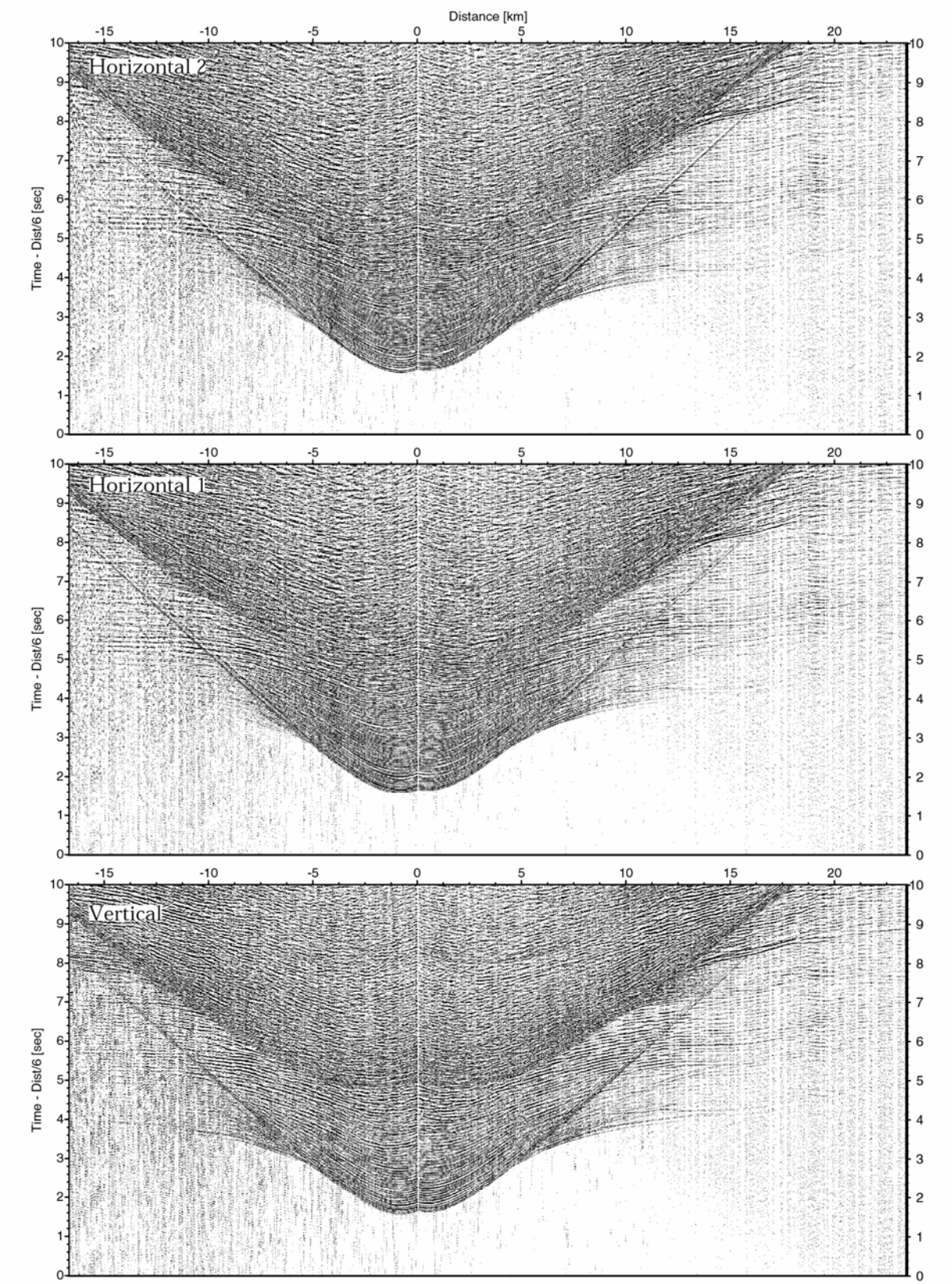

Figure 6.5.19: Record sections from obs 121 OAS/4.5Hz, so186_3 Profile 07.

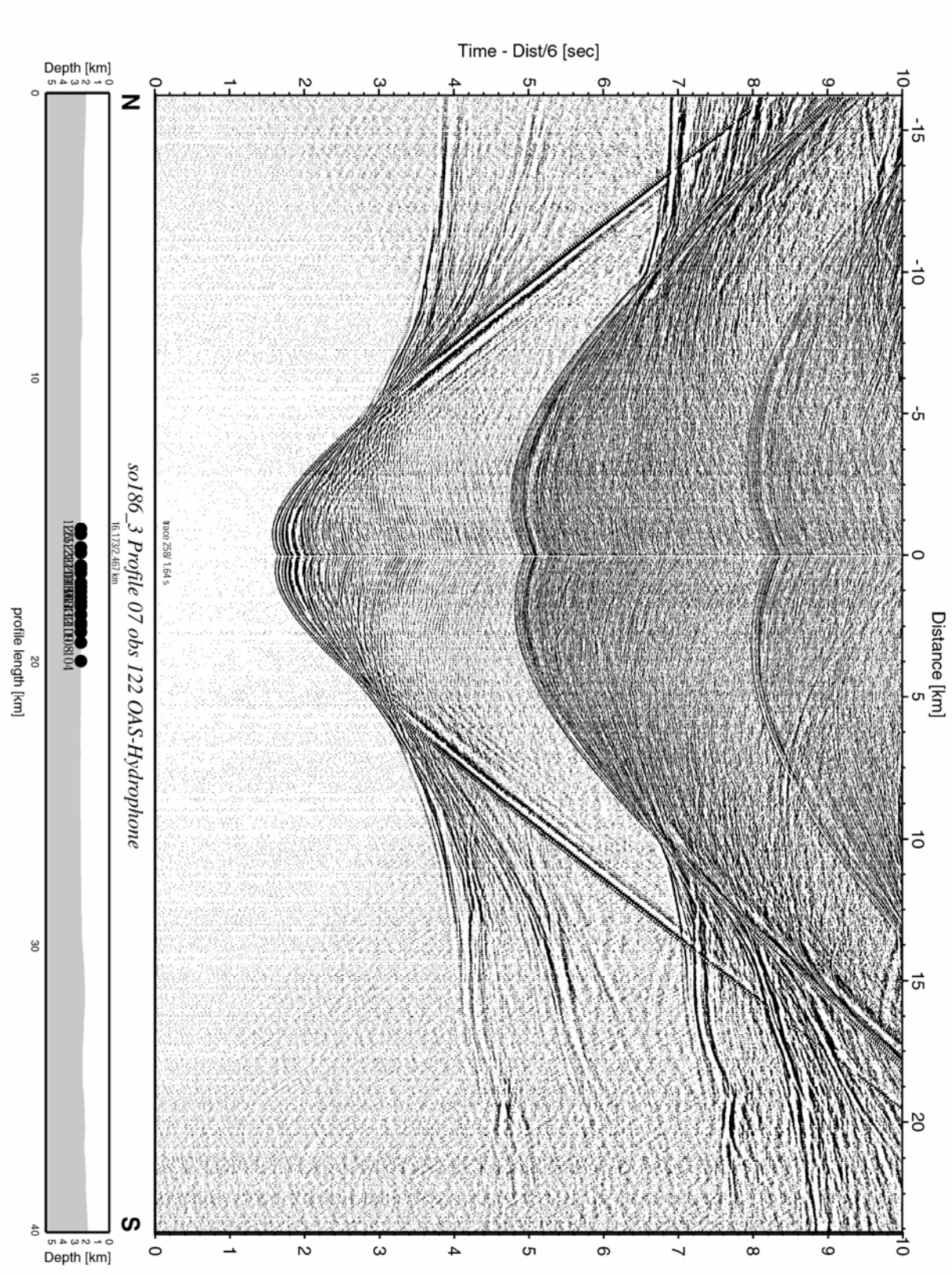

Figure 6.5.20: Record section from obs 122 OAS-Hydrophone, Profile 07.

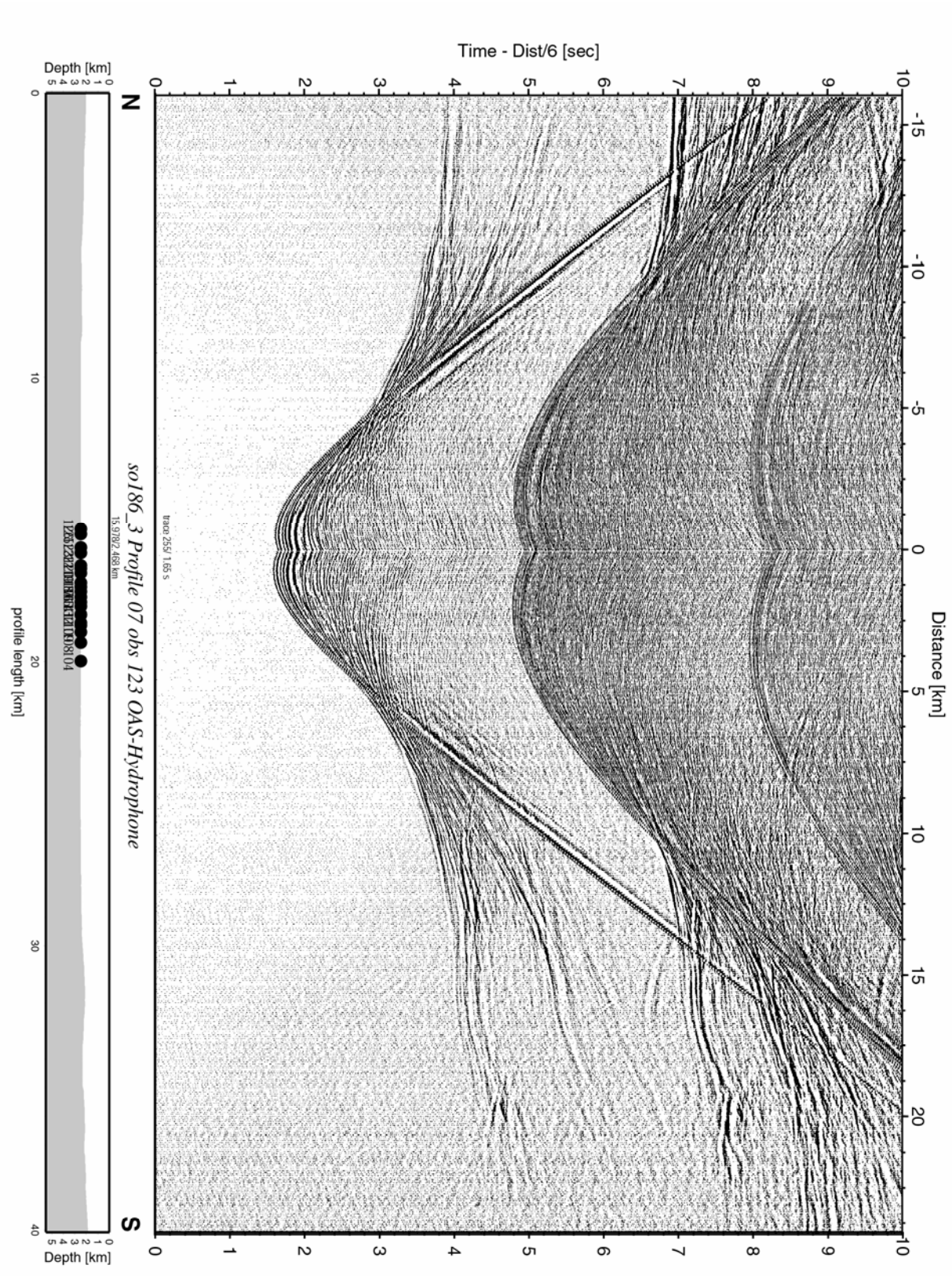

Figure 6.5.21: Record section from obs 123 OAS-Hydrophone, Profile 07.

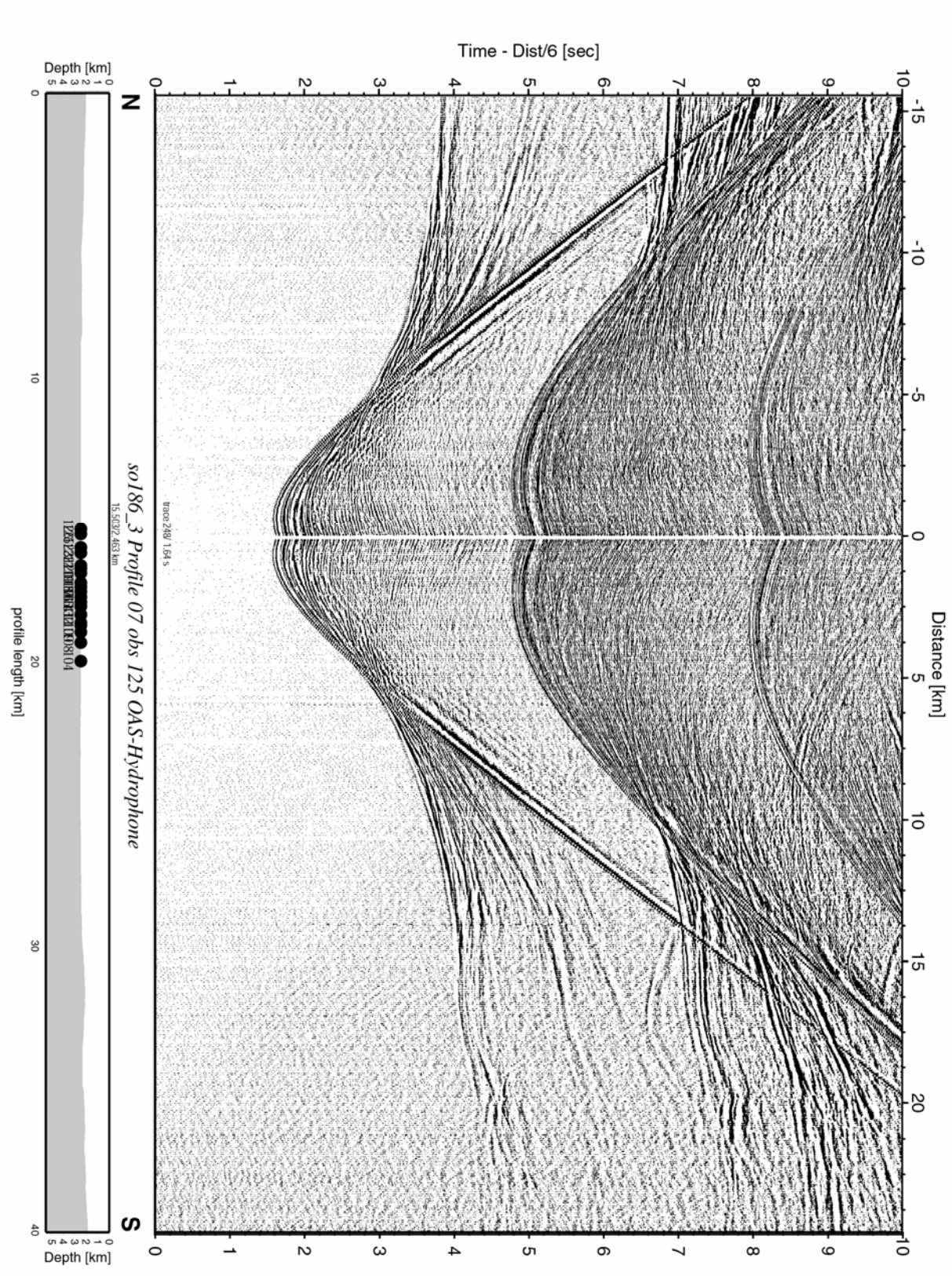

Figure 6.5.22: Record section from obs 125 OAS-Hydrophone, Profile 07.

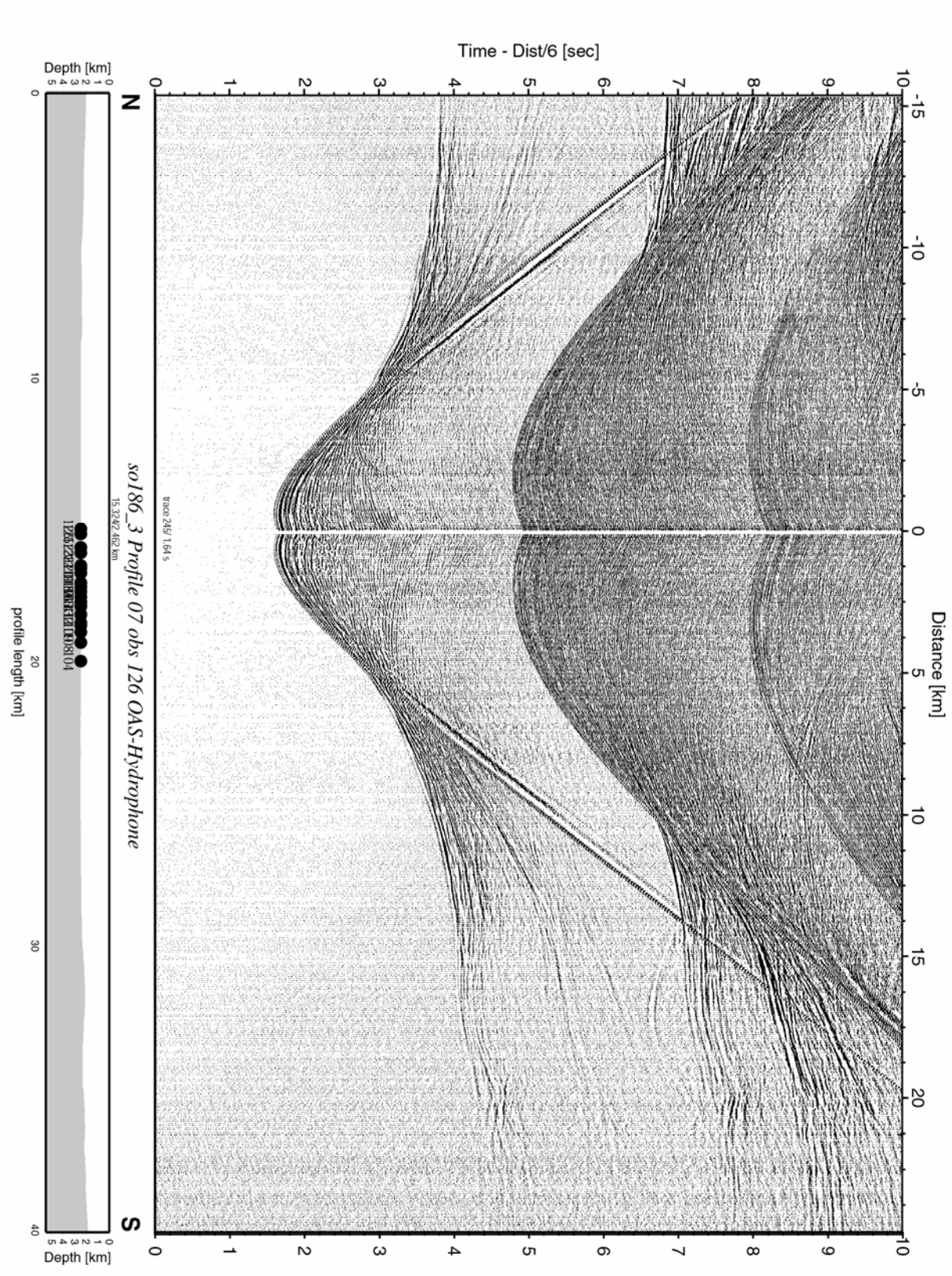

Figure 6.5.23: Record section from obs 126 OAS-Hydrophone, Profile 07.

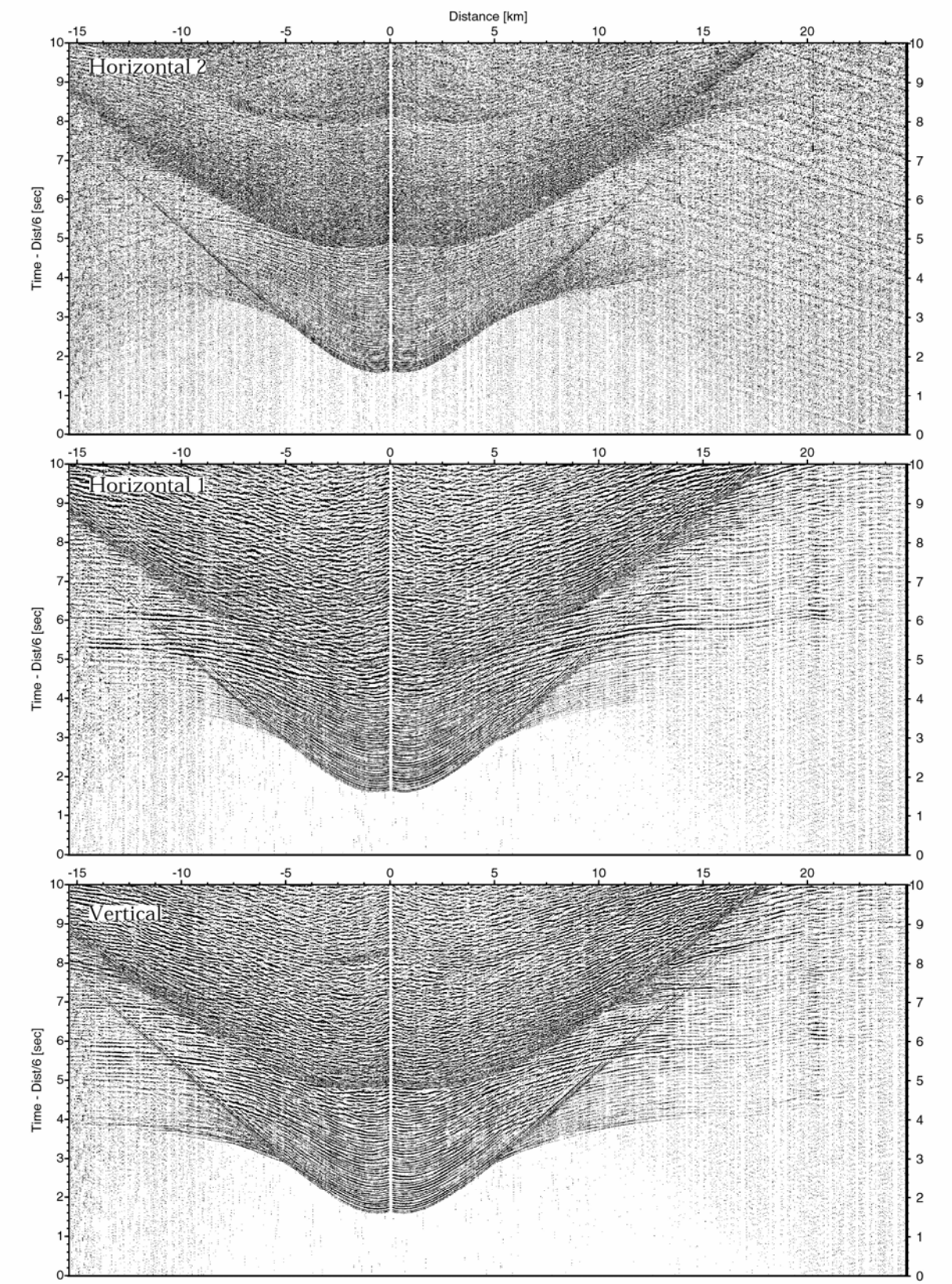

Figure 6.5.24: Record sections from obs 126 OAS/4.5Hz, so186_3 Profile 07.

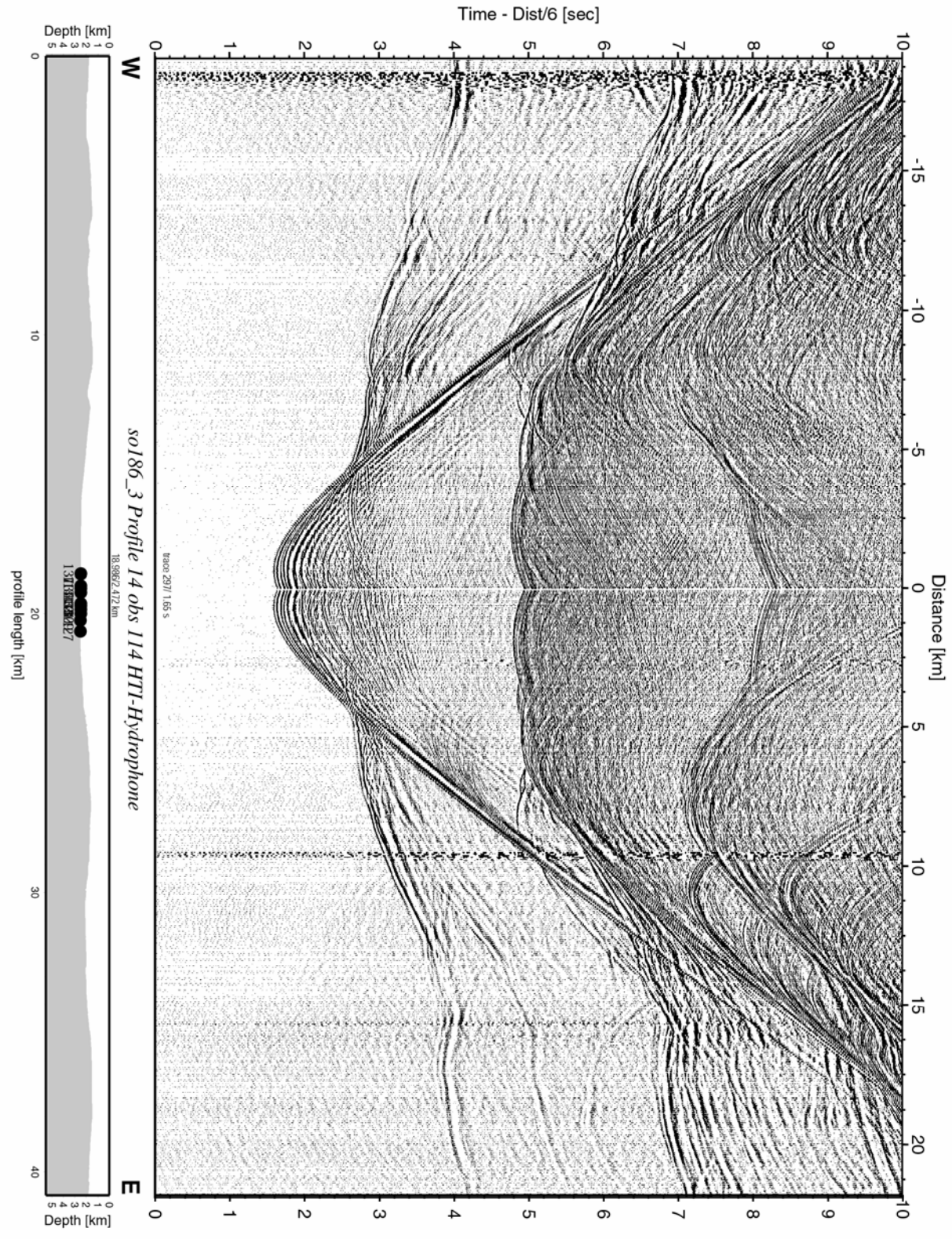

Figure 6.5.25: Record section from obs 114 HTI-Hydrophone, Profile 14.

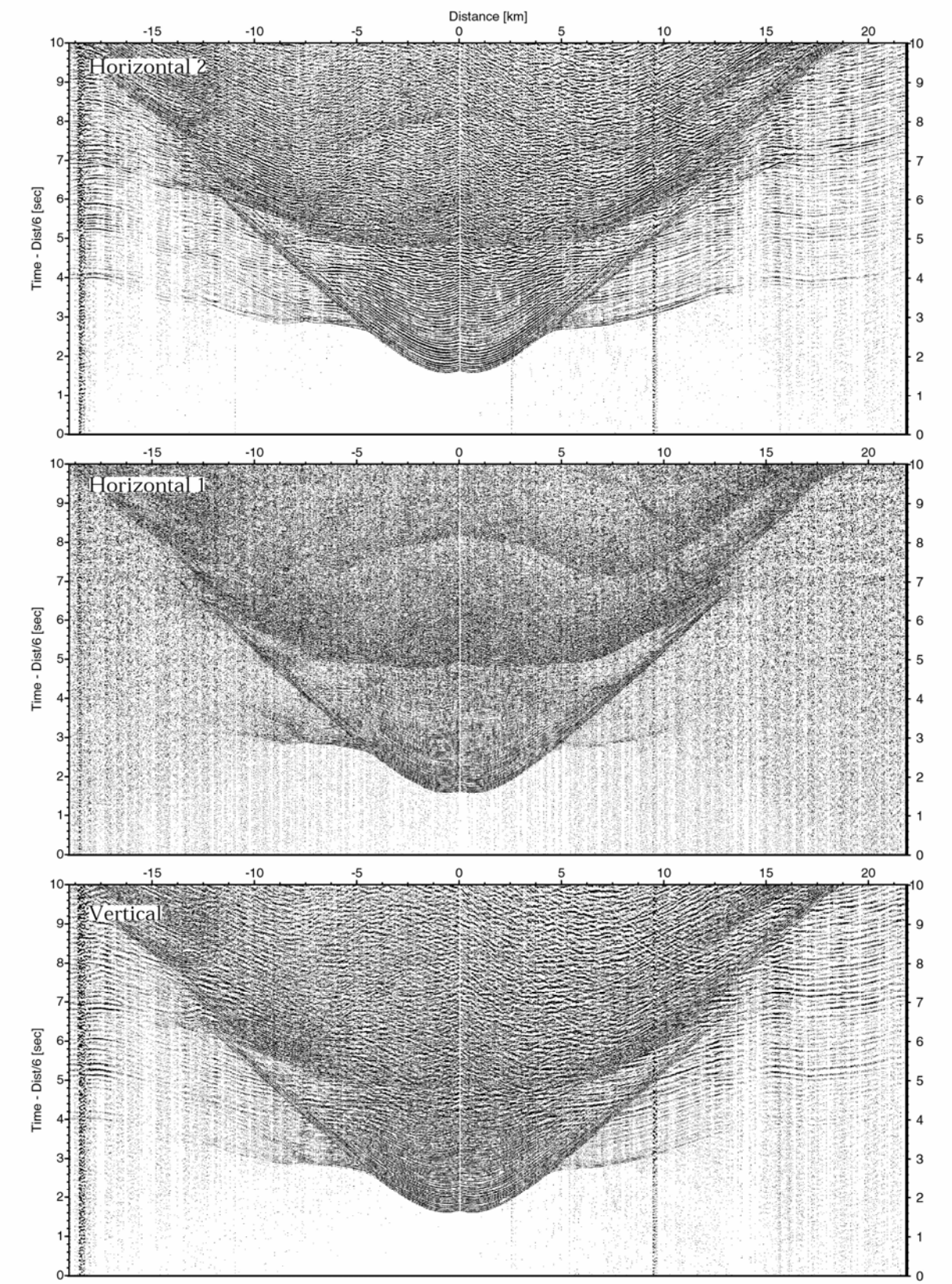

Figure 6.5.26: Record sections from obs 114 HTI/4.5Hz, so186_3 Profile 14.

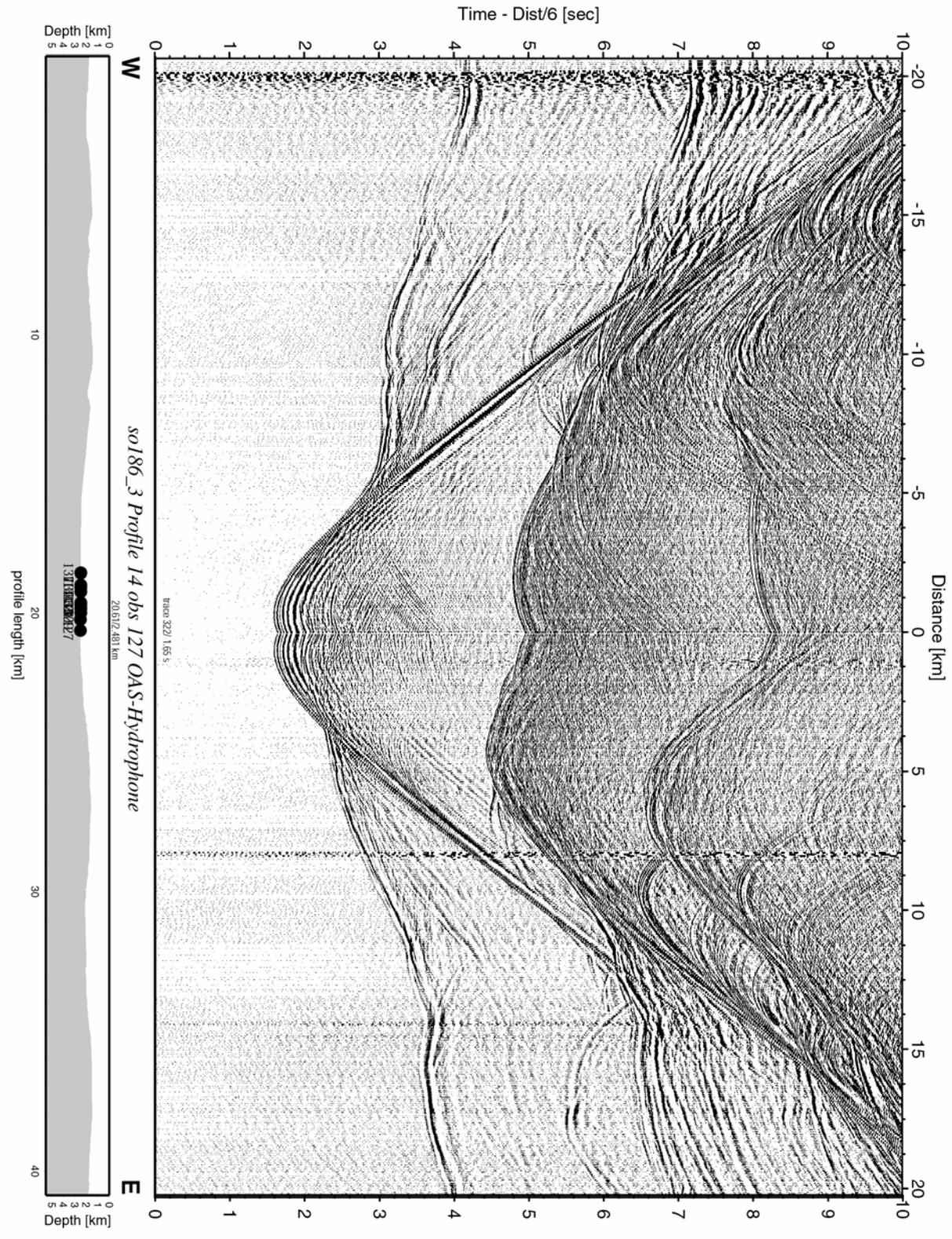

Figure 6.5.27: Record section from obs 127 OAS-Hydrophone, Profile 14.

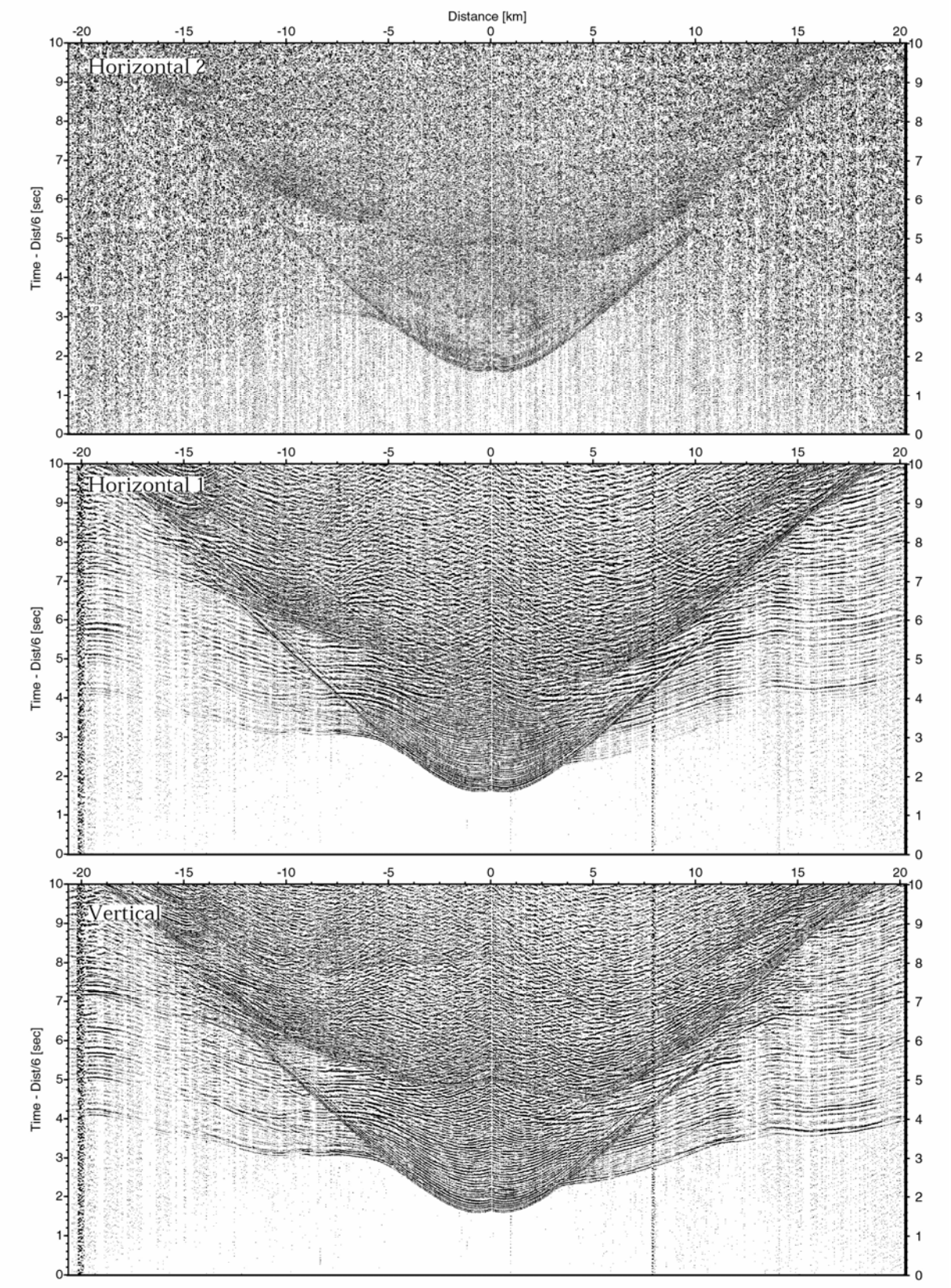

Figure 6.5.28: Record sections from obs 127 OAS/4.5Hz, so186_3 Profile 14.

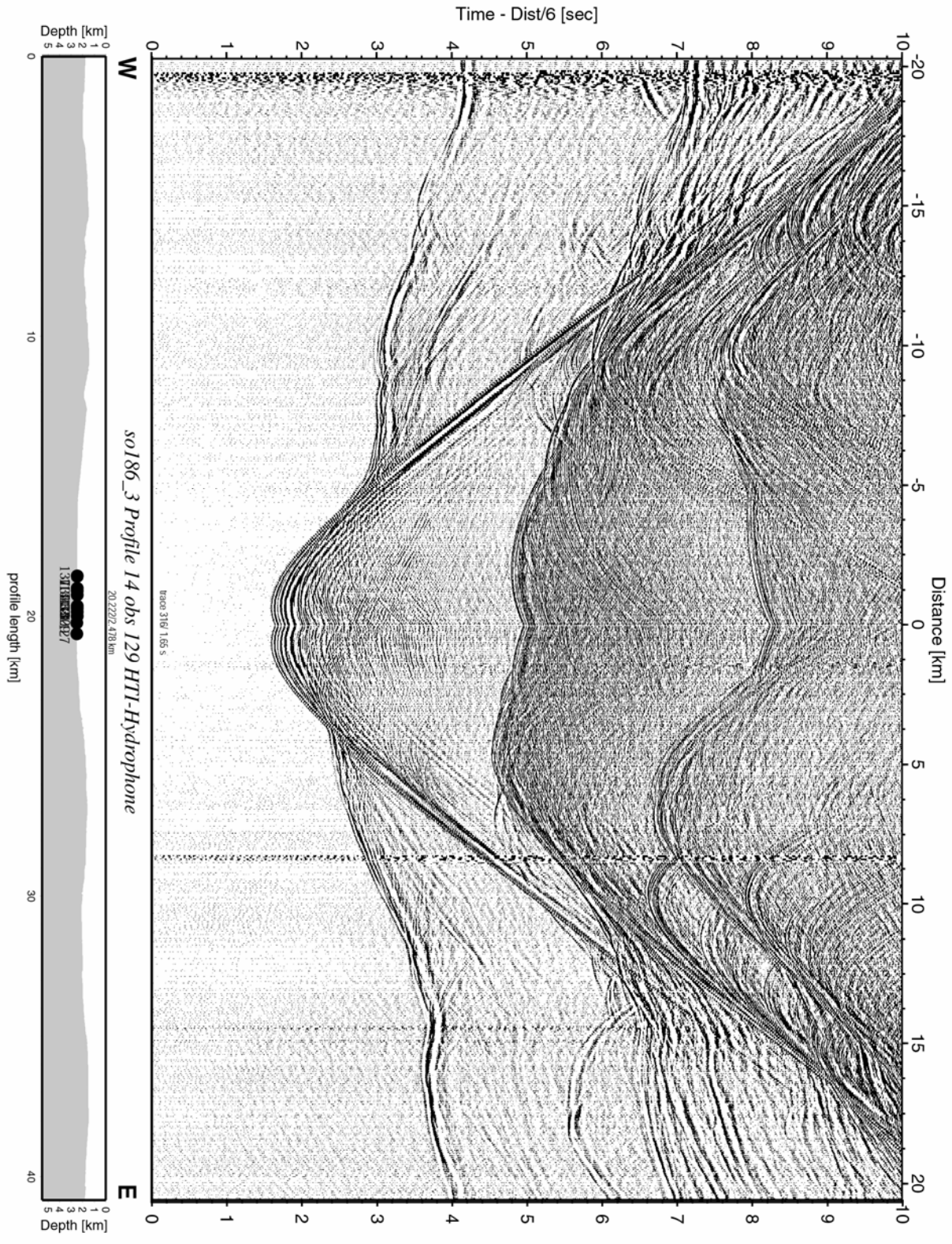

Figure 6.5.29: Record section from obs 129 HTI-Hydrophone, Profile 14.

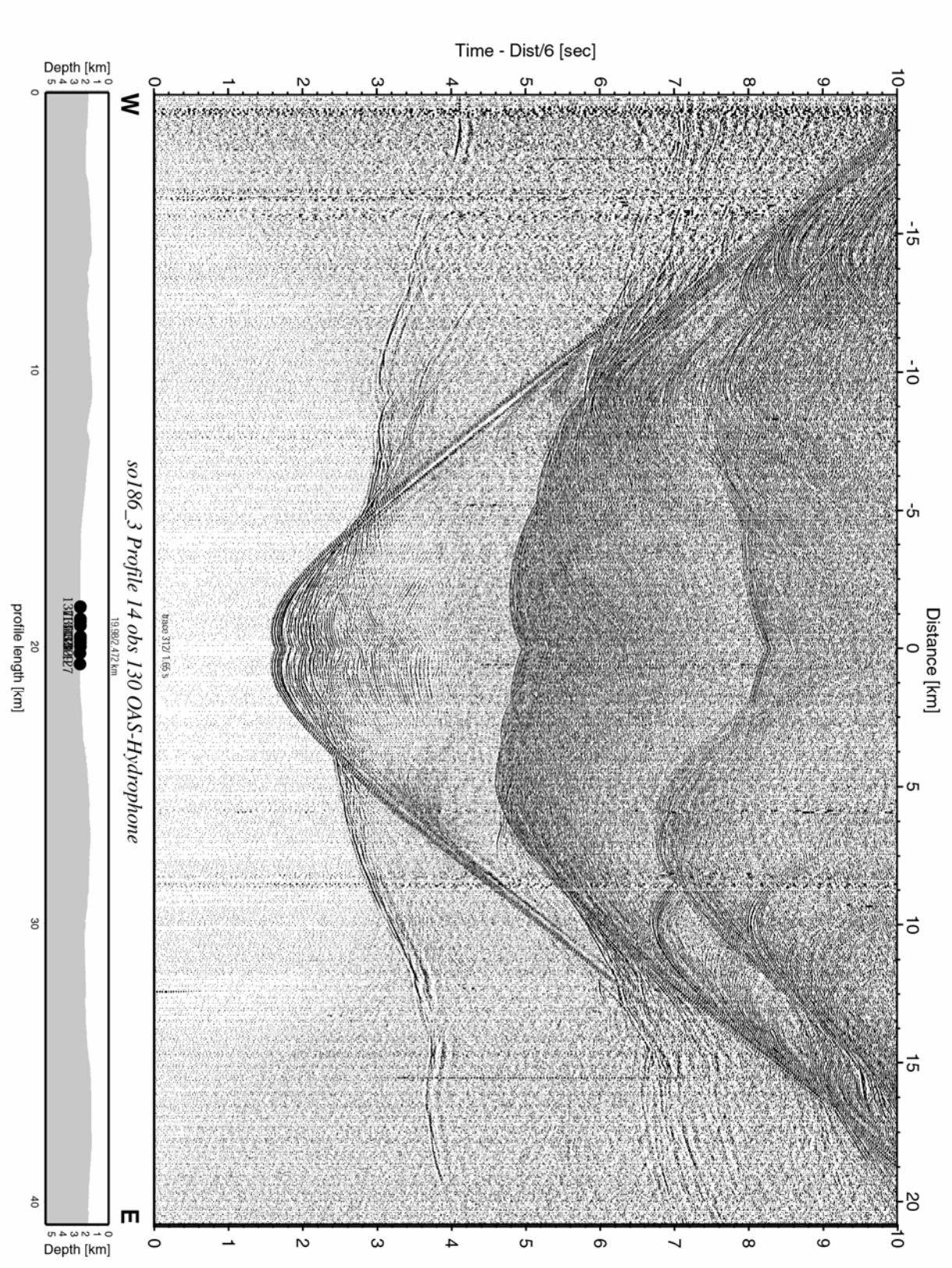

Figure 6.5.30: Record section from obs 130 OAS-Hydrophone, Profile 14.

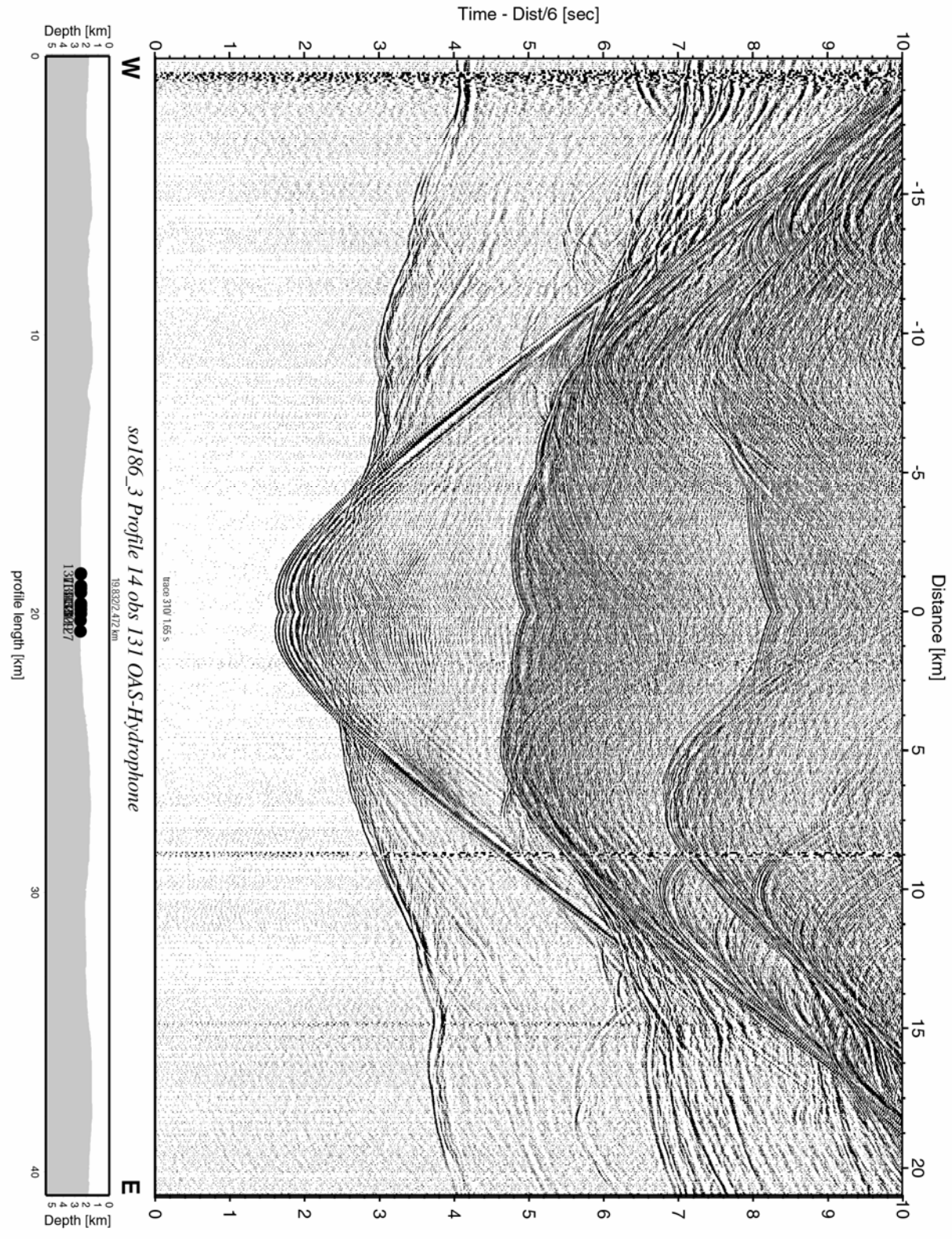

Figure 6.5.31: Record section from obs 131 OAS-Hydrophone, Profile 14.

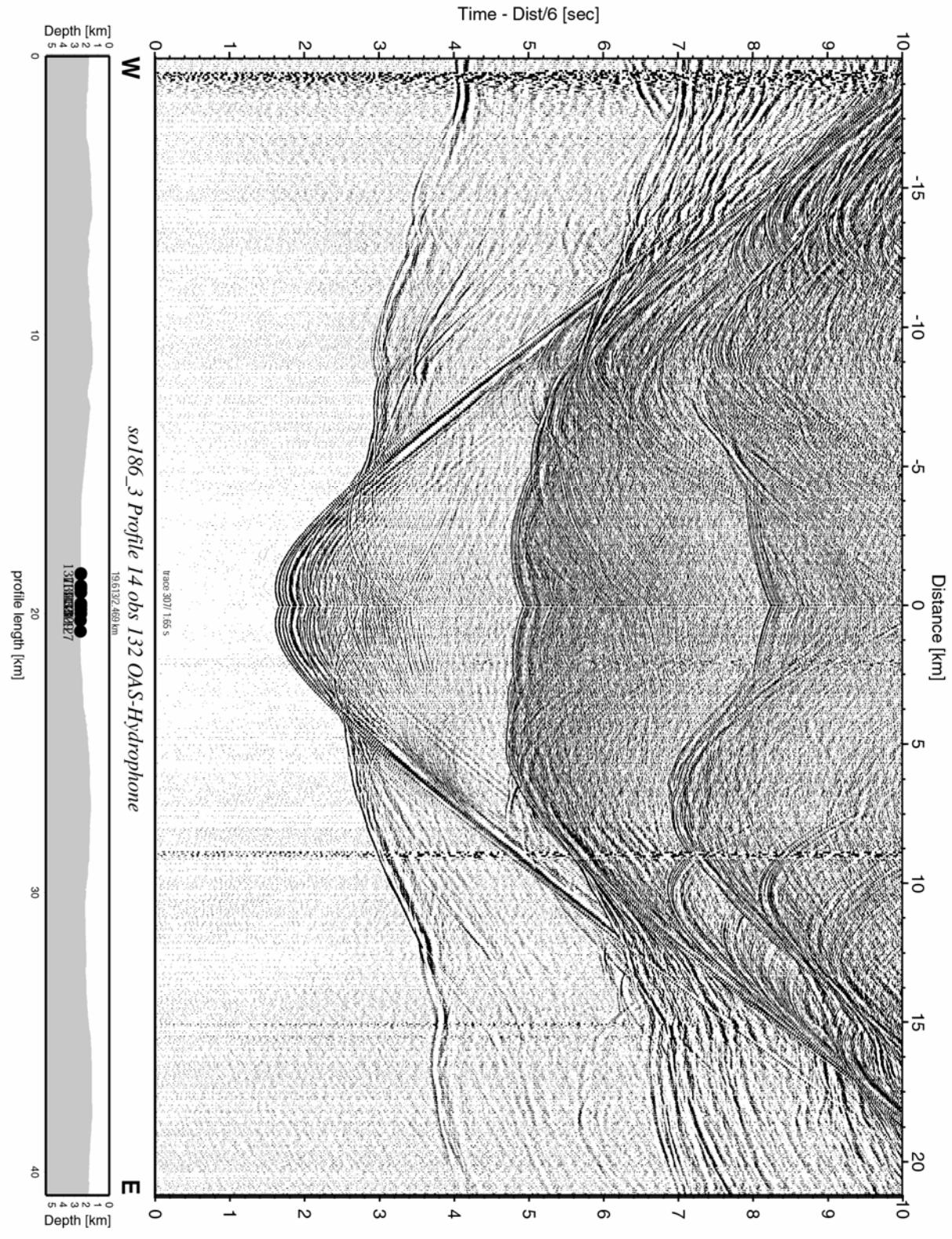

Figure 6.5.32: Record section from obs 132 OAS-Hydrophone, Profile 14.

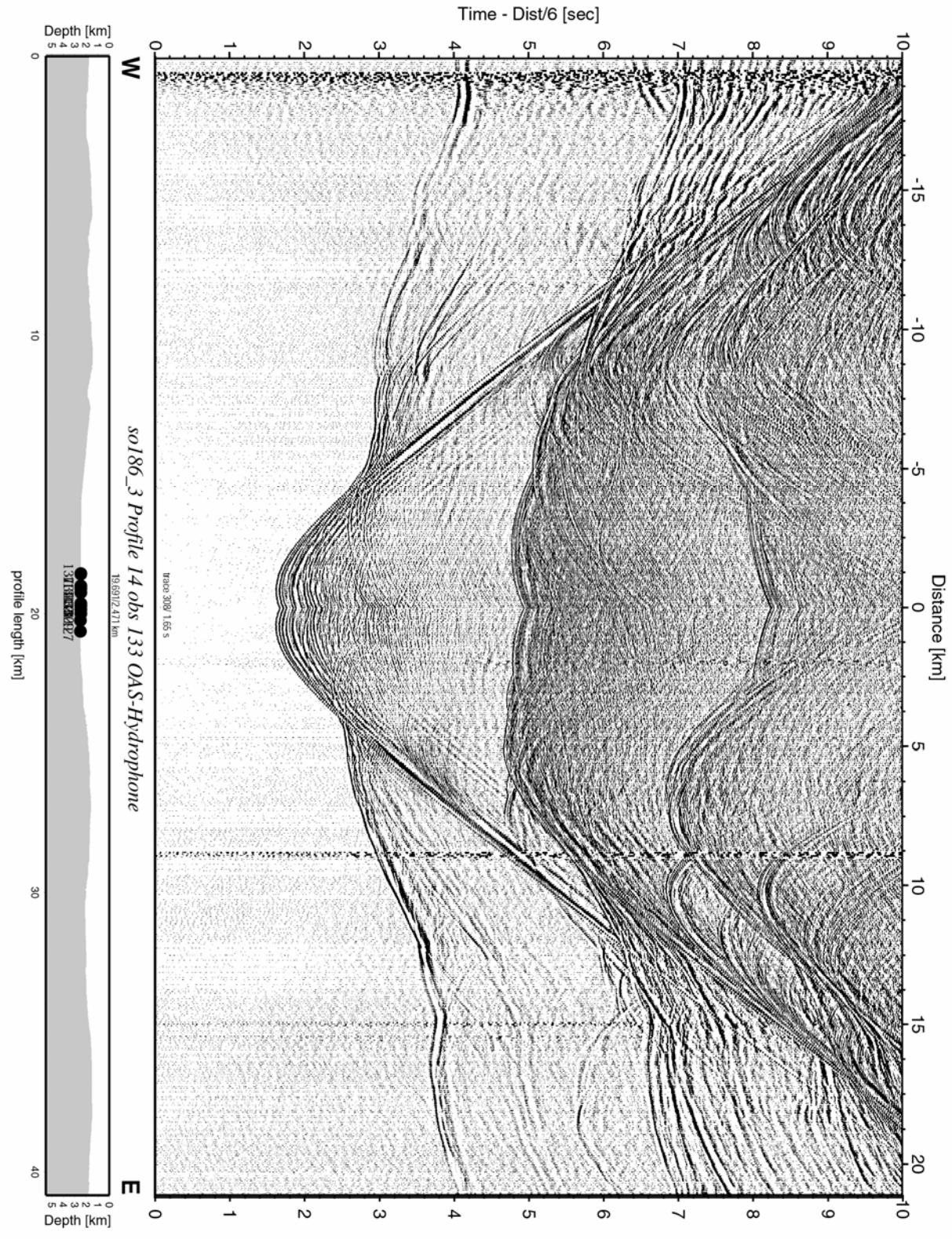

Figure 6.5.33: Record section from obs 133 OAS-Hydrophone, Profile 14.

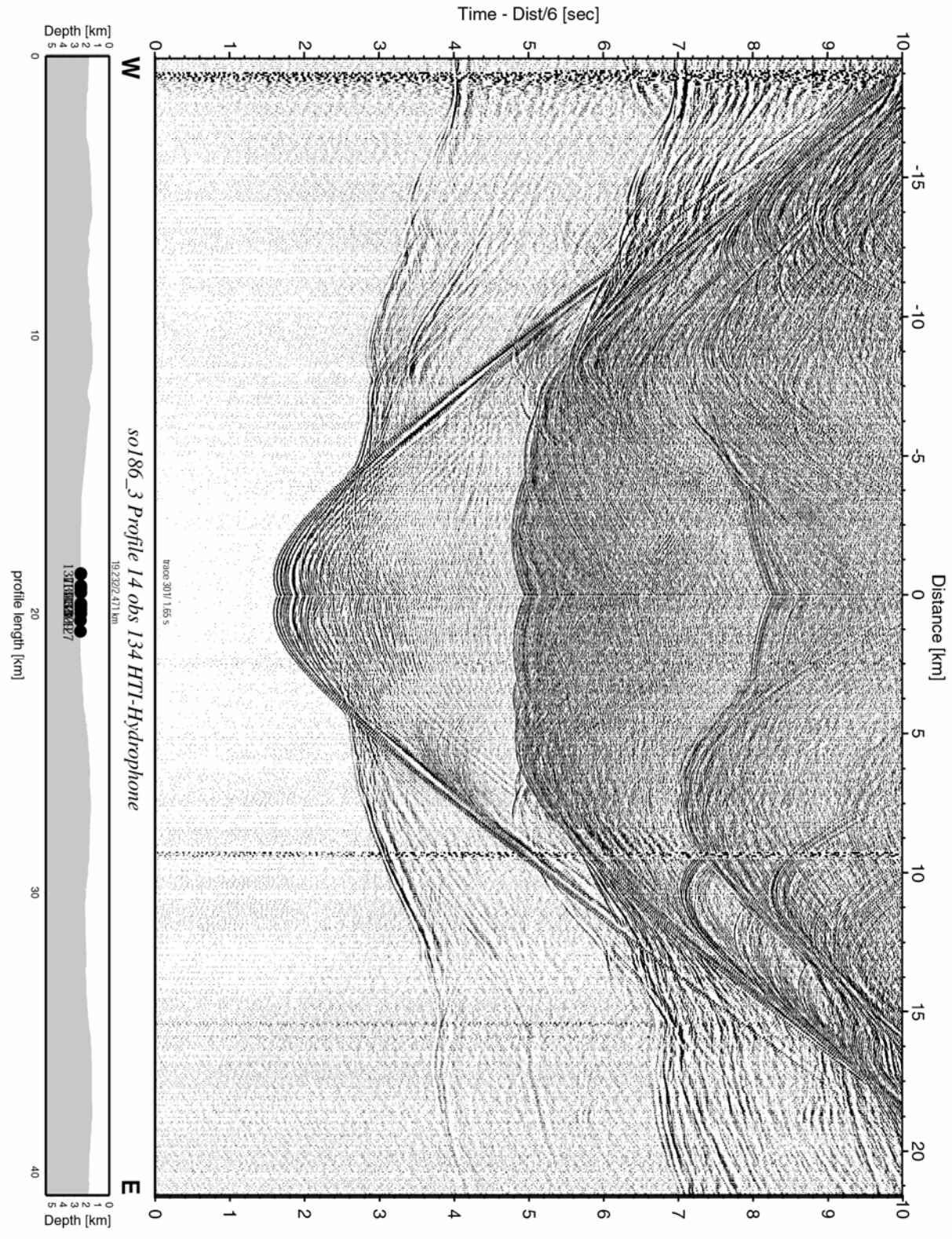

Figure 6.5.34: Record section from obs 134 HTI-Hydrophone, Profile 14.

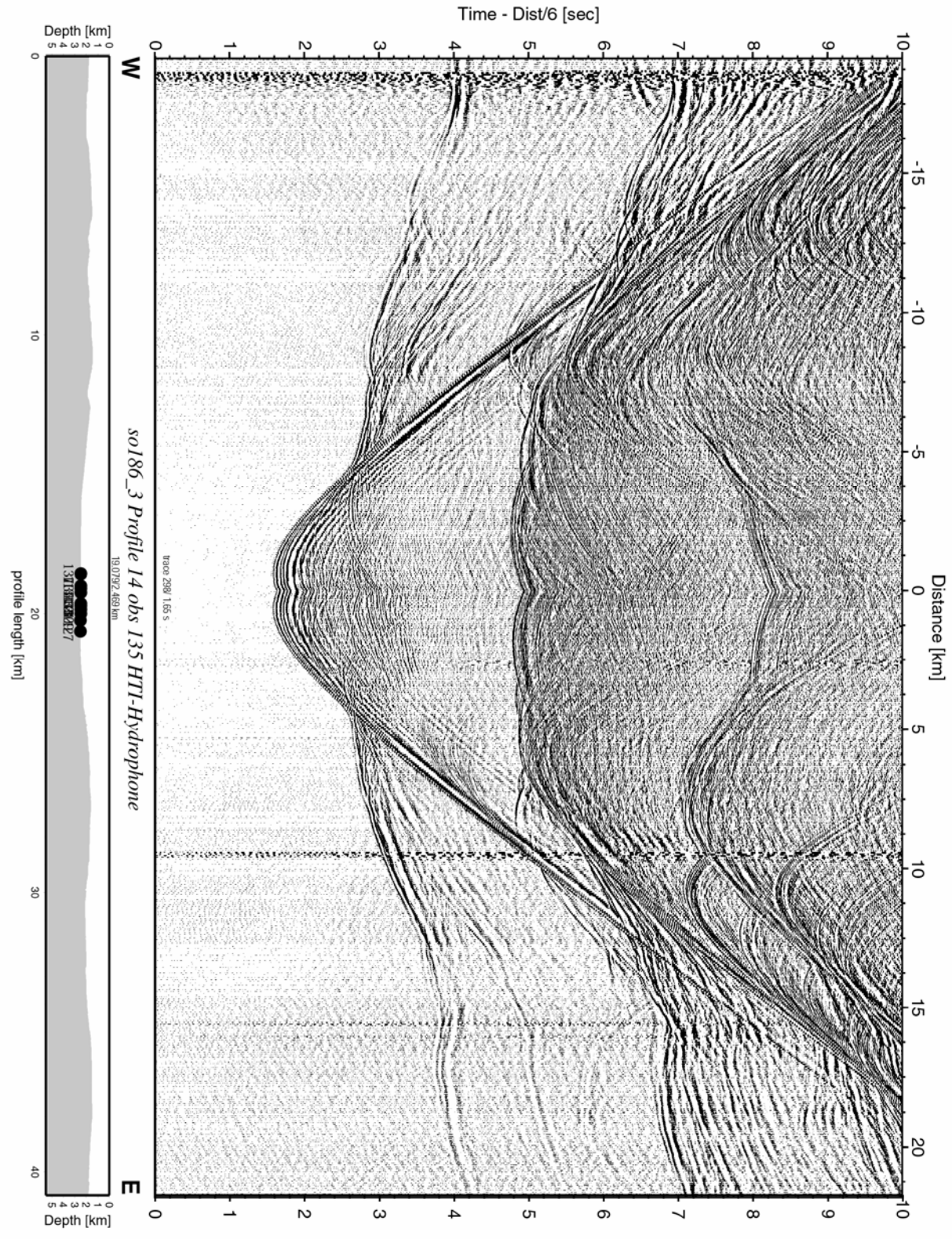

Figure 6.5.35: Record section from obs 135 HTI-Hydrophone, Profile 14.

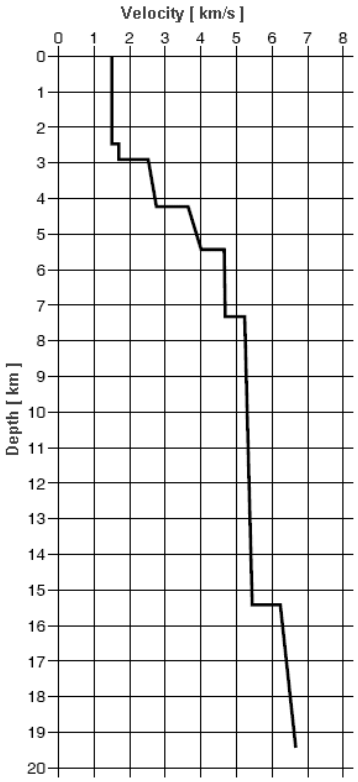

Figure 6.5.36: Velocity-depth model for OBS114 at profile junction of p07 and p14.

6.6 Paroscientific pressure data

Each of the stations OBS 26-29, OBS 37-38, OBS 42, OBS 45, OBS 49, OBS 51, OBS 64, OBS 69, OBS 91 and TOBS and OBU 01B, having been provided with a hydrophone and geophone, was equipped with an additional Paroscientific pressure sensor. The pressure sensors worked reliably, and recorded data was in general very good. Some representative examples are displayed in Figures 6.6.1 to 6.6.3. The upper panel of Figure 6.6.1 shows the entire pressure range, including pressure values reached during both descent in the beginning and during surfacing of the instrument at the end of the recording. The water depth obtained from the SIMRAD echo sounding system during deployment of the instruments is correct for OBS 29, where the water depth is less than 2000 m. There is a consistent deviation at the deeper positioned instruments where the water depth obtained by the SIMRAD system is about 100 m less than the water depth obtained from Paroscientific pressure data. These deviations in the water depth of the instruments compared to the pressure (and thus water depth) recorded by the Paroscientific pressure sensor might originate from a drifting of the instrument during its descent after deployment, or from an improper calibration of the SIMRAD system.

The diurnal tides are registered as well as the monthly cycles as consequence of the gravitational forces acting between the Earth, the Moon, and the Sun. The distances of the Sun, the Earth, and the Moon vary due to their elliptical orbits (Fig. 6.6.4). Increased gravitational influences and tide-raising forces are produced when the Moon is at position of perigee, its closest approach to the Earth (once a month) or when the Earth is at perihelion, its closest approach to the Sun (once a year). The diagram in Figure 6.6.4 also shows the possible coincidence of perigee with perihelion to produce tides of augmented range.

Besides the registration of the long-term pressure variations, earthquakes were recorded. An example of the earthquake signal measured by the Paroscientific pressure sensor is given in Figures 6.6.5 from OBS 26 and 6.6.6 from OBS 37. The earthquake had a magnitude of 5.7 Mw (from the USGS seismological catalogue); it occurred at 18 Dec. 2005 at 04:23,10 UTC north of Simeulue island. It was recorded by several instruments, e.g. OBS 26-29 and OBS 37/38. The seismic signal from the vertical component of the same earthquake registered by OBS 26 is displayed for comparison in Figure 6.6.7 with the same time axis.

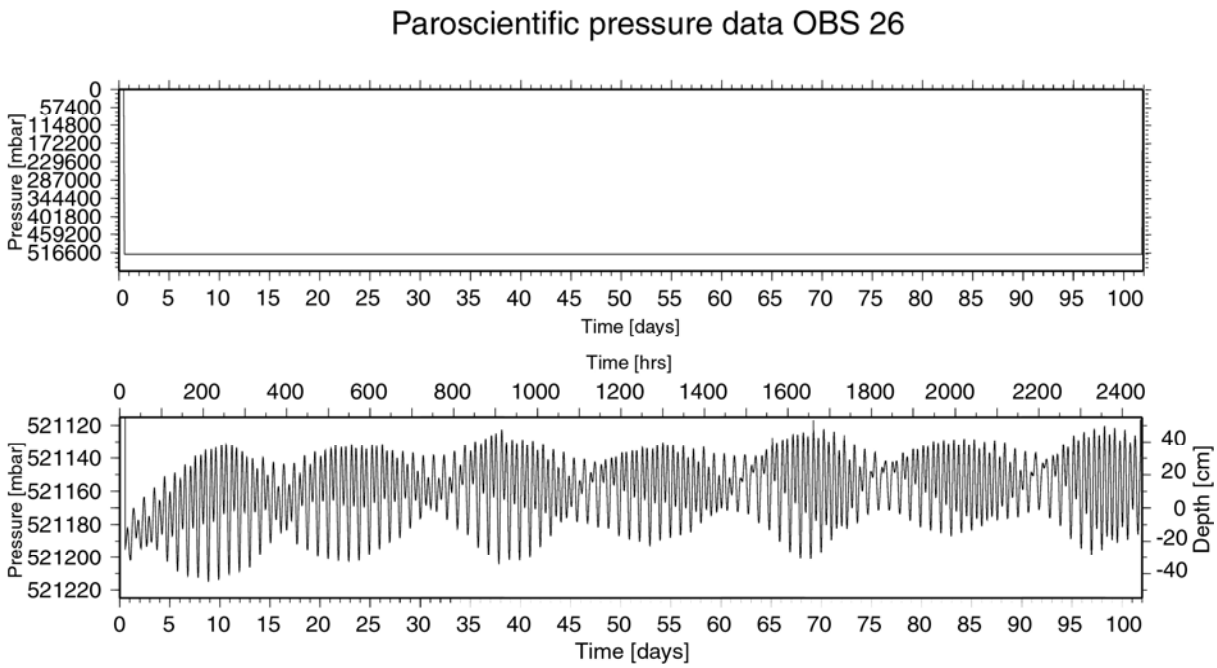

Figure 6.6.1: *Pressure data of OBS 26. Total range (top panel) and zoom (lower panel). Data is displayed from 24.11.2005 to 05.03.2006.*

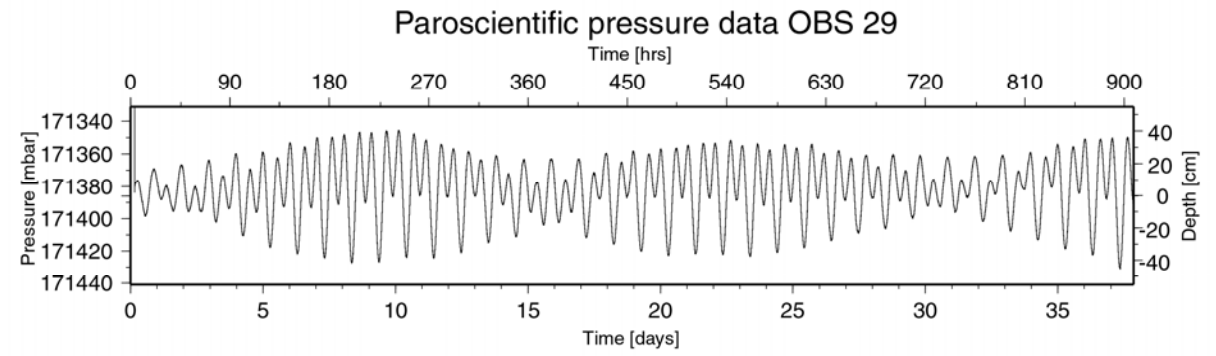

Figure 6.6.2: *Pressure data of OBS 29. Data is displayed from 24.11.2005 to 31.12.2005.*

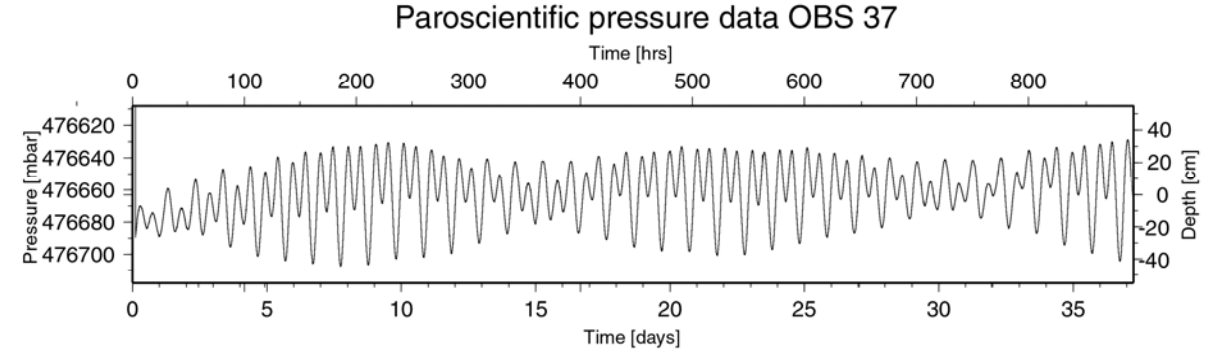

Figure 6.6.3: *Pressure data of OBS 37. Data is displayed from 24.11.2005 to 31.12.2005.*

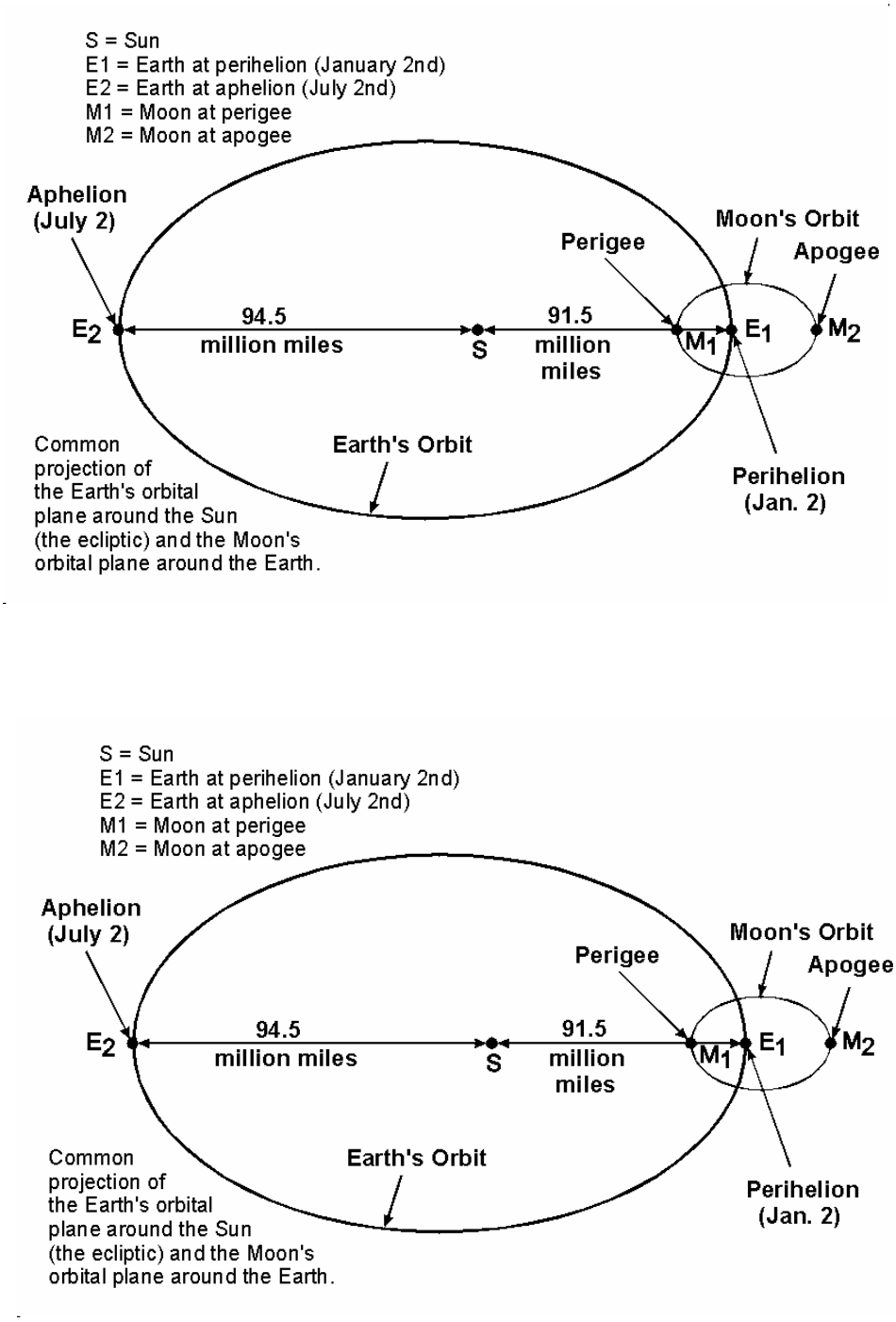

S = Sun
E1 = Earth at perihelion (January 2nd)
E2 = Earth at aphelion (July 2nd)
M1 = Moon at perigee
M2 = Moon at apogee
Aphelion
(July 2)
Moon's Orbit
Perigee
Apogee
E2
94.5
million miles
S
91.5
million
miles
M1
E1
M2
Common
projection of
the Earth's orbital
plane around the Sun
(the ecliptic) and the Moon's
orbital plane around the Earth.
Earth's Orbit
Perihelion
(Jan. 2)

Figure 6.6.4: *Elliptical orbits of Sun, Earth, and Moon, and the distances from their centers of attraction (Fig. from http://www.co-ops.nos.noaa.gov/restles4.html).*

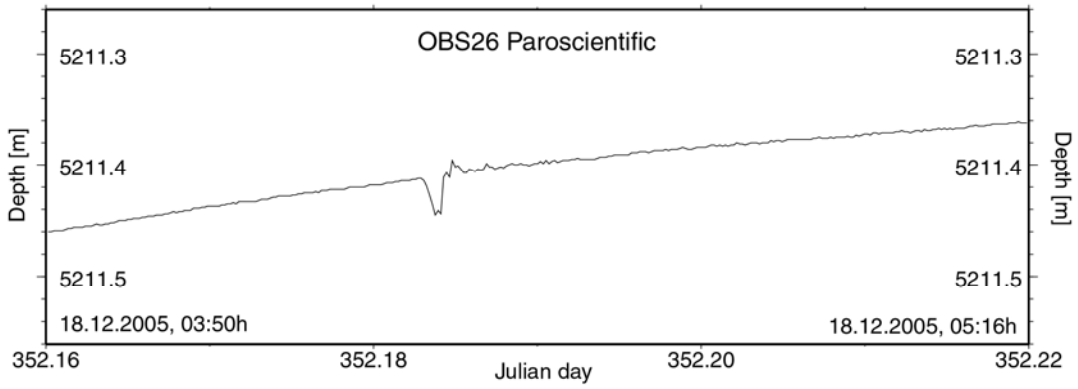

Figure 6.6.5: *Zoom of OBS 26 from18.12.2005. An earthquake occurred north of Simeulue island within the range of 100 km of this instrument.*

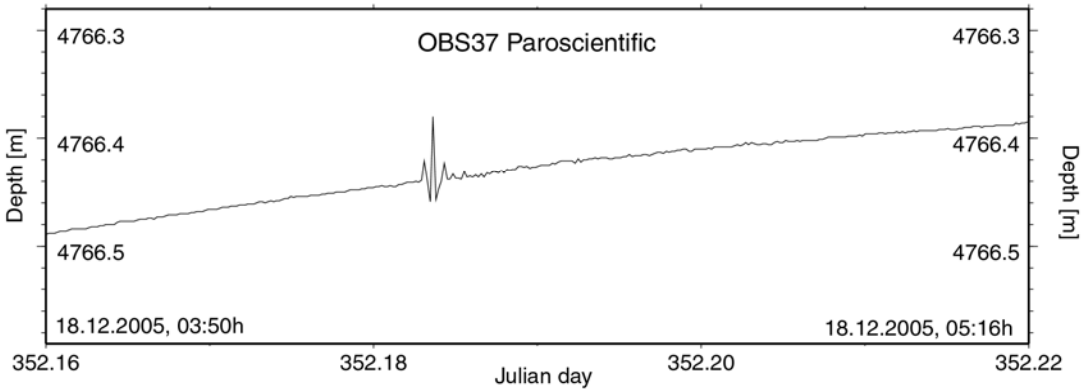

Figure 6.6.6: *Zoom of OBS 37 from18.12.2005. An earthquake occurred north of Simeulue island within the range of 100 km of this instrument.*

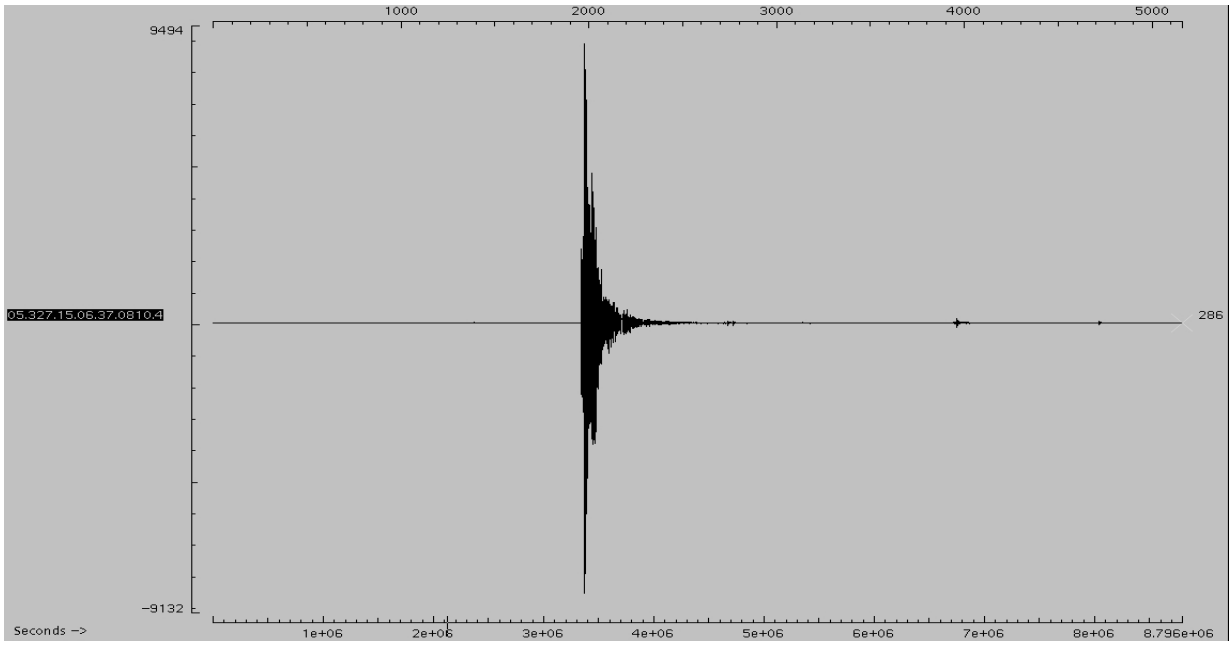

Figure 6.6.7: *Earthquake of 18.12.2005, OBS 26, 4. channel (vertical component). The same range is displayed as in Figures 6.6.4 and 6.6.5.*

6.7 Methane Sensors

In addition to the OBS, five methane sensors were deployed during SO186-3 to measure the methane output at the seafloor. During SONNE-cruise SO186C the methane sensors were already deployed and tested, but the data coverage was very poor then, due to technical problems. After maintenance and exchange of the methane sensor membranes, during this cruise, all sensors were deployed closely spaced for a better calibration and comparison of the data. The sensors were mounted to the conventional OBS-frame, now called OBM (Ocean Bottom Methane sensor), two sensors were mounted on one OBS-frame for OBM 60, OBM 61, both on profile 01, OBM 101/106, OBM 102/107, on profile 02-05/06-13. One sensor was mounted additionally on the frame of a regular OBS, which was also deployed three times during this cruise (OBS/M 59 on profile 01, OBS/M 100/108 on profile 02-05/06-13). See Table 6.7.1 for sensor and recorder specifications for each OBM instrument. After the profiles had been shot, all sensors were recovered and the data was read out. Between profiles 02-05 and 06-13 the OBS/M instruments were recovered, but the recorders were only opened after recovery, i.e. after profile 13.

Each sensor is calibrated under reference condition (25°C, 1 bar, 0 ‰ salinity) for a sensor-specific conversion formula. The output conversion formula describes the relation between the sensor signal output-voltage (U1 and U2) and the concentration of dissolved methane. U1 and U2, methane, and temperature voltage, are converted to the methane concentration C (in µmol/l) and gas temperature T (in °C). The conversion formula for each sensor is given in Figure 6.7.1. Most stations provided reasonable data, which are displayed in Figures 6.7.2 – 6.7.7.

Unfortunately 2 data loggers had no data for an unknown reason (see Table 6.7.1). And the methane concentration could not be plotted for the second deployment (profile 06-13) also for an unknown reason, because the values of voltage were reasonable if compared to the values of the deployment before (profiles 02-05), where we could plot the methane concentration (see Figure 6.7.7).

Station	S/N	Recorder	Data storage and averaging	Data recorded	Remarks
OBM59	T27	B050928	1min / 1min	01.03.06 – 04.03.06	
OBM60	T28	A050928	1min / 1min	01.03.06 – 04.03.06	
OBM60	T31	C050928	10min / 1min	01.03.06 – 04.03.06	
OBM61	T29	A000000	10min / 1min	01.03.06 – 04.03.06	
OBM61	T30	F050928	10min / 1min	01.03.06 – 04.03.06	
OBM100/ 108	T27	B050928	1min / 1min	06.03.06 – 11.03.06	No data
OBM101	T29	A000000	1min / 1min	06.03.06 – 08.03.06	
OBM101	T30	F050928	1min / 1min	06.03.06 – 08.03.06	Division by 0
OBM102	T28	A050928	1min / 1min	06.03.06 – 08.03.06	
OBM102	T31	C050928	1min / 1min	06.03.06 – 08.03.06	
OBM106	T29	A000000	1min / 1min	08.03.06 – 11.03.06	Methane conc. can't be displayed
OBM106	T30	F050928	1min / 1min	08.03.06 – 11.03.06	Methane conc. can't be displayed
OBM107	T28	A050928	1min / 1min	08.03.06 – 11.03.06	Methane conc. can't be displayed
OBM107	T31	C050928	1min / 1min	08.03.06 – 11.03.06	No data

Table 6.7.1: *Methane stations, sensors and recorders.*

Conversion Formula

METS T27

$$C = \exp\left(1.316 * \ln\left(\left(0.910+6.462 * \exp\frac{-U_1}{0.980}\right) * \left(\frac{1}{U_2} - \frac{1}{-1.069 + 6.810 * \exp\frac{-U_1}{1.356}}\right)\right)\right)$$

$$T = (21.573 * U_1) - 3.221$$

METS T28

$$C = \exp\left(1.297 * \ln\left(\left(2.639+7.840 * \exp\frac{-U_1}{0.474}\right) * \left(\frac{1}{U_2} - \frac{1}{-3.477 + 9.401 * \exp\frac{-U_1}{1.949}}\right)\right)\right)$$

$$T = (21.128 * U_1) - 1.438$$

METS T29

$$C = \exp\left(1.314 * \ln\left(\left(1.108+5.893 * \exp\frac{-U_1}{0.799}\right) * \left(\frac{1}{U_2} - \frac{1}{-0.935 + 6.503 * \exp\frac{-U_1}{1.312}}\right)\right)\right)$$

$$T = (21.537 * U_1) - 0.560$$

METS T30

$$C = \exp\left(1.266 * \ln\left(\left(1.043+10.112 * \exp\frac{-U_1}{0.767}\right) * \left(\frac{1}{U_2} - \frac{1}{-0.554 + 5.667 * \exp\frac{-U_1}{1.257}}\right)\right)\right)$$

$$T = (21.375 * U_1) - 4.874$$

METS T31

$$C = \exp\left(1.370 * \ln\left(\left(1.456+6.853 * \exp\frac{-U_1}{0.547}\right) * \left(\frac{1}{U_2} - \frac{1}{1.086 + 6.955 * \exp\frac{-U_1}{0.720}}\right)\right)\right)$$

$$T = (21.340 * U_1) - 3.221$$

Figure 6.7.1: *Calibration formulae for the methane sensors.*

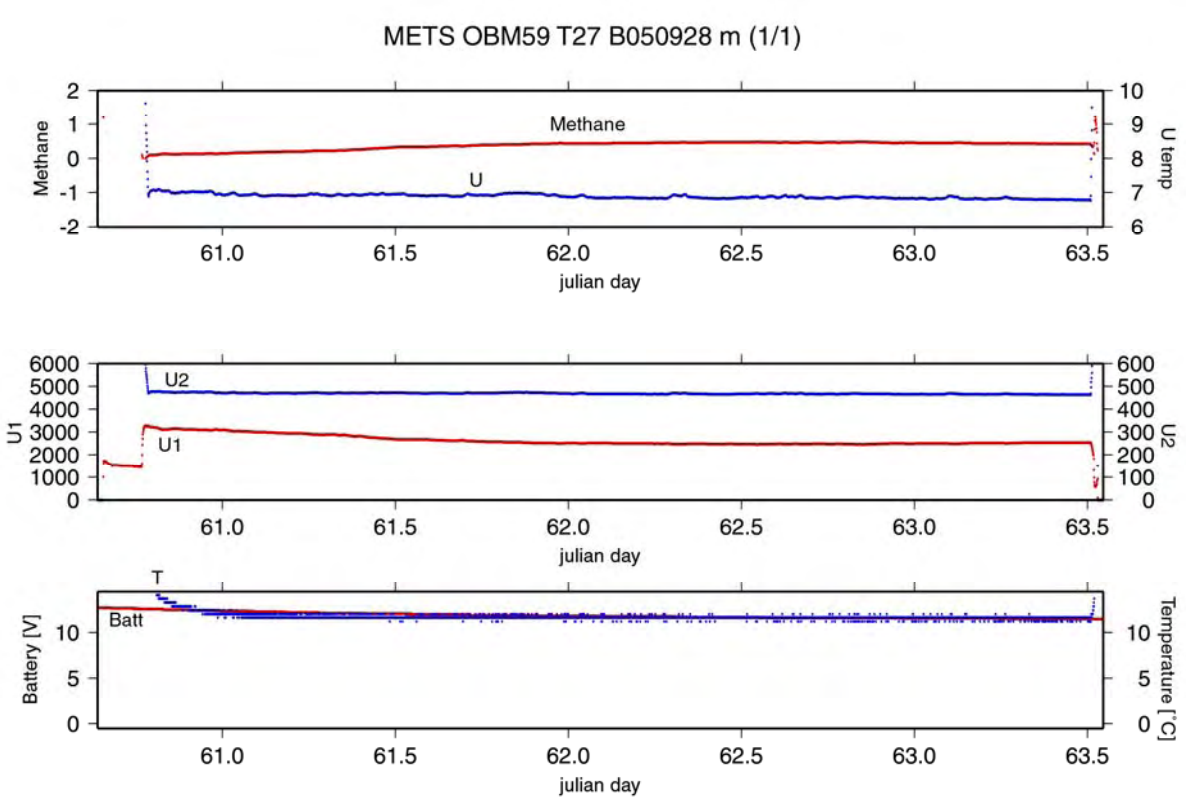

Figure 6.7.2: *Raw data (bottom and middle, U [mv]), methane data (top), OBM59.*

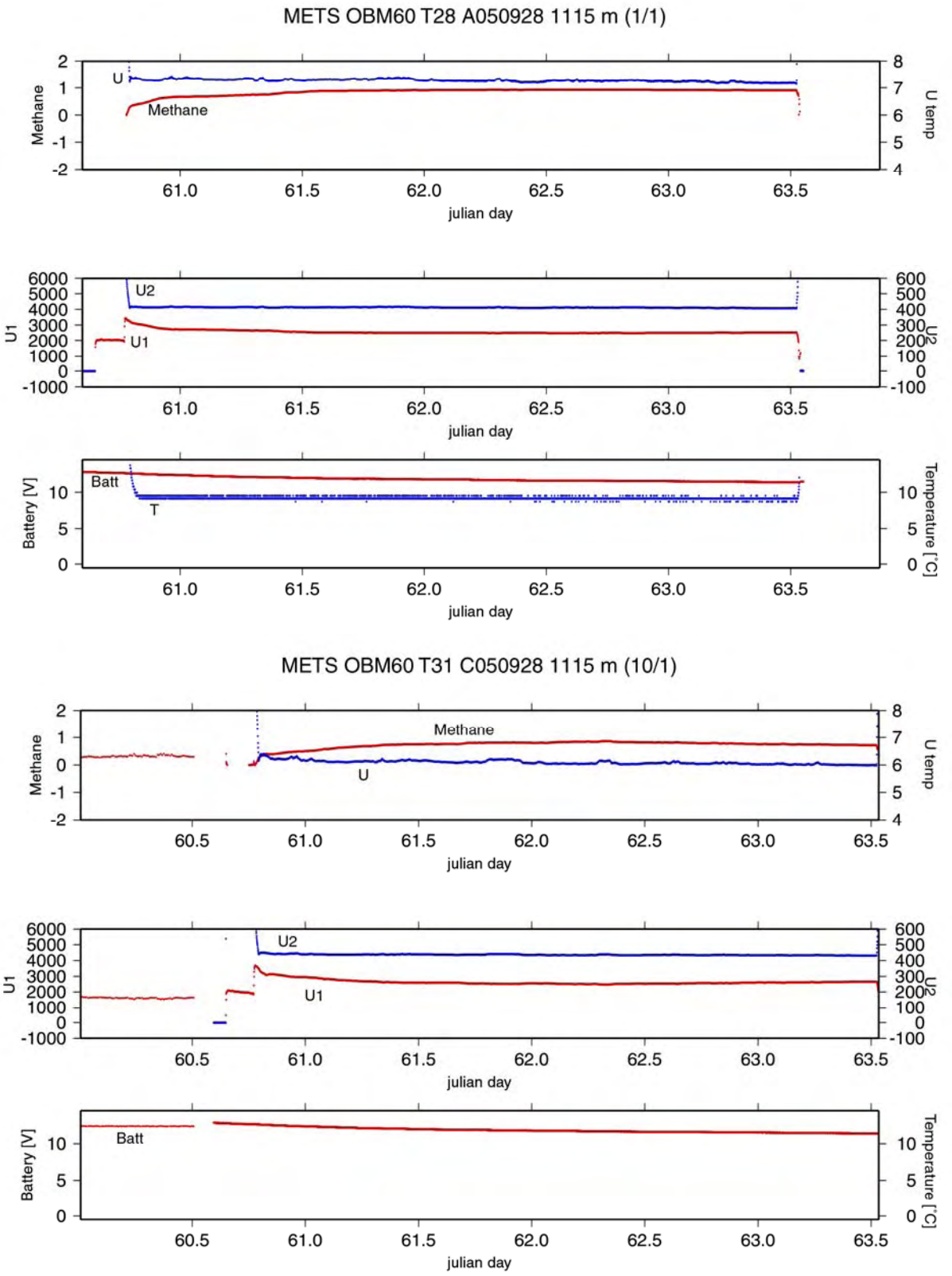

Figure 6.7.3: *Raw data (bottom and middle, U [mv]), methane data (top), OBM60, on top for sensor T28 with recorder A050928 and at the bottom for sensor T31 with recorder C050928.*

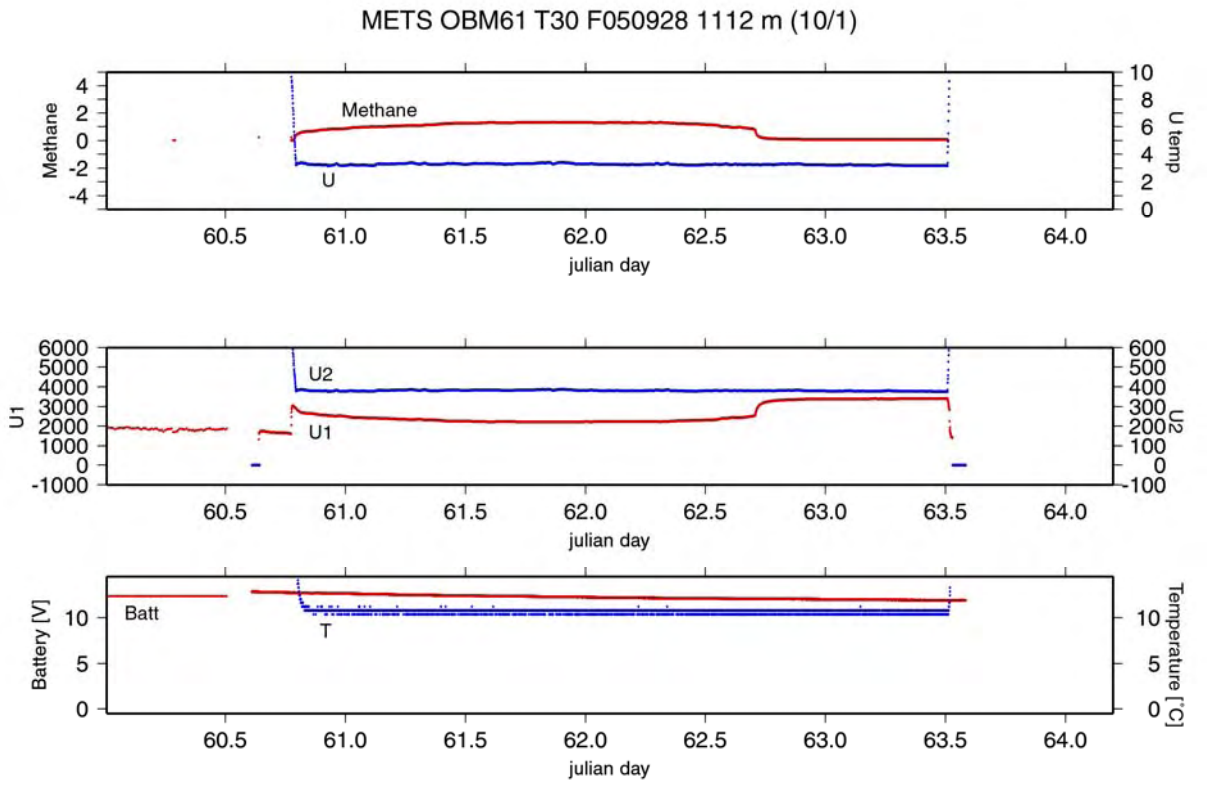

Figure 6.7.4: *Raw data (bottom and middle, U [mv]), methane data (top), OBM61.*

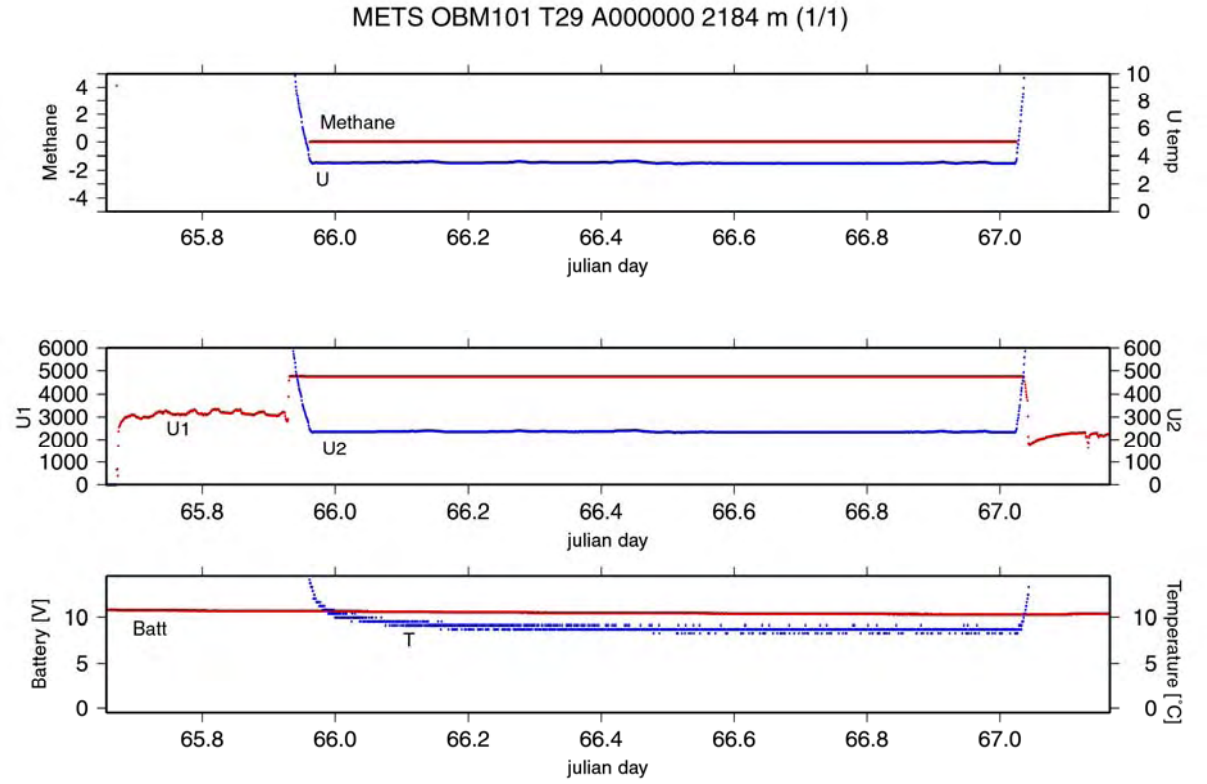

Figure 6.7.5: *Raw data (bottom and middle, U [mv]), methane data (top), OBM101.*

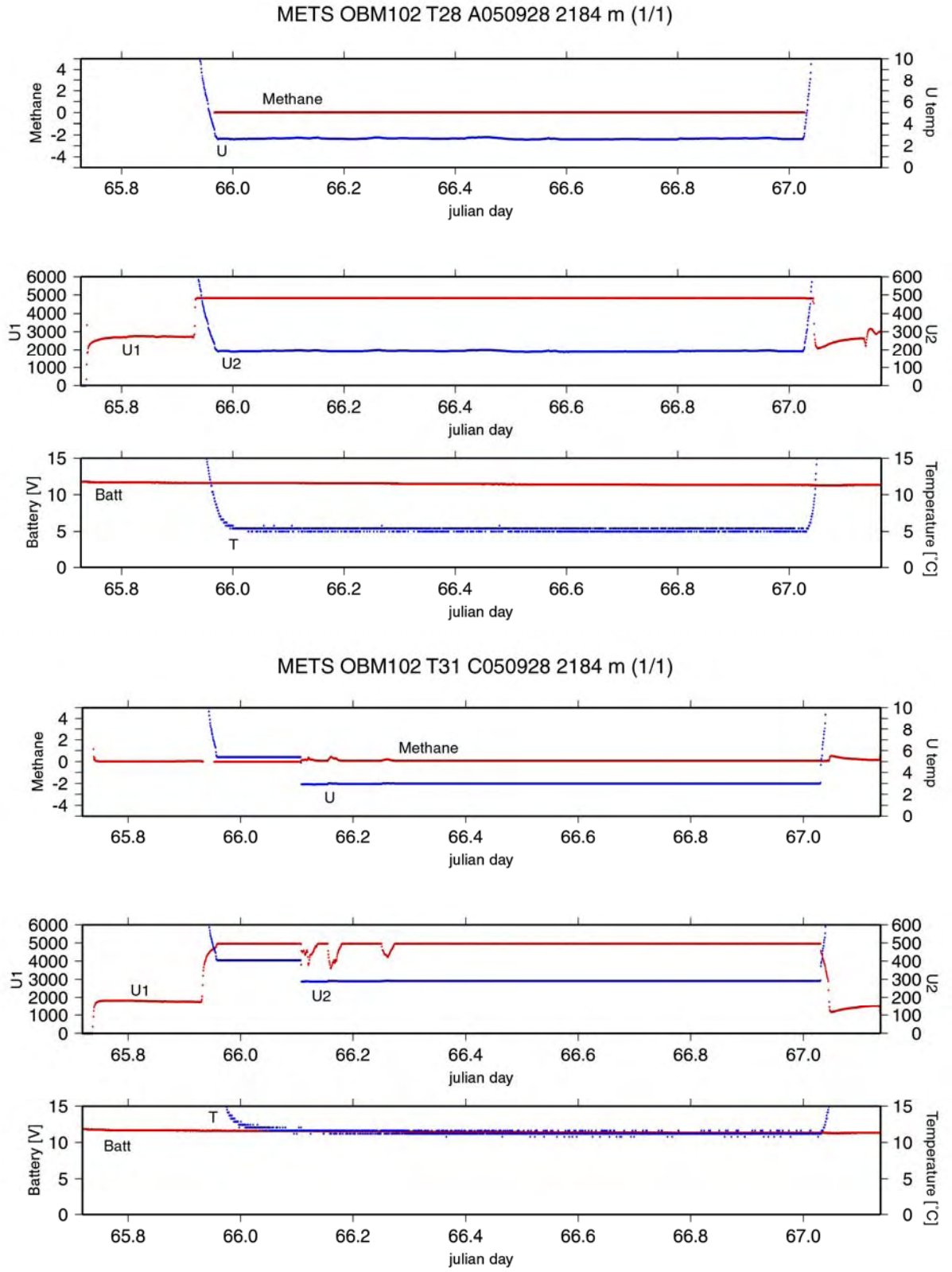

Figure 6.7.6: *Raw data (bottom and middle, U [mv]), methane data (top), OBM102, on top for sensor T28 with recorder A050928 and at the bottom for sensor T31 with recorder C050928.*

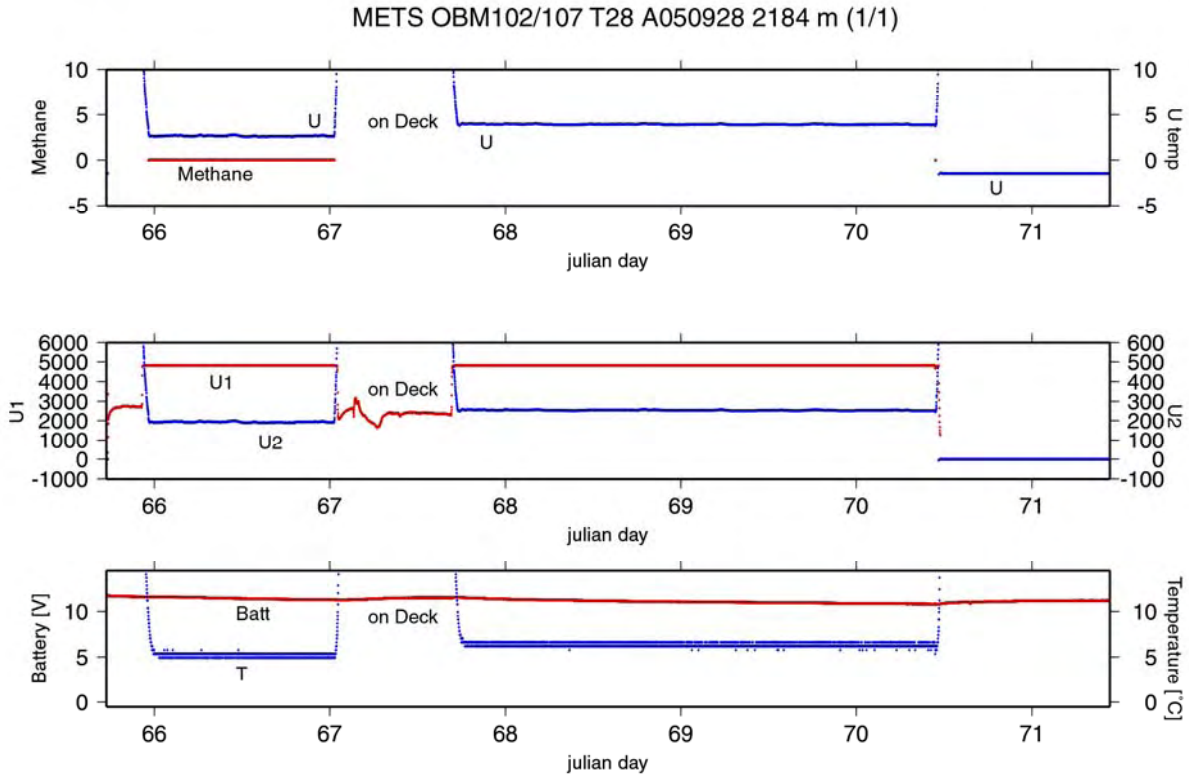

Figure 6.7.7: *Raw data (bottom and middle, U [mv]), methane data (top), OBM102/107.*

7. Acknowledgements

The Cruise SO186-3 was financed within the project SEACAUSE by the German Federal Ministry for Education and Research (Bundesministerium für Bildung und Forschung / BMBF) under Project No. 03G0186B. We are grateful for the continuous support of marine sciences with an outstanding platform such as RV SONNE. The authors wish to express their gratitude to all the colleagues who have supported the work before and during the cruise. Much of the work done during the cruise was only made possible by the scientists' and the crew's experience. Particular thanks are directed to the ship's master, Captain Oliver Meyer and to the entire crew of RV SONNE for their excellent support throughout the cruise.

8. References:

Abercrombie, R., Antolik, M., Felzer, K., and Ekström, G.: The 1994 Java tsunami earthquake: Slip over a subducting seamount, J. Geophys. Res., 106, 6595-6607, 2001.

Ammon, C.J., Ji, C., Thio, H-K., Robinson, D., Ni, S., Hjorleifsdottir, V., Kanamori, H., Lay, T., Das, S., Helmberger, D., Ichinose, G., Polet, J., and Wald, D., Rupture Process of the 2004 Sumatra-Andaman Earthquake, Science 308, 1133-1139, 2005.

Audley-Charles, M.G., Evolution of the southern margin of Thethys (North Australian region) from early Permian to late Cretaceous, in: Gondwana and Thethys, Audley-Charles, M.G., and A. Hallam (eds), Geological Society Special Publication 37, 79-100, 1988.

Bangs, N. L. B., G. K. Westbrook, J. W. Ladd, and P. Buhl, Seismic velocities from the Barbados Ridge Complex: Indicators of high pore fluid pressures in an accretionary complex, J. Geophys. Res., 95, 8767-8782, 1990.

Beaudry, D. and G. F. Moore: Seismic-stratigraphic frame work off Central Sumatra, Sunda Arc, Earth and Plan. Sc. Letts., 54, 17-28, 1981.

Beaudry, D. and G. F. Moore: Seismic stratigraphy and Cenozoic evolution of the West Sumatra forearc basin, Am. Assoc. Petr. Geol. Bull., 69, 5, 742-759, 1985.

Beck, R. H. und P. Lehner: Oceans, new frontier in exploration. Am. Assoc. Petr. Geol. 58, 376-395, 1974.

Benaron, N, A geophysical study of the forearc region south of Java, Indonesia, Master Thesis, University of San Diego, CA, 83 pp, 1982.

Bialas, J., and Flueh, E. R., Ocean Bottom Seismometers, Sea Technology, 40, 4, 41-46, 1999.

Bilham, R., A flying start, then a slow slip. Science 308, 1126-1127, 2005.

Bostock, M. G., R. D. Hyndman, S. Rondenay, and S. M. Peacock, An inverted continental Moho and serpentinization of the forearc mantle, Nature, 417, 536-538, 2002

Brouwer, H. A.: The Geology of the Netherlands East Indies, Macmillan, New York, 1-160, 1925.

Byrne, D. E., W.-H. Wang, and D. M. Davis, Mechanical role of backstops in the growth of forearcs, Tectonics, 12, 1, 123-144, 1993.

Carlson, R. L., and D. J. Miller, Mantle wedge water contents estimated from seismic velocities in partially serpentinized peridotites, Geophys. Res. Lett.,30(5), 1250, doi:10.1029/2002GL016600, 2003

Collot, J.-Y., Marcaillou, B., Sage, F., Michaud, F., Agudelo, W., Charcis, P., Graindorge, D., Gutscher, M.-A., Spence, G., Are rupture zone limits of great subduction earthquakes controlled by upper plate structures? Evidence from multi-channel seismic reflection data acquired across northern Ecuador-southwest Colombia margin. Journ. Geophys. Res., 109, B11103, 1-14, 2004.

Cox, C., Deaton, T., and Webb, S., A Deep-Sea Differentail Pressure Gauge, J. Atmosph. Oceanic Technology, 1, 237-246, 1984.

Curray, J.R., Shor, G.G.Jr., Raitt, R.W., and Henry M., Seismic refraction and reflection studies of crustal structure of the Eastern Sunda and Western Banda arcs, Journal of Geophysical Research, 82, 17, 2479-2489, 1977.

Curray, J. R.: The Sunda Arc: A model for oblique plate convergence, Proc. Snellius-II Symp., Neth. Jl. Sea Res., 24, 131-140, 1989.

Dahlen, F. A., Critical taper model of fold-and-thrust belts and accretionary wedges, Annu. Rev. Earth Planet. Sci., 18, 55-99, 1990.

Davis, D. M., J. Suppe, and F. A. Dahlen, Mechanics of Fold-and-Thrust Belts and Accretionary Wedges, J. Geophys. Res., 88, 1153-1172, 1983.
Davis, D.M., and R.von Huene, Inferences on sediment strength and fault friction from structures at the Aleutian Trench, Geology, 15, 517-522, 1987.
Davis, D. M., Accretionary mechanics with properties that vary in space and time, in: Subduction top to bottom, Geophysical Monograph 96, 39-48, 1996.
Davis, E. E., and R. Hyndman, Accretion and recent deformation of sediments along the northern Cascadia subduction zone, Int. Geological Society of America Bulletin, 101, 1465-1480, 1989.
De Mets, Gordon, R. G., Argus, D. F., and Stein, S. Current plate motions, Geophysical Journal International, 101, 425-478, 1990.
Diament, M., H. Harjono, K. Karta, C. Deplus, D. Dahrin, M. T. Zan, Jr., M. Gerard, O. Lassal, A. Martin, J. Malod, Mentawai fault zone off Sumatra: a new key to the geodynamics of western Indonesia, Geology, 20, 259-262, 1992.
Fine, I. V., Rabinovich A. B. and Thomson, R. E., A dual source region fo rthe 2004 Sumatra tsunami, Geophys. Res. Lett. 32, L16602, doi :10.1029/2005GL023521, 2005.
Fitch, T. J., Plate convergence, transcurrent faults and internal deformation adjacent to Southeast Asia and the Western Pacific, Int. Journal of Geophysical Research, 77, 4432-4460, 1972.
Flueh, E.R., and Bialas, J., A digital, high data capacity ocean bottom recorder for seismic investigations, Int. Underwater Systems Design, 18, 3, 18-20, 1996.
Flueh, E.R. (edt) and Shipboard Science Party, GINCO2 (SONNE Cruise SO-138): Geo-scientific investigations along the active convergence zone between the Eastern Eurasian and Indo-Australian Plates off Indonesia, Cruise Report, Geomar, Kiel, 1999.
Fruehn, J, R. von Huene, and M. A. Fisher, Accretion in the wake of terrane collision: the Neogene accretionary wedge off Kenai peninsula, Alaska, Tectonics, 18, 2, 263-277, 1999.
Gaedicke, C., Cruise report Sonne Cruise So186-2 SeacauseII; BGR, Hannover, Archive Number: 0125999, 144pp, 2006.
Ganie, B., Syafuddin, Superman, A. and Honza, E., Geomorphological features in the eastern Sunda Trench, CCOP Technical Bulletin, 19, 7-12, 1987.
Gasparon, M., and R. Varne, Sumatran granitoids and their relationship to Southeast Asian terranes, Tectonophysics, 251, 277-299, 1995.
Ghose, R., Yoshioka, S., and Oike, K., Three-dimensional numerical simulation of the subduction dynamics in the Sunda arc region, Southeast Asia, Tectonophysics, 181, 223-255, 1990.
Gower, J., Jason 1 detects the 26 December 2004 tsunami, EOS Trans. AGU, 86, 37-38, 2005.
Graeber, F. M., and G. Asch, Three-dimensional models of P wave velocity and P-to-S ratio in the southern central Andes by simultaneous inversion of local earthquake data, J. Geophys. Res., 104, 20,237-20,256, 1999
Grevemeyer, I., T.M. Tiwari, Overriding plate controls spatial distribution of megathrust earthquakes in the Sunda-Andaman subduction zone, Poster, EGU Meeting, Vienna, 2006.
Guilbert, J., Vergoz, J., Schisselé, E., Roueff, A. and Cansi, Y., Use of hydroacoustic and seismic arrays to obersve rupture propagation adn source extent of the Mw=9.0 Sumatra earthquake, Geophys. Res. Lett. 32, L15310, doi :10.1029/2005GL022966, 2005.
Gutscher, M.A., N. Kukowski, J. Malavieille, and S. Lallemand, Cyclical behavior of thrust wedges: insights from high basal friction sandbox experiments, Geology, 24 (2), 135-138, 1996.
Hamilton, W.B., Tectonics of the Indonesian Region, USGS Professional Paper, 1078, 1979.
Hamilton, W., Plate tectonics and island arcs, Geological Society of America Bulletin, 100, 1503-1527, 1988.
Huchon, P. and Le Pichon, X.: Sunda Strait and Central Sumatra fault, Geology, 12, 668-672, 1984.
Hutchinson, C.S., Geological Evolution of South-East Asia, Claredon Press, Oxford, 1989.
Hyndman, R.D, S.M. Peacock, Serpentinization of the forearc mantle, Earth Planet. Sci. Lett. 212, 417-432, 2003
Ishii, M., Shearer, P.M., Houston, H., and Vidale J.E., Extent, duration and speed of the 2004 Sumatra-Andaman earthquake imaged by the Hi-Net array, Nature 435, doi:10.1038/nature03675, 933-936, 2005.
Izart, A., B. Mustafa Kemal, J. A. Malod, Seismic stratigraphy and subsidence evolution of the northwest Sumatra fore-arc basin, Marine Geology, 122, 109-124, 1994.
Jiao, W., P. G. Silver, Y. Fei, and C. T. Prewitt, Do intermediate- and deep-focus earthquakes occur on preexisting weak zones? An examination of the Tonga subduction zone, J. Geophys. Res., 105, 28,125-28,138, 2000
Kamiya, S., and Y. Kobayashi, Seismological evidence for the existence of serpentinized wedge mantle, Geophys. Res. Lett., 27, 819-822, 2000
Karig, D. E., Suparka, S., Moore, G. F., Hehunassa, P. E.: Structure and Cenozoic evolution of the Sunda Arc in the central Sumatra region, Am. Assoc. Petr. Geol. Mem., 29, 223-237, 1979.
Karig, D. E., Lawrence, M. B., Moore, G. F., Curray, J. R.: Structural framework of the forear-arc basin, NW Sumatra, Jl. Geol. Soc. Lon., 137, 77-91, 1980.

Karig, D. E., Moore, G. F., Curray, J. R., Lawrence, M. B.: Morphology and shallow structure of the lower trench slope off Nias island, Sunda Arc, in: D. E. Hays (ed)., The tectonic and geologic evolution of Southeast Asian Seas and Islands, Geoph. Mon., 23, 179-208, 1980.
Kennett, B. L. N. and Cummins, P. R., The relationship of the seismic source and subduction zone structure for the 2004 December 26 Sumatra-Andaman earthquake, Earth and Planet. Sci. Lett. 239, 1-8, 2005.
Khan and Gudmundsson, GPS Analysis of the Sumatra-Andaman Earthquake. EOS, Am. Geophy. Union, 1. März 2005, 86, 9, p. 89 + 94, 2005.
Kirby, S., E. R. Engdahl, and R. Denlinger, Intermediate-depth intraslab earthquakes and arc volcanism as physical expressions of crustal and uppermost mantle metamorphism in subducted slabs, in: Subduction Top to Bottom, Geophys. Monogr. Ser., vol. 96, edited by G. Bebout et al., pp. 195-214, AGU, Washington, DC, 1996
Kobayashi, K., Nakanishi, M., Tamaki, K., Ogawa, Y.: Outer slope faulting associated with the western Kuril and Japan trenches, Geophys. J. Int., 134, 356-372, 1998.
Kopp, H., Crustal Structure Along the Central Sunda Margin, Indonesia, PhD Thesis, University of Kiel, 2001.
Kopp, H., BSR occurrence along the Sunda margin: evidence from seismic data, Earth and Planetary Science Letters, 197, 225-235, 2002.
Kopp, H., D. Klaeschen, E. R. Flueh, J. Bialas, C. Reichert, Crustal structure of the Java margin from seismic wide-angle and multichannel reflection data, Journal of Geophysical Research, 107, B2, 10.1029/2000JB000095, 2002.
Kopp, H. and N. Kukowski, Backstop geometry and accretionary mechanics of the Sunda margin, Tectonics, 6, 22, 10.1029/2002TC001420, 2003.
Kopp, H., Flueh, E., Papenberg, C., Klaeschen, D., SPOC Scientists: Seismic Investigations of the O'Higgins Seamount Group and Juan Fernández Ridge: Aseismic Ridge Emplacement and Lithosphere Hydration, Tectonics, 2, 23, TC2009, 10.1029/2003TC001590, 2004.
Krüger, F., and Ohrnberger, M., Tracking the rupture of the Mw=9.3 Sumatra earthquake over 1,150 km at teleseismic distance. Letters to Nature, doi:10.1038/nature03696, 1-3, 2005.
Kuenen, P. H.: Geological interpretation of bathymetrical results. The Snellius expedition, 5, 1, 1-124, Brill, Leiden, 1935.
Lallemand, S. E., P. Schnuerle, and J. Malavieille, Coulomb theory applied to accretionary and nonaccretionary wedges: Possible causes for tectonic erosion and/or frontal accretion, J. Geophys. Res., 99, 12033-12055, 1994.
Lay, T., Kanamori, H., Ammon, C.J., Nettles, M., Ward, S.N., Aster, R.C., Beck, S.L., Bilek, S.L., Brudzinski, M.R., Butler, R., DeShon, H.R., Ekström, G., Satake, K., and Sipkin, S., The Great Sumatra-Andaman Earthquake of 26 December 2004, Science 308, 1127-1133, 2005.
Lohrmann, J., N. Kukowski, J. Adam, and O. Oncken, The impact of analogue material properties on the geometry, kinematics, and dynamics of convergent sand wedges, Journal of Structural Geology, 25 (10), 1691-1711, 2003.
Lomnitz, C. and Nielsen-Hofseth, S., The Indian Ocean Disaster: Tsunami Physics and Early Warning Dilemmas, EOS 15. February 2005, p. 65 + 70, 2005.
Malod, J. A., K. Karta, M.O. Beslier, M.T. Zen Jr., From normal to oblique subduction: Tectonic relationships between Java and Sumatra, Journal of Southeast Asian Earth Sciences, 12, 85-93, 1995.
Malod, J. A., and B. M. Kemal, The Sumatra margin: oblique subduction and lateral displacement of the accretionary prism, in: Tectonic evolution of Southeast Asia, R. Hall and D. Blundell (edts), Geological Society Special Publication, 106, 19-28, 1996.
Masson, D. G., Parson, L. M., Milsom, J., Nichols, G., Sikumbang, N., Dwiyanto, B., Kallagher, H.: Subduction of seamounts at the Java Trench: a view with long-range sidescan sonar, Tectonophysics, 185, 51-65, 1990.
Masson, D. G.: Fault patterns at outer trench walls, Marine Geophys. Res., 13, 209-225, 1991.
McCaffrey, R., Oblique plate convergence, slip vectors, and forearc deformation, Journal of Geophysical Research, 97, B6, 8905-8915, 1992.
McCaffrey, R., P. C. Zwick, Y. Bock, L. Prawirodirdjo, J. F. Genrich, C. W. Stevens, S. S. O. Puntodewo, C. Subarya, Strain partitioning during oblique plate convergence in northern Sumatra: Geodetic and seismologic constraints and numerical modeling,J ournal of Geophysical Research, 105, 28363-28376, 2000.
McCloskey, J., Nalbant, S. S. and Steacy, S., Earthquake risk from co-seismic stress, Nature 434, 291, 2005.
McCourt, W., M. J. Crow, E. J. Cobbing, and T. C. Amin, Mesozoic and Cenozoic plutonic evolution of SE Asia: evidence from Sumatra, Indonesia, in: Tectonic Evolution of Southeast Asia, R. Hall (edt), Geological Society of London Spec. Publication 106, 321-335, 1996.
Metcalfe, I., Pre-Cretaceous evolution of Se Asian terranes, in: Tectonic Evolution of Southeast Asia, R. Hall (edt), Geological Society of London Spec. Publication 106, 97-122, 1996.
Moore, G. F., J. R. Curray, D. G. Moore, D. E. Karig, Variations in geologic structure along the Sunda fore arc, Northeastern Indian Ocean, in: The tectonic and geologic evolution of Southeast Asian seas and islands, D. Hayes (edt), Geophysical Monograph, 23,145-160, 1980.

Müller, D., W. R. Roest, J. Y. Royer, L. M.Gahagan, and J. G. Sclater, Digital isochrons of the world's ocean floor, Journal of Geophysical Research, 102, 3211-3214, 1997.
Nalbant, S. S., Steacy, S., Sieh, K., Natawidjaja, D. and McCloskey, J., Earthquake risk on the Sunda trench, Nature 435, 756-757, 2005.
Newcomb, K.R., and McCann, W.R., Seismic history and seismotectonics of the Sunda Arc, Journal of Geophysical Research, 92: 421-439, 1987.
Ni, S., Kanamori, H., and Helmberger, D., Energy radiation from the Sumatra earthquake, Nature 434, 582, 2005.
Nishimura, S., and S. Suparka, Tectonic approach to the Neogene evolution of Pacific-Indian Ocean seaways, Tectonophysics, 281, 1-16, 1997.
Park, J., Anderson, K., Aster, R., Butler, R., Lay, T. and Simpson, D., Global seismographic network records the great Sumatra-Andaman earthquake, EOS, Am. Geophy. Union, 8. February 2005, 86, 6, p. 57 + 60-61, 2005.
Park, J., Song, T. A., Tromp, J., Okal, E., Stein, S., Roult, G., Clevede, E., Laske, G., Kanamori, H., Davis, P., Berger, J., Braitenberg, C., Van Camp, M., Lei, X., Sun, H., Xu, H., Rosat, S., Earth's free oscillations excited by the 26 December 2004 Sumatra-Andaman earthquake, Science 308, 1139-1144, 2005b.
Peacock, S., Fluid processes in subduction zones, Science, 248, 329-337, 1990
Peacock, S., Large-scale hydration of the lithosphere above subducting slabs, Chem. Geol., 108, 49-59, 1993
Peacock, S., Are the lower planes of double seismic zones caused by serpentine dehydration in the subducting oceanic mantle?, Geology, 29, 299-302, 2001
Pubellier, M., C. Rangin, J.-P. Cadet, I. Tjashuri, J. Butterlin and C. Mueller, L'ile de Nias, un edifice polyphase sur la bordure interne de la fosse de la Sonde (Archipel de Mentawai, Indonesie), Comptes rendus de l'Academie des sciences, Serie II, 8, 1019-1026, 1992.
Ranero, C. R. and R. von Huene, Subduction erosion along the Middle America convergent margin, Nature, 404, 748-752, 2000.
Ranero, C. R., J. Phipps Morgan, K. McIntosh, and C. Reichert, Bending-related faulting and mantle serpentinization at the Middle America trench, Nature, 425, 367-373, 2003.
Reichert, C. (edt) and Shipboard Science Party, GINCO1 (SONNE Cruise SO-137): Geo-scientific investigations along the active convergence zone between the Eastern Eurasian and Indo-Australian Plates off Indonesia, Cruise Report, BGR, Hannover, 1999.
Ryan, H. F., and D. W. Scholl, The evolution of forearc structures along an oblique convergent margin, Central Aleutian arc, Tectonics, 8, 3 497-516, 1989.
Sabadini, R., Dalla Via, G., Hoogland, M., and Aoudia, A, A Splash in Earth Gravity from the 2004 Sumatra Earthquake. EOS, Am. Geophy. Union, 12. April 2005, 86 (15), p. 149 + 153, 2005.
Samuel, M. A.: The Structural and Stratigraphic Evolution of Islands of the Active Margin of the Sumatra Forearc, Indonesia. PhD-Thesis University of London, pp. 345, 1994.
Samuel, M. A., and N. A. Harbury, The Mentawai fault zone and deformation of the Sumatran forearc in the Nias area, in: Tectonic evolution of Southeast Asia, R. Hall and D. Blundell (edts), Geological Society Special Publication, 106, 337-351, 1996.
Schlueter, H. U., C. Gaedicke, H. A. Roeser, B. Schreckenberger, H. Meyer, C. Reichert, Y. Djajadihardja, and A. Prexl, Tectonic features of the southern Sumatra-western Java forearc of Indonesia-, Tectonics, 21(5), 1047, doi:10.1029/2001TC901048, 2002.
Scholl, D. W., Stuffing continental crustal material into the mantle at subduction zones—evidence, quantities, consequences, http://pangaea.stanford.edu/GP/Scholl.html, 2002.
Schott, B., and H.A. Koyi, Estimating basal friction in accretionary wedges from the geometry and spacing of frontal faults, Earth and Planetary Science Letters, 194, 221-227, 2001.
Seno, T., and Y. Yamanaka, Double seismic zones, compressional deep trench-outer rise events, and superplumes, in: Subduction Top to Bottom, Geophys. Monogr. Ser., vol. 96, edited by G. Bebout et al., pp. 347-355, AGU, Washington, DC, 1996
Seno, T., D. Zhao, Y. Kobayashi, and M. Nakamura, Dehydration of serpentinized mantle: Seismic evidence from southwest Japan, Earth Planets Space, 53, 861-871, 2001
Sieh, K., Aceh-Andaman earthquake : What happened and waht's next ?, Nature 434, 573-574, 2005.
Sieh, K., and D. Natawidjaja, Neotectonics of the Sumatran fault, Indonesia, Journal of Geophysical Research, 105, 12 28295-28326, 2000.
Stein, S. and Okal, E. A., 2005. Speed and size of the Sumatra earthquake, Nature 434, 581-582
Tapponnier, P., G. Peltzer, A. Y. Le Dain, Armijo-Rolando, and P. Cobbold, Propagating extrusion tectonics in Aisa: new insights from simple experiments with plasticine, Geology, 10, 12, 611-616, 1982.
Tregoning et al., 1994
Van Bemmelen, R. W.: The geology of Indonesia, Vol. IA, General Geology, IB Portfolio. Government Printing Office, Nijhoff, The Hague, 1-732, 1949.
Van Weering, T. C. E., Kusnida, D., Tjokrosapoetro, S., Lubis, S., Kridoharto, P., Munadi, S.: The seismic structure of the Lombok and Savu forearc basins, Indonesia, Neth. J. Sea Res., 24, 251-262, 1989.

Vening Meinesz, F. A.: The earth's crust deformtion in the East Indies, Proc. K. Ned. Akad. Wet., 43, 2778-293, 1940.
von Huene, R., and D. W. Scholl, Observations at convergent margins concerning sediment subduction, subduction erosion and the growth of continental crust, Reviews of Geophysics, 29, 279-316, 1991.
von Huene, R., and D. Klaeschen, Opposing gradients of permanent strain in the aseismic zone and elastic strain across the seismogenic zone of the Kodiak shelf and slope, Alaska, Tectonics,18,2, 248-262, 1999.
Von Huene, R., Ranero, C.R. und Watts, P.:Tsunamigenic slope failure along the Middle America Trench in two tectonic settings, Marine Geology, 203, 303-317, 2004.
Widiyantoro, S., and R. van der Hilst, Structure and Evolution of Lithospheric Slab Beneath the Sunda Arc, Indonesia, Science, 271, 1566-1570, 1996.
Wilson, M., Modeling the Sumatra-Andaman earthquake reveals a complex, nonuniform rupture, Physics Today 58, 6, 19-21., 2005.
Yuan, X., Kind, R. and Pedersen, H. A., Seismic monitoring of the Indian Ocean tsunami, Geophys. Res. Lett. 32, L15308, doi :10.1029/2005GL023464, 2005.
Zhao, D., F. Ochi, A. Hasegawa, and A. Yamamoto, Evidence for the location and cause of large crustal earthquakes in Japan, J. Geophys. Res., 105, 13,579-13,594, 2000.

	INST.	LAT (N)	LON (E)	DEPLOY.	RECOV.	DEPTH	REL.	ANT.	REC.	SKEW	SENSORS
		D:M	D:M	DATE	DATE	(m)	CODE	CH.	NO.	(ms)	
SO-186 1A	OBS 01	2°48,024' N	97°12,036' E	15.10.05	01.03.06	834	131351 (05.03. 00:00)	D	MLS 040602	915*	HTI 55 + Owen (4,5Hz)
	OBS 02	2°42,008' N	96°51,044' E	15.10.05	04.03.06	1123	133563 (05.03. 01:00)	C	MLS 040603	1119*	OAS 41 + Owen (4,5Hz)
	OBS 03	2°12,009' N	96°18,012' E	15.10.05	02.11.05	1021	250177 (05.03.06 04:00)	C	MBS 010701	-220	OAS 29 + Owen (4,5Hz)
	OBS 04	1°57,987' N	96°29,981' E	15.10.05	24.11.05	1155	131317 (05.03.06 02:00)	D	MTS 050815	15	OAS 17 + Owen (4,5Hz)
	OBH 05	1°54,020' N	96°12,004' E	15.10.05	24.11.05	2364	A324 (A) (05.03.06 21:15	D	MTS 050814	23	DPG 92
	OBS 06	1°53,990' N	95°59,981' E	15.10.05	05.11.05	3164	133770 (05.03.06 03:00)	C	MTS 050811	23	DPG 95 + Paroscientific
	OBH 07	2°12,047' N	96°00,004' E	15.10.05	10.01.06	1616	C444 (A) (05.03.06 20:00	D	MTS 050816	989 *	DPG 77
	OBH 08	2°00,001' N	95°42,002' E	15.10.05	24.11.05	4444	D634 (A) (05.03.06 22:45	D	MTS 050812	28	DPG 75
	OBS 09	2°12,000' N	95°17,997' E	15.10.05	24.11.05	4668	133736 (05.03.06 05:00)	D	MTS 050813	52	DPG 73 + Paroscientific
	OBS 10	2°24,022' N	95° 42,004' E	15.10.05	02.11.05	749	133664 (05.03.06 06:00)	D	MBS 000614	-104	HTI 57 + Owen 27 (4,5Hz)
	OBS 11	2°36,050' N	95°29,984' E	15.10.05	02.11.05	1057	131245 (05.03.06 07:00)	C	MBS 001006	-30	HTI 51 + Owen 23 (4,5Hz)
	OBS 12	3°12,002' N	95°41,957' E	16.10.05	28.02.06	470	133622 (05.03. 08:00)	C	MLS 010408	781	HTI 56 + Owen(4,5Hz)
	OBH 13	3°06,003' N	96°00,001' E	16.10.05	03.11.05	657	C464 (A) (06.03.06 00:00	D	MLS 020601	60	OAS 07
	OBS 14	3°30,000' N	96°11,984' E	16.10.05	28.02.06	859	134037 (05.03. 09:00)	D	MLS 040304	980*	OAS 45 + Owen (4,5Hz)
	OBS 15	3°18,037' N	96°29,950' E	16.10.05	01.03.06	1013	134123 (05.03. 10:00)	D	MLS 040803	1001*	HTI + Owen (4,5Hz)
	OBS 16	3°00,026' N	96°30,007' E	16.10.05	01.03.06	1087	145206 (05.03. 11:00)	C	MLS 010406	1088*	OAS 03 + Owen (4,5Hz)
	OBS 17	2°53,991' N	96°11,983' E	16.10.05	01.03.06	770	131415 (05.03. 12:00)	D	MLS 010404	1540*	HTI + Owen (4,5Hz)
	OBS 18	2°48,006' N	96°29,996' E	16.10.05	01.03.06	1052	131203 (05.03. 13:00)	C	MLS 000708	-139*	OAS 30 + Owen (4,5Hz)
	OBH 19	2°54,006' N	96°41,996' E	16.10.05	01.03.06	1112	03B3+0355 (05.03 19:00)	D	MLS 000712	1121*	OAS 35
	OBS 20	3°17,988' N	96°48,002' E	16.10.05	01.03.06	996	134071 (05.03 14:00)	C	MLS 040102	716*	HTI + Owen (4,5Hz)
SO-186 1B	OBS 21	2°24,047' N	95°42,044' E	02.11.05	02.03.06	752	250177 (05.03. 04:00)	C	MLS 991233	1123*	OAS 29 + Owen(4,5Hz)
	OBS 22	2°36,062' N	95°30,023' E	02.11.05	28.02.06	1060	133664 (05.03. 06:00)	D	MLS 991234	1145*	HTI 57 + Owen 27 (4,5Hz)
	OBH 23	3°05,964' N	96°00,042' E	03.11.05	28.02.06	647	C464 (A) (06.03. 00:00)	D	MLS 020601	1372*	OAS 07
	OBS 24	2°12,004' N	96°18,011' E	03.11.05	02.03.06	1022	131245 (05.03. 07:00)	C	MLS 991258	1477 *	HTI 51 + Owen 23 (4,5Hz)
	OBS 25	1°53,944' N	95°59,984' E	05.11.05	10.11.05	3162	133770 (05.03.06 03:00)	C	MTS 050811	5	DPG 95 + Paro
SO-186 1C (GITEWS)	OBSTEST	3°32,791 S	99° 29,562 E	18.11.05	20.11.05	5812	427562	C	MTS 050805	1	DPG72 + Gü + Paro 98495
	OBS 26	1°30,010'N	95°59,990' E	24.11.05	05.03.06	5121	430067 (06.03. 02:00)	C	MTS 050810	1474*	DPG 65 + Owen -071 (4,5 Hz) + Paro 98489
	OBS 27	1°40,000' N	96°05,010' E	24.11.05	05.03.06	4793	427623 (06.03. 11:00)	C	MTS 050809	1172*	DPG 68 + Owen -075 (4,5 Hz) + Paro 616
	OBS 28	1°39,970' N	96°24,990' E	24.11.05	05.03.06	2379	430173 (06.03. 09:00)	D	MTS 050817	1085*	DPG 62 + Owen (4,5 Hz) + Paro 612
	OBS 29	1°45,00' N	96°32,99' E	24.11.05	05.03.06	1702	427260 (06.03. 07:00)	D	MTS 050818	935*	DPG 63 + Owen -072 (4,5 Hz) + Paro 22
	OBS 30	2°00,130' N	96°29,740' E	24.11.05	10.01.06	1178	427430 (06.03.06 15:00)	D	MLS 010403	1053 *	OAS 44 + Owen -077 (4,5 Hz)
	OBS 31	1°50,080' N	96°20.010' E	24.11.05	10.01.06	2770	131317	D	MLS 991243	1076 *	OAS 17 + Owen 20 (4,5 Hz)
	OBS 32	1°54,000' N	96°11,854' E	24.11.05	10.01.06	2364	430232 (06.03.06 14:00)	D	MLS 040806	no skew	HTI 31 + Owen -076 (4,5 Hz)
	OBS 33	1°54,104' N	95°59,451' E	24.11.05	10.01.06	3448	430326 (06.03.06 04:00)	D	MTS 050815	1033*	DPG 67 + Owen (4,5 Hz) + Paro
	OBS 34	2°00,006' N	95°41,998' E	24.11.05	16.01.06	4383	133770	D	MLS 991246	no skew	OAS31 + Owen 10 (4,5 Hz)
	OBS 35	1°50,006' N	95°42,001' E	24.11.05	16.01.06	5017	145331 (05.03.06 16:00)	D	MLS 991236	no skew	OAS 25 + Owen (4,5 Hz)
	OBS 36	2°00,065' N	95°29,984' E	24.11.05	16.01.06	4916	C504 (mode A)	D	MLS 991257	no skew	DPG 95 + Owen (4,5 Hz)
	OBS 37	2°12,04' N	95°17,958' E	24.11.05	28.02.06	4674	427476	D	MTS 050814	1074*	DPG 66 +Owen (4,5 Hz) + Paro 98494
	OBS 38	2°30,05' N	95° 20,04' E	24.11.05	28.02.06	1324	133736 (05.03. 05:00)	D	MTS 050812	out of range	DPG 73 + Owen -079 (4,5 Hz) + Paro 98475
	OBH 39	2°42,040' N	95°3,953' E	24.11.05	10.01.06	1104	D634 (mode A)	daue	MLS 991235	-1089187470	DPG 75
	OBH 40	2°48,046' N	94°55,986' E	24.11.05	28.02.06	865	4A49	D	MLS 991259	727*	DPG 92
	TOBU 01	3°43,900' S	99°13,800' E	20.11.05	12.01.06	5290	133525 (05.03.06 15:00)	C	MTS-M 050808	no skew	DPG 61 + Gü + Paro 98469
	TOBS 01	3°43,000' S	99°14,050' E	20.11.05	12.01.06	5228	427562 (06.03.06 12:00)	C	MTS 050805	no skew	DPG 72 + Gü + Paro 98495
	TOBU 02	0°27,132' S	96°50,737' E	23.11.05	11.01.06	3259	430135	C	MTS-M 050807	-638858	DPG 64 + Gü + Paro 98607
	TOBS 02	0°26,687' S	96°52,270' E	23.11.05	11.01.06	3440	145240 (05.03.06 17:00)	C	MTS 050811	1065 *	DPG 71 + Owen -073 (4,5Hz) + Paro 98621

INST.	LAT (N)	LON (E)	DEPLOY.	RECOV.	DEPTH	REL.	ANT.	REC.	at OBS	SENSORS
	D:M	D:M	DATE	DATE	(m)	CODE	CH.	NO.	#	

SO-186 1C	OBM 01	1° 40,014' N	96° 25,075' E	24.11.05	10.01.06	2260	427226 (06.03.06 13:00)	D	B050928	OBS 28	METS T31
	OBM 02	1° 45,580' N	96° 33,150' E	24.11.05	10.01.06	1693	427524 (06.03.06 10:00)	C	F050928	OBS 29	METS T30
	OBM 03	1° 50,020' N	96° 19,960' E	24.11.05	10.01.06	2771	430274 (06.03.06 08:00)	C	C050928	OBS 31	METS T28
	OBM 04	1° 53,985' N	96° 11,940' E	24.11.05	10.01.06	2373	430424 (06.03.06 03:00)	C	A000000	OBS 32	METS T29
	OBM 05	1° 54,067' N	95° 59,666' E	24.11.05	10.01.06	3451	427737	D	A050828	OBS 33	METS T27

	INST.	LAT (N)	LON (E)	DEPLOY.	RECOV.	DEPTH	REL.	ANT.	REC.	SKEW	SENSORS
		D:M	D:M	DATE	DATE	(m)	CODE	CH.	NO.	(ms)	
SO-186 1D	OBH 41	2°12,107' N	96°00,038' E	10.01.06	02.03.06	1608	D634 (A) (05.03. 22:45)	D	MLS 991235	105	DPG 75
	OBS 42	1°52,444' N	96°15,074' E	10.01.06	04.03.06	2573	430326 (06.03. 04:00)	D	MTS 050815	18	DPG 67 + Owen (4,5 Hz) + Paro 8b
	OBS 43	1°59,652' N	96°28,812' E	10.01.06	02.03.06	1303	430232 (06.03. 14:00)	D	MLS 040806	15	HTI 31 + Owen -076 (4,5Hz)
	OBS 44	0°26,520' S	96°50,420' E	11.01.06	11.01.06	3367	430424	C	MTS 050806	0	DPG 77 + Gü + Paro
	TOBS 02B	3°50,585' S	99°31,282' E	14.01.06		4469	427562 (30.01.08 00:00)	C	MTS 050806		DPG 72 + Gü 01 + Paro 98495
	TOBS 01B	0°27,356' S	96°51,733' E	15.01.06	06.03.06	3625	427226 (30.01.2008 00:00	C	MTS 050811	91	DPG 77 + Gü 04 + Paro 98609
	TOBU 01B	0°25,515' S	96°51,658' E	15.01.06	06.03.06	3649	430135 (30.01.08 00:00)	C	MTS 050508	104	DPG 61 + Gü + Paro 98469
	TOBU 01C	0°24,822' S	96°52,727' E	06.03.06		3685	430135 (30.01.08 01:00)	C	MTS 050808		DPG 61 + Gü 02 + Paro 98469
	OBS 45	1°21,918' N	95°52,974' E	16.01.06	05.03.06	4941	145240 (05.03. 17:00)	C	MTS 050816	-14	DPG 71 + Owen -073 (4,5 Hz) + Paro 98621
	OBS 46	1°49,989' N	95°42,003' E	16.01.06	02.03.06	5021	131317 (05.03. 02:00)	D	MLS 991243	82	OAS 17 + Owen (4,5 Hz)
	OBS 47	2°00,005' N	95°30,000' E	16.01.06	02.03.06	4923	427430 (06.03. 15:00)	D	MLS 010403	96	OAS 44 + Owen (4,5 Hz)
	OBS 48	2°09,828' N	95°37,874' E	16.01.06	02.03.06	2762	427737 (06.03. 06:00)	D	MTS 050813	16	HTI 42 + Owen (4,5 Hz)
	OBS 49	2°24,840' N	95°10,120' E	16.01.06	28.02.06	1460	430424 (06.03. 03:00)	C	MTS 050807	no skew	DPG 64 + Gü 03 + Paro 476
	OBS 50	2°39,950' N	95°05,050' E	16.01.06	28.02.06	811	145331	D	MLS 991236	-81	OAS 2 + Owen 72 (4,5 Hz)
	OBS 51	2°59,990' N	95°05,010' E	16.01.06	28.02.06	786	427524 (06.03. 10:00)	D	MTS 050805	-17	DPG 95 + Owen 78 (4,5 Hz) + Paro 98488
	OBH 52	3°09,760' N	95°05,070' E	16.01.06	28.02.06	472	C444 (A) (05.03. 20:00)	D	MLS 991257	low batt	HTI 46
	OBS 53	3°21,000' N	95°05,010' E	16.01.06	28.02.06	801	133770 (05.03. 03:00)	D	MLS 991246	-91	OAS + Owen (4,5 Hz)

	INST.	LAT (N)	LON (E)	DEPLOY.	RECOVERY	DEPTH	REL.	ANT.	REC.	SKEW	SENSORS
		D:M	D:M	DATE	DATE	(m)	CODE	CH.	NO.	(ms)	
SO-186 3 - 1	OBS 54	3°03,540' N	97°06,840' E	01.03.06	04.03.06	262	134037 (05.03. 09:00)	C	MLS 040304	-3	HTI 61 + Owen 3 (4,5 Hz)
	OBS 55	2°59,960' N	97°04,179' E	01.03.06	04.03.06	879	134071 (05.03. 14:00)	D	MLS 040102	-6	OAS 30 + Owen 7 (4,5 Hz)
	OBS 56	2°55,997' N	97°01,223' E	01.03.06	04.03.06	995	145331 (05.03. 16:00)	C	MLS 000708	-25	OAS 37 + Owen (4,5 Hz)
	OBH 57	2°51,987' N	96°58,363' E	01.03.06	04.03.06	1033	03B3+0355 (05.03. 19)	D	MLS 010404	12	OAS 35
	OBS 58	2°48,006' N	96°55,582' E	01.03.06	04.03.06	1080	133736 (05.03. 05:00)	D	MLS 991234	4	HTI 57 + Owen 27 (4,5 Hz)
	OBH/M 59	2°44,029' N	96°52,567' E	01.03.06	04.03.06	1113	134123 (05.03. 10:00)	D	MLS 991257 / B050928	4753	OAS 23+ Owen (4,5 Hz) + METS
	OBM 60	2°43,894' N	96°52,477' E	01.03.06	04.03.06	1115	427476 (06.03. 16:00)	D	A050928 / C050928		METS T27 + METS T29
	OBM 61	2°43,825' N	96°52,411' E	01.03.06	04.03.06	1112	430424 (06.03. 03:00)	C	F050928 / A000000		METS T28 + METS T30
	OBS 02	2°42,008' N	96°51,044' E	15.10.05	04.03.06	1123	133563 (05.03. 01:00)	C	MLS 040603	1119*	OAS 41 + Owen (4,5Hz)
	OBS 62	2°40,027' N	96°49,647' E	01.03.06	04.03.06	1138	427524 (06.03. 10:00)	D	MLS 010406	1	OAS 55 + Owen (4,5 Hz)
	OBS 63	2°36,031' N	96°46,730' E	01.03.06	04.03.06	1148	133770 (05.03. 03:00)	D	MLS 020601	9	OAS 03 + Owen (4,5 Hz)
	OBS 64	2°31,993' N	96°43,834' E	01.03.06	04.03.06	1071	131351 (05.03. 00:00)	C	MTS 050805	0	DPG 66 + Owen (4,5 Hz)
	OBS 65	2°28,002' N	96°40,937' E	01.03.06	04.03.06	605	131203 (05.03. 13:00)	C	MTS 050814	0	DPG 73 + Owen (4,5 Hz) + Paro
	OBS 66	2°24,008' N	96°38,020' E	01.03.06	04.03.06	332	133664 (05.03. 03:00)	D	MLS 991246	-7	OAS 56 + Owen (4,5 Hz)
	OBS 67	2°19,883' N	96°35,010' E	01.03.06	04.03.06	91	145206 (05.03. 11:00)	D	MLS 991236	-5	OAS 31 + Owen 10 (4,5 Hz)
	OBS 68	2°15,979' N	96°32,179' E	01.03.06	04.03.06	72	131415 (05.03. 12:00)	D	MTS 050812	-2	DPG 95 + Owen (4,5 Hz) + Paro
	OBS 69	2°11,921' N	96°29,254' E	01.03.06	04.03.06	1046	4A49 (B) (06.03. 01)	D	MTS 050807	12	DPG 64 + Gü 03 + Paro 476
	OBH 70	2°07,994' N	96°26,336' E	01.03.06	04.03.06	1094	C464 (A) (06.03. 00)	D	MLS 010408	-4	OAS 27
	OBS 71	2°03,978' N	96°23,503' E	02.03.06	04.03.06	1508	133622 (05.03. 08:00)	D	MLS 040602	-3	OAS 45 + Owen 06 (4.5 HZ)
	OBH 72	1°59,937' N	96°20,552' E	02.03.06	04.03.06	1921	C444 (A) (05.03. 20)	D	MLS 991259	-8	HTI 46
	INST.	LAT (N)	LON (E)	DEPLOY.	RECOVERY	DEPTH	REL.	ANT.	REC.	SKEW	SENSORS
		D:M	D:M	DATE	DATE	(m)	CODE	CH.	NO.	(ms)	
	OBS 73	1°56,006' N	96°17,676' E	02.03.06	04.03.06	2055	430232 (06.03. 14:00)	C	MLS 040806	1	HTI 31 + Owen 050906 (4,5 Hz)

SO-186 3 - 1	OBS 42	1°52,444 N	96°15,074 E	10.01.06	04.03.06	2573	430326 (06.03. 04:00)	D	MTS 050815	18	DPG 67 + Owen (4,5 Hz) + Paro 8b
	OBS 29	1°45,00' N	96° 32,99' E	24.11.05	05.03.06	1702	427260 (06.03. 07:00)	D	MTS 050818	935*	DPG 63 + Owen -072 (4,5 Hz) + Paro 22
	OBS 28	1°39,97' N	96°24,99' E	24.11.05	05.03.06	2379	430173 (06.03. 09:00)	D	MTS 050817	1085*	DPG 62 + Owen (4,5 Hz) + Paro 612
	OBS 74	1°48,003' N	96°11,840' E	02.03.06	04.03.06	2752	131245 (07.03. 00:00)	D	MLS 991258	12	OAS 17 + Owen (4,5 Hz)
	OBS 75	1°44,047' N	96°8,951' E	02.03.06	05.03.06	3965	250177 (07.03. 01:00)	D	MLS 991233	4	OAS 44 + Owen (4,5 Hz)
	OBS 27	1°40,000' N	96°05,00'1E	24.11.05	05.03.06	4793	427623 (06.03. 11:00)	C	MTS 050809	1172*	DPG 68 + Owen -075 (4,5 Hz) + Paro 616
	OBS 76	1°36,014' N	96°3,160' E	02.03.06	05.03.06	5040	427737	D	MLS 010403	5	OAS 42 + Owen (4,5 Hz)
	OBS 77	1°31,970' N	96°0,221' E	02.03.06	05.03.06	5103	427430	C	MBS 001002	-12	OAS + Owen (4,5 Hz)
	OBS 26	1°30,01 N	95°59,99' E	24.11.05	05.03.06	5121	430067 (06.03. 02:00)	C	MTS 050810	1474*	DPG 65 + Owen -071 (4,5 Hz) + Paro 98489
	OBS 78	1°28,000' N	95°57,388' E	02.03.06	05.03.06	5100	131317 (07.03. 04:00)	C	MLS 991243	4	OAS + Owen (4,5 Hz)
	OBH 79	1°23,992' N	95°54,432' E	02.03.06	05.03.06	5009	D634 (A) (07.03. 05:00)	D	MLS 040803	0	OAS 25
	OBS 45	1°21,918 N	95°52,974 E	16.01.06	05.03.06	4941	145240 (05.03. 17:00)	C	MTS 050816	-14	DPG 71 + Owen -073 (4,5 Hz) + Paro 98621
	OBH 80	1°19,988' N	95°51,514' E	02.03.06	05.03.06	4906	A324 (A) (07.03. 06:00)	D	MBS 020508	14	OAS 07
SO-186 3 - 2	OBS 81	2°7,062' N	95°56,248' E	06.03.06	08.03.06	2183	134123 (08.03 04:00)	D	MTS 050810	7	DPG 71 + Owen 7 (4,5 Hz) + Paro 489
	OBS 82	2°7,148' N	95°56,237' E	06.03.06	08.03.06	2181	427737 (08.03 04:00)	C	MLS 040803	-23	OAS 30 + Owen KS 0510-079 (4,5 Hz)
	OBS 83	2°7,235' N	95°56,131' E	06.03.06	08.03.06	2176	134037 (08.03 04:00)	C	MLS 991246	-30	HTI 35 + Owen KS 0509-073 (4,5 Hz)
	OBS 84	2°7,290' N	95°56,037' E	06.03.06	08.03.06	2180	250177 (08.03 04:00)	D	MLS 991233	-391	OAS 07 + Owen 60 (4,5 Hz)
	OBS 85	2°7,358' N	95°55,920' E	06.03.06	08.03.06	2181	427524 (08.03 04:00)	C	MBS 001002	-7	OAS 31 + Owen 41 (4,5 Hz)
	OBS 86	2°7,412' N	95°55,908' E	06.03.06	08.03.06	2181	145331 (08.03 04:00)	D	MLS 040304	-34	OAS 25 + Owen 8 (4,5 Hz)
	OBS 87	2°7,469' N	95°55,853' E	06.03.06	08.03.06	2181	133736 (08.03 04:00)	D	MLS 020601	-19	OAS 29 + Owen KS 0509-071 (4,5 Hz)
	OBS 88	2°7,518' N	95°55,802' E	06.03.06	08.03.06	2184	430424 (08.03 04:00)	C	MLS 010406	-4	HTI 57 + Owen KS 0202-022 (4,5 Hz)
	OBS 89	2°7,587' N	95°55,722' E	06.03.06	08.03.06	2182	427226 (08.03 04:00)	D	MLS 040102	-6	HTI 52 + Owen 24 (4,5 Hz)
	OBS 90	2°7,671' N	95°55,644' E	06.03.06	08.03.06	2186	427623 (08.03 04:00)	C/D	MLS 991234	-21	HTI 55 + Owen 59
	OBS 91	2°7,741' N	95°55,570' E	06.03.06	08.03.06	2183	430173 (08.03 04:00)	C/D	MTS 050805	-1	DPG 67 + Owen 23 (4,5 Hz) + Paro (x78277)
	OBS 92	2°7,805' N	95°55,505' E	06.03.06	08.03.06	2183	133664 (08.03 04:00)	D	MLS 991236	-7	HTI 31 + Owen 3 (4,5 Hz)
	OBS 93	2°7,874' N	95°55,448' E	06.03.06	08.03.06	2183	131317 (08.03 04:00)	C	MLS 010404	0	HTI 51 + Owen KS 0509-075 (4,5 Hz)
	OBS 94	2°7,966' N	95°55,345' E	06.03.06	08.03.06	2184	430326 (08.03 04:00)	D	MLS 000708	kein end,kein skew	OAS 41 + Owen KS 0509-076 (4,5 Hz)
	OBS 95	2°8,041' N	95°55,274' E	06.03.06	08.03.06	2186	427260 (08.03 04:00)	C	MLS 040806	-42	OAS 45 + Owen 29 (4,5 Hz)
	OBS 96	2°8,089' N	95°55,183' E	06.03.06	08.03.06	2184	430067 (08.03 04:00)	D	MLS 010408	-4	HTI 42 + Owen 10 (4,5 Hz)
	OBS 97	2°8,212' N	95°55,096' E	06.03.06	08.03.06	2185	131245 (08.03 04:00)	D	MBS 020501	11	OAS 22 + Owen 27 (4,5 Hz)
	OBS 98	2°8,231' N	95°55,080' E	06.03.06	08.03.06	2184	427430 (08.03 04:00)	D	MBS 001005	6	OAS 11 + Owen 9 (4,5 Hz)
	OBS 99	2°8,288' N	95°55,022' E	06.03.06	08.03.06	2185	145240 (08.03 04:00)	D	MLS 040603	-1	DPG 64 + Owen 5 (4.5 Hz)
	OBS/M 100	2°8,360' N	95°54,953' E	06.03.06	11.03.06	2186	145206 (08.03 04:00)	D	MLS 991257/ B050928	-12	HTI 25 + Owen (4,5 Hz) + METS T 27
	OBM 101	2°8,454' N	95°54,858' E	06.03.06	11.03.06	2184	133770 (08.03 04:00)	D	A000000 / F050928		METS T 29 (A) + METS T 30 (F)
	OBM 102	2°8,495' N	95°54,817' E	06.03.06	11.03.06	2184	131351 (08.03 04:00)	D	A050928 / C050928		METS T 28 (A) + METS T 31 (C)
	OBH 103	2°8,641' N	95°54,694' E	06.03.06	08.03.06	1683	C444 (A) (08.03 04:00)	D	MBS 020508	7	OAS 3
SO-186 3 - 3	OBH 104	3°50,134' N	93°54,969' E	08.03.06	11.03.06	1465	C444 (A) (11.03. 22:10)	D	MBS 020508	16	OAS 3
	OBM 106	3°50,217' N	93°54,902' E	08.03.06	11.03.06	2462	133770 (11.03. 22:00)	D	A000000 / F050928		METS T 29 (A) + METS T 30 (F)
	OBM 107	3°50,330' N	93°54,803' E	08.03.06	11.03.06	2462	131351 (11.03. 22:00)	D	A050928 / C050928		METS T 28 (A) + METS T 31 (C)
	OBS/M 108	3°50,427' N	93°54,770' E	08.03.06	11.03.06	2467	145206 (11.03. 22:00)	D	MLS 991257	-12	HTI 25 + Owen (4,5 Hz) + METS T 27
	OBS 109	3°50,516' N	93°54,719' E	08.03.06	10.03.06	2469	145240 (11.03. 22:00)	D	MBS 020505	3	OAS 37 + Owen 5 (4,5 Hz)
	OBS 110	3°50,609' N	93°54,668' E	08.03.06	10.03.06	2464	427260 (11.03. 22:00)	D	MBS 001005	12	OAS 11 + Owen 9 (4,5 Hz)
	OBS 111	3°50,708' N	93°54,618' E	08.03.06	10.03.06	2469	430067 (11.03. 22:00)	C	MBS 980908	3	OAS 45 + Owen 29 (4,5 Hz)
	OBS 112	3°50,815' N	93°54,569' E	08.03.06	10.03.06	2469	133664 (11.03. 22:00)	D	MBS 980906	8	OAS 41 + Owen (4,5 Hz)
	OBS 113	3°50,922' N	93°54,538' E	08.03.06	10.03.06	2467	131245 (11.03. 22:00)	D	MBS 020501	11	OAS 22 + Owen 27 (4,5 Hz)
	OBS 114	3°51,022' N	93°54,511' E	08.03.06	11.03.06	2466	430326 (11.03. 22:00)	D	MBS 990712	-8	HTI 42 + Owen 20 (4,5 Hz)
	INST.	LAT (N)	LON (E)	DEPLOY.	RECOVERY	DEPTH	REL.	ANT.	REC.	SKEW	SENSORS
		D:M	D:M	DATE	DATE	(m)	CODE	CH.	NO.	(ms)	
	OBS 115	3°51,116' N	93°54,468' E	08.03.06	11.03.06	2473	430173 (12.03. 01:00)	C	MBS 010703	-13	HTI 51 + Owen KS 0509-075 (4,5 Hz)
	OBS 116	3°51,206' N	93°54,415' E	08.03.06	11.03.06	2470	131317 (11.03. 22:00)	D	MBS 991292	-16	HTI 61 + Owen (4,5 Hz)
	OBS 117	3°51,303' N	93°54,359' E	08.03.06	11.03.06	2475	250177 (12.03. 01:00)	C	MLS 040803	-23	OAS 30 + Owen KS 0510-079 (4,5 Hz)

SO-186 3 - 3	**OBS 118**	3°51,402' N	93°54,320' E	08.03.06	11.03.06	2471	427737 (12.03. 01:00)	D	MLS 991233	-391	OAS 07 + Owen 60 (4,5 Hz)
	OBS 119	3°51,503' N	93°54,285' E	08.03.06	11.03.06	2470	131203 (12.03. 01:00)	D	MLS 040304	-34	OAS 25 + Owen 8 (4,5 Hz)
	OBS 120	3°51,596' N	93°54,235' E	08.03.06	11.03.06	2467	145331 (12.03. 01:00)	D	MLS 020601	-19	OAS 29 + Owen KS 0509-071 (4,5 Hz)
	OBS 121	3°51,702' N	93°54,193' E	08.03.06	11.03.06	2472	427226 (12.03. 01:00)	C	MBS 001002	-15	OAS 31 + Owen 41 (4,5 Hz)
	OBS 122B	3°51,809' N	93°54,130' E	08.03.06	10.03.06	2465	427524 (12.03. 01:00)	D	MBS 020509	8	HTI 31 + Owen 3 (4,5 Hz)
	OBS 122	3°51,914' N	93°54,068' E	08.03.06	10.03.06	2464	427623 (12.03. 01:00)	C	MBS 001003	11	HTI 55 + Owen (4,5 Hz)
	OBS 123	3°52,020' N	93°54,045' E	08.03.06	10.03.06	2465	133736 (12.03. 01:00)	D	MBS 990901	-6	HTI 52 + Owen 24 (4,5 Hz)
	OBS 124	3°52,123' N	93°54,023' E	08.03.06	10.03.06	2466	430424 (12.03. 01:00)	C	MLS 010406	-4	HTI 57 + Owen KS 0202-022 (4,5 Hz)
	OBS 125	3°52,217' N	93°53,984' E	08.03.06	10.03.06	2465	134037 (12.03. 01:00)	C	MLS 991246	-30	HTI 35 + Owen KS 0509-073
	OBS 126	3°52,310' N	93°53,943' E	08.03.06	10.03.06	2462	134123 (12.03. 01:00)	D	MBS 020507	48	OAS 17 + Owen 7 (4,5 Hz)
SO-186 3 - 4	**OBS 127**	3°51,397' N	93°55,313' E	10.03.06	11.03.06	2476	427623 (12.03. 01:00)	C	MBS 001003	11	OAS 55 + Owen (4,5 Hz)
	OBS 128	3°51,360' N	93°55,215' E	10.03.06	11.03.06	2478	145240 (11.03. 22:00)	D	MBS 020505	3	OAS 37 + Owen 5 (dünn) (4,5 Hz)
	OBS 129	3°51,330' N	93°55,144' E	10.03.06	11.03.06	2475	427524 (12.03. 01:00)	D	MBS 020509	8	HTI 31+ Owen 3 (4,5 Hz)
	OBS 130	3°51,260' N	93°55,024' E	10.03.06	11.03.06	2468	427260 (11.03. 22:00)	D	MBS 001005	12	OAS 11 + Owen 5 (dick) (4,5 Hz)
	OBS 131	3°51,233' N	93°54,943' E	10.03.06	11.03.06	2470	430067 (11.03. 22:00)	C	MBS 980908	3	OAS 45 + Owen 29 (4,5 Hz)
	OBS 132	3°51,197' N	93°54,847' E	10.03.06	11.03.06	2471	133664 (11.03. 22:00)	D	MBS 980906	8	OAS 41 + Owen (4,5 Hz)
	OBS 133	3°51,157' N	93°54,761' E	10.03.06	11.03.06	2468	131245 (11.03. 22:00)	D	MBS 020501	11	OAS 22 + Owen 27 (4,5 Hz)
	OBS 134	3°51,115' N	93°54,667' E	10.03.06	11.03.06	2469	133736 (12.03. 01:00)	D	MBS 990901	-6	HTI 52 + Owen 24 (4,5 Hz)
	OBS 135	3°51,080' N	93°54,570' E	10.03.06	11.03.06	2469	134037 (12.03. 01:00)	C	MLS 991246	-30	HTI 35 + Owen KS 0509-073
	OBS 136	3°51,004' N	93°54,388' E	10.03.06	11.03.06	2473	430424 (12.03. 01:00)	C	MLS 010406	-4	HTI 57 + Owen KS 0202-022 (4,5 Hz)
	OBS 137	3°50,960' N	93°54,294' E	10.03.06	11.03.06	2470	134123 (12.03. 01:00)	D	MBS 020507	48	OAS 17 + Owen 7 (4,5 Hz)

* Schaltsekunde

Refraction Seismic Lines

Line	First SP Lon, Lat	Last SP Lon, Lat	shot interval [s]	date and time [UTC]
SO186-3-01	1 1.28662N, 95.82539 E	1949 3.06217 N, 97.11574 E	60	02.03.2006 23:02 – 04.03.2006 07:30
SO186-3-02	1 1.99306N, 96.06301 E	335 2.24915 N, 95.80646 E	60	07.03.2006 02:07 – 07.03.2006 09:24
SO186-3-02a	1 2.2493N, 95.8022 E	535 1.96616 N, 96.08477 E	40	07.03.2006 07:36 – 07.03.2006 13:32
SO186-3-02b	1 1.96802N, 96.08970 E	350 2.2538 N, 95.80632 E	60 (bb array only)	07.03.2006 13:40 – 07.03.2006 19:29
SO186-3-02c	1 2.25537N, 95.81104 E	296 2.09845 N, 95.96652 E	40 (bb array only)	07.03.2006 19:43 – 07.03.2006 22:59:40
SO186-3-03	1 3.91152 N, 93.87719 E	175 3.99862 N, 93.83813 E	30	08.03.2006 18:50 – 08.03.2006 20:17
SO186-3-03a	1 3.99943 N, 93.84298 E	630 3.66897 N, 93.98991 E	30	08.03.2006 20:24 – 09.03.2006 01:38:30
SO186-3-03b	1 3.66897 N, 93.99660 E	633 3.99779 N, 93.84873 E	30	09.03.2006 01:50 – 09.03.2006 07:06
SO186-3-03c	1 4.00113 N, 93.83501 E	631 3.66899 N, 93.98273 E	30	09.03.2006 07:25 – 09.3.2006 12:40
SO186-3-03d	1 3.66862 N, 93.99371 E	643 4.00342 N, 93.84401 E	30	09.03.2006 12:54 – 09.03.2006 18:15
SO186-3-03e	1 4.00165 N, 93.85189 E	349 3.82752 N, 93.92851 E	30	09.03.2006 18:33 – 09.03.2006 21:22
SO186-3-03f	1 3.82073 N, 93.91760 E	159 3.90658 N, 93.87978 E	30	09.03.2006 21:41 – 09.03.2006 23:00
SO186-3-04	1 3.85211 N, 93.89638 E	289 3.78793 N, 97.75041 E	30	10.03.2006 03:54 – 10.03.2006 06:18
SO186-3-04a	1 3.78073 N, 93.75053 E	643 3.92999 N, 94.08810 E	30	10.03.2006 06:27 – 10.03.2006 11:48
SO186-3-04b	1 3.94119 N, 94.09016 E	653 3.79114 N, 93.75116 E	30	10.03.2006 12:00 – 10.03.2006 17:26

9.2 Appendix

SO186-3-04c	1 3.77426N, 93.75039E	655 3.92366N, 94.08922E	30	10.03.2006 17:44 – 10.03.2006 23:11
SO186-3-04d	1 3.93461N, 94.09122E	677 3.78507N, 93.-75215E	30	10.03.2006 23:21 – 11.03.2006 04:59
SO186-3-04e	1 3.77722N, 93.75071E	425 3.87536N, 93.97173E	30	11.03.2006 05:09 – 11.03.2006 08:41-
SO186-3-04f	1 3.88359N, 93.97316E	139 3.85322N, 93.89917E	30	11.03.2006 08:52 – 11.03.2006 10:01

Abkürzungen / Abbreviation

z.W	zu Wasser
a.D.	an Deck
SL (max.)	(maximale)Seillänge
LT	Lottiefe nach Hydrosweep
W x	eingesetzte Winde
SM	Simrad - Multibeam - Lot
PS	Parasound
rwk:	Rechtweisender Kurs
d:	Distanz
v:	Geschwindigkeit in Knoten
SL:	Seillänge
KL:	Kabellänge

Eingesetzte Geräte

Airguns Bb	19 Profile
Airguns Stb	19 Profile
OBH / OBS	118x Aus + 84 x Ein
TEWS-Boje / TOBU	1x TOBU ein und aus
CTD mit SVP-Sonde	1
SIMRAD-Profil	1

Geräteverluste: Keine

Winde	D/M	Typ	RF-Nr	SO 186-3 Einsatz	Gesamt Einsatz	SO 186-3 S`länge	Gesamt S`länge	Zust.	SO 186-3 gefierte max. L	jemals gefierte max. Länge
W 1	18,2	LWL	812001	0 h	478 h	0 m	241232 m	3-4	0 m	8022 m
W 2	18,2	LWL	120301500	0 h	0 h	0 m	0 m	1	0 m	0 m
W 4	11	NSW	818045	1,5 h	310 h	2000 m	270589 m	3-4	2000 m	8081 m
W 5	11	NSW	818237	0 h	106 h	0 m	100537 m	3	0 m	5861 m
W 6	18,2	Koax	815286	0 h	356 h	0 m	439920 m	2	0 m	6000 m

Station	Datum	UTC	PositionLat	PositionLon	Tiefe [m]	Windstärke [m/s]	Kurs [°]	v [kn]	Gerät	Gerätekürzel	Aktion	Bemerkung
SO186/126-1	28.02.06	00:26	3° 23,49' N	95° 6,09' E	737	SSE 10	204	11,5	OBS/OBH	OBS/OBH	Beginn Station	
SO186/126-1	28.02.06	00:26	3° 23,49' N	95° 6,09' E	737	SSE 10	204	11,5	OBS/OBH	OBS/OBH	OBS ausgelöst	OBS 53
SO186/126-1	28.02.06	00:41	3° 21,58' N	95° 4,66' E	797	ESE 7	209	4,8	OBS/OBH	OBS/OBH	OBS gesichtet	OBS 53
SO186/126-1	28.02.06	00:56	3° 21,12' N	95° 4,94' E	800	SE 5	94	0,3	OBS/OBH	OBS/OBH	OBS an Deck	OBS 53
SO186/126-1	28.02.06	01:54	3° 10,90' N	95° 4,88' E	515	SSE 10	177	10,9	OBS/OBH	OBS/OBH	OBH ausgelöst	OBH 52
SO186/126-1	28.02.06	02:00	3° 10,30' N	95° 4,92' E	477	SSE 6	169	3	OBS/OBH	OBS/OBH	OBH gesichtet	OBS 52
SO186/126-1	28.02.06	02:14	3° 9,82' N	95° 5,18' E	484	E 6	173	3,6	OBS/OBH	OBS/OBH	OBH an Deck	OBS 52
SO186/126-1	28.02.06	02:58	3° 1,46' N	95° 4,92' E	573	SE 10	181	10,8	OBS/OBH	OBS/OBH	OBS ausgelöst	OBS 51
SO186/126-1	28.02.06	03:11	3° 0,38' N	95° 4,93' E	676	SE 6	172	3,3	OBS/OBH	OBS/OBH	OBS gesichtet	OBS 51
SO186/126-1	28.02.06	03:31	3° 0,19' N	95° 4,89' E	754	SE 5	292	0,4	OBS/OBH	OBS/OBH	OBS an Deck	OBS 51
SO186/126-1	28.02.06	04:38	2° 49,92' N	94° 57,40' E	1203	SE 7	216	12,1	OBS/OBH	OBS/OBH	OBH ausgelöst	OBS 40
SO186/126-1	28.02.06	04:48	2° 48,42' N	94° 56,23' E	926	SE 6	223	7,8	OBS/OBH	OBS/OBH	OBH gesichtet	OBH 40
SO186/126-1	28.02.06	04:57	2° 48,01' N	94° 56,05' E	852	ESE 4	97	1	OBS/OBH	OBS/OBH	OBH an Deck	OBH 40
SO186/126-1	28.02.06	05:48	2° 41,27' N	95° 3,56' E	720	SSE 9	126	12	OBS/OBH	OBS/OBH	OBS ausgelöst	OBS 50
SO186/126-1	28.02.06	05:55	2° 40,43' N	95° 4,59' E	799	SE 8	126	8	OBS/OBH	OBS/OBH	OBS gesichtet	OBS 50
SO186/126-1	28.02.06	06:21	2° 39,92' N	95° 5,09' E	841	SE 4	115	1	OBS/OBH	OBS/OBH	OBS an Deck	OBS 50
SO186/126-1	28.02.06	07:23	2° 28,44' N	95° 8,84' E	1522	SE 9	159	12,2	OBS/OBH	OBS/OBH	OBS ausgelöst	OBS 49
SO186/126-1	28.02.06	07:48	2° 25,36' N	95° 9,80' E	1482	SE 4	188	0,9	OBS/OBH	OBS/OBH	OBS gesichtet	OBS 49
SO186/126-1	28.02.06	08:11	2° 24,71' N	95° 9,84' E	1649,6	ESE 2	272	1,2	OBS/OBH	OBS/OBH	OBS an Deck	OBS 49
SO186/126-1	28.02.06	09:15	2° 14,41' N	95° 16,53' E	4351,3	E 8	148	12,6	OBS/OBH	OBS/OBH	OBS ausgelöst	OBS 37
SO186/126-1	28.02.06	10:22	2° 12,02' N	95° 17,80' E	4690,2	ESE 3	108	1,5	OBS/OBH	OBS/OBH	OBS gesichtet	OBS 37
SO186/126-1	28.02.06	10:35	2° 12,01' N	95° 17,89' E	4697,3	ESE 4	106	1,8	OBS/OBH	OBS/OBH	OBS an Deck	OBS 37
SO186/126-1	28.02.06	12:00	2° 27,48' N	95° 19,73' E	1664,7	SE 6	7	12,4	OBS/OBH	OBS/OBH	OBS ausgelöst	OBS 38

Station	Datum	UTC	PositionLat	PositionLon	Tiefe [m]	Windstärke [m/s]	Kurs [°]	v [kn]	Gerät	Gerätekürzel	Aktion	Bemerkung
SO186/126-1	28.02.06	12:23	2° 30,28' N	95° 19,47' E	1482,2	SE 3	143	1	OBS/OBH	OBS/OBH	OBS gesichtet	OBS 38
SO186/126-1	28.02.06	12:36	2° 30,21' N	95° 19,92' E	1381,7	SSE 3	16	0,7	OBS/OBH	OBS/OBH	OBS an Deck	OBS 38
SO186/126-1	28.02.06	13:28	2° 35,12' N	95° 28,37' E	971,5	SE 8	58	12,2	OBS/OBH	OBS/OBH	OBS ausgelöst	OBS 22
SO186/126-1	28.02.06	13:49	2° 36,27' N	95° 29,72' E	1075,3	SSE 3	57	1,1	OBS/OBH	OBS/OBH	OBS gesichtet	OBS 22
SO186/126-1	28.02.06	13:57	2° 36,12' N	95° 30,00' E	1065,5	ESE 5	42	1	OBS/OBH	OBS/OBH	OBS an Deck	OBS 22
SO186/126-1	28.02.06	17:04	3° 11,07' N	95° 41,63' E	90,2	E 8	19	9,4	OBS/OBH	OBS/OBH	OBS ausgelöst	OBS 12
SO186/126-1	28.02.06	17:10	3° 11,68' N	95° 41,82' E	104,7	E 4	16	4,5	OBS/OBH	OBS/OBH	OBS gesichtet	OBS 12
SO186/126-1	28.02.06	17:19	3° 12,12' N	95° 41,78' E	103,8	E 3	339	2,6	OBS/OBH	OBS/OBH	OBS an Deck	OBS 12
SO186/126-1	28.02.06	20:03	3° 28,55' N	96° 9,58' E	946,9	NE 9	55	11,6	OBS/OBH	OBS/OBH	OBS ausgelöst	OBS 14
SO186/126-1	28.02.06	20:26	3° 29,92' N	96° 11,85' E	867,3	NE 4	303	1	OBS/OBH	OBS/OBH	OBS gesichtet	OBS 14
SO186/126-1	28.02.06	20:37	3° 30,04' N	96° 11,87' E	864	NE 4	8	0,1	OBS/OBH	OBS/OBH	OBS an Deck	OBS 14, Sender d.u.
SO186/126-1	28.02.06	22:45	3° 7,33' N	96° 1,80' E	935	ESE 7	205	12,9	OBS/OBH	OBS/OBH	OBS ausgelöst	OBS 23
SO186/126-1	01.03.06	00:34	3° 5,54' N	95° 59,41' E	605	ESE 2	247	1,1	OBS/OBH	OBS/OBH	OBS gesichtet	OBS 23
SO186/126-1	01.03.06	00:37	3° 5,53' N	95° 59,36' E	610	ESE 3	271	0,9	OBS/OBH	OBS/OBH	OBH an Deck	OBH 23
SO186/126-1	01.03.06	02:03	2° 55,69' N	96° 10,33' E	835	S 8	134	12,6	OBS/OBH	OBS/OBH	OBS ausgelöst	OBS 17
SO186/126-1	01.03.06	02:16	2° 54,42' N	96° 11,95' E	804	S 5	186	3,8	OBS/OBH	OBS/OBH	OBS gesichtet	OBS 17
SO186/126-1	01.03.06	02:27	2° 53,89' N	96° 11,98' E	765	SSE 3	168	1	OBS/OBH	OBS/OBH	OBS an Deck	OBS 17
SO186/126-1	01.03.06	03:48	2° 48,86' N	96° 27,33' E	948	SSE 9	105	12,7	OBS/OBH	OBS/OBH	OBS ausgelöst	OBS 18
SO186/126-1	01.03.06	04:06	2° 48,32' N	96° 29,85' E	1051	SE 4	160	2,3	OBS/OBH	OBS/OBH	OBS gesichtet	OBS 18
SO186/126-1	01.03.06	04:14	2° 47,99' N	96° 29,99' E	1056	S 3	161	1	OBS/OBH	OBS/OBH	OBS an Deck	OBS 18
SO186/126-1	01.03.06	05:13	2° 53,01' N	96° 40,04' E	1112	SE 7	63	12,3	OBS/OBH	OBS/OBH	OBH ausgelöst	OBH 19
SO186/126-1	01.03.06	05:31	2° 54,02' N	96° 41,93' E	1113	SSE 1	49	2,1	OBS/OBH	OBS/OBH	OBH gesichtet	OBH 19
SO186/126-1	01.03.06	05:40	2° 54,15' N	96° 41,96' E	1114	S 1	14	1,2	OBS/OBH	OBS/OBH	OBH an Deck	OBH 19
SO186/126-1	01.03.06	06:34	2° 58,78' N	96° 32,42' E	1093	SSE 6	295	13,1	OBS/OBH	OBS/OBH	OBS ausgelöst	OBS 16
SO186/126-1	01.03.06	06:58	2° 59,94' N	96° 30,05' E	1088	SW 2	275	0,3	OBS/OBH	OBS/OBH	OBS gesichtet	OBS 16
SO186/126-1	01.03.06	07:05	3° 0,13' N	96° 29,87' E	1088	SW 2	319	1,3	OBS/OBH	OBS/OBH	OBS an Deck	OBS 16
SO186/126-1	01.03.06	08:17	3° 14,44' N	96° 30,01' E	1042	SW 4	1	12	OBS/OBH	OBS/OBH	OBS ausgelöst	OBS 15
SO186/126-1	01.03.06	08:43	3° 17,68' N	96° 30,00' E	1017	SSW 2	7	0,3	OBS/OBH	OBS/OBH	OBS gesichtet	OBS 15
SO186/126-1	01.03.06	08:55	3° 18,05' N	96° 29,83' E	1018	WSW 2	322	0,5	OBS/OBH	OBS/OBH	OBS an Deck	OBS 15
SO186/126-1	01.03.06	10:21	3° 18,27' N	96° 46,40' E	1002	SSW 6	88	12,1	OBS/OBH	OBS/OBH	OBS ausgelöst	OBS 20
SO186/126-1	01.03.06	10:39	3° 18,16' N	96° 48,01' E	992	SSW 2	132	0,2	OBS/OBH	OBS/OBH	OBS gesichtet	OBS 20
SO186/126-1	01.03.06	10:49	3° 17,96' N	96° 47,95' E	999	WSW 2	221	1	OBS/OBH	OBS/OBH	OBS an Deck	OBS 20
SO186/126-1	01.03.06	12:54	3° 3,57' N	97° 6,83' E	257	NE 2	144	3	OBS/OBH	OBS/OBH	OBS zu Wasser	OBS 54
SO186/126-1	01.03.06	13:25	2° 59,96' N	97° 4,17' E	881	ENE 2	123	2,5	OBS/OBH	OBS/OBH	OBS zu Wasser	OBS 55
SO186/126-1	01.03.06	13:55	2° 56,03' N	97° 1,27' E	999	NE 2	239	3,9	OBS/OBH	OBS/OBH	OBS zu Wasser	OBS 56
SO186/126-1	01.03.06	14:28	2° 52,01' N	96° 58,38' E	1031	SSW 3	216	2,4	OBS/OBH	OBS/OBH	OBS zu Wasser	OBH 57
SO186/126-1	01.03.06	15:38	2° 49,04' N	97° 11,16' E	872	SW 6	83	11,5	OBS/OBH	OBS/OBH	OBS ausgelöst	OBS 01
SO186/126-1	01.03.06	15:48	2° 48,95' N	97° 11,97' E	782	WSW 1	169	2,1	OBS/OBH	OBS/OBH	OBS gesichtet	OBS 01
SO186/126-1	01.03.06	16:18	2° 47,70' N	97° 12,23' E	836	ESE 2	163	1,2	OBS/OBH	OBS/OBH	OBS an Deck	OBS 01
SO186/126-1	01.03.06	17:50	2° 48,01' N	96° 55,58' E	1081	S 4	286	0,7	OBS/OBH	OBS/OBH	OBS zu Wasser	OBS 58
SO186/126-1	01.03.06	18:23	2° 44,01' N	96° 52,56' E	1114	S 4	219	1,3	OBS/OBH	OBS/OBH	OBS zu Wasser	OBS 59

Station	Datum	UTC	PositionLat	PositionLon	Tiefe [m]	Windstärke [m/s]	Kurs [°]	v [kn]	Gerät	Gerätekürzel	Aktion	Bemerkung
SO186/126-1	01.03.06	18:28	2° 43,92' N	96° 52,49' E	1112	S 3	191	0,8	OBS/OBH	OBS/OBH	OBS zu Wasser	OBS 60
SO186/126-1	01.03.06	18:33	2° 43,83' N	96° 52,41' E	1115	SSE 3	215	1,2	OBS/OBH	OBS/OBH	OBS zu Wasser	OBS 61
SO186/126-1	01.03.06	19:03	2° 40,04' N	96° 49,66' E	1138	SSW 4	216	2,3	OBS/OBH	OBS/OBH	OBS zu Wasser	OBS 62
SO186/126-1	01.03.06	19:36	2° 36,03' N	96° 46,73' E	1150	SSW 4	211	2,1	OBS/OBH	OBS/OBH	OBS zu Wasser	OBS 63
SO186/126-1	01.03.06	20:08	2° 31,98' N	96° 43,83' E	1065	S 4	220	2,6	OBS/OBH	OBS/OBH	OBS zu Wasser	OBS 64
SO186/126-1	01.03.06	20:39	2° 28,01' N	96° 40,95' E	607	SSW 4	215	2,9	OBS/OBH	OBS/OBH	OBS zu Wasser	OBS 65
SO186/126-1	01.03.06	21:09	2° 24,00' N	96° 38,02' E	333	SSW 4	216	2,5	OBS/OBH	OBS/OBH	OBS zu Wasser	OBS 66
SO186/126-1	01.03.06	21:40	2° 20,02' N	96° 35,11' E	89	SSW 3	214	2,6	OBS/OBH	OBS/OBH	OBS zu Wasser	OBS 67
SO186/126-1	01.03.06	22:09	2° 16,02' N	96° 32,22' E	64	SW 4	212	2,4	OBS/OBH	OBS/OBH	OBS zu Wasser	OBS 68
SO186/126-1	01.03.06	22:42	2° 11,93' N	96° 29,26' E	1046	WSW 2	203	1,5	OBS/OBH	OBS/OBH	OBS zu Wasser	OBS 69
SO186/126-1	01.03.06	23:27	2° 8,00' N	96° 26,37' E	1093	SW 2	225	2,1	OBS/OBH	OBS/OBH	OBS zu Wasser	OBS 70
SO186/126-1	02.03.06	00:01	2° 1,94' N	96° 28,11' E	1218	SSE 8	166	12,7	OBS/OBH	OBS/OBH	OBS ausgelöst	OBS 43
SO186/126-1	02.03.06	00:22	1° 59,86' N	96° 28,56' E	1304	E 2	187	1,5	OBS/OBH	OBS/OBH	OBS gesichtet	OBS 43
SO186/126-1	02.03.06	00:33	1° 59,48' N	96° 28,80' E	1305	SE 3	156	1,4	OBS/OBH	OBS/OBH	OBS an Deck	OBS 43
SO186/126-1	02.03.06	01:19	2° 3,99' N	96° 23,50' E	1507	ESE 1	324	2,3	OBS/OBH	OBS/OBH	OBS zu Wasser	OBS 71
SO186/126-1	02.03.06	01:50	1° 59,97' N	96° 20,57' E	1917	ESE 4	201	3,6	OBS/OBH	OBS/OBH	OBH zu Wasser	OBH 72
SO186/126-1	02.03.06	02:22	1° 56,02' N	96° 17,69' E	2059	ESE 4	221	3,4	OBS/OBH	OBS/OBH	OBS zu Wasser	OBS 73
SO186/126-1	02.03.06	03:40	2° 10,68' N	96° 17,98' E	1112	SE 5	3	12,1	OBS/OBH	OBS/OBH	OBS ausgelöst	
SO186/126-1	02.03.06	04:06	2° 12,82' N	96° 17,89' E	978	SSE 4	112	2,1	OBS/OBH	OBS/OBH	OBS gesichtet	OBS 24
SO186/126-1	02.03.06	04:28	2° 12,21' N	96° 17,90' E	1016	SE 2	345	1,1	OBS/OBH	OBS/OBH	OBS an Deck	OBS 24
SO186/126-1	02.03.06	05:45	2° 12,23' N	96° 3,25' E	949	SE 5	269	12,9	OBS/OBH	OBS/OBH	OBH ausgelöst	OBH 41
SO186/126-1	02.03.06	06:14	2° 12,15' N	96° 0,07' E	1596	SSE 3	275	1,3	OBS/OBH	OBS/OBH	OBH gesichtet	OBH 41
SO186/126-1	02.03.06	06:22	2° 12,16' N	96° 0,01' E	1607	S 4	273	1,3	OBS/OBH	OBS/OBH	OBH an Deck	OBH 41
SO186/126-1	02.03.06	07:59	2° 22,72' N	95° 44,01' E	742	SSW 6	303	11,8	OBS/OBH	OBS/OBH	OBS ausgelöst	OBS 21
SO186/126-1	02.03.06	08:10	2° 23,87' N	95° 42,50' E	746	S 3	302	4,8	OBS/OBH	OBS/OBH	OBS gesichtet	OBS 21
SO186/126-1	02.03.06	08:22	2° 24,04' N	95° 42,10' E	752	S 4	137	0,6	OBS/OBH	OBS/OBH	OBS an Deck	OBS 21
SO186/126-1	02.03.06	09:22	2° 13,62' N	95° 38,96' E	1616	SW 9	195	11,9	OBS/OBH	OBS/OBH	OBS ausgelöst	OBS 48
SO186/126-1	02.03.06	09:58	2° 9,99' N	95° 37,93' E	2760	SSW 3	58	0,2	OBS/OBH	OBS/OBH	OBS gesichtet	OBS 48
SO186/126-1	02.03.06	10:21	2° 10,01' N	95° 37,76' E	2755	SSW 5	334	1	OBS/OBH	OBS/OBH	OBS an Deck	OBS 48
SO186/126-1	02.03.06	11:12	2° 3,63' N	95° 32,90' E	4850	SW 9	218	11,9	OBS/OBH	OBS/OBH	OBS ausgelöst	OBS 47
SO186/126-1	02.03.06	12:10	1° 59,94' N	95° 30,10' E	4923	SSW 4	214	0,1	OBS/OBH	OBS/OBH	OBS gesichtet	OBS 47
SO186/126-1	02.03.06	12:24	2° 0,23' N	95° 29,89' E	4924	S 4	29	1	OBS/OBH	OBS/OBH	OBS an Deck	OBS 47
SO186/126-1	02.03.06	13:29	1° 53,20' N	95° 38,18' E	4976	SW 8	132	12,2	OBS/OBH	OBS/OBH	OBS ausgelöst	OBS 46
SO186/126-1	02.03.06	14:32	1° 50,23' N	95° 42,05' E	5021	SSW 5	172	2,9	OBS/OBH	OBS/OBH	OBS gesichtet	OBS 46
SO186/126-1	02.03.06	14:56	1° 49,87' N	95° 42,20' E	5021	SSW 4	115	1,3	OBS/OBH	OBS/OBH	OBS an Deck	OBS 46
SO186/126-1	02.03.06	17:33	1° 48,01' N	96° 11,82' E	2755	SSW 2	99	2,4	OBS/OBH	OBS/OBH	OBS zu Wasser	OBS 74
SO186/126-1	02.03.06	18:09	1° 44,03' N	96° 8,95' E	3965	WSW 5	201	1,7	OBS/OBH	OBS/OBH	OBS zu Wasser	OBS 75
SO186/126-1	02.03.06	19:06	1° 36,02' N	96° 3,16' E	5041	WSW 4	215	2	OBS/OBH	OBS/OBH	OBS zu Wasser	OBS 76
SO186/126-1	02.03.06	19:39	1° 32,00' N	96° 0,26' E	5105	WSW 4	226	1,1	OBS/OBH	OBS/OBH	OBH zu Wasser	OBH 77
SO186/126-1	02.03.06	20:13	1° 28,04' N	95° 57,34' E	5100	W 4	183	2,7	OBS/OBH	OBS/OBH	OBH zu Wasser	OBH 78
SO186/126-1	02.03.06	20:49	1° 24,00' N	95° 54,44' E	5010	SW 4	203	1,3	OBS/OBH	OBS/OBH	OBH zu Wasser	OBH 79

Station	Datum	UTC	PositionLat	PositionLon	Tiefe [m]	Windstärke [m/s]	Kurs [°]	v [kn]	Gerät	Gerätekürzel	Aktion	Bemerkung
SO186/126-1	02.03.06	21:23	1° 20,02' N	95° 51,54' E	4906	WSW 4	215	2,5	OBS/OBH	OBS/OBH	OBH zu Wasser	OBH 80
SO186/126-1	02.03.06	21:23	1° 20,02' N	95° 51,54' E	4906	WSW 4	215	2,5	OBS/OBH	OBS/OBH	Ende Station	
SO186/127-1	02.03.06	22:15	1° 14,99' N	95° 47,95' E	4919	SSW 2	34	2,5	Profil	PR	Stationsbeginn	
SO186/127-1	02.03.06	22:29	1° 15,55' N	95° 48,33' E	4912	SSW 2	26	2,9	Profil	PR	Stb-Airgunarray zu Wasser	
SO186/127-1	02.03.06	22:55	1° 16,92' N	95° 49,31' E	4890	SW 1	38	3,8	Profil	PR	Bb-Airgunarray zu Wasser	Softstart
SO186/127-1	02.03.06	22:56	1° 16,97' N	95° 49,35' E	4891	SW 1	32	4,1	Profil	PR	Beginn Profil	# 01, rwK: 036°, d: 132 sm
SO186/127-1	04.03.06	07:30	3° 3,82' N	97° 6,98' E	209	NW 6	34	4,1	Profil	PR	Ende Profil	
SO186/127-1	04.03.06	07:50	3° 4,58' N	97° 7,56' E	102	WNW 4	30	2,8	Profil	PR	Bb-Airgunarray an Deck	
SO186/127-1	04.03.06	08:08	3° 5,32' N	97° 8,07' E	94	W 4	36	3,3	Profil	PR	Stb-Airgunarray an Deck	
SO186/127-1	04.03.06	08:08	3° 5,32' N	97° 8,07' E	94	W 4	36	3,3	Profil	PR	Stationsende	
SO186/128-1	04.03.06	08:11	3° 5,33' N	97° 8,21' E	94	NNE 4	161	4,7	OBS/OBH	OBS/OBH	Beginn Station	
SO186/128-1	04.03.06	08:14	3° 5,01' N	97° 8,07' E	95	NW 5	210	9,2	OBS/OBH	OBS/OBH	OBS ausgelöst	OBS 54
SO186/128-1	04.03.06	08:20	3° 4,18' N	97° 7,45' E	0	WNW 7	216	7,8	OBS/OBH	OBS/OBH	OBS gesichtet	
SO186/128-1	04.03.06	08:35	3° 3,22' N	97° 7,06' E	0	NW 3	179	1,3	OBS/OBH	OBS/OBH	OBS an Deck	OBS 54
SO186/128-1	04.03.06	08:44	3° 2,51' N	97° 6,24' E	0	NW 8	223	11,3	OBS/OBH	OBS/OBH	OBS ausgelöst	OBS 55
SO186/128-1	04.03.06	09:00	3° 0,38' N	97° 4,51' E	0	WNW 6	211	4,6	OBS/OBH	OBS/OBH	OBS gesichtet	OBS 55
SO186/128-1	04.03.06	09:19	2° 59,74' N	97° 4,49' E	0	W 4	118	1,4	OBS/OBH	OBS/OBH	OBS an Deck	OBS 55
SO186/128-1	04.03.06	09:37	2° 58,41' N	97° 3,50' E	0	WNW 10	223	12,6	OBS/OBH	OBS/OBH	OBS ausgelöst	OBS 56
SO186/128-1	04.03.06	09:54	2° 56,21' N	97° 1,53' E	0	WNW 6	217	4,2	OBS/OBH	OBS/OBH	OBS gesichtet	OBS 56
SO186/128-1	04.03.06	10:07	2° 56,01' N	97° 1,36' E	0	W 4	55	0,8	OBS/OBH	OBS/OBH	OBS an Deck	OBS 56
SO186/128-1	04.03.06	10:32	2° 53,31' N	96° 59,38' E	0	W 10	215	11,9	OBS/OBH	OBS/OBH	OBH ausgelöst	OBH 57
SO186/128-1	04.03.06	10:40	2° 52,51' N	96° 58,80' E	0	W 7	216	3,6	OBS/OBH	OBS/OBH	OBH gesichtet	OBH 57
SO186/128-1	04.03.06	10:54	2° 52,01' N	96° 58,45' E	0	W 6	59	0,7	OBS/OBH	OBS/OBH	OBH an Deck	OBH 57
SO186/128-1	04.03.06	11:15	2° 50,12' N	96° 57,09' E	0	W 10	215	12,2	OBS/OBH	OBS/OBH	OBS ausgelöst	OBS 58
SO186/128-1	04.03.06	11:36	2° 47,99' N	96° 55,63' E	0	WSW 3	76	0,1	OBS/OBH	OBS/OBH	OBS gesichtet	OBS 58
SO186/128-1	04.03.06	11:46	2° 47,93' N	96° 55,64' E	0	WSW 5	216	0,6	OBS/OBH	OBS/OBH	OBS an Deck	OBS 58
SO186/128-1	04.03.06	12:00	2° 46,35' N	96° 54,41' E	0	W 9	217	12,2	OBS/OBH	OBS/OBH	OBH ausgelöst	OBH/M 59
SO186/128-1	04.03.06	12:02	2° 46,02' N	96° 54,17' E	0	W 9	217	11,9	OBS/OBH	OBS/OBH	OBH ausgelöst	OBM 61
SO186/128-1	04.03.06	12:25	2° 44,06' N	96° 52,53' E	0	WSW 3	243	1,1	OBS/OBH	OBS/OBH	OBH gesichtet	OBM 59
SO186/128-1	04.03.06	12:28	2° 44,01' N	96° 52,50' E	0	SW 3	177	1,3	OBS/OBH	OBS/OBH	OBH gesichtet	OBM 61
SO186/128-1	04.03.06	12:35	2° 43,92' N	96° 52,56' E	0	WSW 3	132	1,5	OBS/OBH	OBS/OBH	OBH ausgelöst	OBM 60
SO186/128-1	04.03.06	12:36	2° 43,91' N	96° 52,59' E	0	SSW 3	86	1,6	OBS/OBH	OBS/OBH	OBH an Deck	OBM 59
SO186/128-1	04.03.06	12:40	2° 43,95' N	96° 52,65' E	0	WSW 3	55	1,4	OBS/OBH	OBS/OBH	OBH an Deck	OBM 61
SO186/128-1	04.03.06	12:48	2° 43,84' N	96° 52,66' E	0	W 3	226	1,3	OBS/OBH	OBS/OBH	OBH gesichtet	OBM 60
SO186/128-1	04.03.06	12:50	2° 43,82' N	96° 52,63' E	0	W 4	227	1,1	OBS/OBH	OBS/OBH	OBS ausgelöst	OBS 02
SO186/128-1	04.03.06	12:54	2° 43,79' N	96° 52,57' E	0	WNW 4	312	0,8	OBS/OBH	OBS/OBH	OBH an Deck	OBM 60
SO186/128-1	04.03.06	13:06	2° 43,04' N	96° 51,90' E	0	WNW 8	219	12	OBS/OBH	OBS/OBH	OBS gesichtet	OBS 02
SO186/128-1	04.03.06	13:14	2° 42,10' N	96° 51,15' E	0	WNW 6	219	4,6	OBS/OBH	OBS/OBH	OBS ausgelöst	OBS 62
SO186/128-1	04.03.06	13:20	2° 41,93' N	96° 51,04' E	0	NW 3	205	1	OBS/OBH	OBS/OBH	OBS an Deck	OBS 02
SO186/128-1	04.03.06	13:28	2° 41,36' N	96° 50,64' E	0	NW 7	216	11,3	OBS/OBH	OBS/OBH	OBS gesichtet	OBS 62
SO186/128-1	04.03.06	13:41	2° 39,98' N	96° 49,75' E	0	NW 4	225	1,7	OBS/OBH	OBS/OBH	OBS an Deck	OBS 62

Station	Datum	UTC	PositionLat	PositionLon	Tiefe [m]	Windstärke [m/s]	Kurs [°]	v [kn]	Gerät	Gerätekürzel	Aktion	Bemerkung
SO186/128-1	04.03.06	14:01	2° 38,11' N	96° 48,28' E	0	NW 7	213	11,9	OBS/OBH	OBS/OBH	OBS ausgelöst	OBS 63
SO186/128-1	04.03.06	14:15	2° 35,98' N	96° 47,17' E	0	W 3	180	4,7	OBS/OBH	OBS/OBH	OBS gesichtet	OBS 63
SO186/128-1	04.03.06	14:33	2° 36,04' N	96° 46,74' E	0	NW 2	254	0,5	OBS/OBH	OBS/OBH	OBS an Deck	OBS 63
SO186/128-1	04.03.06	14:49	2° 34,35' N	96° 45,55' E	0	W 8	211	12,3	OBS/OBH	OBS/OBH	OBS ausgelöst	OBS 64
SO186/128-1	04.03.06	15:10	2° 31,91' N	96° 43,94' E	0	WSW 3	303	1,8	OBS/OBH	OBS/OBH	OBS gesichtet	OBS 64
SO186/128-1	04.03.06	15:18	2° 31,98' N	96° 43,80' E	0	WSW 2	273	0,7	OBS/OBH	OBS/OBH	OBS an Deck	OBS 54
SO186/128-1	04.03.06	15:34	2° 30,08' N	96° 42,66' E	0	WNW 7	212	11,8	OBS/OBH	OBS/OBH	OBS ausgelöst	OBS 65
SO186/128-1	04.03.06	15:44	2° 28,41' N	96° 41,61' E	0	NW 6	212	10,1	OBS/OBH	OBS/OBH	OBS gesichtet	OBS 65
SO186/128-1	04.03.06	16:00	2° 28,02' N	96° 40,83' E	0	NNW 3	312	1,3	OBS/OBH	OBS/OBH	OBS an Deck	OBS 65
SO186/128-1	04.03.06	16:22	2° 25,32' N	96° 39,12' E	0	NW 6	212	11,6	OBS/OBH	OBS/OBH	OBS ausgelöst	OBS 66
SO186/128-1	04.03.06	16:28	2° 24,39' N	96° 38,40' E	0	NW 7	225	11,5	OBS/OBH	OBS/OBH	OBS gesichtet	OBS 66
SO186/128-1	04.03.06	16:40	2° 24,07' N	96° 37,95' E	0	NW 2	292	1,8	OBS/OBH	OBS/OBH	OBS an Deck	OBS 66
SO186/128-1	04.03.06	17:03	2° 20,80' N	96° 35,78' E	0	NW 6	211	12,4	OBS/OBH	OBS/OBH	OBS ausgelöst	OBS 67
SO186/128-1	04.03.06	17:05	2° 20,43' N	96° 35,57' E	0	NW 6	210	12,6	OBS/OBH	OBS/OBH	OBS gesichtet	OBS 67
SO186/128-1	04.03.06	17:13	2° 19,93' N	96° 35,06' E	0	N 3	302	0,6	OBS/OBH	OBS/OBH	OBS an Deck	OBS 67
SO186/128-1	04.03.06	17:36	2° 16,65' N	96° 32,86' E	0	NNW 5	211	12	OBS/OBH	OBS/OBH	OBS ausgelöst	OBS 68
SO186/128-1	04.03.06	17:39	2° 16,21' N	96° 32,55' E	0	NW 5	216	8,8	OBS/OBH	OBS/OBH	OBS gesichtet	OBS 68
SO186/128-1	04.03.06	17:46	2° 15,91' N	96° 32,12' E	0	N 3	258	1,3	OBS/OBH	OBS/OBH	OBS an Deck	OBS 68
SO186/128-1	04.03.06	17:58	2° 14,39' N	96° 31,09' E	0	NNW 6	216	12,3	OBS/OBH	OBS/OBH	OBS ausgelöst	OBS 69
SO186/128-1	04.03.06	18:17	2° 11,93' N	96° 29,36' E	0	NNW 3	234	3,2	OBS/OBH	OBS/OBH	OBS gesichtet	OBS 69
SO186/128-1	04.03.06	18:22	2° 11,91' N	96° 29,16' E	0	N 4	269	2	OBS/OBH	OBS/OBH	OBS an Deck	OBS 69
SO186/128-1	04.03.06	18:33	2° 10,58' N	96° 28,21' E	0	NNW 5	211	11,7	OBS/OBH	OBS/OBH	OBS ausgelöst	OBS 70
SO186/128-1	04.03.06	18:42	2° 9,05' N	96° 27,28' E	0	N 4	211	11,9	OBS/OBH	OBS/OBH	OBS gesichtet	OBS 70
SO186/128-1	04.03.06	18:55	2° 8,06' N	96° 26,36' E	0	NNW 2	248	1,4	OBS/OBH	OBS/OBH	OBS an Deck	OBS 70
SO186/128-1	04.03.06	19:08	2° 6,49' N	96° 25,28' E	0	N 4	212	11,4	OBS/OBH	OBS/OBH	OBS ausgelöst	OBS 71
SO186/128-1	04.03.06	19:37	2° 4,14' N	96° 23,47' E	0	NNW 3	248	0,6	OBS/OBH	OBS/OBH	OBS gesichtet	OBS 71
SO186/128-1	04.03.06	19:44	2° 4,23' N	96° 23,33' E	0	NE 4	347	1,3	OBS/OBH	OBS/OBH	OBS an Deck	OBS 71
SO186/128-1	04.03.06	19:58	2° 2,59' N	96° 22,31' E	0	N 4	205	11,4	OBS/OBH	OBS/OBH	OBS ausgelöst	OBS 72
SO186/128-1	04.03.06	20:26	2° 0,18' N	96° 20,75' E	0	NNE 4	99	1	OBS/OBH	OBS/OBH	OBS gesichtet	OBS 72
SO186/128-1	04.03.06	20:40	2° 0,11' N	96° 20,46' E	0	NE 3	327	1,1	OBS/OBH	OBS/OBH	OBS an Deck	OBS 72
SO186/128-1	04.03.06	20:48	1° 59,83' N	96° 20,21' E	0	NNE 1	211	8,6	OBS/OBH	OBS/OBH	OBS ausgelöst	OBS 73
SO186/128-1	04.03.06	21:15	1° 56,39' N	96° 18,02' E	0	NNW 1	222	2,1	OBS/OBH	OBS/OBH	OBS gesichtet	OBS 73
SO186/128-1	04.03.06	21:36	1° 56,15' N	96° 17,64' E	0	NNE 2	302	0,4	OBS/OBH	OBS/OBH	OBS an Deck	OBS 73
SO186/128-1	04.03.06	21:51	1° 54,39' N	96° 16,49' E	0	NNE 4	210	11,9	OBS/OBH	OBS/OBH	OBS ausgelöst	OBS 42
SO186/128-1	04.03.06	22:30	1° 52,55' N	96° 15,19' E	0	WSW 10	111	0,2	OBS/OBH	OBS/OBH	OBS gesichtet	OBS 42
SO186/128-1	04.03.06	22:40	1° 52,50' N	96° 15,11' E	0	WSW 8	288	0,5	OBS/OBH	OBS/OBH	OBS an Deck	OBS 42
SO186/128-1	04.03.06	22:42	1° 52,51' N	96° 15,10' E	0	WSW 9	275	0,7	OBS/OBH	OBS/OBH	OBS ausgelöst	OBS 74
SO186/128-1	04.03.06	23:17	1° 48,05' N	96° 11,93' E	0	W 6	239	3,2	OBS/OBH	OBS/OBH	OBS gesichtet	OBS 74
SO186/128-1	04.03.06	23:29	1° 48,07' N	96° 11,90' E	0	WSW 3	353	0,9	OBS/OBH	OBS/OBH	OBS an Deck	OBS 74
SO186/128-1	05.03.06	01:08	1° 45,41' N	96° 29,91' E	1781	NNW 6	98	12	OBS/OBH	OBS/OBH	OBS ausgelöst	OBS 29
SO186/128-1	05.03.06	01:35	1° 45,09' N	96° 32,82' E	1718	ESE 3	159	1	OBS/OBH	OBS/OBH	OBS gesichtet	OBS 29

Station	Datum	UTC	PositionLat	PositionLon	Tiefe [m]	Windstärke [m/s]	Kurs [°]	v [kn]	Gerät	Gerätekürzel	Aktion	Bemerkung
SO186/128-1	05.03.06	01:45	1° 45,07' N	96° 32,99' E	1700	ESE 6	112	0,2	OBS/OBH	OBS/OBH	OBS an Deck	OBS 29
SO186/128-1	05.03.06	02:10	1° 42,90' N	96° 29,63' E	1339	NE 3	237	12,7	OBS/OBH	OBS/OBH	OBS ausgelöst	OBS 28
SO186/128-1	05.03.06	03:10	1° 40,36' N	96° 25,07' E	0	NNE 6	295	0,3	OBS/OBH	OBS/OBH	OBS gesichtet	OBS 28
SO186/128-1	05.03.06	03:20	1° 40,07' N	96° 24,87' E	2477	NNE 2	214	0,7	OBS/OBH	OBS/OBH	OBS an Deck	OBS 28
SO186/128-1	05.03.06	04:21	1° 42,79' N	96° 14,02' E	3284	NE 6	285	12,6	OBS/OBH	OBS/OBH	OBS ausgelöst	OBS 75
SO186/128-1	05.03.06	05:29	1° 44,02' N	96° 8,83' E	0	NE 3	316	1,2	OBS/OBH	OBS/OBH	OBS gesichtet	OBS 75
SO186/128-1	05.03.06	05:43	1° 44,00' N	96° 8,69' E	0	ESE 1	256	2,1	OBS/OBH	OBS/OBH	OBS an Deck	OBS 75
SO186/128-1	05.03.06	05:45	1° 43,94' N	96° 8,59' E	0	ENE 1	216	5,4	OBS/OBH	OBS/OBH	OBS ausgelöst	OBS 27
SO186/128-1	05.03.06	06:15	1° 39,32' N	96° 5,08' E	0	NNE 4	217	12,1	OBS/OBH	OBS/OBH	OBS ausgelöst	OBS 76
SO186/128-1	05.03.06	07:05	1° 39,77' N	96° 4,64' E	0	NE 3	17	2	OBS/OBH	OBS/OBH	OBS gesichtet	OBS 27
SO186/128-1	05.03.06	07:19	1° 40,11' N	96° 4,88' E	0	ENE 3	35	0,9	OBS/OBH	OBS/OBH	OBS an Deck	OBS 27
SO186/128-1	05.03.06	08:08	1° 36,77' N	96° 3,32' E	0	E 6	189	10,3	OBS/OBH	OBS/OBH	OBS gesichtet	OBS 76
SO186/128-1	05.03.06	08:09	1° 36,61' N	96° 3,27' E	0	ENE 4	203	9,9	OBS/OBH	OBS/OBH	OBH ausgelöst	OBH 77
SO186/128-1	05.03.06	08:23	1° 36,05' N	96° 2,91' E	0	E 3	335	0,5	OBS/OBH	OBS/OBH	OBS an Deck	OBS 76
SO186/128-1	05.03.06	08:40	1° 34,14' N	96° 1,66' E	0	E 5	215	11,6	OBS/OBH	OBS/OBH	OBS ausgelöst	OBS 26
SO186/128-1	05.03.06	09:06	1° 30,81' N	95° 59,33' E	0	ENE 4	217	11,6	OBS/OBH	OBS/OBH	OBH ausgelöst	OBH 78
SO186/128-1	05.03.06	09:31	1° 30,60' N	95° 59,58' E	0	ENE 8	36	11	OBS/OBH	OBS/OBH	OBS gesichtet	OBS 77
SO186/128-1	05.03.06	09:46	1° 31,93' N	96° 0,09' E	0	E 3	96	0,1	OBS/OBH	OBS/OBH	OBS an Deck	OBS 77
SO186/128-1	05.03.06	09:58	1° 31,05' N	96° 0,06' E	0	E 4	186	7,7	OBS/OBH	OBS/OBH	OBS gesichtet	OBS 26
SO186/128-1	05.03.06	10:18	1° 30,00' N	95° 59,79' E	0	E 2	231	0,6	OBS/OBH	OBS/OBH	OBS an Deck	OBS 26
SO186/128-1	05.03.06	10:50	1° 27,99' N	95° 57,15' E	0	SE 1	226	0,2	OBS/OBH	OBS/OBH	OBH ausgelöst	OBH 79
SO186/128-1	05.03.06	11:00	1° 28,00' N	95° 57,12' E	0	SE 2	256	0,6	OBS/OBH	OBS/OBH	OBH gesichtet	OBH 78
SO186/128-1	05.03.06	11:17	1° 28,47' N	95° 57,08' E	0	SE 2	47	0,1	OBS/OBH	OBS/OBH	OBH an Deck	OBH 78
SO186/128-1	05.03.06	11:38	1° 26,02' N	95° 55,42' E	0	SSW 7	213	11,6	OBS/OBH	OBS/OBH	OBS ausgelöst	OBS 45
SO186/128-1	05.03.06	11:54	1° 23,35' N	95° 53,61' E	0	S 7	215	12	OBS/OBH	OBS/OBH	OBH ausgelöst	OBH 80
SO186/128-1	05.03.06	12:03	1° 23,39' N	95° 53,94' E	0	SSE 4	23	9,4	OBS/OBH	OBS/OBH	OBH gesichtet	OBH 79
SO186/128-1	05.03.06	12:14	1° 23,94' N	95° 54,50' E	0	S 2	91	1,5	OBS/OBH	OBS/OBH	OBH an Deck	OBH 79
SO186/128-1	05.03.06	12:54	1° 21,94' N	95° 52,82' E	0	SSE 2	62	0,9	OBS/OBH	OBS/OBH	OBS gesichtet	OBS 45
SO186/128-1	05.03.06	13:04	1° 21,85' N	95° 52,97' E	0	SSE 3	167	1,2	OBS/OBH	OBS/OBH	OBS an Deck	OBS 45
SO186/128-1	05.03.06	13:27	1° 20,25' N	95° 51,30' E	0	SSE 4	232	3,8	OBS/OBH	OBS/OBH	OBS gesichtet	OBH 80
SO186/128-1	05.03.06	13:42	1° 19,88' N	95° 51,63' E	0	SSW 3	132	1,1	OBS/OBH	OBS/OBH	OBH an Deck	OBH 80
SO186/128-1	05.03.06	13:42	1° 19,88' N	95° 51,63' E	0	SSW 3	132	1,1	OBS/OBH	OBS/OBH	Stationsende	
SO186/129-1	05.03.06	23:50	0° 24,16' S	96° 50,15' E	3788	SE 10	128	12,3	OBS/OBH	OBS/OBH	Beginn Station	
SO186/129-1	05.03.06	23:50	0° 24,16' S	96° 50,15' E	3788	SE 10	128	12,3	OBS/OBH	OBS/OBH	OBH ausgelöst	TOBU 01B
SO186/129-1	06.03.06	00:37	0° 25,49' S	96° 51,52' E	3647	SE 2	3	0,6	OBS/OBH	OBS/OBH	OBS ausgelöst	TOBS 01 B
SO186/129-1	06.03.06	01:13	0° 25,41' S	96° 51,66' E	3649	SE 5	52	1,4	OBS/OBH	OBS/OBH	OBH gesichtet	TOBU 01B
SO186/129-1	06.03.06	01:16	0° 25,42' S	96° 51,68' E	3652	SSE 4	176	0,4	OBS/OBH	OBS/OBH	OBH an Deck	TOBU 01B
SO186/129-1	06.03.06	01:36	0° 26,68' S	96° 51,77' E	3571	SE 6	177	3,8	OBS/OBH	OBS/OBH	OBS gesichtet	TOBS 01B
SO186/129-1	06.03.06	01:54	0° 27,42' S	96° 51,76' E	3684	SE 4	213	0,4	OBS/OBH	OBS/OBH	OBS an Deck	TOBS 01B
SO186/129-1	06.03.06	01:55	0° 27,43' S	96° 51,76' E	3651	SE 4	195	0,9	OBS/OBH	OBS/OBH	Ende Station	
SO186/130-1	06.03.06	01:59	0° 27,47' S	96° 51,74' E	3704	SE 4	167	0,2	CTD	CTD	Beginn Station	

Station	Datum	UTC	PositionLat	PositionLon	Tiefe [m]	Windstärke [m/s]	Kurs [°]	v [kn]	Gerät	Gerätekürzel	Aktion	Bemerkung
SO186/130-1	06.03.06	01:59	0° 27,47' S	96° 51,74' E	3704	SE 4	167	0,2	CTD	CTD	zu Wasser	SL 20m OFOS-CTD ; SL: 40m SVP-Sonde
SO186/130-1	06.03.06	02:49	0° 27,54' S	96° 51,74' E	3675	SE 5	311	0,5	CTD	CTD	auf Tiefe	Sl: 2000m
SO186/130-1	06.03.06	03:30	0° 27,43' S	96° 51,71' E	3643	SE 3	141	0,2	CTD	CTD	an Deck	
SO186/130-1	06.03.06	03:30	0° 27,43' S	96° 51,71' E	3643	SE 3	141	0,2	CTD	CTD	Ende Station	
SO186/131-1	06.03.06	04:07	0° 24,75' S	96° 52,64' E	3694	SE 5	160	0,8	OBS/OBH	OBS/OBH	Beginn Station	
SO186/131-1	06.03.06	05:09	0° 24,82' S	96° 52,72' E	3692	ESE 5	48	1,5	OBS/OBH	OBS/OBH	OBS zu Wasser	TOBU 01c
SO186/131-1	06.03.06	05:10	0° 24,82' S	96° 52,75' E	3685	ESE 4	79	1,9	OBS/OBH	OBS/OBH	Ende Station	
SO186/132-1	06.03.06	20:50	2° 6,39' N	95° 56,08' E	2189	SE 3	14	5,4	OBS/OBH	OBS/OBH	Beginn Station	
SO186/132-1	06.03.06	21:05	2° 7,05' N	95° 56,25' E	2183	NNW 1	0	1,8	OBS/OBH	OBS/OBH	OBS zu Wasser	OBS 81
SO186/132-1	06.03.06	21:09	2° 7,14' N	95° 56,22' E	2182	WNW 2	321	1	OBS/OBH	OBS/OBH	OBS zu Wasser	OBS 82
SO186/132-1	06.03.06	21:14	2° 7,22' N	95° 56,14' E	2181	SW 2	327	2,1	OBS/OBH	OBS/OBH	OBS zu Wasser	OBS 83
SO186/132-1	06.03.06	21:17	2° 7,28' N	95° 56,06' E	2181	WNW 2	307	2,2	OBS/OBH	OBS/OBH	OBS zu Wasser	OBS 84
SO186/132-1	06.03.06	21:20	2° 7,34' N	95° 55,98' E	2182	NW 2	311	2,1	OBS/OBH	OBS/OBH	OBS zu Wasser	OBS 85
SO186/132-1	06.03.06	21:23	2° 7,41' N	95° 55,90' E	2181	WNW 2	307	1,8	OBS/OBH	OBS/OBH	OBS zu Wasser	OBS 86
SO186/132-1	06.03.06	21:26	2° 7,48' N	95° 55,85' E	2182	W 2	303	1,7	OBS/OBH	OBS/OBH	OBS zu Wasser	OBS 87
SO186/132-1	06.03.06	21:30	2° 7,55' N	95° 55,77' E	2182	W 2	323	2	OBS/OBH	OBS/OBH	OBS zu Wasser	OBS 88
SO186/132-1	06.03.06	21:33	2° 7,61' N	95° 55,70' E	2182	SW 2	311	1,9	OBS/OBH	OBS/OBH	OBS zu Wasser	OBS 89
SO186/132-1	06.03.06	21:36	2° 7,68' N	95° 55,63' E	2179	W 2	334	2,1	OBS/OBH	OBS/OBH	OBS zu Wasser	OBS 90
SO186/132-1	06.03.06	21:40	2° 7,77' N	95° 55,54' E	2183	WSW 2	331	2	OBS/OBH	OBS/OBH	OBS zu Wasser	OBS 91
SO186/132-1	06.03.06	21:43	2° 7,84' N	95° 55,48' E	2184	WSW 2	334	2,2	OBS/OBH	OBS/OBH	OBS zu Wasser	OBS 92
SO186/132-1	06.03.06	21:46	2° 7,90' N	95° 55,42' E	2183	WSW 2	312	1,7	OBS/OBH	OBS/OBH	OBS zu Wasser	OBS 93
SO186/132-1	06.03.06	21:49	2° 7,97' N	95° 55,35' E	2185	SW 2	285	1,8	OBS/OBH	OBS/OBH	OBS zu Wasser	OBS 94
SO186/132-1	06.03.06	21:53	2° 8,04' N	95° 55,27' E	2186	SW 2	346	2,3	OBS/OBH	OBS/OBH	OBS zu Wasser	OBS 95
SO186/132-1	06.03.06	21:57	2° 8,12' N	95° 55,19' E	2187	SW 2	317	1,8	OBS/OBH	OBS/OBH	OBS zu Wasser	OBS 96
SO186/132-1	06.03.06	22:00	2° 8,18' N	95° 55,13' E	2188	WSW 2	297	1,5	OBS/OBH	OBS/OBH	OBS zu Wasser	OBS 97
SO186/132-1	06.03.06	22:04	2° 8,26' N	95° 55,06' E	2185	SW 2	287	1,5	OBS/OBH	OBS/OBH	OBS zu Wasser	OBS 98
SO186/132-1	06.03.06	22:07	2° 8,31' N	95° 55,00' E	2184	SSW 2	313	1,7	OBS/OBH	OBS/OBH	OBS zu Wasser	OBS 99
SO186/132-1	06.03.06	22:11	2° 8,39' N	95° 54,92' E	2187	SSW 2	341	1,9	OBS/OBH	OBS/OBH	OBS zu Wasser	OBS/M 100
SO186/132-1	06.03.06	22:15	2° 8,47' N	95° 54,84' E	2184	SSW 2	288	1,7	OBS/OBH	OBS/OBH	OBS zu Wasser	OBM 101
SO186/132-1	06.03.06	22:18	2° 8,53' N	95° 54,78' E	2184	SSW 2	274	1,8	OBS/OBH	OBS/OBH	OBS zu Wasser	OBM 102
SO186/132-1	06.03.06	22:37	2° 8,66' N	95° 54,74' E	2182	SSW 1	22	0,4	OBS/OBH	OBS/OBH	OBH zu Wasser	OBH 103
SO186/132-1	06.03.06	22:37	2° 8,66' N	95° 54,74' E	2182	SSW 1	22	0,4	OBS/OBH	OBS/OBH	Ende Station	
SO186/133-1	07.03.06	01:29	1° 57,96' N	96° 5,30' E	2608	ESE 1	324	4,5	Profil	PR	Stationsbeginn	
SO186/133-1	07.03.06	01:44	1° 58,67' N	96° 4,61' E	2605	SSW 2	309	3,8	Profil	PR	Bb-Airgunarray zu Wasser	
SO186/133-1	07.03.06	01:59	1° 59,34' N	96° 3,97' E	2145	SSW 3	310	3,8	Profil	PR	Stb-Airgunarray zu Wasser	
SO186/133-1	07.03.06	02:02	1° 59,47' N	96° 3,84' E	2149	SW 3	314	3,9	Profil	PR	Beginn Profil	# 02, rwK: 315; d: 22 sm
SO186/133-1	07.03.06	07:25	2° 15,02' N	95° 48,29' E	1816	WSW 5	315	3,9	Profil	PR	Ende Profil	äK: 135°; d:1 sm
SO186/133-2	07.03.06	07:35	2° 14,93' N	95° 48,14' E	1853	WSW 4	135	3,1	Profil	PR	Beginn Profil	# 03, rwK: 135°, d: 24 sm
SO186/133-2	07.03.06	13:32	1° 57,89' N	96° 5,14' E	2615	SW 5	118	3,8	Profil	PR	Ende Profil	
SO186/133-3	07.03.06	13:39	1° 58,30' N	96° 5,28' E	2607	SSW 5	312	4,3	Profil	PR	Beginn Profil	# 04, rwK: 315°, d: 24 sm
SO186/133-3	07.03.06	19:25	2° 15,11' N	95° 48,46' E	1795	SSW 5	305	3,9	Profil	PR	Ende Profil	

Station	Datum	UTC	PositionLat	PositionLon	Tiefe [m]	Windstärke [m/s]	Kurs [°]	v [kn]	Gerät	Gerätekürzel	Aktion	Bemerkung
SO186/133-4	07.03.06	19:39	2° 15,42' N	95° 48,55' E	1737	SW 5	133	2,8	Profil	PR	Beginn Profil	# 05, rwK: 135°, d: 14 nm
SO186/133-4	07.03.06	22:36	2° 6,92' N	95° 56,94' E	2172	SSE 4	119	4,2	Profil	PR	Stb-Airgunarray an Deck	
SO186/133-4	07.03.06	23:00	2° 5,78' N	95° 58,09' E	2187	SW 2	126	4,2	Profil	PR	Ende Profil	
SO186/133-4	07.03.06	23:24	2° 4,58' N	95° 59,24' E	2180	SSE 2	140	4,7	Profil	PR	Bb-Airgunarray an Deck	
SO186/133-4	07.03.06	23:24	2° 4,58' N	95° 59,24' E	2180	SSE 2	140	4,7	Profil	PR	Stationsende	
SO186/134-1	07.03.06	23:44	2° 5,97' N	95° 57,60' E	2187	N 5	315	7,6	OBS/OBH	OBS/OBH	Beginn Station	
SO186/134-1	07.03.06	23:44	2° 5,97' N	95° 57,60' E	2187	N 5	315	7,6	OBS/OBH	OBS/OBH	OBS ausgelöst	OBS 81
SO186/134-1	07.03.06	23:48	2° 6,29' N	95° 57,26' E	2186	N 5	315	5,9	OBS/OBH	OBS/OBH	OBS ausgelöst	OBS 82
SO186/134-1	07.03.06	23:51	2° 6,45' N	95° 57,08' E	2184	N 5	289	4,4	OBS/OBH	OBS/OBH	OBS ausgelöst	OBS 83
SO186/134-1	07.03.06	23:53	2° 6,53' N	95° 56,98' E	2183	NNE 4	325	4	OBS/OBH	OBS/OBH	OBS ausgelöst	OBS 84
SO186/134-1	08.03.06	00:00	2° 6,74' N	95° 56,71' E	0	NNE 3	310	2,3	OBS/OBH	OBS/OBH	OBS ausgelöst	OBS 85
SO186/134-1	08.03.06	00:01	2° 6,76' N	95° 56,69' E	0	NNE 4	316	1,3	OBS/OBH	OBS/OBH	OBS ausgelöst	OBS 86
SO186/134-1	08.03.06	00:04	2° 6,78' N	95° 56,66' E	0	NNE 3	11	1,1	OBS/OBH	OBS/OBH	OBS ausgelöst	OBS 87
SO186/134-1	08.03.06	00:07	2° 6,81' N	95° 56,64' E	0	NE 3	259	1	OBS/OBH	OBS/OBH	OBS ausgelöst	OBS 88
SO186/134-1	08.03.06	00:09	2° 6,83' N	95° 56,63' E	0	NE 2	246	1	OBS/OBH	OBS/OBH	OBS ausgelöst	OBS 89
SO186/134-1	08.03.06	00:10	2° 6,84' N	95° 56,62' E	0	NE 2	16	0,9	OBS/OBH	OBS/OBH	OBS ausgelöst	OBS 90
SO186/134-1	08.03.06	00:12	2° 6,86' N	95° 56,61' E	0	NE 2	324	0,8	OBS/OBH	OBS/OBH	OBS ausgelöst	OBS 91
SO186/134-1	08.03.06	00:15	2° 6,89' N	95° 56,58' E	0	NE 3	349	1	OBS/OBH	OBS/OBH	OBS ausgelöst	OBS 92
SO186/134-1	08.03.06	00:17	2° 6,90' N	95° 56,57' E	0	NE 3	335	0,7	OBS/OBH	OBS/OBH	OBS ausgelöst	OBS 93
SO186/134-1	08.03.06	00:17	2° 6,90' N	95° 56,57' E	0	NE 3	335	0,7	OBS/OBH	OBS/OBH	OBS gesichtet	OBS 81
SO186/134-1	08.03.06	00:18	2° 6,91' N	95° 56,56' E	0	NE 3	276	0,5	OBS/OBH	OBS/OBH	OBS gesichtet	OBS 82
SO186/134-1	08.03.06	00:19	2° 6,92' N	95° 56,56' E	0	NE 2	237	0,4	OBS/OBH	OBS/OBH	OBS ausgelöst	OBS 94
SO186/134-1	08.03.06	00:22	2° 6,96' N	95° 56,52' E	0	NE 2	285	1,7	OBS/OBH	OBS/OBH	OBS ausgelöst	OBS 95
SO186/134-1	08.03.06	00:22	2° 6,96' N	95° 56,52' E	0	NE 2	285	1,7	OBS/OBH	OBS/OBH	OBS gesichtet	OBS 83
SO186/134-1	08.03.06	00:23	2° 6,98' N	95° 56,50' E	0	NE 2	317	1,7	OBS/OBH	OBS/OBH	OBS gesichtet	OBS 84
SO186/134-1	08.03.06	00:23	2° 6,98' N	95° 56,50' E	0	NE 2	317	1,7	OBS/OBH	OBS/OBH	OBS ausgelöst	OBS 96
SO186/134-1	08.03.06	00:24	2° 6,99' N	95° 56,48' E	0	ENE 2	333	2	OBS/OBH	OBS/OBH	OBS ausgelöst	OBS 97
SO186/134-1	08.03.06	00:26	2° 7,03' N	95° 56,44' E	0	ENE 2	283	1,9	OBS/OBH	OBS/OBH	OBS gesichtet	OBS 85
SO186/134-1	08.03.06	00:26	2° 7,03' N	95° 56,44' E	0	ENE 2	283	1,9	OBS/OBH	OBS/OBH	OBS ausgelöst	OBS 98
SO186/134-1	08.03.06	00:29	2° 7,11' N	95° 56,36' E	0	ENE 2	305	2,5	OBS/OBH	OBS/OBH	OBS ausgelöst	OBS 99
SO186/134-1	08.03.06	00:30	2° 7,14' N	95° 56,34' E	0	ENE 2	305	2,6	OBS/OBH	OBS/OBH	OBS an Deck	OBS 81
SO186/134-1	08.03.06	00:30	2° 7,14' N	95° 56,34' E	0	ENE 2	305	2,6	OBS/OBH	OBS/OBH	OBS ausgelöst	OBS 100
SO186/134-1	08.03.06	00:31	2° 7,17' N	95° 56,31' E	0	ENE 2	318	2,5	OBS/OBH	OBS/OBH	OBS gesichtet	OBS 86
SO186/134-1	08.03.06	00:32	2° 7,20' N	95° 56,29' E	0	NNE 3	315	2,2	OBS/OBH	OBS/OBH	OBS ausgelöst	OBS 101
SO186/134-1	08.03.06	00:34	2° 7,24' N	95° 56,24' E	0	NNE 3	279	1,5	OBS/OBH	OBS/OBH	OBS gesichtet	OBS 87
SO186/134-1	08.03.06	00:35	2° 7,25' N	95° 56,22' E	0	NNE 3	269	0,7	OBS/OBH	OBS/OBH	OBS ausgelöst	OBS 102
SO186/134-1	08.03.06	00:36	2° 7,27' N	95° 56,22' E	0	NE 2	209	1,7	OBS/OBH	OBS/OBH	OBS gesichtet	OBS 88
SO186/134-1	08.03.06	00:36	2° 7,27' N	95° 56,22' E	0	NE 2	209	1,7	OBS/OBH	OBS/OBH	OBS gesichtet	OBS 89
SO186/134-1	08.03.06	00:36	2° 7,27' N	95° 56,22' E	0	NE 2	209	1,7	OBS/OBH	OBS/OBH	OBS gesichtet	OBS 90
SO186/134-1	08.03.06	00:37	2° 7,28' N	95° 56,21' E	0	NE 2	356	1,3	OBS/OBH	OBS/OBH	OBS gesichtet	OBS 91
SO186/134-1	08.03.06	00:43	2° 7,32' N	95° 56,20' E	0	NE 2	227	0,9	OBS/OBH	OBS/OBH	OBS gesichtet	OBS 92

Station	Datum	UTC	PositionLat	PositionLon	Tiefe [m]	Windstärke [m/s]	Kurs [°]	v [kn]	Gerät	Gerätekürzel	Aktion	Bemerkung
SO186/134-1	08.03.06	00:44	2° 7,33' N	95° 56,20' E	0	NE 2	238	0,7	OBS/OBH	OBS/OBH	OBS gesichtet	OBS 93
SO186/134-1	08.03.06	00:46	2° 7,35' N	95° 56,20' E	0	NE 2	4	0,7	OBS/OBH	OBS/OBH	OBS an Deck	OBS 82
SO186/134-1	08.03.06	00:49	2° 7,37' N	95° 56,18' E	0	NE 2	318	1,1	OBS/OBH	OBS/OBH	OBS gesichtet	OBS 94
SO186/134-1	08.03.06	00:54	2° 7,45' N	95° 56,08' E	0	NE 2	327	2,3	OBS/OBH	OBS/OBH	OBS gesichtet	OBS 95
SO186/134-1	08.03.06	00:55	2° 7,47' N	95° 56,05' E	0	NE 2	302	2	OBS/OBH	OBS/OBH	OBS an Deck	OBS 83
SO186/134-1	08.03.06	00:55	2° 7,47' N	95° 56,05' E	0	NE 2	302	2	OBS/OBH	OBS/OBH	OBS gesichtet	OBS 96
SO186/134-1	08.03.06	01:02	2° 7,63' N	95° 55,81' E	0	NNE 2	322	3,2	OBS/OBH	OBS/OBH	OBS an Deck	OBS 84
SO186/134-1	08.03.06	01:03	2° 7,66' N	95° 55,78' E	0	NNE 3	291	1,7	OBS/OBH	OBS/OBH	OBS gesichtet	OBS 97
SO186/134-1	08.03.06	01:08	2° 7,71' N	95° 55,73' E	0	NE 2	345	1	OBS/OBH	OBS/OBH	OBS gesichtet	OBS 98
SO186/134-1	08.03.06	01:10	2° 7,74' N	95° 55,71' E	0	NE 2	263	1,4	OBS/OBH	OBS/OBH	OBS an Deck	OBS 85
SO186/134-1	08.03.06	01:13	2° 7,78' N	95° 55,68' E	0	NE 2	316	1,1	OBS/OBH	OBS/OBH	OBS gesichtet	OBS 99
SO186/134-1	08.03.06	01:13	2° 7,78' N	95° 55,68' E	0	NE 2	316	1,1	OBS/OBH	OBS/OBH	OBS gesichtet	OBS 100
SO186/134-1	08.03.06	01:14	2° 7,79' N	95° 55,67' E	0	NE 2	320	1,5	OBS/OBH	OBS/OBH	OBS gesichtet	OBS 101
SO186/134-1	08.03.06	01:17	2° 7,84' N	95° 55,63' E	0	NE 2	298	1,2	OBS/OBH	OBS/OBH	OBS an Deck	OBS 86
SO186/134-1	08.03.06	01:23	2° 7,92' N	95° 55,55' E	0	NNE 2	277	1,2	OBS/OBH	OBS/OBH	OBS an Deck	OBS 87
SO186/134-1	08.03.06	01:24	2° 7,94' N	95° 55,54' E	0	NNE 2	278	1,7	OBS/OBH	OBS/OBH	OBS gesichtet	OBS 102
SO186/134-1	08.03.06	01:30	2° 8,12' N	95° 55,39' E	0	N 3	342	2,4	OBS/OBH	OBS/OBH	OBS an Deck	OBS 88
SO186/134-1	08.03.06	01:37	2° 8,34' N	95° 55,23' E	0	NNE 2	6	2,2	OBS/OBH	OBS/OBH	OBS an Deck	OBS 89
SO186/134-1	08.03.06	01:46	2° 8,56' N	95° 55,12' E	0	NNE 2	321	1,4	OBS/OBH	OBS/OBH	OBH ausgelöst	OBH 103
SO186/134-1	08.03.06	01:46	2° 8,56' N	95° 55,12' E	0	NNE 2	321	1,4	OBS/OBH	OBS/OBH	OBS an Deck	OBS 90
SO186/134-1	08.03.06	01:56	2° 8,75' N	95° 55,02' E	0	NNE 1	325	1,2	OBS/OBH	OBS/OBH	OBS an Deck	OBS 91
SO186/134-1	08.03.06	02:03	2° 8,87' N	95° 54,96' E	0	SW 1	302	1,2	OBS/OBH	OBS/OBH	OBS an Deck	OBS 92
SO186/134-1	08.03.06	02:09	2° 8,96' N	95° 54,90' E	0	WNW 1	328	1,3	OBS/OBH	OBS/OBH	OBS an Deck	OBS 93
SO186/134-1	08.03.06	02:15	2° 9,07' N	95° 54,78' E	0	SSW 1	324	2,1	OBS/OBH	OBS/OBH	OBS an Deck	OBS 94
SO186/134-1	08.03.06	02:22	2° 9,19' N	95° 54,63' E	0	WNW 2	266	1,2	OBS/OBH	OBS/OBH	OBS an Deck	OBS 95
SO186/134-1	08.03.06	02:29	2° 9,28' N	95° 54,50' E	0	NNE 1	293	1,2	OBS/OBH	OBS/OBH	OBS an Deck	OBS 96
SO186/134-1	08.03.06	02:33	2° 9,34' N	95° 54,44' E	0	SSW 1	328	1,3	OBS/OBH	OBS/OBH	OBS an Deck	OBS 97
SO186/134-1	08.03.06	02:47	2° 9,60' N	95° 54,31' E	0	N 2	344	1,6	OBS/OBH	OBS/OBH	OBS an Deck	OBS 98
SO186/134-1	08.03.06	02:54	2° 9,72' N	95° 54,23' E	0	ENE 1	359	2,5	OBS/OBH	OBS/OBH	OBH gesichtet	OBH 103
SO186/134-1	08.03.06	02:55	2° 9,73' N	95° 54,22' E	0	NE 1	8	2,6	OBS/OBH	OBS/OBH	OBS an Deck	OBS 99
SO186/134-1	08.03.06	03:03	2° 9,85' N	95° 54,11' E	0	NNE 2	288	1,3	OBS/OBH	OBS/OBH	OBS an Deck	OBS 100
SO186/134-1	08.03.06	03:12	2° 10,07' N	95° 53,90' E	0	NNE 2	338	1,7	OBS/OBH	OBS/OBH	OBS an Deck	OBS 101
SO186/134-1	08.03.06	03:19	2° 10,21' N	95° 53,76' E	0	NNW 2	289	1,2	OBS/OBH	OBS/OBH	OBS an Deck	OBS 102
SO186/134-1	08.03.06	03:29	2° 9,92' N	95° 53,94' E	0	ENE 2	168	0,9	OBS/OBH	OBS/OBH	OBH an Deck	OBH 103
SO186/134-1	08.03.06	03:33	2° 9,87' N	95° 53,92' E	0	ENE 1	241	1,2	OBS/OBH	OBS/OBH	Ende Station	
SO186/135-1	08.03.06	16:09	3° 50,01' N	93° 54,94' E	2464	SW 2	305	1,4	OBS/OBH	OBS/OBH	Beginn Station	
SO186/135-1	08.03.06	16:25	3° 50,12' N	93° 54,96' E	2463	S 1	71	0,5	OBS/OBH	OBS/OBH	OBH zu Wasser	OBH 104
SO186/135-1	08.03.06	16:34	3° 50,23' N	93° 54,90' E	2467	NW 1	344	2,4	OBS/OBH	OBS/OBH	OBS zu Wasser	OBS 105
SO186/135-1	08.03.06	16:38	3° 50,33' N	93° 54,81' E	2467	SW 2	300	0,5	OBS/OBH	OBS/OBH	OBS zu Wasser	OBS 106
SO186/135-1	08.03.06	16:43	3° 50,42' N	93° 54,77' E	2464	SW 1	347	1,9	OBS/OBH	OBS/OBH	OBS zu Wasser	OBS 107
SO186/135-1	08.03.06	16:48	3° 50,51' N	93° 54,72' E	2468	SW 3	312	1	OBS/OBH	OBS/OBH	OBS zu Wasser	OBS 108

Station	Datum	UTC	PositionLat	PositionLon	Tiefe [m]	Windstärke [m/s]	Kurs [°]	v [kn]	Gerät	Gerätekürzel	Aktion	Bemerkung
SO186/135-1	08.03.06	16:52	3° 50,59' N	93° 54,67' E	2471	SW 4	286	0,9	OBS/OBH	OBS/OBH	OBS zu Wasser	OBS 109
SO186/135-1	08.03.06	16:57	3° 50,71' N	93° 54,62' E	2468	WSW 3	337	2,1	OBS/OBH	OBS/OBH	OBS zu Wasser	OBS 110
SO186/135-1	08.03.06	17:00	3° 50,79' N	93° 54,58' E	2467	SW 2	332	1,7	OBS/OBH	OBS/OBH	OBS zu Wasser	OBS 111
SO186/135-1	08.03.06	17:04	3° 50,90' N	93° 54,54' E	2466	SW 3	321	0,9	OBS/OBH	OBS/OBH	OBS zu Wasser	OBS 112
SO186/135-1	08.03.06	17:08	3° 51,01' N	93° 54,52' E	2470	SSW 3	329	1,4	OBS/OBH	OBS/OBH	OBS zu Wasser	OBS 113
SO186/135-1	08.03.06	17:12	3° 51,12' N	93° 54,47' E	2473	SSW 4	333	2	OBS/OBH	OBS/OBH	OBS zu Wasser	OBS 114
SO186/135-1	08.03.06	17:15	3° 51,19' N	93° 54,43' E	2468	SSW 5	330	1,9	OBS/OBH	OBS/OBH	OBS zu Wasser	OBS 115
SO186/135-1	08.03.06	17:20	3° 51,31' N	93° 54,36' E	2469	SSW 6	343	2,7	OBS/OBH	OBS/OBH	OBS zu Wasser	OBS 116
SO186/135-1	08.03.06	17:24	3° 51,40' N	93° 54,32' E	2468	SSW 4	338	1,2	OBS/OBH	OBS/OBH	OBS zu Wasser	OBS 117
SO186/135-1	08.03.06	17:28	3° 51,49' N	93° 54,29' E	2470	SW 4	324	1,5	OBS/OBH	OBS/OBH	OBS zu Wasser	OBS 118
SO186/135-1	08.03.06	17:32	3° 51,59' N	93° 54,24' E	2475	SW 3	345	2,3	OBS/OBH	OBS/OBH	OBS zu Wasser	OBS 119
SO186/135-1	08.03.06	17:36	3° 51,69' N	93° 54,20' E	2471	SSW 3	309	1	OBS/OBH	OBS/OBH	OBS zu Wasser	OBS 120
SO186/135-1	08.03.06	17:41	3° 51,81' N	93° 54,13' E	2466	SSW 4	337	2,4	OBS/OBH	OBS/OBH	OBS zu Wasser	OBS 121
SO186/135-1	08.03.06	17:45	3° 51,90' N	93° 54,07' E	2469	SSW 5	312	1	OBS/OBH	OBS/OBH	OBS zu Wasser	OBS 122
SO186/135-1	08.03.06	17:50	3° 52,02' N	93° 54,05' E	2467	SSW 4	357	2	OBS/OBH	OBS/OBH	OBS zu Wasser	OBS 123
SO186/135-1	08.03.06	17:54	3° 52,12' N	93° 54,03' E	2467	SSW 4	346	2,4	OBS/OBH	OBS/OBH	OBS zu Wasser	OBS 124
SO186/135-1	08.03.06	17:58	3° 52,21' N	93° 53,99' E	2463	SSW 4	280	0,8	OBS/OBH	OBS/OBH	OBS zu Wasser	OBS 125
SO186/135-1	08.03.06	18:02	3° 52,31' N	93° 53,94' E	2462	SW 3	345	1,9	OBS/OBH	OBS/OBH	OBS zu Wasser	OBS 126
SO186/135-1	08.03.06	18:03	3° 52,33' N	93° 53,93' E	2463	SW 3	341	1,9	OBS/OBH	OBS/OBH	Ende Station	
SO186/136-1	08.03.06	18:11	3° 52,38' N	93° 53,62' E	2451	SW 5	294	4,2	Profil	PR	Stationsbeginn	
SO186/136-1	08.03.06	18:25	3° 53,26' N	93° 53,30' E	2460	SW 3	319	3,8	Profil	PR	Bb Airgun zu Wasser	
SO186/136-1	08.03.06	18:39	3° 54,11' N	93° 52,88' E	2459	WSW 3	324	4	Profil	PR	Stb Airgun zu Wasser	
SO186/136-1	08.03.06	18:50	3° 54,77' N	93° 52,58' E	2450	W 3	336	3,8	Profil	PR	Beginn Profil	# 06, rwK: 336°, d: 6 sm
SO186/136-1	08.03.06	20:17	3° 59,98' N	93° 50,24' E	2007	NE 4	348	4,4	Profil	PR	Ende Profil	
SO186/136-2	08.03.06	20:22	4° 0,03' N	93° 50,48' E	2000	NE 5	144	4,9	Profil	PR	Beginn Profil	# 07, rwK: 156°, d: 22 sm
SO186/136-2	09.03.06	01:39	3° 39,99' N	93° 59,42' E	1830	WSW 3	155	4,1	Profil	PR	Ende Profil	
SO186/136-3	09.03.06	01:50	3° 40,22' N	93° 59,70' E	1785	NW 2	337	4,3	Profil	PR	Beginn Profil	# 08; rwK: 336 ; d: 22 sm
SO186/136-3	09.03.06	07:06	4° 0,00' N	93° 50,89' E	1982	NE 3	334	4	Profil	PR	Ende Profil	
SO186/136-4	09.03.06	07:24	4° 0,00' N	93° 50,05' E	2045	WNW 2	167	3,5	Profil	PR	Beginn Profil	# 09, rwK: 156°, d: 22 sm
SO186/136-4	09.03.06	12:40	3° 40,05' N	93° 58,99' E	1939	W 3	155	4,2	Profil	PR	Ende Profil	
SO186/136-5	09.03.06	12:53	3° 40,15' N	93° 59,59' E	1781	SW 4	276	3,7	Profil	PR	Beginn Profil	# 10, rwK: 336° , d: 22 sm
SO186/136-5	09.03.06	18:15	4° 0,31' N	93° 50,54' E	1976	NNW 6	316	4	Profil	PR	Ende Profil	
SO186/136-6	09.03.06	18:32	4° 0,07' N	93° 51,11' E	1890	NNW 1	153	3,9	Profil	PR	Beginn Profil	# 11, rwK: 156°, d: 12 sm
SO186/136-6	09.03.06	21:26	3° 49,61' N	93° 55,71' E	2476	WNW 3	151	4,5	Profil	PR	Ende Profil	
SO186/136-7	09.03.06	21:39	3° 49,21' N	93° 55,04' E	2459	NNW 6	333	4,1	Profil	PR	Beginn Profil	# 12, rwK: 336°, d: 6 sm
SO186/136-7	09.03.06	23:00	3° 54,48' N	93° 52,71' E	2452	NNW 4	338	4,3	Profil	PR	Ende Profil	
SO186/136-7	09.03.06	23:25	3° 56,11' N	93° 52,03' E	2397	NNE 5	338	4,8	Profil	PR	Bb-Airgunarray an Deck	
SO186/136-7	09.03.06	23:48	3° 54,84' N	93° 52,37' E	2449	NE 9	161	4,2	Profil	PR	Stb-Airgunarray an Deck	
SO186/136-7	09.03.06	23:48	3° 54,84' N	93° 52,37' E	2449	NE 9	161	4,2	Profil	PR	Stationsende	
SO186/137-1	09.03.06	23:51	3° 54,64' N	93° 52,44' E	2452	NE 10	159	4,3	OBS/OBH	OBS/OBH	Beginn Station	
SO186/137-1	09.03.06	23:52	3° 54,57' N	93° 52,47' E	2447	NE 10	160	4,3	OBS/OBH	OBS/OBH	OBS ausgelöst	OBS 126

Station	Datum	UTC	PositionLat	PositionLon	Tiefe [m]	Windstärke [m/s]	Kurs [°]	v [kn]	Gerät	Gerätekürzel	Aktion	Bemerkung
SO186/137-1	09.03.06	23:56	3° 54,24' N	93° 52,58' E	2449	NE 8	156	5,1	OBS/OBH	OBS/OBH	OBS ausgelöst	OBS 125
SO186/137-1	09.03.06	23:58	3° 54,06' N	93° 52,65' E	2452	NE 9	160	6,1	OBS/OBH	OBS/OBH	OBS ausgelöst	OBS 124
SO186/137-1	10.03.06	00:01	3° 53,78' N	93° 52,76' E	2453	NE 8	154	6	OBS/OBH	OBS/OBH	OBS ausgelöst	OBS 123
SO186/137-1	10.03.06	00:04	3° 53,50' N	93° 52,87' E	2456	NE 8	161	5,9	OBS/OBH	OBS/OBH	OBS ausgelöst	OBS 122
SO186/137-1	10.03.06	00:07	3° 53,22' N	93° 52,99' E	2452	NE 8	157	6,1	OBS/OBH	OBS/OBH	OBS ausgelöst	OBS 122 b
SO186/137-1	10.03.06	00:27	3° 52,21' N	93° 53,76' E	2456	NNE 9	176	1,5	OBS/OBH	OBS/OBH	OBS gesichtet	OBS 126
SO186/137-1	10.03.06	00:31	3° 52,18' N	93° 53,78' E	2457	NE 7	183	1	OBS/OBH	OBS/OBH	OBS gesichtet	OBS 125
SO186/137-1	10.03.06	00:33	3° 52,17' N	93° 53,80' E	2459	NNE 6	107	1,6	OBS/OBH	OBS/OBH	OBS gesichtet	OBS 124
SO186/137-1	10.03.06	00:35	3° 52,16' N	93° 53,87' E	2461	N 6	73	2,7	OBS/OBH	OBS/OBH	OBS gesichtet	OBS 123
SO186/137-1	10.03.06	00:38	3° 52,19' N	93° 53,97' E	2464	NE 6	85	1,6	OBS/OBH	OBS/OBH	OBS an Deck	OBS 126
SO186/137-1	10.03.06	00:39	3° 52,19' N	93° 53,99' E	2466	NE 5	58	1	OBS/OBH	OBS/OBH	OBS gesichtet	OBS 122
SO186/137-1	10.03.06	00:39	3° 52,19' N	93° 53,99' E	2466	NE 5	58	1	OBS/OBH	OBS/OBH	OBS gesichtet	OBS 122 b
SO186/137-1	10.03.06	00:40	3° 52,20' N	93° 54,01' E	2464	NE 5	64	1	OBS/OBH	OBS/OBH	OBS an Deck	OBS 125
SO186/137-1	10.03.06	00:44	3° 52,21' N	93° 54,07' E	2471	NE 3	36	0,7	OBS/OBH	OBS/OBH	OBS an Deck	OBS 124
SO186/137-1	10.03.06	00:49	3° 52,22' N	93° 54,21' E	2470	ENE 3	103	0,8	OBS/OBH	OBS/OBH	OBS an Deck	OBS 123
SO186/137-1	10.03.06	00:50	3° 52,21' N	93° 54,23' E	2470	ENE 2	96	1	OBS/OBH	OBS/OBH	OBS ausgelöst	OBS 113
SO186/137-1	10.03.06	00:52	3° 52,18' N	93° 54,27' E	2471	ESE 3	159	1,8	OBS/OBH	OBS/OBH	OBS ausgelöst	OBS 112
SO186/137-1	10.03.06	00:53	3° 52,16' N	93° 54,28' E	2474	ESE 3	154	0,8	OBS/OBH	OBS/OBH	OBS an Deck	OBS 122
SO186/137-1	10.03.06	00:56	3° 52,11' N	93° 54,29' E	2472	E 3	191	0,9	OBS/OBH	OBS/OBH	OBS ausgelöst	OBS 111
SO186/137-1	10.03.06	00:59	3° 52,08' N	93° 54,30' E	2481	E 3	155	0,9	OBS/OBH	OBS/OBH	OBS ausgelöst	OBS 110
SO186/137-1	10.03.06	01:00	3° 52,07' N	93° 54,30' E	2474	E 3	148	0,6	OBS/OBH	OBS/OBH	OBS an Deck	OBS 122b
SO186/137-1	10.03.06	01:02	3° 52,05' N	93° 54,32' E	2474	E 3	151	0,9	OBS/OBH	OBS/OBH	OBS ausgelöst	OBS 109
SO186/137-1	10.03.06	01:25	3° 51,73' N	93° 54,28' E	2474	ESE 7	164	0,6	OBS/OBH	OBS/OBH	OBS gesichtet	OBS 113
SO186/137-1	10.03.06	01:27	3° 51,68' N	93° 54,30' E	2469	SE 7	163	2,7	OBS/OBH	OBS/OBH	OBS gesichtet	OBS 112
SO186/137-1	10.03.06	01:30	3° 51,46' N	93° 54,37' E	2473	SSE 8	157	5,8	OBS/OBH	OBS/OBH	OBS gesichtet	OBS 111
SO186/137-1	10.03.06	01:33	3° 51,26' N	93° 54,41' E	2470	SSW 10	165	2,6	OBS/OBH	OBS/OBH	OBS gesichtet	OBS 110
SO186/137-1	10.03.06	01:35	3° 51,21' N	93° 54,46' E	2471	SSE 10	117	2,3	OBS/OBH	OBS/OBH	OBS an Deck	OBS 113
SO186/137-1	10.03.06	01:37	3° 51,20' N	93° 54,53' E	2473	SSW 7	97	0,8	OBS/OBH	OBS/OBH	OBS gesichtet	OBS 109
SO186/137-1	10.03.06	01:43	3° 51,14' N	93° 54,67' E	2470	SSW 10	100	1,3	OBS/OBH	OBS/OBH	OBS an Deck	OBS 112
SO186/137-1	10.03.06	01:49	3° 51,08' N	93° 54,80' E	2468	SSW 9	122	1,6	OBS/OBH	OBS/OBH	OBS an Deck	OBS 111
SO186/137-1	10.03.06	01:57	3° 50,96' N	93° 54,95' E	2468	SSW 9	132	1,2	OBS/OBH	OBS/OBH	OBS an Deck	OBS 110
SO186/137-1	10.03.06	02:02	3° 50,84' N	93° 55,01' E	2467	SSW 9	152	2	OBS/OBH	OBS/OBH	OBS an Deck	OBS 109
SO186/137-1	10.03.06	02:08	3° 50,79' N	93° 55,04' E	2466	SSW 7	348	0,3	OBS/OBH	OBS/OBH	Ende Station	
SO186/138-1	10.03.06	02:25	3° 51,43' N	93° 55,43' E	2476	SSE 8	267	2	OBS/OBH	OBS/OBH	Beginn Station	
SO186/138-1	10.03.06	02:28	3° 51,39' N	93° 55,31' E	2478	S 8	253	2,1	OBS/OBH	OBS/OBH	OBS zu Wasser	OBS 127
SO186/138-1	10.03.06	02:31	3° 51,37' N	93° 55,23' E	2475	SSW 8	254	1,4	OBS/OBH	OBS/OBH	OBS zu Wasser	OBS 128
SO186/138-1	10.03.06	02:37	3° 51,32' N	93° 55,14' E	2473	SSW 7	228	1,4	OBS/OBH	OBS/OBH	OBS zu Wasser	OBS 129
SO186/138-1	10.03.06	02:40	3° 51,27' N	93° 55,05' E	2470	SSW 8	248	1,9	OBS/OBH	OBS/OBH	OBS zu Wasser	OBS 130
SO186/138-1	10.03.06	02:43	3° 51,24' N	93° 54,97' E	2472	SSW 6	272	1,9	OBS/OBH	OBS/OBH	OBS zu Wasser	OBS 131
SO186/138-1	10.03.06	02:47	3° 51,20' N	93° 54,85' E	2471	SSW 6	254	2	OBS/OBH	OBS/OBH	OBS zu Wasser	OBS 132
SO186/138-1	10.03.06	02:50	3° 51,15' N	93° 54,77' E	2471	SW 7	246	2	OBS/OBH	OBS/OBH	OBS zu Wasser	OBS 133

Station	Datum	UTC	PositionLat	PositionLon	Tiefe [m]	Windstärke [m/s]	Kurs [°]	v [kn]	Gerät	Gerätekürzel	Aktion	Bemerkung
SO186/138-1	10.03.06	02:52	3° 51,13' N	93° 54,70' E	2471	SSW 7	251	1,8	OBS/OBH	OBS/OBH	OBS zu Wasser	OBS 134
SO186/138-1	10.03.06	02:55	3° 51,09' N	93° 54,60' E	2472	SSW 7	257	2,5	OBS/OBH	OBS/OBH	OBS zu Wasser	OBS 135
SO186/138-1	10.03.06	03:01	3° 51,01' N	93° 54,39' E	2467	SW 7	250	2	OBS/OBH	OBS/OBH	OBS zu Wasser	OBS 136
SO186/138-1	10.03.06	03:04	3° 50,96' N	93° 54,30' E	2464	SW 7	243	2,3	OBS/OBH	OBS/OBH	OBS zu Wasser	OBS 137
SO186/138-1	10.03.06	03:04	3° 50,96' N	93° 54,30' E	2464	SW 7	243	2,3	OBS/OBH	OBS/OBH	Ende Station	
SO186/139-1	10.03.06	03:11	3° 50,95' N	93° 54,08' E	2463	W 8	337	3,4	Profil	PR	Stationsbeginn	
SO186/139-1	10.03.06	03:27	3° 51,69' N	93° 53,85' E	2458	SSW 7	315	2,3	Profil	PR	Bb Airgun zu Wasser	
SO186/139-1	10.03.06	03:45	3° 51,11' N	93° 53,97' E	2459	WSW 8	173	1,5	Profil	PR	Stb Airgun zu Wasser	
SO186/139-1	10.03.06	03:53	3° 51,13' N	93° 53,71' E	2453	S 7	255	3,5	Profil	PR	Beginn Profil	# 13: rwK: 246° d: 10 sm
SO186/139-1	10.03.06	06:17	3° 47,25' N	93° 44,99' E	1708	SSE 4	240	3,6	Profil	PR	Ende Profil	
SO186/139-2	10.03.06	06:26	3° 46,87' N	93° 45,10' E	1734	SE 5	73	4,8	Profil	PR	Beginn Profil	# 14, rwK: 066°, d: 22 sm
SO186/139-2	10.03.06	11:48	3° 55,87' N	94° 5,39' E	1759	SSW 2	70	4,3	Profil	PR	Ende Profil	
SO186/139-3	10.03.06	11:59	3° 56,46' N	94° 5,41' E	1770	S 4	239	4,5	Profil	PR	Beginn Profil	# 15, rwK: 246°, d: 22 sm
SO186/139-3	10.03.06	17:25	3° 47,45' N	93° 45,01' E	1711	ESE 2	251	4,2	Profil	PR	Ende Profil	
SO186/139-4	10.03.06	17:43	3° 46,46' N	93° 45,04' E	1622	NE 3	68	3,9	Profil	PR	Beginn Profil	# 16, rwK: 066°, d: 22 sm
SO186/139-4	10.03.06	23:10	3° 55,44' N	94° 5,38' E	1832	SSE 2	60	3,9	Profil	PR	Ende Profil	
SO186/139-5	10.03.06	23:20	3° 56,07' N	94° 5,42' E	1754	NNE 2	247	3,6	Profil	PR	Beginn Profil	# 17, rwK: 246°, d: 22 sm
SO186/139-5	11.03.06	04:59	3° 47,03' N	93° 44,96' E	1698	SSE 4	249	3,8	Profil	PR	Ende Profil	
SO186/139-6	11.03.06	05:08	3° 46,63' N	93° 45,11' E	1641	SSE 4	67	4,5	Profil	PR	Beginn Profil	# 18, rwk: 066°, d: 14 sm
SO186/139-6	11.03.06	08:40	3° 52,53' N	93° 58,34' E	1590	NNW 3	70	4,4	Profil	PR	Ende Profil	
SO186/139-7	11.03.06	08:51	3° 53,03' N	93° 58,31' E	1556	WNW 4	262	3	Profil	PR	Beginn Profil	# 19, rwK: 246°, d: 5 sm
SO186/139-7	11.03.06	10:00	3° 51,15' N	93° 53,85' E	2455	WNW 4	240	4,1	Profil	PR	Ende Profil	
SO186/139-7	11.03.06	10:21	3° 50,64' N	93° 52,60' E	2377	WNW 4	243	4,2	Profil	PR	Bb-Airgunarray an Deck	
SO186/139-7	11.03.06	10:40	3° 50,09' N	93° 51,40' E	0	NW 4	248	4,9	Profil	PR	Stb-Airgunarray an Deck	
SO186/139-7	11.03.06	10:41	3° 50,06' N	93° 51,33' E	0	NW 5	248	4,3	Profil	PR	Stationsende	
SO186/140-1	11.03.06	10:43	3° 49,97' N	93° 51,26' E	0	SW 5	136	3,6	OBS/OBH	OBS/OBH	Beginn Station	
SO186/140-1	11.03.06	10:44	3° 49,95' N	93° 51,31' E	0	SSW 4	83	3,8	OBS/OBH	OBS/OBH	OBS ausgelöst	OBS/M 108
SO186/140-1	11.03.06	10:47	3° 49,97' N	93° 51,59' E	0	WSW 1	88	7	OBS/OBH	OBS/OBH	OBS ausgelöst	OBM 107
SO186/140-1	11.03.06	10:51	3° 50,00' N	93° 52,10' E	0	NW 3	80	8	OBS/OBH	OBS/OBH	OBS ausgelöst	OBM 106
SO186/140-1	11.03.06	11:05	3° 50,94' N	93° 53,90' E	0	WNW 5	47	11,1	OBS/OBH	OBS/OBH	OBH ausgelöst	OBH 104
SO186/140-1	11.03.06	11:18	3° 50,72' N	93° 54,78' E	0	W 2	161	3,7	OBS/OBH	OBS/OBH	OBS gesichtet	OBS/M 108
SO186/140-1	11.03.06	11:20	3° 50,62' N	93° 54,80' E	0	WNW 2	167	1,5	OBS/OBH	OBS/OBH	OBS gesichtet	OBM 107
SO186/140-1	11.03.06	11:24	3° 50,57' N	93° 54,82' E	0	WNW 2	141	1,2	OBS/OBH	OBS/OBH	OBS gesichtet	OBM 106
SO186/140-1	11.03.06	11:28	3° 50,53' N	93° 54,85' E	0	WNW 3	157	0,7	OBS/OBH	OBS/OBH	OBS an Deck	OBM 107
SO186/140-1	11.03.06	11:31	3° 50,50' N	93° 54,88' E	0	WNW 3	105	0,7	OBS/OBH	OBS/OBH	OBS an Deck	OBS/M 108
SO186/140-1	11.03.06	11:35	3° 50,46' N	93° 54,94' E	0	WNW 2	106	1	OBS/OBH	OBS/OBH	OBS an Deck	OBM 106
SO186/140-1	11.03.06	11:36	3° 50,46' N	93° 54,95' E	0	WNW 2	130	0,7	OBS/OBH	OBS/OBH	OBH gesichtet	OBH 104
SO186/140-1	11.03.06	11:36	3° 50,46' N	93° 54,95' E	0	WNW 2	130	0,7	OBS/OBH	OBS/OBH	OBS ausgelöst	OBS 127
SO186/140-1	11.03.06	11:41	3° 50,39' N	93° 55,00' E	0	WNW 3	184	0,7	OBS/OBH	OBS/OBH	OBH an Deck	OBH 104
SO186/140-1	11.03.06	11:42	3° 50,38' N	93° 55,01' E	0	NW 3	154	0,7	OBS/OBH	OBS/OBH	OBS ausgelöst	OBS 129
SO186/140-1	11.03.06	11:45	3° 50,34' N	93° 55,04' E	0	W 3	108	2,2	OBS/OBH	OBS/OBH	OBS ausgelöst	OBS 129 b

Station	Datum	UTC	PositionLat	PositionLon	Tiefe [m]	Windstärke [m/s]	Kurs [°]	v [kn]	Gerät	Gerätekürzel	Aktion	Bemerkung
SO186/140-1	11.03.06	11:55	3° 51,06' N	93° 55,84' E	0	WNW 5	44	9,3	OBS/OBH	OBS/OBH	OBS ausgelöst	OBS 130
SO186/140-1	11.03.06	12:00	3° 51,53' N	93° 55,80' E	0	WNW 5	296	3,2	OBS/OBH	OBS/OBH	OBS ausgelöst	OBS 131
SO186/140-1	11.03.06	12:09	3° 51,50' N	93° 55,55' E	0	NNW 3	276	1,1	OBS/OBH	OBS/OBH	OBS gesichtet	OBS 127
SO186/140-1	11.03.06	12:11	3° 51,51' N	93° 55,51' E	0	NW 3	282	1,1	OBS/OBH	OBS/OBH	OBS ausgelöst	OBS 132
SO186/140-1	11.03.06	12:13	3° 51,51' N	93° 55,48' E	0	NW 4	288	1,6	OBS/OBH	OBS/OBH	OBS gesichtet	OBS 129
SO186/140-1	11.03.06	12:14	3° 51,51' N	93° 55,47' E	0	WNW 4	206	1	OBS/OBH	OBS/OBH	OBS an Deck	OBS 127
SO186/140-1	11.03.06	12:15	3° 51,50' N	93° 55,46' E	0	WNW 4	245	0,8	OBS/OBH	OBS/OBH	OBS ausgelöst	OBS 133
SO186/140-1	11.03.06	12:18	3° 51,48' N	93° 55,42' E	0	NW 3	242	0,9	OBS/OBH	OBS/OBH	OBS gesichtet	OBS 129 b
SO186/140-1	11.03.06	12:19	3° 51,48' N	93° 55,40' E	0	NW 3	250	1,4	OBS/OBH	OBS/OBH	OBS an Deck	OBS 129
SO186/140-1	11.03.06	12:21	3° 51,46' N	93° 55,37' E	0	WNW 4	235	0,9	OBS/OBH	OBS/OBH	OBS ausgelöst	OBS 134
SO186/140-1	11.03.06	12:24	3° 51,44' N	93° 55,33' E	0	NW 4	267	1,3	OBS/OBH	OBS/OBH	OBS an Deck	OBS 129 b
SO186/140-1	11.03.06	12:26	3° 51,42' N	93° 55,29' E	0	NW 4	242	1,3	OBS/OBH	OBS/OBH	OBS ausgelöst	OBS 135
SO186/140-1	11.03.06	12:27	3° 51,42' N	93° 55,28' E	0	WNW 4	250	1,1	OBS/OBH	OBS/OBH	OBS gesichtet	OBS 130
SO186/140-1	11.03.06	12:31	3° 51,37' N	93° 55,19' E	0	NW 3	240	1,9	OBS/OBH	OBS/OBH	OBS ausgelöst	OBS 114
SO186/140-1	11.03.06	12:32	3° 51,37' N	93° 55,19' E	0	NW 3	240	1,9	OBS/OBH	OBS/OBH	OBS an Deck	OBS 130
SO186/140-1	11.03.06	12:32	3° 51,36' N	93° 55,16' E	0	NW 4	234	1,2	OBS/OBH	OBS/OBH	OBS gesichtet	OBS 131
SO186/140-1	11.03.06	12:36	3° 51,32' N	93° 55,09' E	0	WNW 4	258	0,9	OBS/OBH	OBS/OBH	OBS an Deck	OBS 131
SO186/140-1	11.03.06	12:39	3° 51,29' N	93° 55,06' E	0	WNW 3	221	1,2	OBS/OBH	OBS/OBH	OBS ausgelöst	OBS 136
SO186/140-1	11.03.06	12:41	3° 51,26' N	93° 55,01' E	0	NNW 4	239	1,9	OBS/OBH	OBS/OBH	OBS gesichtet	OBS 132
SO186/140-1	11.03.06	12:42	3° 51,25' N	93° 54,98' E	0	WNW 4	231	1,8	OBS/OBH	OBS/OBH	OBS ausgelöst	OBS 137
SO186/140-1	11.03.06	12:45	3° 51,23' N	93° 54,91' E	0	NNW 4	254	1,1	OBS/OBH	OBS/OBH	OBS an Deck	OBS 132
SO186/140-1	11.03.06	12:49	3° 51,22' N	93° 54,85' E	0	NW 4	252	0,6	OBS/OBH	OBS/OBH	OBS gesichtet	OBS 133
SO186/140-1	11.03.06	12:51	3° 51,22' N	93° 54,83' E	0	NW 3	291	0,6	OBS/OBH	OBS/OBH	OBS ausgelöst	OBS 115
SO186/140-1	11.03.06	12:53	3° 51,22' N	93° 54,82' E	0	NW 4	189	0,1	OBS/OBH	OBS/OBH	OBS gesichtet	OBS 134
SO186/140-1	11.03.06	12:56	3° 51,22' N	93° 54,81' E	0	NNW 3	338	0,5	OBS/OBH	OBS/OBH	OBS an Deck	OBS 133
SO186/140-1	11.03.06	12:58	3° 51,22' N	93° 54,80' E	0	NW 3	177	0,2	OBS/OBH	OBS/OBH	OBS ausgelöst	OBS 116
SO186/140-1	11.03.06	13:00	3° 51,23' N	93° 54,80' E	0	NW 3	355	0,4	OBS/OBH	OBS/OBH	OBS an Deck	OBS 134
SO186/140-1	11.03.06	13:01	3° 51,23' N	93° 54,80' E	0	NW 4	317	0,9	OBS/OBH	OBS/OBH	OBS gesichtet	OBS 135
SO186/140-1	11.03.06	13:04	3° 51,22' N	93° 54,78' E	0	NW 3	219	0,5	OBS/OBH	OBS/OBH	OBS gesichtet	OBS 114
SO186/140-1	11.03.06	13:06	3° 51,21' N	93° 54,77' E	0	NW 4	206	0,5	OBS/OBH	OBS/OBH	OBS an Deck	OBS 135
SO186/140-1	11.03.06	13:07	3° 51,21' N	93° 54,77' E	0	NW 4	227	0,8	OBS/OBH	OBS/OBH	OBS ausgelöst	OBS 117
SO186/140-1	11.03.06	13:12	3° 51,17' N	93° 54,69' E	0	NW 3	236	0,9	OBS/OBH	OBS/OBH	OBS an Deck	OBS 114
SO186/140-1	11.03.06	13:13	3° 51,16' N	93° 54,68' E	0	NW 3	239	0,6	OBS/OBH	OBS/OBH	OBS gesichtet	OBS 136
SO186/140-1	11.03.06	13:14	3° 51,16' N	93° 54,67' E	0	NW 3	261	0,4	OBS/OBH	OBS/OBH	OBS ausgelöst	OBS 118
SO186/140-1	11.03.06	13:14	3° 51,16' N	93° 54,67' E	0	NW 3	261	0,4	OBS/OBH	OBS/OBH	OBS gesichtet	OBS 137
SO186/140-1	11.03.06	13:20	3° 51,12' N	93° 54,60' E	0	NW 3	217	1	OBS/OBH	OBS/OBH	OBS ausgelöst	OBS 119
SO186/140-1	11.03.06	13:22	3° 51,10' N	93° 54,56' E	0	NNW 3	242	1,6	OBS/OBH	OBS/OBH	OBS gesichtet	OBS 115
SO186/140-1	11.03.06	13:24	3° 51,08' N	93° 54,52' E	0	NNW 3	268	1,3	OBS/OBH	OBS/OBH	OBS an Deck	OBS 136
SO186/140-1	11.03.06	13:27	3° 51,06' N	93° 54,48' E	0	NNW 3	218	0,5	OBS/OBH	OBS/OBH	OBS an Deck	OBS 137
SO186/140-1	11.03.06	13:27	3° 51,06' N	93° 54,48' E	0	NNW 3	218	0,5	OBS/OBH	OBS/OBH	OBS ausgelöst	OBS 120
SO186/140-1	11.03.06	13:30	3° 51,06' N	93° 54,45' E	0	NNW 3	275	1	OBS/OBH	OBS/OBH	OBS gesichtet	OBS 116

Station	Datum	UTC	PositionLat	PositionLon	Tiefe [m]	Windstärke [m/s]	Kurs [°]	v [kn]	Gerät	Gerätekürzel	Aktion	Bemerkung
SO186/140-1	11.03.06	13:33	3° 51,10' N	93° 54,43' E	0	NNW 3	343	0,9	OBS/OBH	OBS/OBH	OBS ausgelöst	OBS 121
SO186/140-1	11.03.06	13:36	3° 51,14' N	93° 54,43' E	0	NW 3	311	0,7	OBS/OBH	OBS/OBH	OBS an Deck	OBS 115
SO186/140-1	11.03.06	13:40	3° 51,19' N	93° 54,45' E	0	WNW 3	38	1,2	OBS/OBH	OBS/OBH	OBS gesichtet	OBS 117
SO186/140-1	11.03.06	13:40	3° 51,19' N	93° 54,45' E	0	WNW 3	38	1,2	OBS/OBH	OBS/OBH	OBS an Deck	OBS 116
SO186/140-1	11.03.06	13:44	3° 51,26' N	93° 54,45' E	0	NW 4	1	1	OBS/OBH	OBS/OBH	OBS an Deck	OBS 117
SO186/140-1	11.03.06	13:47	3° 51,30' N	93° 54,45' E	0	NW 3	10	0,9	OBS/OBH	OBS/OBH	OBS gesichtet	OBS 118
SO186/140-1	11.03.06	13:52	3° 51,37' N	93° 54,46' E	0	WNW 4	23	0,8	OBS/OBH	OBS/OBH	OBS gesichtet	OBS 119
SO186/140-1	11.03.06	13:54	3° 51,39' N	93° 54,46' E	0	WNW 3	28	0,9	OBS/OBH	OBS/OBH	OBS an Deck	OBS 118
SO186/140-1	11.03.06	13:58	3° 51,45' N	93° 54,46' E	2471	NW 3	359	1,2	OBS/OBH	OBS/OBH	OBS an Deck	OBS 119
SO186/140-1	11.03.06	14:00	3° 51,49' N	93° 54,45' E	2476	WNW 3	354	2	OBS/OBH	OBS/OBH	OBS gesichtet	OBS 120
SO186/140-1	11.03.06	14:04	3° 51,58' N	93° 54,42' E	2474	NW 4	322	1,1	OBS/OBH	OBS/OBH	OBS gesichtet	OBS 121
SO186/140-1	11.03.06	14:06	3° 51,62' N	93° 54,40' E	2473	NW 4	324	0,8	OBS/OBH	OBS/OBH	OBS an Deck	OBS 120
SO186/140-1	11.03.06	14:11	3° 51,70' N	93° 54,38' E	2476	WNW 3	296	0,7	OBS/OBH	OBS/OBH	OBS an Deck	OBS 121
SO186/140-1	11.03.06	14:17	3° 51,76' N	93° 54,37' E	2474	WNW 4	13	0,9	OBS/OBH	OBS/OBH	Ende Station	
SO186/141-1	11.03.06	14:52	3° 50,01' N	94° 0,03' E	1968	W 3	68	11,9	Vermessung	PROFIL	Beginn Profil	rwK: 065°, d: 28 sm
SO186/141-1	11.03.06	17:06	4° 1,97' N	94° 25,94' E	1490	WNW 5	63	12,7	Vermessung	PROFIL	Kursänderung	rwK: 231°, d: 27 sm
SO186/141-1	11.03.06	19:32	3° 45,08' N	94° 5,11' E	1841	WNW 9	232	11,4	Vermessung	PROFIL	Kursänderung	rwK: 135°, d: 7 sm
SO186/141-1	11.03.06	20:06	3° 40,12' N	94° 9,93' E	1898	WNW 4	134	12,4	Vermessung	PROFIL	Kursänderung	rwK: 048°, d: 39 sm
SO186/141-1	11.03.06	23:08	4° 6,00' N	94° 39,00' E	767	WNW 5	60	13	Vermessung	PROFIL	Kursänderung	rwK: 073°, d: 24 sm
SO186/141-1	12.03.06	01:03	4° 13,10' N	95° 2,01' E	1578	W 6	1	10,4	Vermessung	PROFIL	Kursänderung	rwK: 353° d: 110 sm
SO186/141-1	12.03.06	09:32	5° 59,97' N	94° 49,03' E	586	ENE 10	354	13,2	Vermessung	PROFIL	Kursänderung	rwK: 028°, d: 19 sm
SO186/141-1	12.03.06	11:04	6° 16,99' N	94° 57,92' E	1077	NE 10	40	12,3	Vermessung	PROFIL	Kursänderung	rwK: 094°, d: 28 sm
SO186/141-1	12.03.06	13:26	6° 14,95' N	95° 26,00' E	1541	NE 8	137	10,2	Vermessung	PROFIL	Kursänderung	rwK: 180° d: 7 sm
SO186/141-1	12.03.06	14:00	6° 8,05' N	95° 25,98' E	1534	NE 5	171	11,7	Vermessung	PROFIL	Kursänderung	rwK: 090° d: 20 sm
SO186/141-1	12.03.06	15:54	6° 8,00' N	95° 46,01' E	1227	NNE 7	104	9,9	Vermessung	PROFIL	Kursänderung	rwK: 108° d: 42 sm
SO186/141-1	12.03.06	20:00	5° 54,79' N	96° 26,76' E	1341	NNW 4	109	10,4	Vermessung	PROFIL	Ende Profil	

Station SO 186-3	CTD / Ro	Airguns	w 10	W 11	OBH / OBS Aufnahme	OBH / OBS Auslage	TEWS-Boje / TOBU	EM 120 / Parasound-Profil	Hilfskräne Einsatzzeit	Stationszeit	W 4 Zeit	Seismikprofilzeit	EM 120 / Parasound- Zeit	Stationszeit in sm	Länge W 4	Seismikprofil in sm	EM120/Parasound-Verm. in sm	Bemerkungen
SO186/126-1					26	27				69,0				629				Aufnahme und Auslage OBS / OBH
SO186/127-1		1	1	1						1,3		32,6		4		132		Seismiik-Profil 01
SO186/128-1					34					29,5				177				Aufnahme OBS / OBH
SO186/129-1					1		1			2,1				6				Aufnahme TOBU 01b + TOBS 01b
SO186/130-1	1									1,5	1,5				2000			Schallprofil für SIMRAD-Lot
SO186/131-1							1			1,1				3				Sichtkontrolle TEWS-Boje 01b + Auslage TOBU 01b
SO186/132-1						23				1,8				2				Auslage OBH / OBS
SO186/133-1		1	1	1						0,5		5,4		2		22		Seismiik-Profil 02
SO186/133-2		1	1	1						0,2		5,9		1		24		Seismiik-Profil 03
SO186/133-3		1	1	1						0,1		5,8				24		Seismiik-Profil 04
SO186/133-4		1	1	1						0,6		3,4		3		14		Seismiik-Profil 05
SO186/134-1					23					3,9				7				Aufnahme OBS / OBH
SO186/135-1						23				1,9				3				Auslage OBH / OBS
SO186/136-1		1	1	1						0,6		1,5		2		6		Seismik-Profil 06
SO186/136-2		1	1	1						0,1		5,3				22		Seismik-Profil 07
SO186/136-3		1	1	1						0,2		5,3		1		22		Seismik-Profil 08
SO186/136-4		1	1	1						0,3		5,3		1		22		Seismik-Profil 09
SO186/136-5		1	1	1						0,2		5,4		1		22		Seismik-Profil 10
SO186/136-6		1	1	1						0,3		2,9		1		12		Seismik-Profil 11
SO186/136-7		1	1	1						1,0		1,3		3		6		Seismik-Profil 12
SO186/137-1					11					2,3				1				Aufnahme OBS / OBH
SO186/138-1						11				0,6				1				Auslage OBH / OBS
SO186/139-1		1	1	1						0,7		2,6		1		10		Seismik-Profil 13
SO186/139-2		1	1	1						0,1		5,4				22		Seismik-Profil 14
SO186/139-3		1	1	1						0,2		5,4		1		22		Seismik-Profil 15
SO186/139-4		1	1	1						0,3		5,5		1		22		Seismik-Profil 16
SO186/139-5		1	1	1						0,2		5,6		1		22		Seismik-Profil 17
SO186/139-6		1	1	1						0,1		3,5				14		Seismik-Profil 18
SO186/139-7		1	1	1						0,9		1,2		4		5		Seismik-Profil 19
SO186/140-1					23					3,6				6				Aufnahme OBS / OBH
SO186/141-1								1					29,1			350		SIMRAD EM-Profil
Total:	**1**	**19**	**19**	**19**	**118**	**84**	**2**	**1**	**0**	**125**	**1,5**	**109**	**29,1**	**862**	**2000**	**795**	**0**	
maximal gefierte															2000			
Seillänge SO 186-3																		